

https://dspace.org/

# The suitability of South African coal discard for the production of carbon based building composites

**Eterigho-Ikelegbe, Orevaoghene**

**2023**

University of the Witwatersrand, Johannesburg

https://hdl.handle.net/10539/49011

Eterigho-Ikelegbe, Orevaoghene. (2023). The suitability of South African coal discard for the production of carbon based building composites. [PhD thesis, University of the Witwatersrand, Johannesburg]. WIReDSpace. https://hdl.handle.net/10539/49011

Downloaded from a DSpace repository. https://dspace.org/




# The suitability of South African coal discard for the production of carbon-based building composites

**Orevaoghene ETERIGHO-IKELEGBE**

**2023**

# The suitability of South African coal discard for the production of carbon-based building composites

Orevaoghene ETERIGHO-IKELEGBE

A thesis submitted to the Faculty of Engineering and the Built Environment, University of the Witwatersrand, in fulfilment of the requirements for the degree of Doctor of Philosophy in Engineering.

Supervisor: Associate Professor Samson O. Bada

Johannesburg, 2023

## Declaration

I, **Orevaoghene Eterigho-Ikelegbe** with student number **1794557** hereby declare in terms of the university‘s rule G27 that:

1. I fully understand what plagiarism is, and I am aware of the university‘s policy in this regard.
2. This doctoral thesis is my original work. Where other peoples‘ work was used (either from a printed source, the internet, or any other source), this has been properly acknowledged and referenced following the university‘s requirements.
3. Where my own published works from this research were used verbatim, copyright permissions were duly obtained from the publishers, and proofs of the clearance certificate are attached in the appendix.
4. This thesis and all its contents have not been submitted before for any degree or examination to any other University.
5. I have not used work previously produced by another student or any other person to hand in as my own.
6. I have not allowed and will not allow anyone to copy my work to pass it off as his or her work.



Signature of Candidate

12th / September / 2023

## Abstract

The South African coal mining industries have been discarding their mining and coal preparation waste residues for many years. Estimates suggest that over 60 mega tonnes of coal waste is generated annually in South Africa. When poorly managed these residues are a significant environmental hazard as they occupy useful land and are prone to generating acid mine and spontaneous combustion. The ultimate goal of this research is to transform the coal-based waste problem into a material input for carbon-building materials in construction applications. The research presented in this thesis relates to the characterisation and assessment of coal or carbon ceramic composites produced from the pyrolysis of South African coal waste and preceramic polymer. The composites were prepared by curing and controlled pyrolysis of coal waste mixed with a preceramic polymer (PCP). The different South African coal wastes investigated are Greenside tailing slurry (GTS), Likeflow coal slurry (LCS), Proteas coal discard (PCD), GG1 (a discard from the washing plant), GT (a fine from the mined semi-soft coking coal), GS (from the Witbank coalfield) and fly ash (FA) sample. For the first part of the study, coal composites were produced from coal wastes using Semplastics formulated preceramic polymer (X-MAT®) as the ceramic-forming binder. Later on, commercial preceramic polymer (SPR-212) was investigated as the binder for coal wastes to produce the coal composites. Proximate, ultimate, total sulphur, hydrogen/carbon ratio, oxygen/carbon ratio, X-ray diffraction, X-ray fluorescence, Fourier Transform Infrared spectroscopy, Raman spectroscopy, thermogravimetric and Brunauer-Emmett-Teller analyses were used to obtain descriptions of the coal wastes. The various analyses conducted on the composites, which are up to 80% coal waste, indicated that the physicochemical properties of the coal waste play a huge role in the performance of the composites. For

instance, when a propriety PCP was used, GTS and LCS samples containing carbonyl functional groups, a hydrogen/carbon ratio of ~0.7%, volatile matter between 22.6 and 23.7% and ash content between 15.6 and 30.7%, respectively, produced good-quality composites. The GTS composite recorded flexural strength of 36.5 megapascals (MPa), compressive strength of 130 MPa, and water absorption as low as 3.4%. This suggests that a high hydrogen/carbon ratio and the presence of carbonyl groups in these coal wastes favoured binding or fuseability with the PCP during curing and pyrolysis. On the other hand, PCD of a hydrogen/carbon ratio of ~0.3%, volatile matter of 10.7%, and ash content of 39.8% experienced inertness and lower internal heat transfer with the PCP during pyrolysis. As a result, the PCD composite recorded low mass/shrinkage loss but high water absorption of 10.1%, low compressive strength of 83 MPa and low flexural strength of 27.5 MPa. By extending the range of the coal wastes investigated using discarded fine semi-soft coking coal (i.e., GT coal) mixed with a commercial PCP (SPR-212) as the ceramic-forming binder, coal composites of very poor quality were produced. The GT's hydrogen/carbon ratio was 0.09%, with a volatile matter of 32.7% and ash content of 11.4%. Hence, GT composites recorded volumetric shrinkage up to 36% during pyrolysis, water absorption of 15%, and compressive strength of 278 MPa. This was attributed to the swelling nature of the coal and the residual total carbon of the composite (up to 63%). As a result, the mechanical strength was compromised and the composites' susceptibility to heat during thermal analysis increased. Conversely, GG1 of 5.4% fixed carbon, 10% volatile matter, an ash content of 81.3% and a hydrogen/carbon ratio of 1.7% bonded well with the SPR-212 polymer. Consequently, quality GG1 composites recorded 19.7% volumetric shrinkage, 11% water absorption, and a compressive strength of 392 MPa. However, due to the high ash content of GG1 (81.3%) and the moderate weight loss that

occurred during pyrolysis, the composites recorded densities up to 2.5 grams per cubic centimetre. Additional composite properties reported in this research include textural properties, morphology, the form of carbon, chemical bonds, thermal stability (continuous operating temperature), efflorescence potential, surface properties utilising the angle of contact with water, volume resistivity and leaching potential. Based on the results collated, the coal composites could be designed into technical building parts such as bricks, panels, roofing tiles, etc. Optimisation of the mixing ratio of coal waste and preceramic polymer and the production process is expected to lower the processing temperature and yield coal composites that meet or exceed many conventional building parts.

**Keywords:** Building materials, Carbon, Ceramic, Circularity, Coal waste, Coal discard, Composites, Construction materials, Mechanical strength, Preceramic polymer, Water absorption

## Dedication

*my parents Patrick and Regina*

*my siblings*

*in memory of Mrs Anna Ono Obrifor (1949-2013)*

## Acknowledgement

Everything that has a beginning has an ending. Also, nobody knows what they are doing until they do it. On this note,

- First and foremost, my heartfelt and deep appreciation to God as well as His Son Jesus Christ for carrying me through the postgraduate study journey.
- To my supervisor, Associate Professor Samson Bada for his tremendous help, inexhaustible patience, direction, motivation and for everything he did for me during this research.
- To my family for their prayers, patience, support and encouragement - Mr Patrick, Mrs Regina, Mr Oghenekaro, Dr Omamuzo, Mrs Okeoghene, Mr Akpololohor Eterigho-Ikelegbe. To my cousins, I would like to thank you for your constant love, support and encouragement - Mr Okeoghene Obrifor and Engineer Ajirioghene Agbada.
- To Every Nation Rosebank Church, I extend my sincere appreciation.
- To every researcher in the Clean Coal Technology research group and the administrative staff of the School of Chemical and Metallurgical Engineering, my sincere gratitude for their generous assistance. Thank you for the wonderful time together.
- To the colleagues who helped with data collection and experimental work, I gratefully acknowledge your immeasurable contributions and knowledge sharing - Mr Andrew Morgan, Mr Motlatsi Phali, Mrs Petra Dinham, Associate Professor Rudolph Erasmus, Mr Samuel Onyedikachi
- To my friends and colleagues (in no particular order) who shared and offered words of encouragement during this journey, I extend my gratitude - Mrs Ngozi Enemuo, Dr Olawumi Sadare, Dr Kelvin Yoro, Dr Oluwaseun Ajayi, Professor Michael Daramola,

Dr Patrick Sekoai, Dr Michael Bodunrin, Mr Nino Neels, Mr Olatunde Johnson Lawal, Mr Frank Chime, Mrs Chinwe Unuigbe, Miss Onome Ogujor, Mr Tega Umukoro, Professor Bekir Genc, Professor Adeshola Ilemobade, Professor Nnamdi Elleh, Professor Sunny Iyuke.

- To Lebohang Maduna and Millicent Ramuatho, thank you for your labor.
- To the editors, reviewers and examiners, thank you for your assistance in improving the manuscripts and thesis.
- To Semplastics EHC LLC (Oviedo, FL) and X-MAT®, the Advanced Materials Division of Semplastics, thank you for producing the composites. To Ryan Trammell, I would like to say thank you for responding to my questions and for your support in generating the publications.
- To the German Academic Exchange Service (DAAD), thank you for sponsoring my research stay in Germany under the short-term research grants (57552337).
- To the Department of Science and Innovation National Research Foundation (DSI-NRF) through the South African Research Chairs Initiative Clean Coal Technology Grant (Grant Number: 86421), I gratefully acknowledge their financial support for this research. The opinions, findings, and conclusions expressed are not necessarily to be attributed to the National Research Foundation and other institutions mentioned in this thesis as they accept no liability in this regard.
- To everyone I met and who helped me out along the way that contributed to this in no small measure. It would not be possible without you all! huge thanks to you.
- Lastly, to the readers, hopefully, you find my thesis educating and interesting.

I wish everyone all the best for their careers and for their lives. **Thank you! Danke! Siyabonga!**

## PhD Outputs

The thesis contains the following peer-reviewed journal articles based on work from this study.

**Peer-reviewed publications**

I. **Eterigho-Ikelegbe, O**., Trammell, R., & Bada, S. (2021). Preparation and characterisation of ceramic composites from South Africa coal discard. *Construction and Building Materials*, *302*, 124164. https://doi.org/10.1016/j.conbuildmat.2021.124164

II. **Eterigho-Ikelegbe, O**., Yoro, K. O., & Bada, S. (2021). Coal as a Filler in Polymer Composites: A Review. *Resources, Conservation and Recycling*, *174*, 105756. https://doi.org/10.1016/j.resconrec.2021.105756

III. **Eterigho-Ikelegbe, O**., Trammell, R., & Bada, S. O. (2022). Novel ceramic composites produced from coal discards with potential application in the building and construction sectors. *Journal of the Southern African Institute of Mining and Metallurgy*, *122*(8), 421–428. https://doi.org/10.17159/2411-9717/2001/2022

IV. **Eterigho-Ikelegbe, O.,** Trammell, R., Ricohermoso, E., & Bada, S. (2023). Mechanism of bonding, surface property, electrical behaviour, and environmental friendliness of carbon/ceramic composites produced via the pyrolysis of coal waste with polysiloxane polymer. *Environmental Science and Pollution Research*, *30*(41), 93786–93799. https://doi.org/10.1007/s11356-023-28661-z

V. **Eterigho-Ikelegbe, O**., Ricohermoso, E., Harrar, H., Riedel, R., & Bada, S. (2023). Strong, lightweight, thermally stable, and hydrophobic sustainable structural composites produced from coal-based waste and polymer-derived SiOC

ceramics. *Clean Technologies and Environmental Policy*. https://doi.org/10.1007/s10098-023-02589-x

**Conference, symposium and seminar presentations**

- 'Innovative options for coal/coal-based waste in the circular economy', *Wits Inter-faculty Symposium on Climate, Sustainability and Inequality*, 23-24 August 2023, University of the Witwatersrand **(Oral presentation)**
- 'Towards Circularity and Sustainable Coal Waste Management', *Southern African Coal Processing Society International Coal Conference*: '*The role of coal beneficiation in a low carbon economy*', 15-17 August 2023 **(Oral presentation)**
- 'Coal composites: An option for coal waste in the circular economy', *Postgraduate Seminar (CHEMET-PGS-2023),* 30 May 2023, University of the Witwatersrand **(Oral Presentation)**
- 'Structural composites from coal waste using polysiloxane polymer as ceramic binder: physicochemical/microstructural investigation, thermal stability, compressive strength, and surface property', *2nd International Centre for Sustainable Carbon (ICSC) Energy Transition Workshop: The future of coal in a transitioning energy landscape*, 19-20 April 2023, Cape Town South Africa **(Oral Presentation)**
- 'Investigation of carbon/ceramic composites from coal waste and polysiloxane polymer: Application as sustainable construction materials', *6th International Conference on Engineering for a Sustainable World (ICESW 2022)*, 28-30 November 2022, Covenant University, Nigeria **(Oral Presentation)**

- ‘Carbon/ceramic composites from coal waste and preceramic polymer – potential for building applications’, *The Wits PhD Seminar*, 12-16 September 2022, University of the Witwatersrand **(Oral Presentation)**
- ‘Coal value chain and coal in the circular economy’, *Wits Inter-faculty Symposium on Climate, Sustainability, and Inequality*, 3-4 August 2022, University of the Witwatersrand **(Oral presentation)**
- **‘**Properties of carbon/ceramic composites from South African coal wastes’**,** *The 13th Cross-Faculty Postgraduate Symposium,* 11 July 2022, University of the Witwatersrand **(Poster presentation)**
- ‘Preparation and characterisation of structural composites from South Africa coal discard’, *Southern African Coal Processing Society International Coal Conference*: ‘*Coal Processing and Our Role in the Drive for Cleaner Coal*’, 12-14 October 2021 **(Oral presentation)**
- ‘Ceramic composites from South Africa coal discard: a preliminary investigation’, *The 12th Cross-Faculty Postgraduate Symposium,* 26-28 July 2021, University of the Witwatersrand **(Poster presentation)**

**Report contribution**

- Samson Bada, Jibril Abdulsalam, **Orevaoghene Eterigho-Ikelegbe.** The alternative uses of coal in the production of advanced materials and lightweight products for the sustainability of the South African coal industry. *Project Number: P2023 - 1*

**Award**

- Short-Term Doctoral Grant, 2021 (57552337), The German Academic Exchange Service (DAAD) visiting scholar for further study and training at the Technische Universität Darmstadt, Germany.

# Table of Contents

**Declaration** ..... **i**

**Abstract** ..... **ii**

**Dedication** ..... **v**

**Acknowledgement** ..... **vi**

**PhD Outputs** ..... **viii**

Peer-reviewed publications ..... viii

Conference, symposium and seminar presentations ..... ix

Report contribution ..... x

Award ..... xi

**Table of Contents** ..... **xii**

**List of Figures** ..... **xviii**

**List of Tables** ..... **xxii**

**Abbreviations, Acronyms and Units** ..... **xxiv**

**1 Introduction** ..... **1**

1.1 Motivation and background ..... 1

1.2 Problem statement ..... 4

1.3 Research questions ..... 5

1.4 Research aim and objectives ..... 6

1.5 Significance and relevance of the research ..... 7

1.6 Thesis organisation ..... 9

**2 Coal as a filler in polymer composites: a review** ..... **11**

Abstract ..... 12

2.1 Introduction ..... 13

2.2 Non-energy application of coal ..... 15

2.3 Polymeric character and macromolecular structure of coal ..... 17

2.4 Coal as a filler in the development of polymer composites ..... 20
2.5 Production of coal/polymer composites ..... 23
2.6 Research and development of coal as an organic filler in polymer composites 26
2.6.1 Polymeric gradient materials consisting of coal ..... 26
2.6.2 Effect of coal structure on the interfacial interaction between coal fillers and polymers ..... 31
2.6.3 Effect of coal content on the mechanical strength of the composites ..... 33
2.6.4 Thermal stability and flame retardancy effect of coal fillers ..... 36
2.6.5 Additional features of coal/polymer composites ..... 40
2.6.6 Life cycle and techno-economic assessment of coal/polymer composites 41
2.7 Technical challenges in developing coal/polymer composites ..... 43
2.7.1 Role of coupling agents and compatibilisers ..... 44
2.8 Coal and preceramic polymer resin ..... 52
2.9 Comparison of coal fillers with other filler materials ..... 53
2.10 Conclusions ..... 60
2.11 Future research focus and needs ..... 61
**3 Experimental ..... 64**
3.1 Chemicals, coal wastes and fabrication of the coal/ceramic composites ..... 65
3.2 Characterisation techniques ..... 66
3.3 Characterisation of the coal composites ..... 67
3.4 Resources and equipment ..... 69
3.5 Summary ..... 74
**4 Preparation and characterisation of ceramic composites from South Africa coal discard ..... 75**
Abstract ..... 76
4.1 Introduction ..... 77

4.2 Experimental ..... 79
4.2.1 Analysis of the coal discard utilised and the synthesised composites ..... 79
4.2.2 Preparation of the composites ..... 81
4.2.3 Physicomechanical characterisation ..... 82
4.3 Results and discussion ..... 83
4.3.1 Proximate and ultimate analysis ..... 83
4.3.2 Fourier Transform Infrared spectroscopy ..... 85
4.3.3 X-ray diffraction ..... 87
4.3.4 Thermogravimetric analysis ..... 90
4.3.5 Morphology ..... 92
4.3.6 Physicomechanical properties ..... 94
4.3.6.1 Pyrolysis shrinkage and pyrolysis mass loss of composite specimens . 94
4.3.6.2 Porosity and water absorption test ..... 95
4.3.6.3 Flexural strength and compression strength ..... 98
4.4 Conclusion ..... 100
**5 Novel composites produced from coal discards with potential application in the building and construction sectors ..... 101**
Abstract ..... 102
5.1 Introduction ..... 103
5.2 Experimental ..... 105
5.2.1 Materials and method ..... 105
5.2.2 Characterisation of coal discard and coal/ceramic composite ..... 106
5.3 Results and discussion ..... 108
5.3.1 Properties of the coal discard samples ..... 108
5.3.2 Morphological characterisation of the coal composites ..... 111
5.3.3 Flexural strength and water absorption properties ..... 112

5.3.4 Continuous operating temperature ..... 115
5.3.5 Chemical resistance ..... 117
5.3.6 Efflorescence ..... 120
5.4 Conclusions ..... 121
**6 Mechanism of bonding, surface property, electrical behaviour, and environmental friendliness of carbon/ceramic composites produced via the pyrolysis of coal waste with polysiloxane polymer ..... 122**
Abstract ..... 124
6.1 Introduction ..... 125
6.2 Materials and methods ..... 129
6.2.1 Materials ..... 129
6.2.2 Preparation of the carbon/ceramic composites ..... 130
6.3 Characterisation and testing ..... 131
6.3.1 Textural properties of the coal samples and the carbon/ceramic composites ……131
6.3.2 Wettability evaluation ..... 132
6.3.3 Form of carbon/Raman analysis ..... 132
6.3.4 Electrical resistivity measurement ..... 132
6.3.5 Environmental friendliness of the composites ..... 133
6.4 Results and discussion ..... 134
6.4.1 Mechanism of bonding ..... 134
6.4.2 Textural analysis of the coal samples and carbon/ceramic composites .. 136
6.4.3 Water contact angle analysis ..... 139
6.4.4 Raman spectra ..... 140
6.4.5 Electrical resistivity evaluation ..... 145
6.4.6 Leachability analysis ..... 148
6.5 Conclusion ..... 151

**7 Strong, lightweight, thermally stable, and hydrophobic structural composites produced from coal-based waste and polymer-derived SiOC ceramics..... 153**

Abstract ..... 155

7.1 Introduction ..... 156

7.2 Experimental and characterisation ..... 159

7.2.1 Materials and preparation of the composites ..... 159

7.2.2 Physicochemical and microstructural characterisation of the coal-based wastes and composites ..... 161

7.2.3 Physicomechanical and surface properties of the composites ..... 163

7.3 Results and discussion ..... 164

7.3.1 Physicochemical assessment of the coal-based waste and coal composites ……164

7.3.2 Functional group and microstructural analysis of the coal-based wastes and coal composite ..... 166

7.3.2.1 Fourier transform infrared spectra analysis ..... 166

7.3.2.2 X-ray diffraction analysis ..... 170

7.3.2.3 Scanning electron and optical imaging ..... 172

7.3.2.4 Raman analysis ..... 175

7.3.2.5 Thermal stability/continuous operating temperature of the composites ……..177

7.3.3 Physical and mechanical analysis of the composites ..... 179

7.3.3.1 Weight loss and shrinkage during pyrolysis ..... 179

7.3.3.2 Density, water absorption and apparent porosity of the composites ..... 181

7.3.3.3 Surface property of the composites ..... 184

7.3.3.4 Compressive strength performance ..... 185

7.4 Conclusion ..... 191

**8 General conclusions and recommendations..... 192**

8.1 Conclusions ..... 193

8.2 Recommendations ..... 194

**References ..... 195**

**Appendix A ..... 231**

**Appendix B ..... 237**

**Appendix C ..... 242**

## List of Figures

Figure 1-1 The anticipated benefits of coal composites derived from coal waste over traditional building products from virgin materials..... 9
Figure 2-1 Non-energy value products from coal ..... 16
Figure 2-2 (a) Three-dimensional crosslinked two-component macromolecular model of coal (Adapted from Haenel (1992)), (b) Molecular structure model of bituminous coal (Adapted from Shinn (1984)) ..... 20
Figure 2-3 Examples of polymer feedstocks for the development of coal/polymer composites ..... 21
Figure 2-4 Schematic representation for the fabrication of coal/polymer composites... 24
Figure 2-5 Schematic of coal/polymer gradient composite preparation based on the centrifugal casting method (Adapted from Stabik and Chomiak (2011)) ..... 28
Figure 2-6 (a) Flexure and (b) tensile properties of coal plastic composites composed of 0 to 60 weight percent (wt.%) of Pittsburgh No. 8 coal (Phillips et al., 2019) ..... 34
Figure 2-7 Mechanical properties as a function of (a) the percentage mass of coal and (b) the particle size (Hu et al., 2017, reproduced with permission from Elsevier) ..... 36
Figure 2-8 Mechanical properties of the SBR1500 rubber filled with coal slime with different ash content (Tan et al., 2019, reproduced with permission from Elsevier) ..... 47
Figure 2-9 Reaction scheme of coal particles and titanate coupling agent (Adapted from Cheng et al. (2014)) ..... 50
Figure 2-10 (a) impact strength and (b) elongation at break of pure polypropylene (0/0), and polypropylene/ethylene-propylene-diene monomer/coal composites (Adapted and modified from Bai et al. (2019)) ..... 51
Figure 2-11 Schematic of coal/ceramic composite preparation ..... 53
Figure 3-1 Summary of single batch production of the coal composites ..... 65
Figure 3-2 A summary of techniques used to analyse the coal wastes..... 67
Figure 3-3 A summary of the techniques used to characterise and test the performance of the coal composites..... 69
Figure 3-4 Resources used in the fabrication of the coal composites: (a) SPR-212 preceramic polymer, (b) 20 mm diameter moulds for shaping, (c) compression moulding machine, (d) oven for curing the moulded mixture of coal and the preceramic polymer,

(e) high temperature furnace for pyrolysis of the cured moulded body and (f) compression testing equipment..... 70
Figure 3-5 Some products obtained and tests conducted: (a) fresh mixture of coal waste and preceramic polymer, (b) cured/green samples, (c, d) pyrolysed samples, (e) efflorescence testing and hot water absorption test, (f) prepared composite sections for scanning electron microscopy analysis, (g) leachate obtained from crushed composite samples and (h, i) pyrolysed samples ..... 71
Figure 4-1 A schematic representation of the experimental procedure for producing coal composites ..... 81
Figure 4-2 Image of coal discard (left) and coal composites formed (right)..... 82
Figure 4-3 Spectra of the raw coal discard samples ..... 86
Figure 4-4 Spectra of the coal composites ..... 87
Figure 4-5 X-ray diffraction patterns of pulverised coal discard samples ..... 88
Figure 4-6 X-ray diffraction patterns obtained for coal/ceramic composite specimens. 89
Figure 4-7 Thermogravimetric curves for coal discard samples and coal composite specimens ..... 91
Figure 4-8 Microstructure of the top surface of coal composite specimens (a) Likeflow coal slurry (LCS), (b) Greenside tailing slurry (GTS) and (c) Proteas coal discard (PCD), and the fractured surface of (d) LCS, (e) GTS and (f) PCD..... 93
Figure 4-9 Summary of flexural strength, pyrolysis mass loss and pyrolysis shrinkage of coal composite specimens ..... 94
Figure 4-10 Mechanism of the binding scheme between discard coal particles and the preceramic polymer resin ..... 97
Figure 5-1 Schematic of coal/ceramic composites production..... 106
Figure 5-2 Scanning electron microscopy images of the (a) Greenside tailing slurry, (b) Proteas coal discard and (c) Likeflow coal slurry composites ..... 112
Figure 5-3 Water absorption and flexural strength properties of the composites ..... 113
Figure 5-4 X-ray diffraction patterns of the composites ..... 115
Figure 5-5 (a) Weight loss curves and (b) derivative thermogravimetric (DTG) curves of coal discard composites and conventional roof materials ..... 116

Figure 5-6 Coal composites and conventional roof tiles exposed to different chemicals: (a) citric acid, (b) potassium hydroxide, (c) ammonium chloride and (d) lactic acid solution ..... 118
Figure 6-1 Assessment of the physicochemical characteristics of the coal wastes (air-dried) (a) Proximate analysis (b) Ultimate analysis ..... 130
Figure 6-2 A summary of the production of the carbon/ceramic composites ..... 131
Figure 6-3 Pictorial images of the carbon/ceramic composites..... 131
Figure 6-4 Arrangement of the four-point probe resistance measurement of the carbon/ceramic composites..... 133
Figure 6-5 Hypothetical mechanisms of the curing and pyrolysis of coal waste and the polysiloxane preceramic polymer..... 136
Figure 6-6 Comparison of the pore size distributions of the coal samples and the carbon/ceramic composites..... 137
Figure 6-7 The water contact angle of the carbon/ceramic composites at room temperature ..... 140
Figure 6-8 Raman spectra of the coal waste and the carbon/ceramic composites with their corresponding curve-fitting bands ..... 143
Figure 6-9 Variation in the peak intensity ratio ($A_D/A_G$) and the size of the carbon cluster crystallites of the coal and their composites ..... 145
Figure 6-10 Measured volume electrical resistivity of the composites ..... 146
Figure 7-1 Preparation of the composites..... 161
Figure 7-2 Fourier Transform Infrared spectrum of the native polysiloxane SPR-212 167
Figure 7-3 Fourier Transform Infrared spectra of the coal waste and their corresponding composites ..... 169
Figure 7-4 A comparison of the X-ray diffraction patterns of the coals and coal composites ..... 172
Figure 7-5 Scanning electron microscopy secondary electron image (a), back-scattered images (d, g, j), energy dispersive X-ray spectroscopy analysis (b, e, h, k) and optical micrographs (c, f, i, l) of the as-fabricated composites. (a, b, c) GG1; (d, e, f) FA; (g, h, i) GT; (j, k, l) GS composites..... 174
Figure 7-6 Raman spectra of the composites..... 176

Figure 7-7 Thermal analysis (TGA) profiles of the composites under (a) Oxygen (b) Air environment ..... 178
Figure 7-8 Average pyrolysis mass loss and shrinkage of the composites ..... 181
Figure 7-9 Bulk, geometric and apparent densities of the composites ..... 183
Figure 7-10 Average apparent porosity and water absorption of the composites ..... 184
Figure 7-11 The water contact angle of the composites measured by the sessile drop method and FTIR of the nonpolar C-H group (right) ..... 185
Figure 7-12 Average ultimate compressive stress and specific compressive strength of the composites ..... 187
Figure 7-13 The correlation between (a) hydrogen/carbon ratio (b) ash content (c) volatile matter of CBW on the key performance properties of the composites ..... 189

## List of Tables

Table 2-1 Key properties of the evaluated coals ..... 47
Table 2-2 Properties of tensile and flexural strength of representative polymer composites ..... 55
Table 2-3 Summary of investigations of composites developed using coal and polymer ..... 57
Table 3-1 The list of analytical facilities and equipment used for this research ..... 72
Table 4-1 Summary of formula ..... 83
Table 4-2 Summary of properties of coal discard samples and coal composite specimens ..... 84
Table 4-3 Physicomechanical properties of the coal composite specimens ..... 95
Table 4-4 Comparison of key data of the composites developed in this study to other structural composites in the literature ..... 99
Table 5-1 The major and minor element content of the coal discards ..... 109
Table 5-2 Physicochemical properties of the coal discard and coal composites ..... 111
Table 5-3 Summary of data extracted from the weight loss curves in Figure 5-5a ..... 117
Table 5-4 Chemical resistance performance of coal composites and conventional roof tiles ..... 119
Table 6-1 Textural information of the coal samples and the carbon/ceramic composites ..... 137
Table 6-2 Comparison of the other graphitisation indices obtained from deconvoluted Raman spectra of the coal samples and carbon/ceramic composites and calculated using Equations 6-2 to 6-5 ..... 142
Table 6-4 Leached concentrations of heavy metal elements and inorganic anions from the composites compared with the LCT and TCLP limits ..... 150
Table 7-1 Particle size distribution and textural properties of the CBW samples ..... 161
Table 7-2 Physicochemical composition of the coal-based wastes (wt. %, air-dried basis) ..... 165
Table 7-3 Elemental composition of the pyrolysed composites ..... 165
Table 7-4 Summary of the various functional groups within the coal structure and coal composites ..... 170
Table 7-5 Graphitisation indices of the composites ..... 176

Table 7-6 Summary of the thermogravimetric analysis of the composites shown in Figure 7-7 ..... 179
Table 7-7 The physicomechanical performance of the composites produced in this study compared to other composites for building applications in the literature ..... 190

## Abbreviations, Acronyms and Units

Å – angstrom

% – percent(age)

~ – approximate

°C/min – degree Celsius per minute

µL – microlitre

µL/s – microlitre per second

µm – micrometre

Ω – ohm

Ω-cm – ohms centimetres

a.d. – air-dried

ASTM – American Society for Testing Materials

BET – Brunauer, Emmett and Teller

CA – contact angle

CBC – coal-based waste

CPC – coal plastic composite

EPA – Environmental Protection Agency

EPDM – ethylene-propylene-diene monomer

FA – fly ash

FTIR – Fourier Transform Infrared

g – grams

g/L – grams per litre

GG1 – discard from the washing plant

GPa – gigapascal

GS – coal waste collected from the Witbank coalfield

GT – fine coal waste from the mined semi-soft coking coal

Gt – gigatonne

GTS – Greenside tailing slurry

H/C – hydrogen to carbon atomic ratio

HDPE – high-density polyethylene

ISO – International Standard Organization

IEA – International Energy Agency

KH-570 – γ-methacryloxypropyltrimethoxysilane

LCS – Likeflow coal slurry

LCT – leachable concentrations threshold

LOI – loss on ignition

$L_a$ – size of carbon crystallites

$L_D$ – distance between defects

MAPE – maleic anhydride grafted polyethylene

mg – milligram

mL – millilitre

mL/g – millilitre per gram

MPa – megapascal

Mt – megaton

n.d. – not detected

$n_D$ – defect density

nm – nanometre

O/C – oxygen to carbon atomic ratio

PCD – Proteas coal discard

PCP – preceramic polymer

PDC – polymer-derived ceramic

PSXs – poly(organosiloxanes)

SDBS – sodium dodecylbenzene sulphonate

SEM-EDS – scanning electron microscopy-energy dispersive x-ray spectrometry

T – tonnes

T5% – temperature at 5% weight loss

$T_g$ – glass transition temperature

TGA – thermogravimetric analysis

wt.% – Percentage by weight

XRD – X-ray diffraction

XRF – X-ray fluorescence

# 1 Introduction

This chapter presents the motivation and background to the thesis. The research aim, research questions and objectives, and the organisation of the thesis are clearly outlined.

## 1.1 Motivation and background

Coal is a vastly abundant and affordable natural resource that has facilitated economic growth in both the developing and developed world (Magazzino et al., 2020). Coal is significantly used in chemical, steel, and cement production and for generating electricity (Longwell et al., 1995; Pudasainee et al., 2020). According to the International Energy Agency (IEA, 2020), South Africa is ranked seventh in coal production worldwide. The country is almost entirely dependent on coal for its domestic demands and is a leader in using coal as feedstock for chemical production. However, the use of coal beyond energy production is attracting great interest (Schobert & Song, 2002; Hu et al., 2017; Al-Majali et al., 2019). By taking advantage of the carbon atoms in coal, researchers are exploring different approaches to utilise coal as raw material feedstock, a precursor or filler material in producing products of high significance (Reid, 2018).

The technological uses of coal for non-energy applications are summarised in the New Carbon Age Report Fact Sheet (NCC, 2019). It includes carbon electrodes, carbon foams, activated carbons, carbon foam, carbon nanotubes, etc. Other high-end non-energy products that can be produced from coal feedstock are carbon fibres, carbon composite materials, high-density carbon products, graphene, and supercapacitors (Romey & Hein, 1981; Jagtoyen et al., 1993; Derbyshire et al., 1994; Song et al., 2005; Frank et al., 2012; Zhao et al., 2014; Reid, 2018; Liu et al., 2019; Zabihi et al., 2019; Gagarin et al., 2020).

For example, Keller et al. (2016) reported that coal's broad range of electrical properties could be tapped for processing thin films for electronic devices. Moreso, coal is considered a promising filler material that can improve the performance of many thermoplastic and thermosetting polymers due to its chemistry and chemical stability. According to Bai et al. (2019), the active side chain alkyl, hydroxyl, carbonyl and methoxyl groups within the structural units of coal could enhance the compatibility between coal powder and polymer. Hence, coal is investigated as an organic reinforcement for polymer modification to extend the polymer with novel functionalities. Other researchers have incorporated coal with plastic to increase the mechanical and microstructure properties of plastics (Zhu et al., 2010; Hu et al., 2017; Al-Majali et al., 2019; Phillips et al., 2019).

Within the last two decades, hybrid or composite materials have emerged as fundamental building blocks for modern technological and scientific research (Foresight, 2013). Ceramics is an outstanding material explored to develop composite material (Fridlyander et al., 1992; Raether, 2013). Conventionally, ceramics are produced by mixing ceramic powder (obtained via powder synthesis) with additives, shaped (powder processing) and then sintered via a process known as the 'powder technology'. The conventional process of producing ceramics involves high temperature and high pressure, induces shape and size limitations, making it unsuitable for fabricating geometrically complex ceramics (Magnant et al., 2012). To overcome this challenge, preceramic polymers (PCPs) containing inorganic or organometallic compounds that convert to ceramics upon pyrolysis were proposed (Greil, 1995; Colombo et al., 2010). The ceramics from these polymers, called polymer-derived ceramics (PDCs), can be obtained at relatively low processing temperatures (Colombo et al., 2010; Eckel et al., 2016). Due to

the exceptional properties of the PDCs, PCPs have been used to create useful end products such as clutches for racing cars, brakes for conventional automobiles, coatings, micro components, etc. (Riedel et al., 2006; Colombo et al., 2010; Xia et al., 2020; Wen et al., 2022).

Recently, Hill and Easter (2019, 2021) reported an innovative route to produce carbon/ceramic composites from two United States medium-volatile bituminous coals using PCP resin as a binder. The authors found that the lower-grade coal yielded composites of higher linear shrinkage (19.4%) and lower char yield (68.3%). In contrast, the higher-grade coal yielded superior composites of linear shrinkage and char yield of 18% and 80%, respectively. In terms of weight and strength, the higher-grade coal resulted in a lighter and higher-strength composite than the lower-grade coal. Furthermore, a fire test conducted with a propane torch could not cause significant damage to the composites, thus, reflecting their excellent fire resistance. The results documented by the investigators suggest that these carbon/ceramic composites can be moulded into building materials such as bricks, roof shingles, tiles, panels, etc.

Falcon (1986) established that coal from different regions does not have the same characteristics. The carboniferous coals of the northern hemisphere and the Permian coals of the southern hemisphere vary in composition and degree of maturity. This is due to the origin, vegetation, and climate at the time of formation, coalification age, and subsequent events in the geological history of coal development in both regions. The coals from the southern hemisphere have lower sulphide, pyrite, chlorine, and poisonous trace elements but are higher in ash and inert organic matter than the northern hemisphere coals. It is important to select coals for specific utilisation fields because of these differences, as they can be directly related to performance (Falcon, 1986). Therefore, it is anticipated that

South African coal and the United States coal utilised by Hill and Easter (2019, 2021) would react differently with the PCP due to the difference in their organic matter and inorganic minerals. The research documented in this thesis explores the suitability of South African coals as a suitable feedstock to obtain ceramic composites comparable in properties to conventional building materials.

## 1.2 Problem statement

Coal is the primary source of energy in South Africa and is used in the chemical and steel industries. However useful it may be, coal mining companies and related sectors must deal with the disposal of coal waste, an unwanted by-product growing steadily with about 60 Mt (megatonne) generated annually in South Africa (Department of Mineral and Energy, 2021). These coal wastes are stored in discard (tailing) dumps. Disposing of these wastes is a challenge to the industry due to high processing costs and long-term care while stockpiling them is often associated with violations of environmental and social standards. The landfill disposal of coal waste causes latent environmental problems since the heavy metal in the coal waste cannot be contained within the landfill boundaries forever. Landfill disposal of coal waste also means using space, which is considered a limited resource. Other threats of stockpiling coal waste include spontaneous combustion, air pollution and contamination of aquifers (Munawer, 2018; Moyo et al., 2018, 2019). Repurposing and recycling are potential solutions to this ever-growing problem. Despite efforts locally and internationally, the recycling rates of coal waste remain low. Furthermore, most coal waste recycling options are still under research in the laboratory stage. Therefore, an innovative and effective strategy is required to increase the recycling rates of coal waste that will enhance the sustainability of the coal sector.

Meanwhile, the world's construction industry consumes more raw materials than any other economic activity. As the urban population is expected to rise over the next decades up to 9.8 billion in 2050 (OECD, 2015), with 65% in urban areas, the continuous exploitation and growing demand for raw materials would lead to substantial depletion of high-quality materials e.g., clay/sand for the building and construction industries (Lemeshev et al., 2004; Abdrakhimov & Abdrakhimova, 2017; Fomina & Yu. Stolboushkin, 2019). The variety of coal wastes in South Africa regarding their mineral and chemical composition could impose a considerable qualitative, quantitative, and technological assessment of their sustainability for obtaining structural composites. If coal waste bonded with PCP resin can be harnessed, the accumulation of huge quantities of coal waste could be prevented by converting them to high-volume composites. Additionally, using coal waste instead of virgin raw materials would lead to energy savings, job creation and resource conservation, creating a closed-loop material cycle and enabling a circular economy. The relatively new concept of using South African coal wastes pyrolyzed with a PCP resin to produce composites leaves room for extensive exploration. Therefore, this study sought to address the gap in knowledge by investigating the suitability of South African coal wastes to produce coal composites.

## 1.3 Research questions

The following questions were posed and investigated in this research:

i. How does the different microstructures of South African coal wastes influence the physicomechanical properties and the continuous operating temperature of coal composites fabricated using a proprietary polysiloxane PCP resin as the ceramic-forming binder?

ii. How does the variations in chemical composition of South African coal wastes influence the physicomechanical properties of the coal composites and their application as structural composites? Also, what is the effect of prolonged exposure of the coal composites to various chemicals compared to those of traditional building materials (e.g., roof tiles)?

iii. What is the mechanism of bonding, surface property, electrical property and the environmental friendliness of the coal composites produced from South African coal wastes and the proprietary polysiloxane PCP resin?

iv. How does the variations in the physicochemical properties of South African coal wastes affect the physicomechanical properties, microstructure, surface property and the continuous operating temperature of coal composites produced using a commercial PCP (SPR-212) as the ceramic-forming binder?

## 1.4 Research aim and objectives

The study aimed to investigate the suitability of South African coal discards or wastes to produce structural coal composites using PCPs as ceramic-forming binders. This study further aimed to understand the effect of the physicochemical characteristics of coal wastes on the final properties of the composites.

Hence, the objectives of this study were as follows:

i. To evaluate the physicomechanical properties and the continuous operating temperature of coal composites produced by Semplastics EHC LLC (Oviedo, FL, USA) from various South African coal wastes and a polysiloxane PCP resin as the ceramic-forming binder.

ii. To provide additional scientific information on the properties of the composites evaluated in (i) based on the chemical compositions of the various coal wastes and also to compare the composites' chemical resistance and efflorescence potential with those of traditional building materials (e.g., ceramic and concrete roof tiles).

iii. To propose the mechanism of bonding that adequately describes the pyrolytic conversion of coal/polymer to carbon/ceramic composites and to investigate the surface property, electrical property and environmental friendliness of the composites produced in (i).

iv. To produce coal composites from a variety of South African coal wastes and commercial PCP (SPR-212) and to evaluate their microstructure, physicomechanical, continuous operating temperature and surface property.

## 1.5 Significance and relevance of the research

At this time, it is difficult to imagine South Africa without coal despite the uncertainties surrounding coal as a source of energy. Even so, the process of mining and preparing clean coal leaves behind abundant low-value coal waste that violates environmental and social standards. There is only one study that has reported the possibility of producing structural composites from coal and PCP resin (Hill & Easter, 2019, 2021). Using South African coal waste to produce structural composites has not been studied before, thus, making the contributions of this study novel and significant as it provides this information. This study sought to acquire understanding in this area by providing extensive information on the physicochemical and physicomechanical characteristics of the coal composites that make them suitable as building materials. As well as the knowledge on the conversion of coal waste and PCP to coal/ceramic composites. Accordingly, it is anticipated that South African coal waste bonded with PCP

resin could produce composite building parts. If a significant amount of coal waste can be used to produce composite building parts, the disposal problem would be eliminated, and valuable products would be created. Where contributions to improve the sustainability and circularity of the coal sector is receiving research attention, this study is important in that it would provide a platform for future research to improve the quality of the composites. The eventual success and implementation of this research would pave the way to process huge quantities of coal waste to high-volume composites compared to other valorisation solutions that use small volumes of coal waste. Besides, using coal waste as raw material input for producing composite building parts instead of virgin raw materials will prevent their accumulation, might lead to energy savings, job creation, revenue for the mining communities and resource conservation.

The rationale for investigating South African coal waste as feedstock for producing building composites is illustrated in Figure 1-1. Repurposing coal waste aligns with the theme of waste valorisation and management, the circular economy and sustainability under the Sustainable Development Goals 8, 12 and 13 that focus on economic growth, responsible consumption and climate action. The significance of this study is further reinforced by the fact that the proposed solution is preferred to disposal/disposal and may be considered a practical solution to coal waste pollution issues. To meet the Sustainable Development Goals, it is imperative to investigate the suitability of various South African coal wastes as raw material for producing coal composites for building applications.

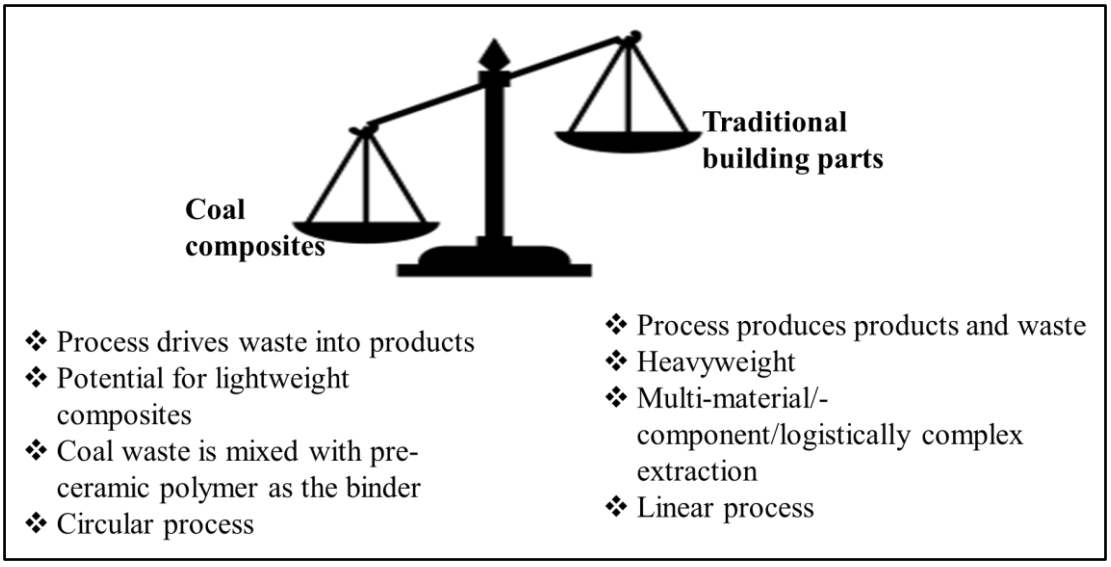



Figure 1-1 The anticipated benefits of coal composites derived from coal waste over traditional building products from virgin materials

## 1.6 Thesis organisation

The thesis contains works that have previously been published. Copyright permissions have been obtained for the publications used verbatim in this thesis (see Appendix B). The thesis is divided into eight chapters, including an introductory chapter. A brief description of each chapter in the thesis is provided below.

**Chapter 1**, the general introduction, includes the background and motivation for the investigation. The problem statement, aim, objectives, and scope of the study are also provided.

In **Chapter 2**, the research and development of coal as an organic filler in polymer composites are thoroughly reviewed. The polymeric nature of coal, as well as the implications of coal structure and the content of coal on the composites' properties , are discussed. This chapter has been published in *Resources, Conservation & Recycling*.

**Chapter 3** summarises the general methodology of the study. The materials, preparation method of the coal composites, analytical techniques and performance evaluation of the coal composites are outlined.

**Chapters 4**, **5**, and **6** provide detail investigations on the properties of coal composites produced by Semplastics EHC LLC (Oviedo, FL, USA) using a proprietary PCP. I recommended the coal wastes used to produce the composites after thoroughly reviewing the literature. The documentation of the properties of the coal waste and the coal composites was done by me. Chapter 4 has been published in *Construction and Building Materials*. Chapter 5 was presented at the *Southern African Coal Processing Society International Coal Conference* 2021 and published in the *Southern African Institute of Mining and Metallurgy* journal. Chapter 6 was presented at the *6th International Conference on Engineering for a Sustainable World* 2022 and has been published in *Environmental Science and Pollution Research*.

In **Chapter 7**, the microstructural characterisation and physicomechanical properties of the coal composites produced using other coal wastes and a commercial PCP as the binder is evaluated and discussed. Chapter 7 was presented at the *2nd International Centre for Sustainable Carbon Energy Transition Workshop* and has been published in *Clean Technologies and Environmental Policy*.

**Chapter 8** is a summary of the research's crucial findings. It includes the concluding remarks and a list of recommendations for future research.

These published chapters are included in the thesis as they appear in the journals with minimum changes. All references used in this study are captured in the list of references.

# 2 Coal as a filler in polymer composites: a review

This chapter is published in:

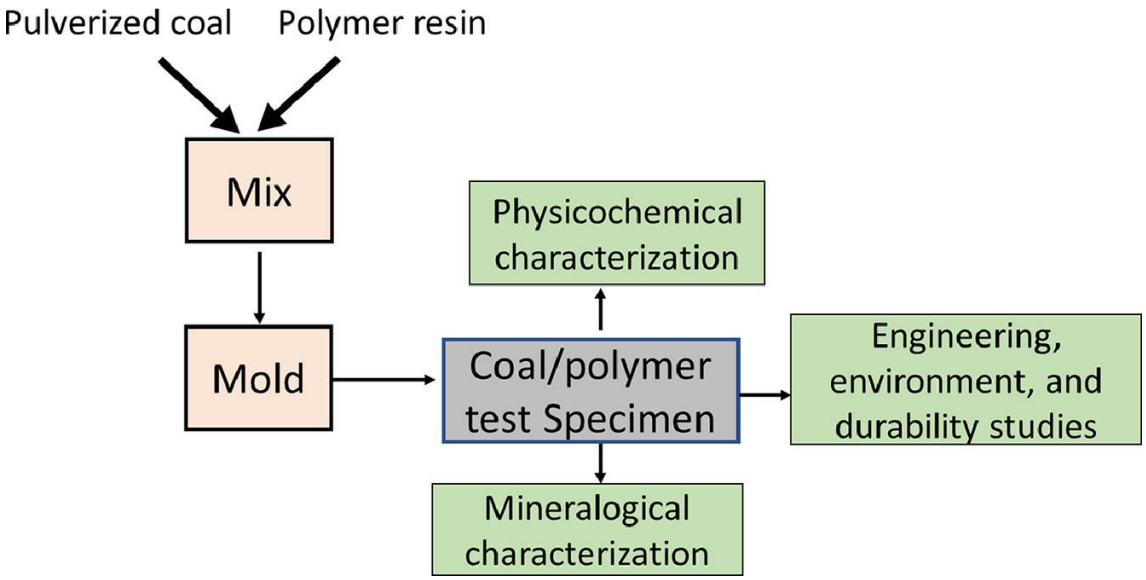
**Eterigho-Ikelegbe, O**., Yoro, K. O., & Bada, S. (2021). Coal as a Filler in Polymer Composites: A Review. *Resources, Conservation and Recycling*, *174*, 105756.

https://doi.org/10.1016/j.resconrec.2021.105756

**Preamble**

This chapter explains in detail, with reference to the literature, the use of coal as a filler material in developing polymer composites for different applications. The properties of the composites and the technical issues associated with bonding coal particles with polymer materials to produce coal/polymer composites of desirable properties was extensively reviewed.

**Graphical Abstract**



**Abstract**

There is rapidly growing interest in non-energy coal applications. In addition, the demand for non-traditional specialised materials is on the rise. Therefore, this review systematically presents cutting-edge updates on the development of polymer composites using coal as a feedstock. The review begins by exploring the polymeric nature and macromolecular structure of coal. The paper then reviews the results of published experimental studies relating to the use of coal as a filler in polymeric composites. Previous studies have demonstrated that coal can serve as a filler to extend the use and processing of polymer materials. Based on the articles reviewed, the content of coal, the structure of the coal, and the interfacial bonding between coal particles and the polymer matrix are the main factors that influence the mechanical performance of the final coal/polymer composite material. Not to mention, coupling agents could be introduced to alter the surface of the coal particles as a strategy to increase the compatibility between coal and polymer and, ultimately, the composite's performance. However, further studies involving the use of modelling and simulation capable of predicting the influence of processing parameters on the overall performance of the final composites are necessary. More positive results demonstrating the technical feasibility and sustainable utilisation of coal as a filler in polymer composites production beyond the laboratory scale could pave the way for its large-scale applications.

**Keywords:** Agglomeration, Coal, Organic filler, Preceramic polymer, Reinforcement

## 2.1 Introduction

Coal is a heterogeneous complex rock containing organic materials with inorganic mineralised inclusions dispersed within and around its internal structure (Davidson, 1982; Schweinfurth, 2003; Pudasainee et al., 2020). Coal is abundantly available and, for many decades, has been used as a source of affordable energy, thereby enhancing industrial and economic growth globally (Magazzino et al., 2020). Currently, the most significant use of coal is for the generation of steam for electricity production (IEA, 2019). Energy projections indicated that coal would continue to play an indispensable role as a source of fuel for the world's electricity generation, petrochemical, metallurgical reductant, and production of cement, aluminium, and glass (IEA, 2019). However, a recent report on world energy by the BP Statistical Review of World Energy (2020) indicates that the use of coal is declining steadily, especially in power generation. This decline could be attributed to the long-term concerns regarding greenhouse gas emissions, putting pressure on the environment. Furthermore, the preference for renewables and the stiff pricing competition of coal with natural gas for power generation also contribute to the current decline in coal usage (BP Statistical Review of World Energy, 2019, 2020; Gagarin et al., 2020). As countries switch to natural gas and renewables for electricity generation, there is a need to diversify the use of coal beyond the production of electricity and chemicals.

Research to combat the environmental impacts of coal combustion has progressed massively in recent times, with significant attention shifting towards diversifying the inherently rich carbon and mineral chemistry of coal to produce sustainable non-energy products. One of the non-energy products derived from coal to enhance its economic and environmental value is the production of composite materials. Composite or hybrid materials are increasingly gaining popularity due to their attractiveness and the significant

roles they play in modern applications such as biomedical implants, electronic components, and construction and auto-part structures (Mohanty et al., 2018; Rajak et al., 2019). In producing composites, two or more components synergistically combine to produce a new material with improved mechanical, electrical and physicochemical properties compared to a single material (Rajak et al., 2019). Research and development regarding the use of coal as a promising filler material to improve the performance of thermoplastic and thermosetting polymers can be dated back to the 1960s (Attalla, 1989). Coal in fine form is used in reinforcing a polymeric matrix (continuous phase) to produce coal/polymer composites displaying interesting chemical and physical properties that are different from the original properties of the polymer (Stabik & Chomiak, 2011; Phillips et al., 2019).

A review of the different forms of carbon materials used as modifiers or enhancers for engineering polymeric composite was reported by Stabik et al. (2012). The current review presents past studies and advances in research on the use of coal as a natural filling agent in the development of coal/polymer composites. To the best of our knowledge, this is the first review article to present research updates on coal/polymer composites, with valuable input in the focus area. The review begins with a discussion on the polymeric attribute of coal, followed by highlighting the properties of coal that make it valuable as an organic filler in composite production. Methods of preparation, the effect of coal structure, coal content, the flame-retardant effect of coal filler and other composite characteristics are also reported. The paper examines the role of coupling agents and compatibilisers, highlighting concerns that limit the broader adoption of the developed composites. In addition, it discusses future research areas for the development of high-performance coal/polymer composites.

## 2.2 Non-energy application of coal

Schobert and Song (2002), Reid (2018), and the New Carbon Age Report Fact Sheet (NCC, 2019) presented an extensive study on the non-energy applications of coal. These studies confirm significant opportunities for coal as a feedstock to create high-speciality carbon-based products. Reports from other studies have established that coal can be used to produce carbon fibres, composite materials, carbon nanotubes, high-density carbon, activated carbons, soil amendments, life-science biosensors, carbon foam, graphene, and carbon electrodes for the aluminium industry (Tsyntsarski et al., 2010; Frank et al., 2012; Zhao et al., 2014; Saha et al., 2018; Liu et al., 2019; Zabihi et al., 2019; Abdulsalam et al., 2020a; Gagarin et al., 2020). In addition, Keller et al. (2016) confirmed that coal possesses a wide array of electrical properties that could be exploited for processing thin films for electronic devices. Furthermore, researchers have demonstrated that rare earth elements can be obtained from coal (Honaker et al., 2016, 2018, 2019; Laudal et al., 2018; Zhang et al., 2018; Zhang & Honaker, 2020).

The non-energy application of coal is summarised in Figure 2-1. In some of the applications in Figure 2-1, coal is used as a precursor under carbonisation and different pre-treatment techniques with harsh chemicals, as well as high pressures and temperature stages in their production. For instance, activated carbon can be made directly by carbonising coal, while carbon molecular sieves can be produced by co-carbonising coal with solvents or tar pitches (Abdulsalam et al., 2019, 2020a; Yang et al., 2019). Other materials, like carbon fibres, are made from spinning coal-derived precursors (coal tar pitch) (Frank et al., 2012; Liu et al., 2019). Fullerenes and carbon nanotubes are made by chemically modifying coal, while synthetic graphite is made from crushed coal mixed with coal tar pitch as the binder, followed by other high-temperature treatments (Song et

al., 2005; Kieush, 2019; Silva et al., 2020; Li et al., 2021). Another recent area of coal utilisation is synthesising graphene or activated carbon as carbon materials for supercapacitors through electrolysis. Supercapacitors are advanced energy storage systems with excellent storage system properties such as high specific capacitance, high power density, excellent cycle efficiency, long cycle stability and fast start/stop technologies attributed to their fast charging-discharging kinetics (Ding et al., 2020). With coal electrolysis, clean hydrogen and carbon dioxide gas can be produced, as well as low-cost solid carbon (char), used as a precursor in the synthesis of carbon materials. The aforementioned advanced materials are produced through various clean coal technology pathways leading to increased coal efficiency with less environmental impact. In other applications, coal can be used directly or with minimal pre-treatment as a feedstock or filler to produce sustainable construction materials like ceramic and plastic composites (Hu et al., 2017; Al-Majali et al., 2019; Hill & Easter, 2019).

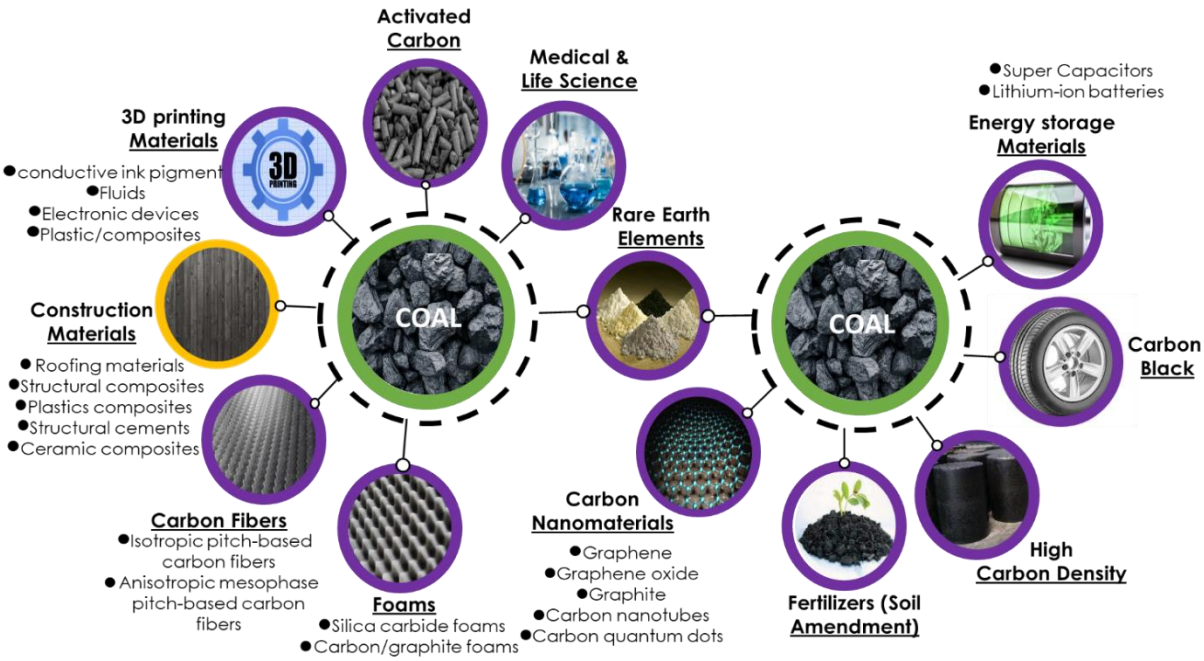



Figure 2-1 Non-energy value products from coal

Coal-filled polymeric materials are investigated for applications such as building materials, manufacturing plastic films, and producing tribological materials (Rojek et al., 2011; Stabik & Chomiak, 2013; Hu et al., 2017; Al-Majali et al., 2019). Also, the incorporation of hard coal as an antistatic filler for non-conductive polymers to develop graded composites is investigated by the Polish Silesian University and Institute of Coal Chemistry (Stabik & Chomiak, 2011, 2016a). Besides being cheap and readily available, the increasing interest in blending coal with polymer materials stems from the fact that composites with a wide range of properties (mechanical, chemical, electrical, thermal, flammability, magnetic and optical) can be developed (Rojek et al., 2011; Stabik & Chomiak, 2016a). Furthermore, the ease of processing coal/polymer composites using traditional polymer technology such as moulding techniques and extrusion, and the possibility of obtaining low-density composites makes their development attractive (Stabik & Chomiak, 2013; Rajak et al., 2019). In comparison with coal combustion or other coal conversion processes, the direct utilisation of coal as filler material has been shown to yield little or no emissions and associated criteria pollutants (Phillips et al., 2019).

## 2.3 Polymeric character and macromolecular structure of coal

The use of coal as filler in polymer composite development requires knowledge of its polymeric character, as well as its macromolecular structure. Coal is a mixture of plant remains consisting of protein, cellulose, lignin, resins, polysaccharides, lipids, and pigments (Haenel, 1992; Sekhohola et al., 2013; Bardet & Pournou, 2017). These plant tissues contain biopolymers whose chemical content upon coalification determines the chemical structure of the coal formed. As coalification progresses, the plant tissues

gradually change to a more crystalline structure such as graphite (Whitehurst, 1978; Wert & Weller, 1982; Nip et al., 1992; Schmitz, 2018).

There are different views regarding the macromolecular structure of coal. For example, Marzec (2002) reported diverging opinions in the literature suggesting that coal's macromolecular feature is similar to many polymers and behaves like a polymer. Howard (1936) presented experimental evidence to prove that bituminous coal is a polymer, while Weller and Wert (1983) reported that internal friction for many coals displays general characteristic damping peaks like those found in wood, amber, oil shale, and those reported in many synthetic polymers. Fundamental contributions by Song et al. (1993, 2005) highlighted that coal is a complex polymeric structure with weak bonds formed by the interaction of composites of aromatics and low molecular weight species. Derbyshire et al. (1989) and Sun et al. (2015) described coal as a three-dimensional crosslinked macromolecular structure comprised of molecular components trapped within its pores. According to the authors, these macromolecules are primarily composed of carbon and hydrogen with significant amounts of oxygen, nitrogen and sulphur. Other schools of thought regard coal mainly as a connected structure of smaller molecules joined together by minor interactions of π-π interactions, hydrogen bonds and charge-transfer complexes (Painter et al., 2010). Wert and Weller (1982) and Ahamed et al. (2019) reported that coal consists of aromatic ring structures that are connected by aliphatic carbon chains to form cohesive units of varying size.

More uniquely, low-rank coals such as lignite and sub-bituminous are characterised by smaller aromatic ring clusters joined by high proportions of weak crosslinks compared to bituminous and anthracite coals (Song et al., 1992). Jian et al. (2019) indicated that the molecular structure, which is the primary portion of coal, is a

crosslinked polymer with a dimensional network structure consisting of covalent and non-covalent crosslinks. The authors further stated that covalent crosslinks are generally chemical crosslinks with high-energy bonds that are difficult to open, while the non-covalent crosslinks, i.e., physical crosslinks, contain many hydrogen and polar bonds in a considerable proportion that are easy to open. The same authors also remarked that the molecular structures of lignite and sub-bituminous coals have an inclusion of many side chains and functional groups, e.g., carboxyl, hydroxyl, alkyl, carbonyl (C=O), methoxyl (R-O-$CH_3$) groups, and other oxygen-containing groups, compared to highly volatile bituminous and bituminous coals. Whereas Painter et al. (1987, 2010) stated that lignite and sub-bituminous coals are polar and they interact via hydrogen bonds involving polar groups such as carboxylic acids and phenolic hydroxyl. Bai et al. (2019) reported that the active side chain groups associated with the coal matrix can be explored to increase compatibility between the coal fines and polymer. Furthermore, Hu et al. (2017) reported that coal, especially lignite, sub-bituminous and weathered coals, could bind with polymers to produce new products due to the hydrogen bonds present within its molecules. Based on the excellent macromolecular characteristics and polymeric nature of coal, it has attracted interest as a rigid filler for polymer modification. A typical molecular structure of coal is shown in Figure 2-2.

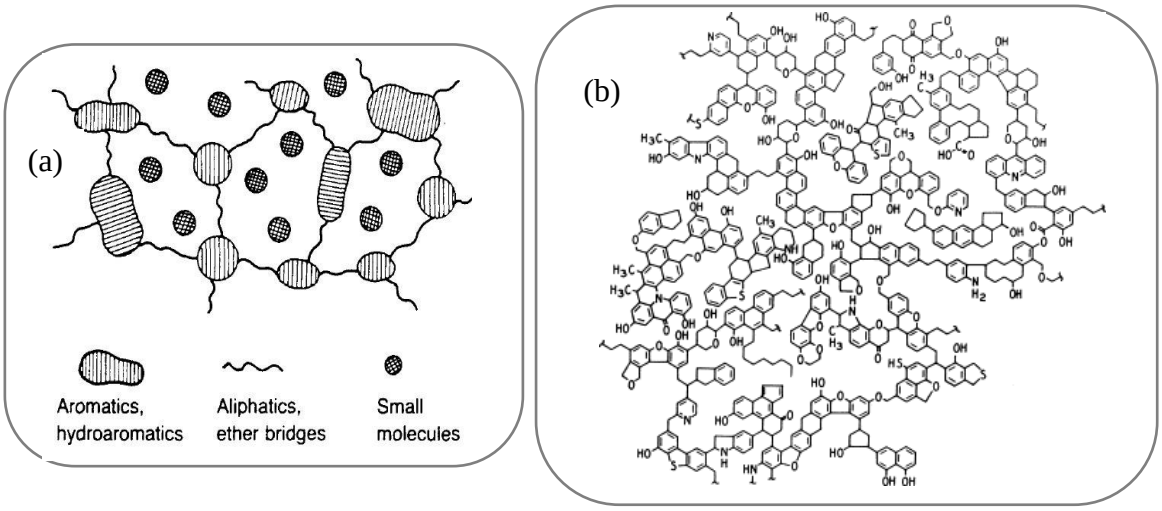



Figure 2-2 (a) Three-dimensional crosslinked two-component macromolecular model of coal (Adapted from Haenel (1992)), (b) Molecular structure model of bituminous coal (Adapted from Shinn (1984))

## 2.4 Coal as a filler in the development of polymer composites

Polymeric materials are also known as plastic materials and are composed of long polymer molecular chains formed from many repeating units (monomeric units) joined by intermolecular forces or chemical bonds (Stabik & Chomiak, 2013; Tanzi et al., 2019). The main purpose of incorporating fillers into polymers is that they can yield several desirable and improved polymers compared to unfilled polymers, thereby allowing for wider application. These effects include but are not limited to increased stiffness, antistatic properties, suppressed mechanical vibrations, reduced coefficient of thermal expansion, increased electrical conductivity, reduced combustibility, improved creep resistance, high fracture toughness and reduced cost of the finished product (Stabik et al., 2010; Ai et al., 2018; Gnatowski & Kazik, 2019). Coal/polymer composites can be produced from various coals and different polymers, as depicted in Figure 2-3. It is important to note that the choice of a polymer depends on the reactivity of the polymer with the coal particulate matter and the end-use of the composites. Compared to other

matrix materials, the polymer matrix allows the manufacturing of complex body parts of low density (Hsissou et al., 2021). According to the review article on composite materials, Rajak et al. (2019) reported that thermosetting polymers are more studied owing to their stability at higher temperatures, chemical resistance and good strength. However, if the objective is to achieve high-impact resistance, recyclable and printable composites, then thermoplastic polymers are recommended.

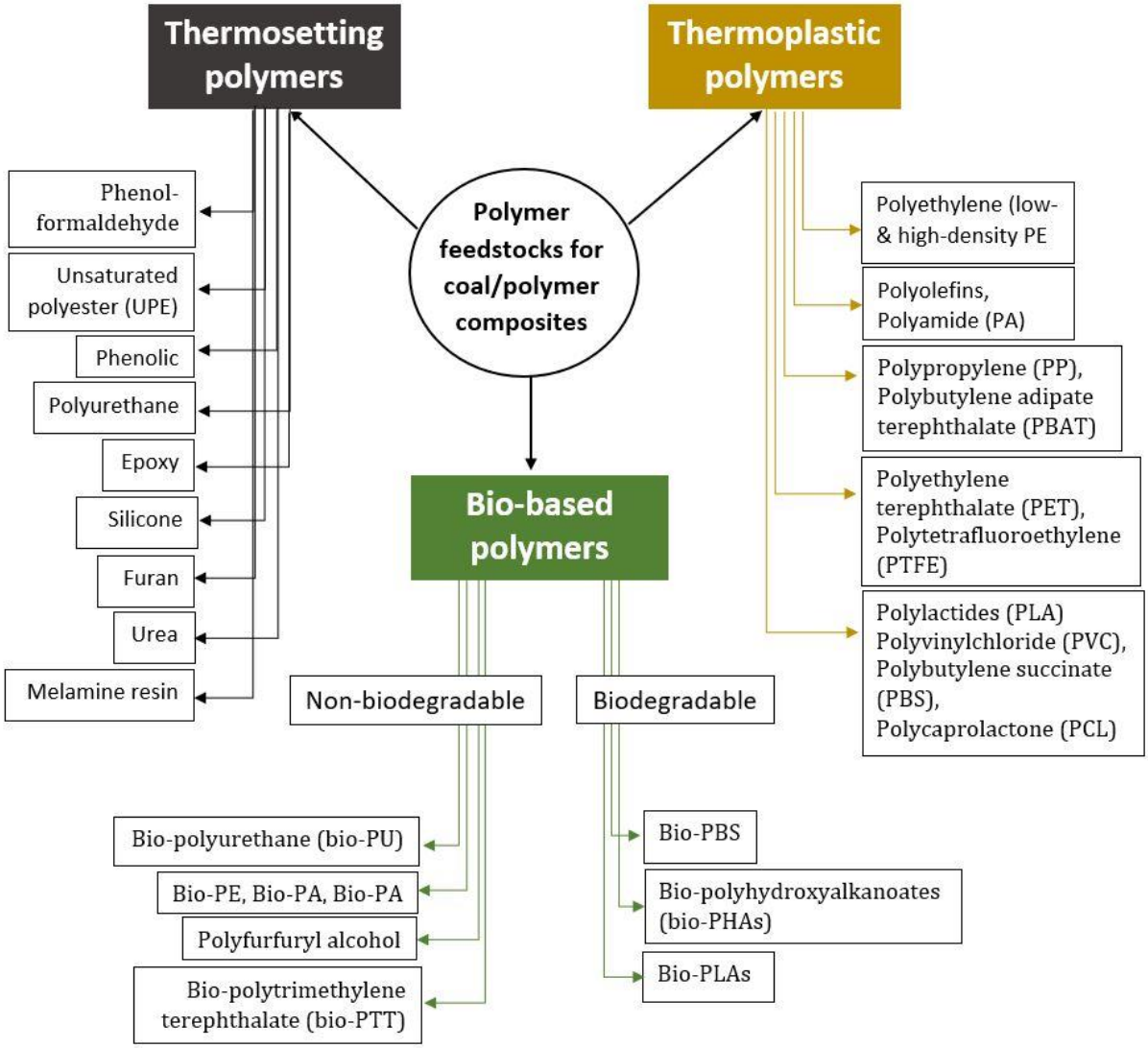



Figure 2-3 Examples of polymer feedstocks for the development of coal/polymer composites

As discussed in the introductory section, composite materials are developed by combining different matrices (base materials) and fillers (dispersed phase) (Stabik & Chomiak, 2013). In composite development, the fillers may be organic or inorganic and may take the form of powder (wood flour, chalk, FA, talc, chamotte powder and coal), fibres (natural, metal, cellulose, glass, aramid and carbon), or gas cavity (foam). Other researched fillers include lignin, graphene oxide and calcium carbonate (Stabik et al., 2010; Rojek et al., 2011; Ai et al., 2018; Tan et al., 2019). Fillers operate in different ways depending on their structure (physical and chemical), shape, degree of fineness, aspect ratio and the nature of the interaction at the matrix-filler boundary (Stabik & Chomiak, 2013). It is reported that white carbon black (silica) and carbon black are extensively used as active reinforcing fillers in developing rubber-based composites in the rubber industry (Mohanty et al., 2018; Tan et al., 2019). This is due to their large surface area, better surface activity and superior polymer-filler interaction. Amongst the existing fillers, Pusz et al. (2015) and Rojek et al. (2011) reported that apart from the disadvantage of limited heat resistance, carbon and organic fillers are attractive because of their low density, low price, availability and ease of recycling.

Compared to other carbon materials like graphite, diamond, carbon black and coke, obtained through expensive conversion processes, coal is considered an alternative attractive filler and modifier for improving the performance of polymers due to its chemical stability and low cost of production (Rojek et al., 2011; Phillips et al., 2019). Rojek et al. (2011) reported that compared to other fillers, coal is characterised by higher heat resistance, albeit this property varies with the type of coal and that the use of coal filler significantly alters or adds unique features to the polymeric material. Likewise, Pusz et al. (2015) showed that rigid fillers like coal can be used to hinder polymer chain motion

and to increase the glass transition temperature of polymers. Zhu et al. (2010) also reported that the carbonaceous and silicate supports (such as clay minerals kaolinite and montmorillonite) in coal act as intumescent barriers to the polymeric matrix during burning and are a good candidate as a benign flame retardant. Phillips et al. (2019) reported that the natural antifungal properties, resistance to insect attack and low water absorption capacity of coal could be used to develop highly durable composites that require no additives and coatings. Bai et al. (2019) also reported that good compatibility and dispersion between coal particles and polymer could contribute to developing composites with unique functionalities like antistatic properties, electrical conductivity, and antibacterial properties beyond mechanical, chemical and thermal stability. These desirable properties of coal in combination with its polymeric character, which depends on the coal type, grade and condition of formation, have instigated research in the field of coal/polymer composites. The following sections describe the production of coal/polymer composites and address the effect of coal as a filler on the final properties of various polymers.

## 2.5 Production of coal/polymer composites

Modern industrial practices are moving at a fast pace and many polymeric materials rarely meet the required property demand. Incorporating coal as a filler to fabricate polymer composites or as a modifier to enhance the properties of polymeric materials is an important strategy to extend the non-energy application and sustainability of coal. The literature shows that different process pathways can be used to develop coal/polymer composites owing to different end-uses. The general preparation route of producing coal/polymer composites is depicted in Figure 2-4.

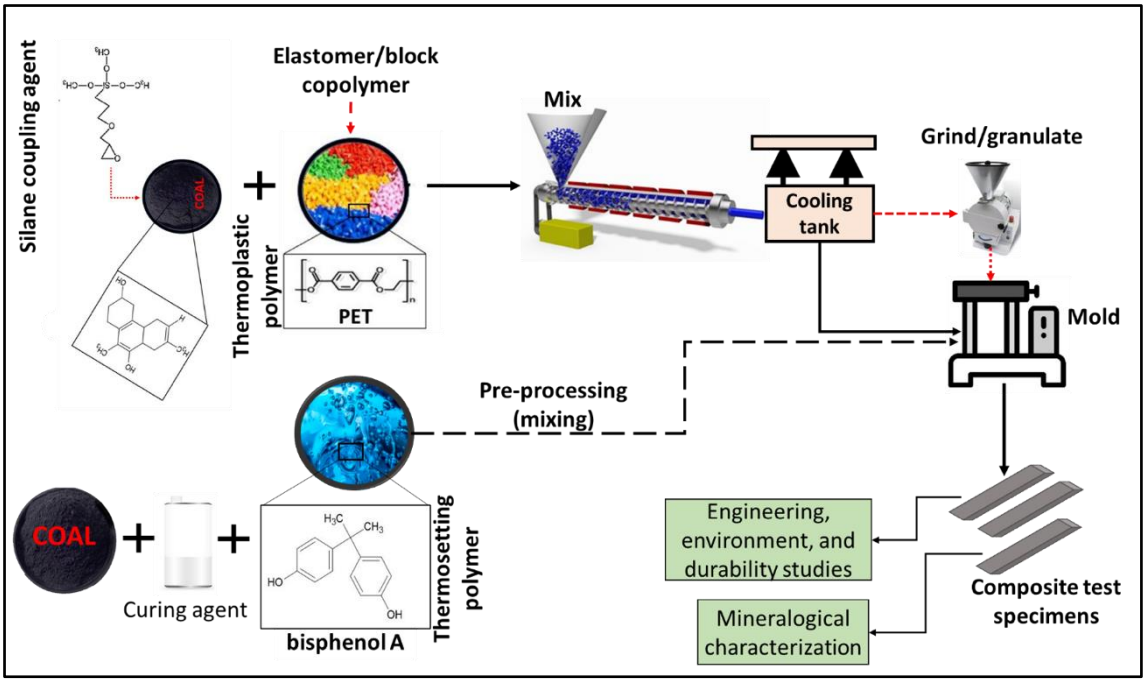



Figure 2-4 Schematic representation for the fabrication of coal/polymer composites

Typically, the production process begins by characterising the raw materials being coal and polymer to provide knowledge of their intrinsic properties and structure. The coal is dried to remove any adsorbed moisture on the surface and then pulverised to a suitable particle size distribution. Depending on the structure of the coal particles, the coal surface may be modified using a coupling agent to enhance the dispersion of the coal particles in the polymer (Bai et al., 2019). An example of a surface modification protocol is reported in an investigation conducted by Bai et al. (2019). Based on the studies conducted so far, coupling agents have only been reported for use with thermoplastic polymers. Thermoplastic polymers have also been blended with compatibilisers, such as copolymers or elastomers, to allow for sufficient mixing and to enhance the toughness and impact strength of the polymer (Bai et al., 2019). On the other hand, thermosetting polymers like bisphenol A are co-reacted with a curing agent or hardener (Stabik et al., 2010; Pusz et al., 2015; Stabik & Chomiak, 2016b; Das et al., 2018) via a crosslinking reaction known as curing.

For thermosetting polymers, coal and polymer are mixed in a predetermined ratio at room temperature or any other temperature as desired and then cured in air or an oven (thermoforming). The mixture could also be transferred straight to a compression moulding machine for shaping before it is cured. In the case of thermoplastic polymers, the main reaction between the coal and the polymer occurs during the melt mixing or blending leading to adhesion at the coal particles and polymer matrix boundary. The melt mixing process can be carried out using a batch mixer (Pardo et al., 2010; Al-Majali et al., 2019), a compounder (Phillips et al., 2019), or an extruder (Bai et al., 2019; Kijo-Kleczkowska et al., 2020). The exiting mixture from the blending process is cooled to eliminate any residual or internal stress in the material. The injection or compression moulding machine is then used to develop the blend into test specimens (Guang-Heng et al., 2006; Wang & Zhou, 2011; Al-Majali et al., 2019; Kijo-Kleczkowska et al., 2020).

Remarkably, the mixing and moulding equipment opens a window for the optimisation of coal/polymer composites to attain different optimal performances and wider applications. Al-Majali et al. (2019) reported the preparation of coal/polymer composites using a unique route. In this approach, the composite obtained from the meltmixing of coal and polymer was pulverised before being injected into the mould to produce the test specimens. In another investigation by Bai et al. (2019), the coal and polymer mix exiting the extruder was heated to 120 °C and then cooled to produce the composites. Phillips et al. (2019) pelletised the extruded composite, heated it to 180 °C, then applied compression moulding under heat to produce test specimens before cooling it to room temperature. An alternative approach was used by Rojek et al. (2011) whereby the extruded composites were granulated, dried and charged into the injection moulding

machine. Despite the different process routes employed, the technique should have the ability to produce a composite with a continuous phase morphology.

## 2.6 Research and development of coal as an organic filler in polymer composites

### *2.6.1 Polymeric gradient materials consisting of coal*

A polymeric gradient material represents a unique class of functionally graded materials exhibiting a gradation of properties or parameters, such as density, microstructure, density, and chemical composition in their structure (Krawczak, 2010; Stabik et al., 2010; Stabik and Chomiak, 2011; Stabik & Chomiak, 2016a, 2016b). Stabik and Chomiak (2013) reported that the main advantage of polymeric gradient materials is the ability to combine regions of materials with non-identical properties and without definite boundaries. Polymeric gradient materials are of interest as insulators in electrical and electronics engineering, manufacturing equipment parts, and in the chemical and coal mining industry (Stabik et al., 2010; Stabik & Chomiak, 2011).

Polymeric materials, for example, epoxy resins have high electrical resistance and a strong tendency to accumulate static charges on their surface. Static electricity poses a danger in the chemical and coal industries due to the gathering of excessive dust on the surface of equipment fabricated with polymeric materials, leading to sparks and eventually fire and explosion. Adding electro-conductive additives or antistatic agents like pulverised hard coal to the polymer in a graded manner to gradually increase the resistance in the composite volume is one way to decrease the excessive build-up of electrostatic charges on the surface of the polymer (Stabik et al., 2010; Stabik & Chomiak, 2016a, 2016b). The fundamental challenge in designing these materials is determining the relationship between the variation of properties and the variation of parameters.

Another challenge is the design of a macroscopic continuous gradation with narrow interlayers and interfaces between regions of various compositions and structures (Stabik & Chomiak, 2011; Stabik & Chomiak, 2016a).

Polymeric gradient materials based on coal fillers are produced by the sedimentation process via the casting method. The casting technology may rely on gravity without applying pressure (Stabik et al., 2010; Stabik & Chomiak, 2013) or may be achieved under the effect of centrifugal force (Stabik & Chomiak, 2011, 2016a, 2016b). The casting method allows a one-dimensional gradient of the component material in the liquid polymer matrix following matrix solidification. Figure 2-5 presents a schematic of the preparation of a coal/polymer-classified composite based on the centrifugal casting method. According to this figure, the coal filler is thoroughly mixed with the polymer resin. For thermosetting polymers, hardeners or curing agents are added. The mixture is deaerated in a vacuum drier and then cast into a mould. The mould containing the mixture is then mounted on a centrifugal casting device and rotated around one or two perpendicular axes of the mould. As a result of the centrifugal force applied, one of the components of the mixture gradually settles towards the wall of the mould. The rotation is stopped when the solidification of the composite is attained. A detailed centrifugal casting process for the development of graded coal/polymer composites can be found in the report published by Stabik and Chomiak (2011).

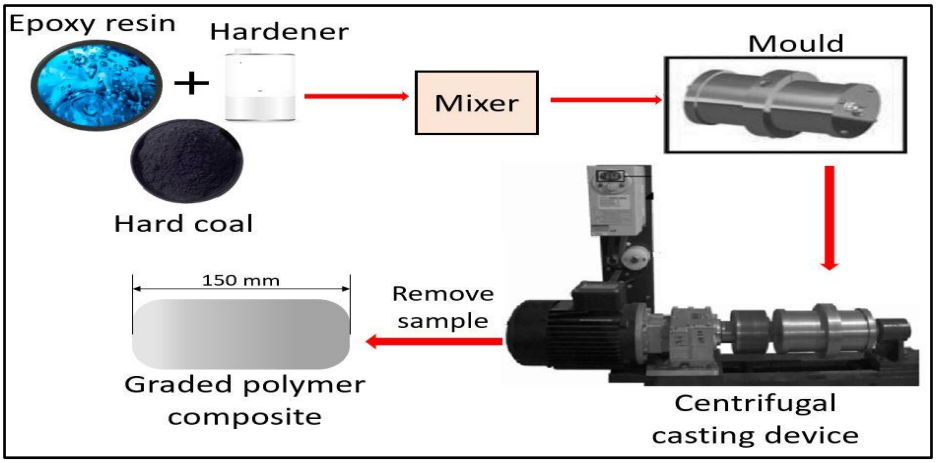



Figure 2-5 Schematic of coal/polymer gradient composite preparation based on the centrifugal casting method (Adapted from Stabik and Chomiak (2011))

The effect of the coal filler and the centrifugal rotational casting velocity on the surface resistivity of each layer of the composites containing different contents of coal was analysed by Stabik and Chomiak (2011). Two types of coal, anthracite (ash = 3.37%) and hard coal (ash = 16.70%) in the range of 3 to 12 weight percentage volume (wt.% vol) and rotational velocities (535.3 to 617.7 revolutions per minute) were investigated. Epidain 6 epoxy resin was used as the polymer and cured at room temperature with a hardener. The results showed that the content of the coal filler changed the surface resistivity of the outer layers to levels that prevented the accumulation of charges. It should be noted that four layers in each graded composite were analysed. Based on the filler contents and rotational velocities, anthracite coal produced surface resistivities in the range of $6.83 \times 10^{8}$ Ω to $1.26 \times 10^{11}$ Ω. On the other hand, the surface resistivities measured considering all four layers were in the range of $5.29 \times 10^{9}$ Ω to $> 1.25 \times 10^{13}$ Ω for hard coal. Based on the EN 13463-1 standard requirement for nonelectrical equipment or materials, the surface resistivity limit to accumulate electrostatic charges and hence from igniting should be below $1.00 \times 10^{8}$ to $1.00 \times 10^{11}$ Ω (Stabik & Chomiak, 2011, 2016b). Compared to hard coal, graded composites filled with anthracite coal recorded

lower surface resistivity values. Statistically, by using a central composite design, the lowest resistivity values were recorded at an optimum coal filler content of about 11 wt.% volume.

Stabik and Chomiak (2016b) investigated the correlation between the surface resistivity of cylindrical coal/polymer-graded composites produced by the centrifugal casting method and the gradation of coal filler content. Epoxy resins were used in the study together with curing agents. Three different types of hard coals were investigated – orthocoking, bigger than average-size anthracite and smaller than average-size anthracite coals. In all cases, adding hard coal particles to the polymer resin decreased the surface resistivity of the outer surface. The study also confirmed that increasing the content of coal filler, especially that of bigger than average-sized anthracite, remarkably reduced the outer surface resistivity of the polymer, the lowest being $7.00 \times 10^{10}$ Ω compared to cured, unfilled epoxy polymer with a resistivity of $10^{16}$ Ω. Compared to orthocoking coal, anthracite coal produced lower resistivity and it was attributed to a higher degree of carbonisation of the coal. Based on the resistivity values, the study confirmed that the addition of coal particles reduced the ability of the epoxy polymer to accumulate electrostatic charges.

A study was also conducted to investigate the influence of coal particles on the wear resistance of polymeric-graded composites developed using the gravitational casting technique (Stabik & Chomiak, 2013). Pulverised anthracite coal (ash content of 3.37% and carbon content of 90.1%) and hard coal (ash content of 16.78% and carbon content of 71.5%) were used as antistatic agents without sizing or surface modification. Based on the wear and abrasion resistance analysis, introducing hard or anthracite coal particles (15 to 40 wt.% vol.) into bisphenol A epoxy resin changed these properties slightly. The

addition of 26 wt.% vol. of both types of coals resulted in minimum loss of wear and abrasion resistance. The authors demonstrated that for less than 26 wt.% vol. addition, the wear resistance of composites developed using hard coal was better than anthracite coal, while above 26 wt.% vol., the reverse was the case. In summary, incorporating coal fillers into epoxy resin to form polymer-graded composites decreased the abrasion and wear resistance slightly compared to cured polymer resin without coal filler particles. It was proposed that future research should investigate the influence of coupling agents on the wear and abrasion properties of coal/polymer-graded composites.

Stabik et al. (2010) developed composites exhibiting different electrical properties across the cross-section of epoxy resin and evaluated their electrical resistivity in sequential layers of functionally polymeric-graded composites. The composites produced by gravitational casting contained layers of different amounts of hard coal throughout the thickness of the specimens. The epoxy resin used in preparing and casting these composites was cured using a Z-1 hardener at room temperature. The authors demonstrated that as the depth of the content of hard coal filler increased up to the plain epoxy resin layer, the surface resistivity increased gradually along the depth of the composite's layers. According to the authors, composites with this attribute may be attractive in applications where static electricity must be avoided on one surface (reduced tendency to electrostatic charge accumulation) while simultaneously retaining high resistivity on the other surface. This feature will be significant to manufacturing mining machines, electronic elements, explosives parts, etc. Further investigation on the effect of the coal filler composition in specified layers of gradient composite was proposed for future research.

It is reported that thermoplastic and thermosetting polymers may be used as matrix material to develop polymer-graded composites (Stabik et al., 2010). However, the available information in the public domain only provided information concerning coal fillers mainly blended with epoxy resins. It is worth highlighting that the research in this area was mainly carried out in Poland, with coal that is different from those found in the southern hemisphere. Exploring the influence of coal inorganic minerals (clay types and quartz content), processing conditions, coal size, etc., in future research may pave the way for obtaining different coal/polymer-graded composites.

### *2.6.2 Effect of coal structure on the interfacial interaction between coal fillers and polymers*

The structure and composition of coals vary depending on the origin and formation process (Falcon, 1987; Ahmed & Jones, 1990; Okolo et al., 2015; Wu et al., 2017). The effects of coal structure on the properties of the composites formed from coal of different ranks as a filler were studied by Wang and Zhou (2011). The authors added 10 grams (g) of coal to 65 g of soy protein isolate plastics and 25 g of glycerol as a plasticiser. The mixture was homogenised for 24 hours at 4 °C in a closed container, and the homogenised mixture was compressed at a temperature of 150 °C and a pressure of 20 MPa (megapascal) for five minutes. The mould with the blended sheet composites was cooled to approximately 50 °C before removal. Surface functional group and Fourier Transform Infrared (FTIR) analyses of the coal samples indicated that as the coal rank increased from lignite to bituminous, oxygen-containing groups (hydroxyl, carbonyl and carboxyl), aliphatic chains and the oxygen/carbon ratio decreased while aromatic hydrogen increased. Due to the reactive structure of the carboxyl and hydroxy groups found in lignite and sub-bituminous coal particles, the coal macromolecules formed a

strong interaction with soy protein chains, resulting in strong but brittle composites. The authors demonstrated that lignite and sub-bituminous coals rich in groups containing reactive and aliphatic chains reacted with the active polar amino side chains in soy protein through hydrogen bonding, charge-charge and dipole-dipole intermolecular interactions. Stronger amide linkages, hydrogen bonds and interfacial interactions between the macromolecules of lignite and sub-bituminous coal and soy protein chains were formed compared to the bituminous coals. As a result, the water resistance, tensile strength, glass transition temperature and bending strength of coal-soy protein isolate composites decreased as the coal rank increased.

Pusz et al. (2015) investigated the effect of raw anthracite and thermally treated anthracite on the cure behaviour of epoxy composites. Commercial-grade epoxy resin (diglycidyl ether of bisphenol A) and a crosslinking agent (aliphatic amine-tetramethylenediamine) were used. The epoxy and coal mixture was stirred at 80 °C for 24 hours, sonicated and degassed before adding the curing agent. The mixture was poured into a steel mould and placed in an oven for two hours at 80 °C and 120 °C for curing. The authors observed that functional groups containing oxygen, such as hydroxyl or carboxyl groups, on the surface of pristine anthracite coal particles accelerated curing reactions and enhanced the physical and chemical interactions between the raw anthracite fillers and polymer. In contrast, treating the raw anthracite coal thermally at 2000 °C ordered its structure and led to the loss of oxygen, hydrogen, and nitrogen. As a result, the thermally treated anthracite had no significant effect on the curing reactions, the same for the pristine resin. To further confirm the contribution of functional groups in coal, the glass transition temperature, $T_g$, of 5 wt.% of anthracite and thermally treated anthracite increased to 139 °C and 142 °C, respectively from 137 °C of neat epoxy resin. The

researchers noted that the $T_g$ increased due to good interaction or bonding between coal and the epoxy polymer. Moreover, a reduction in damping amplitude indicated that the polymer chains were significantly hindered, and this effect was more evident for raw anthracite coal with functional groups on their surface.

### *2.6.3 Effect of coal content on the mechanical strength of the composites*

The goal of polymer modification is to improve the properties of the new polymer formed. It is, therefore, expected that the content or amount of coal filler would profoundly affect the performance of the coal/polymer composite formed. To obtain a good balance of properties, Al-Majali et al. (2019) melt-mixed 15 to 60 wt.% fine coal in the as-received form with high-density polyethylene (HDPE) to produce coal plastic composites (CPCs) via injection moulding. The CPCs were fabricated as a potential replacement for commercial wood-plastic composites used for building materials. The investigation's results demonstrated the highest flexural strength of 42.9 MPa obtained from 60% fine coal of particle size less than 125 μm (micrometre) coal. The flexural strength of the composites surpassed that of pure HDPE (33.0 MPa) and commercial wood-plastic composites (30.4 to 36.7 MPa). The strong HDPE material used in the study, the optimised process parameters and the use of 40 to 60% coal content improved the dispersion of coal particles and increased the flexural strength of the CPCs produced. Regarding the flexural modulus, i.e., the ability of the composites to resist bending when subjected to a load, commercial wood-plastic composites (2.0 to 3.0 GPa (gigapascal)) were comparable to the fabricated CPCs (0.9 to 1.9 GPa). Nonetheless, the values of flexural modulus obtained in the study exceeded the International Building Code for deflection, thus certifying the composites for application as a building material.

A recent investigation on the effect of the amount of pulverised bituminous coal (Pittsburgh No. 8) on HDPE as the matrix material was conducted by Phillips et al. (2019). The coal sample was dried, blended and compounded using a twin-screw compounder. The blend was extruded as a pelletised composite, heated to 180 °C then moulded under heat to form CPCs. By varying the coal content from 0 to 60 wt.%, 30 wt.% coal content produced the best flexural strength of coal/polymer composites. While 60 wt.% coal content displayed the least flexural strength, it was still higher than the flexural strength of pure HDPE (Figure 2-6). On the other hand, the composites' tensile strength decreased as the content of coal in the polymer matrix increased from 0 to 60 wt.% owing to the poor interfacial bonding between the coal fillers and the polymer matrix. With a proper design, the mixing and fabrication processes could be optimised to improve the dispersion of coal particles in the polymer matrix.

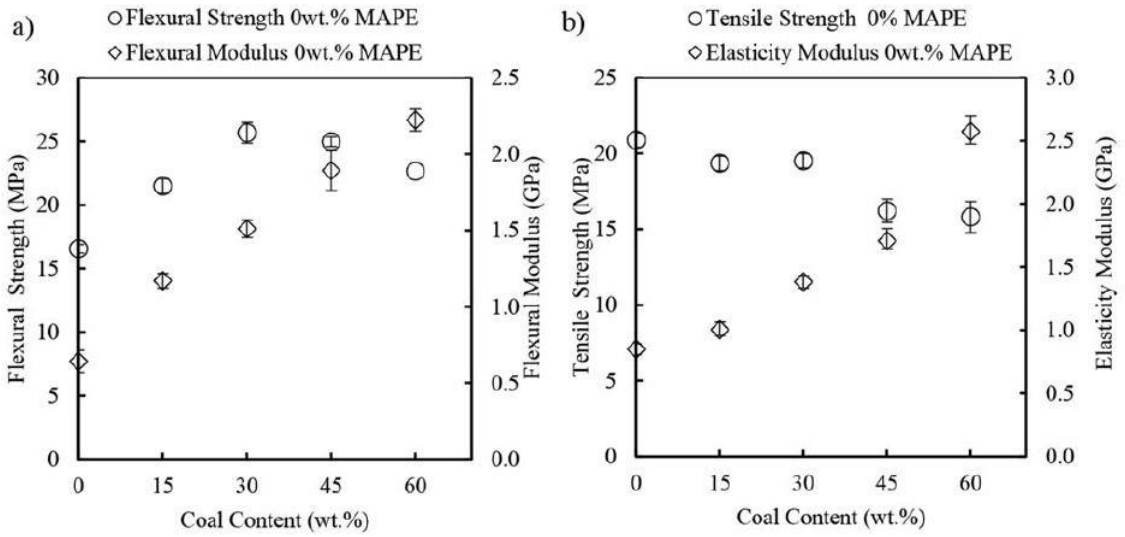



Figure 2-6 (a) Flexure and (b) tensile properties of coal plastic composites composed of 0 to 60 weight percent (wt.%) of Pittsburgh No. 8 coal (Phillips et al., 2019)

In an investigation conducted by Hu et al. (2017) weathered coal was treated with sodium hydroxide to extract humic acid as sodium humate to produce a polymeric composite. The mixture was heated in a water bath at 60 °C while stirring to produce

polymeric composite materials for possible application as plastic bags and films. The undissolved coal particles were used as a filler and blended with sodium humate, polyvinyl alcohol, carboxymethyl starch as the flexible polymer matrix, and deionised water. The authors selected the matrix materials based on the expected large amount of hydrogen bonding in the polyvinyl alcohol/carboxymethyl starch mixture to bond with coal. The reacting components and the reaction process were varied, and the resulting mixture was poured on a horizontal glass plate to produce plastic films. From Figure 2-7(a), the relationship between tensile strength and the percentage of coal was not linear, indicating an optimal amount of coal required to obtain maximum tensile and breaking elongation properties. The figure also showed that blending 30 % coal yielded the best breaking elongation property, i.e., the point at which the hydrogen bond strength gradually reached saturation. It was established that the undissolved coal particles served as filler and reinforcement to increase the toughness. Also, the sodium humate extracted from the coal reacted and bonded with the polyvinyl alcohol/carboxymethyl starch mixture in water via hydrogen bonds to strengthen the plastic film. Figure 2-7(b) indicates that the fine particle size of coal was instrumental in increasing the tensile strength and breaking elongation of the plastic film.

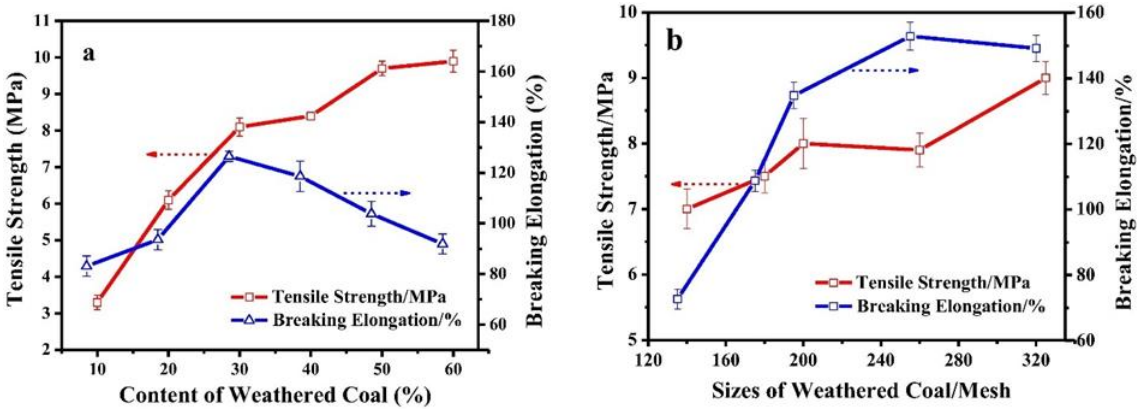



Figure 2-7 Mechanical properties as a function of (a) the percentage mass of coal and (b) the particle size (Hu et al., 2017, reproduced with permission from Elsevier)

### *2.6.4 Thermal stability and flame retardancy effect of coal fillers*

Apart from the strength enhanced from blending coal fillers with polymers, coal/polymer composites have also been reported to show flame retardancy and thermal stability properties. The thermal properties of coal/polymer composites are evaluated using a variety of analyses. The thermal stability effect of adding anthracite coal in different proportions to virgin polymer was investigated by Pusz et al. (2015) using thermogravimetric analysis. The initial decomposition temperature, the temperature of the maximum rate of weight loss and the percentage weight loss at 800 °C were used to determine the composites' stability. From the results obtained, both neat polymer matrix and composite samples were stable up to about 320 °C. However, the weight loss at 800 °C for pure epoxy recorded 93%, which was higher than composites developed from different blends of anthracite coal and epoxy (67 to 90%). The authors confirmed that adding anthracite coal to pure epoxy polymer improved the polymer's thermal stability, which was attributed to the fine dispersion of coal particles in the polymer matrix.

The influence of dimensional sensitivity to changes in temperature of coal/polymer composites in terms of coefficient of thermal expansion was investigated by Al-Majali et al. (2019). The authors demonstrated that with an increasing coal content

in the mixture, the composites' coefficient of thermal expansion also increased ($0.5 \times 10^{-4}$/°C to $1.4 \times 10^{-4}$/°C) and was lower compared to the neat HDPE polymer (1.8 to $2.0 \times 10^{-4}$/°C). Low thermal expansion recorded for the composites has been attributed to the presence of covalent bonding in coal. Al-Majali et al. (2019) also investigated the flame retardancy of coal/polymer composites in terms of oxidative induction time (measured in minutes), surface burning rate (measured in millimetres/minute), and flash/self-ignition temperature. In terms of oxidative induction time that defines the thermal-oxidative degradation and the service life of the composites, the study showed that increasing the coal content from 40 to 60% increased the oxidative induction time from 23.9 to 43.1 minutes corresponding to an 80% increase. The incorporation of more coal resulted in delaying the onset of composite decomposition, and consequently, increased the composites' service life. It should be noted that while both polymer and coal are combustible materials, thermal degradation is hindered by adding primary (aromaticity) and/or secondary (e.g., sulphur-based) antioxidants to the polymer matrix (Al-Majali et al., 2019). Therefore, the combined synergy of aromaticity and sulphur in coal acted as the antioxidant. This presents the unique advantage of using coal as a filler in preventing the decomposition of the composites over wood with only aromaticity. 60% weight coal in the polymer blend also recorded higher flash/self-ignition temperature values (420 °C/460 °C) compared to commercial wood-plastic composites (370 to 387 °C/394 to 395 °C). This meant that the minimum temperature at which the flammable gases in the composites are initiated or ignited occurs at a higher temperature for coal/polymer composites compared to their commercial counterparts. In summary, the coal/polymer composites developed by Al-Majali et al. (2019) showed lower

flammability potential without applying fire retardants or antioxidants over commercial wood-plastic composites.

The differential thermal gravimetric analysis was also utilised in determining the thermal stability of the plastic film produced from the addition of sodium humate extracted from coal and 30% coal compared to the mixture containing only carboxymethyl starch/polyvinyl alcohol by Hu et al. (2017). The delay in the degradation of the composite was attributed to the strong and greater number of hydrogen bonding present in the coal particles, resulting in the high energy required to break the hydrogen bonds. In another investigation conducted by Zhu et al. (2010), the addition of ammonium polyphosphate, an intumescent coating for polyethylene terephthalate polymers, was found to reduce the degradation temperature (380 °C) and accelerate the degradation rate of polyethylene terephthalate. The authors thought that the well-dispersed silicate supports and carbonaceous ingredients in the coal would act as intumescent barriers for polymers during burning. With further research on the effect of the content of pulverised coal and ammonium polyphosphate blended with polyethylene terephthalate, 30% coal and ammonium polyphosphate synergistically acted as flame retardants for polyethylene terephthalate. However, the composites' strength was drastically compromised because of the degradation of polyethylene terephthalate and the poor interfacial adhesion between polyethylene terephthalate and ammonium polyphosphate compared to neat polyethylene terephthalate. The strength of the composites could be enhanced by optimising the amount of each component in the mixture, adding coupling agents (e.g., silane maleic anhydride) to the blend and/or thermally treating the coal.

Bai et al. (2019) demonstrated that increasing the amount of pulverised coal in a polypropylene/ethylene-propylene-diene monomer mixture delayed the initial

decomposition temperature of pure polypropylene. Thermal analysis was conducted by heating the composites from 25 to 600 °C at a heating rate of 10 °C per minute (°C/min) under argon. From the results obtained, it was clear that compatibilising the polymer with an elastomer material increases the initial decomposition temperature from 399.29 °C for the neat polymer to 419.23 °C for the polymer blend. As the coal content in the mixture increased, the decomposition temperature increased up to 431.02 °C, while the temperature at which the highest weight loss occurred increased from 461.27 °C to 464.06 °C compared to the neat polymer (447.79 °C). The delay in the decomposition temperature could be attributed to the composite's unique microstructure and the carbonisation and steric hindrance of the coal's aromatic structure, which reduced the degree of deformation of the polymer chain in the composite. The thermal property of the coal/polymer composite, i.e., the glass transition temperature, has also been reported to be affected by the coal's structure (Wang & Zhou, 2011). In this investigation, the authors demonstrated that low-rank coals increase the glass transition temperature of the polymer as a result of the strong interfacial interaction between low-rank coals and the polymer in the composite.

Clay minerals in coal might play a positive role in enhancing the thermal stability of coal/polymer composites; therefore, their effect deserves further scrutiny. It is also important to note that one factor that could lead to poor thermal stability or heat resistance of the coal/polymer composites is poor interaction or compatibility between coal and the polymer. This challenge can be overcome by adding compatibilisers or coupling agents, as discussed in Section 2.7.

### *2.6.5 Additional features of coal/polymer composites*

Composites developed from coal particles and polymers are anticipated for use as construction materials to replace wood polymer composites. Apart from checking the mechanical integrity of the developed composites, some researchers have conducted additional analyses to investigate the durability of the composites using the absorption test, leaching test, life cycle analysis, etc., as discussed in this section.

In a study conducted by Al-Majali et al. (2019), coal composites produced were subjected to a water absorption test for two hours and 24 hours in deionised water to analyse the durability of the composites. The result shows that the weight increase noted in the composite immersed in water after 24 hours exceeded that of the two-hour tests. In both cases, the weight gain was between 0.047 and 22%, equivalent to less than a 1% increase in weight. The authors compared this result with wood polymer composites; the coal composite had less water uptake than the wood polymer composites. Unlike the hydrophilic nature of the wood, the authors attributed the impressive water absorption results of coal/polymer composites to the hydrophobic nature of coal, which depends on the coal constituent.

Concerning the composites developed using coal as a filler, it is well known that coal contains different levels of major and minor toxic elements. The exposure of these composites to extreme weather conditions may lead to leaching of these elements into the environment. The mobility of toxic contaminants into the environment caused by the leaching of coal or the composites produced could lead to legacy environmental and health issues, which need to be adequately studied. Based on this knowledge, Al-Majali et al. (2019) investigated the leaching characteristic of ground coal/polymer composites using the Toxicity Characteristic Leaching Procedure, United States Environmental

Protection Agency (EPA) Method 1311. The result showed that the heavy metal concentrations from both coal and coal/polymer composites were below the United States EPA limits, suggesting that the leached metals will not be a threat to the environment. More studies on the leaching characteristics of coal/polymer composites need to be conducted to establish the safe utilisation of such composites.

### *2.6.6 Life cycle and techno-economic assessment of coal/polymer composites*

When implementing a new process or technology, it is important to estimate and compare the economic viability and environmental friendliness of the process. To perform these assessments, a techno-economic analysis and a life cycle assessment are performed. At the time of publication, no full case studies have examined the techno-economic analysis of coal/polymer composites. This is expected because the research in coal utilisation for coal/polymer composites is still growing. Although Al-Majali et al. (2019) modelled the manufacturing process (mass and energy balance) of coal/composite, coupled with the low drying and cooling requirement compared to wood fillers, the authors anticipated lower operational costs at high filler content and suggested that the use of coal filler was techno-economically feasible and had an advantage over wood fillers. Notwithstanding, it is important to conduct a full techno-economic analysis as it opens a window for developing and conducting further studies in coal/polymer composites processing. With the techno-economic analysis, informed decisions can be provided to the private and public sectors interested in this area of research. A complete techno-economic analysis provides a technical assessment (mass and energy balances), and a financial assessment covering operating expenditure, capital expenditure and net present value/net present costs. In addition, sensitivity analysis could be incorporated into the techno-economic analysis model as it is critical to check to what extent variation in

process parameters would impact the profitability of developing coal/polymer composites.

Life cycle assessment is a tool used to assess the benefits of one product over another by calculating the product's energy inputs, material inputs, associated emissions and waste outputs. Life cycle assessment of polymer composites can be terminated halfway to the production stage (cradle-to-gate) or it can be carried out over the entire life cycle, from the acquisition of raw material to the ultimate disposal of the composites. The guideline for a life cycle assessment study is provided by the International Standard Organization, ISO 14044. Proprietary software that houses data from previous life cycle assessment studies in combination with surrogate data from other studies and public databases can be consulted to perform a detailed life cycle assessment. In the research conducted by Al-Majali et al. (2019), a cradle-to-gate life cycle assessment of the greenhouse gas emission and energy associated with the process of developing coal/polymer composites was examined. The analysis was modelled on the premise that one tonne of composite material is composed of 40 wt.% HDPE and 60 wt.% wood or coal filler. The life cycle assessment results indicated that the energy associated with developing coal/polymer composites was higher (2516.2 megajoules per tonne for coal/polymer composite) compared to 952.7 megajoules per tonne for wood polymer composites. Likewise, from the modelling of specific greenhouse gas emissions, the total emissions associated with developing coal/polymer composites were also higher (265.9 kilograms of carbon dioxide per tonne of composite) compared to wood polymer composites (148.6 kilograms of carbon dioxide per tonne composite). The difference in energy and total emissions suggests that wood polymer composites performed better in terms of energy and emissions. However, the life cycle assessment in the study omits

other phases and parameters of the composites' life cycle and only one study on the subject cloud judgement. Hence, additional and full life cycle assessment research considering all parameters and phases is required to cement these conclusions. Moreover, it would be interesting to extend the comparison of life cycle assessment studies of coal/polymer composites to other non-energy applications of coal.

## 2.7 Technical challenges in developing coal/polymer composites

Weak adhesion or interfacial interaction between a reinforcement and matrix material is a significant challenge in composites production that greatly influences the composites' behaviour (Qi et al., 2006; Rojek et al., 2011; Mohanty et al., 2018). For instance, poor dispersion and reduced compatibility between hydrophobic polymers and hydrophilic fibres have led to weak adhesion in fibre composite development (Keener et al., 2004; Mohanty et al., 2018). Research has shown that lower-rank coals (lignite and sub-bituminous) are weakly hydrophobic, with hydrophobicity increasing with rank. However, for medium-volatile and low-volatile bituminous coals, the hydrophobicity reaches a maximum while it decreases for anthracite (Ding & Laskowski, 2009; Kumar et al., 2014). The oxygen/carbon ratio can also be used as an indicator of coal's hydrophilicity. As the rank increases, the ratio declines, and the hydrophilic groups on the coal surface tend to fall off (Zhou et al., 2015). According to Ding and Laskowski (2009), hydrophobic particles dispersed in water (polar medium) are likely to agglomerate to create a network of interacting particles. It is, therefore, conceivable that hydrophilic coal, for example, weathered or oxidised coal dispersed in a hydrophobic polymer would result in the aggregation and clustering of coal particles. The ripple effect of this is poor interfacial bonding between the coal particles and the polymer matrix, and eventually poorly dispersed coal composite structures of degraded mechanical strength. Phillips et

al. (2019) reported that it is desirable for composites to have good interfacial bonding and for filler and polymers to have high bond strength (Rojek et al., 2011) to obtain products with good properties. Otherwise, the filler particles will disconnect from the matrix base when the composite is under tensile stress. Weak interfacial bonding creates inherent flaws that could act as stress concentrators. These stress concentrators limit the stress transfer from the matrix to the load-bearing filler, initiate cracks, and can markedly compromise the overall mechanical performance of coal/polymer composites (Guang-Heng et al., 2006; Mohanty et al., 2018; Bai et al., 2019; Phillips et al., 2019).

### *2.7.1 Role of coupling agents and compatibilisers*

To overcome the persistent challenge of weak adhesion between the coal particles and polymer matrix, several studies have recommended modifying the surface of coal particles using surfactants or coupling agents to enhance the properties of the coal/polymer composite (Pardo et al., 2010; Rojek et al., 2011; Stabik & Chomiak, 2013). Coupling agents play a role in preventing coal filler particles from agglomerating and reducing interfacial tension while promoting interfacial interaction between coal filler and the polymer material. Their introduction has been reported to enhance the strength of the composite and its deformation capacity (Keener et al., 2004; Pardo et al., 2010; Phillips et al., 2019). Regarding the fabrication of coal/polymer composites, coupling agents are introduced to modify the surface functionality of coal particles by providing more bonding opportunities for coal particles with the polymer material.

Regarding the introduction of coupling agents in developing coal/polymer composites, Cheng et al. (2014) first investigated the dispersion of coal particles in anhydrous ethanol. The authors observed that coal particles were poorly dispersed and agglomerated as a result of the presence of hydroxyl groups on the coal particle surface.

To overcome this challenge, the researchers further investigated the effectiveness of three different coupling agents: γ-methacryloxypropyltrimethoxysilane (KH-570), di(dioctylpyrophosphato) ethylene titanate, and vinyltrimethoxysilane on the surface of pristine coal particles. The investigation revealed that the side groups of the main chain of the coupling agents reacted with the hydroxyl groups from coal particles to form a complex on the surface of the coal particles, hindering the interaction among the particles. The authors recommended that coal particles modified using di(dioctylpyrophosphato) ethylene titanate could be used for rubber or plastic blends to obtain better performance and a longer life cycle.

Owing to its structure, a low-rank coal slime constituting the tailings from coal processing was found useful as an active filler for rubber composite (Tan et al., 2019). The coal contained 35.59 wt.% ash and 21.13 wt.% volatile matter (air-dried basis), 75.18 wt.% total carbon, 5.85 wt.% hydrogen and 17.17 wt.% oxygen. The structure of the coal slime was also found to contain active oxygen-based functional groups and aliphatic chains, which imparted the coal with good chemical reactivity. Furthermore, the coal slime was considered biphasic material since it contained carbon black and clay/quartz components. These components are found to improve the composite's thermal stability, gas barrier performance and mechanical properties. According to the test carried out, the coal slime was first carbonised at 600 °C for one hour in a nitrogen atmosphere, then cooled to ambient temperature. The product was mixed with 3 wt%. coupling agent in a planetary ball mill container in isopropanol solution to obtain modified coal slime. Four different coupling agents – cetyltrimethylammonium bromide, silane KH-Si69, aluminate and sodium dodecylbenzene sulphonate (SDBS) – were used. Conventional melt mixing was used in blending the modified coal with SBR1500 rubber to prepare the

composites. The authors found that coal slime modified with SDBS displayed the best particle mixture with good monodispersed and loosely stacked products. Based on the functional group analysis, it was revealed that the SDBS modifier decreased the number of hydroxyl groups on the surface of the coal particles. As a result, the hydrophobicity of the particles increased. The applied treatment promoted the uniform dispersion of coal filler in the rubber matrix, enhanced its compatibility with the rubber, and enhanced the binding force and slip resistance of rubber molecules on the coal particle's surface. It was reported that the surface of the HL-C-SDBS coal particles contained carbonyl, aliphatic chains and sulphonate, leading to high reactivity and the formation of chemical bonds with the rubber molecules. As a result, SDBS-modified coal produced the best reinforcement composites. The researchers also studied the effect of different ash content on the strength of the SDBS-modified coal slime rubber composites. The result is presented in Figure 2-8 and shows that the composites formed with 30% ash content produced the highest tensile strength of 18.80 MPa. Apart from that, the elongation at break increased as the ash content increased. It was reported that the clay minerals in the coal did not bond well with the rubber matrix, thereby causing the rubber chains on the surface of the coal particles to slip greatly.

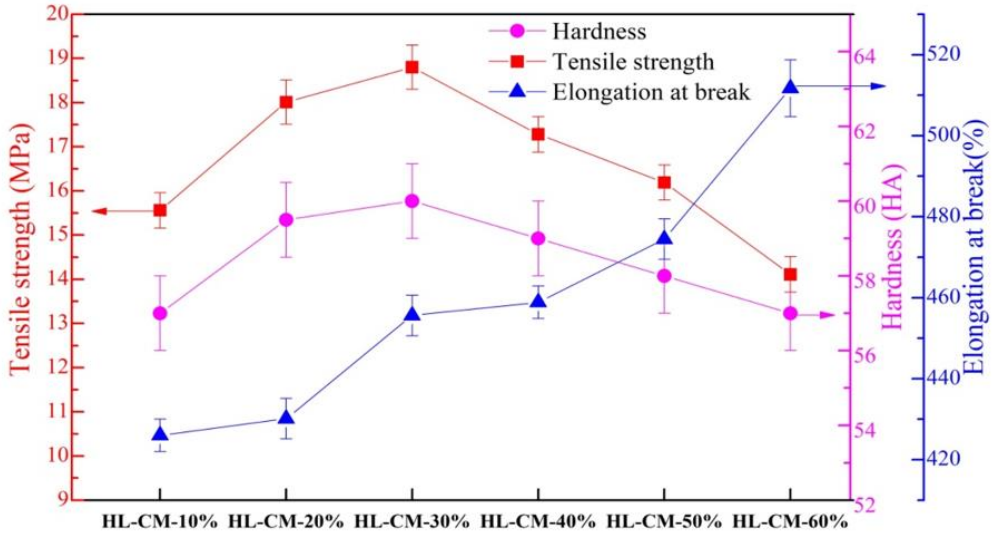



Figure 2-8 Mechanical properties of the SBR1500 rubber filled with coal slime with different ash content (Tan et al., 2019, reproduced with permission from Elsevier)

The effect of three types of bituminous coal (properties in Table 2-1) (0 to 60%) coupled with 3 wt.% maleic anhydride grafted polyethylene (MAPE) coupling agent on the mechanical performance of coal/HDPE composites was investigated by Phillips et al. (2019). Compared to pure HDPE, the addition of 30 wt.% coal improved the flexural strength and flexural modulus of HDPE by 16.5 to 28% and 41.7 to 65.5%, respectively. Pitt No. 8 coal displayed the best flexural strength and flexural modulus composites, being 20.92 MPa and 1.604 GPa, respectively.

Table 2-1 Key properties of the evaluated coals

| Property (wt. %) | Pitt No. 8 | Kittanning | Upper Freeport |
|---|---|---|---|
| Carbon | 74.84 | 72.65 | 57.05 |
| Fixed carbon | 56.12 | 56.82 | 41.05 |
| Ash | 9.1 | 6.84 | 18.96 |

On the other hand, Phillips et al. (2019) observed that the tensile strengths of 30 wt.% coal composites were drastically reduced by 28 to 50% compared to virgin HDPE with about 61 to 71% increase in the modulus of elasticity. The stress concentration sites around the coal particles caused by insufficient interfacial interaction between the coal particles and the polymer matrix were responsible for the inadequate stress transfer to the coal particles throughout the polymer matrix. Hence, the decrease in tensile strength. By eliminating any trapped air bubbles in the mixture using a vacuum oven, the tensile strength of the composites could improve. Therefore, placing the mixture in a vacuum oven to release the air bubbles before moulding might prove productive. Also, the dispersion of coal particles in the polymer matrix may be enhanced by properly designing the mixing and/or fabrication processes, then optimisation.

Although it has been reported that an appropriate precoating process employing a coupling agent could enhance and contribute to the good interfacial microstructure and strength of the composites, this is not always the case. Modifying coal fillers with coupling agents has also been shown to produce negative or no effect on the final properties of the coal/polymer composites. Phillips et al. (2019) investigated the effect of the content of MAPE coupling agent (0 to 3%) on the mechanical properties of coal/HDPE composites. The results revealed that the addition of 0.5% MAPE produced no clear effect on the flexural strength of the composites, and within the range of the amount of coupling agent investigated, MAPE impacted little on the elastic modulus of the composites. The author also observed that one and three wt%. MAPE markedly produced a negative effect on the flexural and tensile strength as the coal content in the mixture increased from 15 to 60%. Using MAPE coupling agent produced even lower flexural strength composites than composites with MAPE. The author expected that the

coal particle's hydroxyl group would be ideal for causing a reaction with the grafted maleic acid in the MAPE coupling agent. However, by probing further into the reason for the negative effect of MAPE on the composites, the authors observed that the amounts of hydroxyl groups on the coal surface were below the detection limit. The low availability of hydroxyl groups led to insufficient reaction sites for bonding with the coupling agent. Hence, the poor adhesion between the coal filler and the polymer matrix.

Rojek et al. (2011) compared the coupling efficiency of 1% titanates and silanes to hard coal (7%, 14% and 21%) blended with polyamide polymer. The results indicated that the mechanical strength (toughness, elongation, breaking elongation and tensile strength) of the modified hard coal/polymer composites decreased as the content of coal filler in the mixture increased. It was also observed that titanates produced polyamide composites with better mechanical properties than silane coupling agents. The reduction in the composite's strength was closely linked to the formation of coal particle agglomerates in the polymer matrix, which acted as internal notches or stress concentration sites. A typical reaction mechanism between the coal particles and the titanate coupling agent is presented in Figure 2-9. The hydroxyl groups on the surface of the coal particles function as reaction sites and are bonded chemically to the coupling agent, which is replaced with the -O-$CH_2$- of ethylene titanate molecules upon alcoholysis reaction to form a layer on the surface of the coal particles. This changed the surface of the coal particles from hydrophilic to hydrophobic. During blending, the polymer portion of the coupling agent, if any, bonds to the polymer matrix.

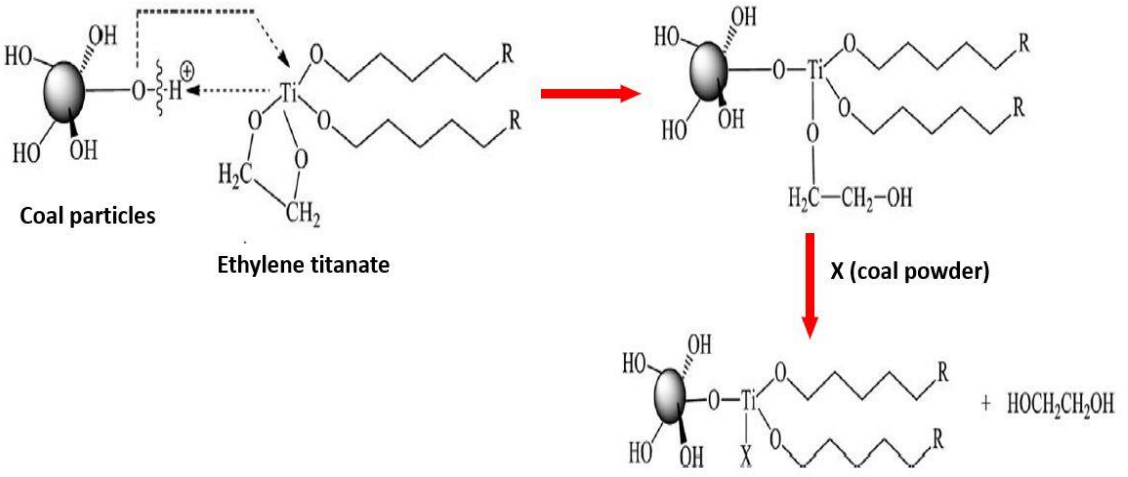



Figure 2-9 Reaction scheme of coal particles and titanate coupling agent (Adapted from Cheng et al. (2014))

Compatibilisers such as block copolymers or elastomers could be added to manipulate the interface property of the polymer via ex-situ modification or in-situ process to enhance polymer reactivity (Mohanty et al., 2018; Bai et al., 2019). Coupling agent and compatibilisation strategies were explored by Bai et al. (2019) using KH-570 as a coupling agent to improve the superficial capacity of coal particles. The modified coal was mixed with ethylene-propylene-diene monomer (EPDM) as the compatibiliser in different compositions, then with polypropylene polymer using a co-rotating twin-screw extruder. The results indicated that the use of a coupling agent increased the contact angle of the coal particles from 33.8 ° to 91.6 ° in water. This implied that the surface hydrophobicity increased and the surface free energy of the coal particles decreased. This increase was found to improve the dispersion of coal particles in the PP/EPDM blend. This finding agreed with the result obtained by Cheng et al. (2014), where the contact angle of coal particles in water was found to increase after modifying coal particles with coupling agents. The high contact angle was attributed to the increase in surface hydrophobicity of coal particles and a reduction of the surface free energy. The effect of

adding modified coal with EPDM elastomer on the mechanical strength of pure polypropylene is presented in Figure 2-10. The authors demonstrated that the impact strength and elongation at break for modified coal (6%) with EPDM (26%) and polypropylene (70%) improved the strength of the polymer but adding pulverised coal (8% and 12%) led to visible cracks. The authors attributed the decrease in the strength of the composite using coal of 8% and 12% to the strong polarity of hydroxyl groups, which caused the coal particles to agglomerate. These conditions consequently led to strong coal-coal interaction but weak coal/polypropylene-EPDM interfacial bonding. It is important to point out that if compatibilisers are used, they should be compatible with both the polymer and coal particles to assure the formation of strong interfacial adhesion and good mechanical strength.

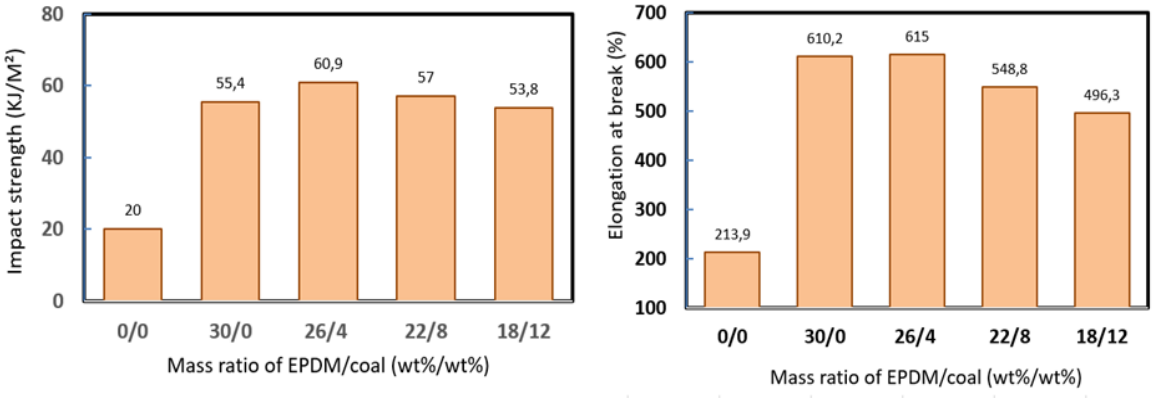



Figure 2-10 (a) impact strength and (b) elongation at break of pure polypropylene (0/0), and polypropylene/ethylene-propylene-diene monomer/coal composites (Adapted and modified from Bai et al. (2019))

From these findings, modifying the surface of the coal particles can change the surface of coal fillers from hydrophilic to hydrophobic and promote the dispersibility of coal fillers in the polymer matrix. However, it is not yet clear the influence of the amount of coupling agent on the physicochemical properties of the resultant composite. Also,

some coals, especially anthracite or hard coal, have little or no reaction sites to react with the coupling agent, hence, an attempt to use coupling agents most likely may prove unproductive. On the other hand, using renewable, low-cost, green coupling agents like furfuryl palmitate and palmitic acid has shown interesting results for the development of fly ash/polymer reinforced composites (Mistri et al., 2010; Sengupta et al., 2011, 2012, 2013) and could be investigated for such coals. In addition, more tests and analyses on modified coal particles using conventional coupling agents should be conducted to establish their effect on the performance of coal/polymer composites. Likewise, it would be beneficial to understand the different mechanisms of the reaction of modified coal with thermoplastic and thermosetting polymers.

## 2.8 Coal and preceramic polymer resin

A unique procedure for producing coal/polymer blends was patented by Hill and Easter (2019). The investigators blended a propriety PCP resin with different coal types and grades and compared the properties of the coal composite formed. The composition of the propriety PCP resin used by Hill and Easter in this investigation was not provided, but according to the literature, PCP resins are noted to contain organometallic compounds (Riedel et al., 2006; Manoj Kumar & Kim, 2011; Eckel et al., 2016; Peterson, 2016; Wang et al., 2019). Figure 2-11 depicts a schematic preparation of the coal/ceramic composites. The process involves the blending of coal fines and polymer resin along with a curing agent, surfactant and/or stabiliser, which may be added to create a slurry. The mixture is then subjected to pressure in a press, pelletised, extruded, or three-dimensionally printed into complex shapes. The complex shapes produced are cured, cooled and pyrolysed in a furnace under a non-oxidising or reactive atmosphere. The results obtained by Hill and Easter (2019) showed that the medium-volatile bituminous run-of-mine coal sourced

from the United States produced composites with higher strength, stiffness and toughness, as well as other remarkable properties compared to the composites produced from synthetic graphite and pre-pyrolysed coal particles. The authors attributed the outstanding performance of the coal/ceramic composites to the hydrogen in the coal and to the thermochemical decomposition of the organic materials that occurred during pyrolysis. Also, the outstanding performance of the coal/ceramic composites could be due to the fine coal particles used in the study. Fine coal particles would provide better surface contact and diffusion reaction with the PCP resin during pyrolysis.

The variation in coal's inherent properties, degree of curing, range of pyrolysis schedules, the ratio of coal/polymer resin and the use of various PCP precursors available commercially could pave the way for the fabrication of multifunctional coal ceramic composites with unique properties.

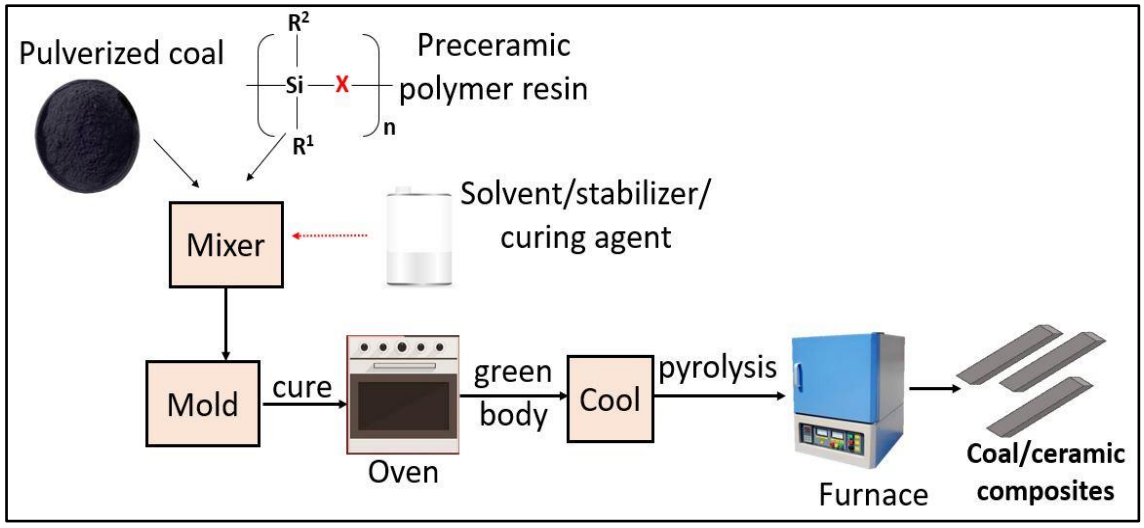



Figure 2-11 Schematic of coal/ceramic composite preparation

## 2.9 Comparison of coal fillers with other filler materials

From the literature surveyed, different properties were reported or analysed for coal/polymer composites produced. This is not surprising as different researchers are in search of different applications because such composites could find applications in a

variety of industries. Table 2-3 summarises the coal/polymer mix, the manufacturing technique and the methods used to characterise the produced coal/polymer composites in the literature. From Table 2-3, the two most reported or consistent properties, tensile and flexural strength provides information about the strength of the composites. Table 2-2 compares the tensile strength and flexural strength of coal/polymer composites to polymer composites developed using other fillers.

Table 2-2 Properties of tensile and flexural strength of representative polymer composites

| Filler | Resin | Tensile strength/MPa | Flexural strength/MPa | Comments | Reference |
|---|---|---|---|---|---|
| Kaolinite | Styrene butadiene rubber | 2.87 to 19.62 | – | Kaolinite modified with KH-Si69 | Zhang et al., 2016 |
| Fly ash + fibre | Epoxy | 40 | – | Fibre treated in sodium hydroxide solution | Kumar et al., 2016 |
| Fly ash + fibre | Polyester | 65 to 74 | – | Fly ash reduced tensile strength fibre/polymer composites | Ramachandran and Kalita, 2014 |
| Fly ash + fibre | Unsaturated polyester | 32.3 to 28.94 | – | Tensile strength reduced on adding fly ash | Manikandan et al., 2015 |
| Expandable graphite (EG) | Polypropylene | 24.6 to 28.3 | – | EG functionalised with phosphorus-containing flame retardant | Qi et al., 2017 |
| Fly ash | HDPE | 23.60 to 28.79 | 21.6 | Prepared using a co-rotating twin-screw extruder | Ahmad and Mahanwar, 2010 |
| Coal | HDPE | – | 30.4 to 42.9 | Flexural strength outperformed commercial alternatives | Al-Majali et al., 2019 |
| Coal | APP + PET | 19.0 to 39.9 | 31.7 to 74.8 | Flexural and tensile strength lower than pure PET | Zhu et al., 2010 |
| Coal | CMS and polyvinyl alcohol | ≈ 3 to 10 | – | For plastic film application | Hu et al., 2017 |
| Wood flour | HDPE | 10.2 to 30.2 | 22 to 58.8 | MAPE used as coupling agent | Li, 2012 |
| Wood | Polypropylene | 31.6 to 35.9 | – | Propolis extract silane used as a coupling agent | Odalanowska et al., 2021 |

| | | | | | |
|---|---|---|---|---|---|
| Sawdust teak + sal wood flour | Epoxy | 16.25 | 52.76 | 67% wood flour produced the best mechanical strength | Jain and Gupta, 2018 |
| Saw dust | Phenolic resin | 34.50 | 61.82 | 60:40 % wt. vol. Application for construction sector | Lette et al., 2018 |
| Various | Various | 13.50 to 34.11 | 28.90 to 75.5 | Sawdust flour + polypropylene (50/50) = best mechanical strength | Khan et al., 2019 |
| Carbon black (CB) | Polyester resin | 23.5 | – | The addition of CB decreased tensile and flexural strength | Alam et al., 2014 |
| CB | Epoxy resin | – | 10 to 40 | PMMA used as spacers | Phua et al., 2017 |

APP – ammonium polyphosphate; CMS – carboxymethyl starch; HDPE – high-density polyethylene; KH-Si69 – bis-(γ-triethoxysilyl-propyl)-tetrasulfide; MAPE – maleic anhydride grafted polyethylene; PET – polyethylene terephthalate; PMMA – polymethylmethacrylate

Table 2-3 Summary of investigations of composites developed using coal and polymer

| No | Coal + polymer (wt.%) | Preparation technique | Surface and mineralogical characterisation | Properties studied | Reference |
|---|---|---|---|---|---|
| 1 | Hard coal + coal sludge + Polyamide PA6 | Extruder (NT = 240 °C; RSS = 190 rpm + injection moulding (optimised parameters) | – | Thermal (DSC and TGA-DTG) | Kijo-Kleczkowska et al., 2020 |
| 2 | Coal + coupling agent (KH-570) + elastomer (EPDM) + polypropylene (70%) | Melt blending using a twin-screw extruder (NT = 190 °C, RSS = 12 rpm, FS = 6 rpm). Melting temperature = 120 °C | Contact angle, FTIR, SEM | TGA, impact strength, elongation at break | Bai et al., 2019 |
| 3 | Coal (< 125 μm) (15 to 60 wt. %) + HDPE | Melt blending using a batch mixer (100 rpm, 10 minutes, 180 °C) + cool + grounding + extrusion + injection moulding (180 °C) | – | Flexural strength, flexural modulus, CTE, flammability (OIT, surface burning rate, FIT/SIT), water absorption, metal leaching, LCA | Al-Majali et al., 2019 |
| 4 | Coal mine overburden (70 to 100 μm) (0 to 40 wt.%) + epoxy + hardener | Hand mixing, composite cured at room temperature for 24 hours, design of experiment (Taguchi) | – | Compressive strength, sliding wear test (dry) | Das et al., 2018 |
| 5 | Coal (< 12 μm) + soy protein plastic + glycerol as plasticiser | Mechanically mixed at 48 °C, aged (4 °C, 24 hours), compression moulding (140 °C, 20 MPa, 5 minutes) | FTIR, XPS, SEM | DTG, tensile strength, elongation at break, water absorption | Guang-Heng et al., 2006 |
| 6 | Demineralised coal (around 10 μm) + soy protein isolate (10 g) + glycerol (25 g) as plasticiser | Mechanically mixed (4 °C, 24 hours), compression moulding (140 °C, 20 MPa, 5 minutes) | FTIR | DSC, tensile strength, impact strength, water absorption | Wang and Zhou, 2011 |

| | | | | | |
|---|---|---|---|---|---|
| 7 | Coal + polyethylene terephthalate + and ammonium polyphosphate (flame retardant) | High speed batch mixer + injection machine (die temperature ≈ 275 °C | SEM, XRD, char yield | TGA, oxygen index, fire performance, tensile and flexural strength | Zhu et al., 2010 |
| 8 | Hard coal (3 to 12%) + epoxy resin, Epidian 6 + Z-1 hardener | Gravitational casting into a mould | – | Surface resistivity | Stabik et al., 2010 |
| 9 | Orthocoking coal/ anthracite coal + epoxy resins Epidian 6/Epidian 6011; triethylenetetramine (Z-1)/triethylenetetraimene adduct hardener | Centrifugal casting + multifactorial, rotatable central composite design of experiments | Microscopic observations in radial direction | Surface resistivity | Stabik and Chomiak, 2016a, 2016b |
| 10 | Anthracite coal + epoxy resin, Epidian 6 + Z-1 hardener | Centrifugal casting | – | Surface resistivity | Stabik and Chomiak, 2011 |
| 11 | Hard coal + polyamide 6 | Twin-screw extruder + granulator | Mass flow rate index analysis | – | Stabik et al., 2009 |
| 12 | Anthracite/hard coal + Bisphenol A epoxy resin | Gravitational casting | – | Wear or abrasion resistance test | Stabik and Chomiak, 2013 |
| 13 | Bituminous coal (15 to 60 wt. %) + maleic anhydride polyethylene + HDPE | Dry mix + twin-screw compounder (RSS = 20 rpm, barrel T = 160 °C) + compression moulding (ten minutes, 18 tonnes) | SEM | Flexural strength and modulus, tensile strength | Phillips et al., 2019 |
| 14 | Hard coal + titanate polyamide 6 | Twin-screw extruder + granulator + injection moulding | – | Tensile strength, impact strength, density | Rojek et al., 2011 |
| 15 | Coal (< 75 μm) + carboxymethyl starch (CMS) + polyvinyl alcohol (PVA) | Different ratios PVA, CMS, sodium hydroxide, and deionised water mixed at 60 °C | FTIR, XPS, SEM, AFM | TGA-DTG, tensile strength, percentage elongation, (elongation at break) | Hu et al., 2017 |
| 16 | Anthracite (raw and thermally treated, 5 and 20%) + epoxy resin + Tetramethylenediamine hardener | Mechanical stirrer (80 °C, 24 hours) + sonicated (one hour) + mechanical mixing (2000 rpm, | SEM, optical microscopy, FTIR, Raman, XRD | Thermal (DSC and TGA-DTG), dynamic mechanical studies | Pusz et al., 2015 |

| | |
|---|---|
| | five minutes) + mould (two hours at 80 and 120 °C) |

AFM – atomic force microscopy; CTE – coefficient of thermal expansion; DSC – differential scanning calorimetry; EPDM – ethylene-propylene-diene monomer; FIT/SIT – flash/self-ignition temperatures; FS – feeder speed; FTIR – Fourier Transform Infrared spectroscopy; HDPE – high-density polyethylene; KH-570 – γ-methacryloxypropyltrimethoxysilane; LCA – life cycle analysis; NT – nozzle temperature; OIT – oxidation induction time; RSS – rotation screw speed; TGA-DTG – thermogravimetric analysis-derivative thermogravimetric; SEM – scanning electron microscope; XPS – X-ray photoelectron spectroscopy; XRD – X-Ray diffraction

## 2.10 Conclusions

Despite the increasing use of coal as an energy resource, the need to use coal in an environmentally friendly and economic manner requires research to be extended to its non-energy applications. Therefore, articles on coal/polymer composites were examined to provide important information on the various bench-scale investigations. The literature shows that the availability of functional groups like hydroxyl, carboxylic and aliphatic groups on coal particles imparts good reactivity between coal and polymer materials. Consequently, a strong binding force is formed between the coal particles and the polymer matrix. On the other hand, the strong presence of polar hydroxyl and carboxyl functional groups in the structure of coal promotes hydrophilicity in coal. Hydrophilic coal is not good from the standpoint that the composite formed may absorb significant moisture from the environment causing the composites to degrade easily. It can also cause coalescing of coal particles due to strong hydrogen bonds, resulting in low dispersion of coal particles in the polymer matrix. Therefore, to develop coal/polymer composites with good dispersion, strong adhesion, and ultimately improved performance, it is necessary to consider the type of polymer and the interfacial interaction between the surface of the coal particles and the polymer. Therefore, polymers with coal-like features are recommended. Moreover, coupling agents with reactive groups compatible with the chemical nature of coal and the polymer are envisaged to enhance the dispersion and compatibility of coal in non- or weak polar polymer materials. By so doing, the adhesive strength between coal filler and polymer material can be greatly improved. That said, the coupling agent must be chosen carefully and in optimal quantity.

In summary, using low-cost coal with minimal pre-treatment before mixing it with polymer-based materials to produce coal/polymer composites presents promising

direction for the non-energy application of coal. However, until additional findings demonstrating the benefits of coal/polymer composites are reported, the implementation of coal/polymer composites as functional composites might not be expedited.

## 2.11 Future research focus and needs

The need to expand the existing application of coal other than a source of energy stimulates research into the use of coal as a filler to produce coal/polymer composites. Based on a detailed analysis of the available literature, additional research and challenges that need to be addressed are:

(i) Unlike other fillers, coal is attractive because it is cheap, easily accessible and could reduce the cost of the final composite materials. However, the vast variation in the chemical nature of coal and polymer poses a challenge to developing coal/polymer composites. At the same time, these variations can be exploited to produce new coal/polymer composites exhibiting various unique and interesting properties that can be used for diverse applications.

(ii) This review has shown that it is possible to produce high-quality polymer-graded composites by adding pulverised hard coal as an antistatic agent or as electro-conducting additives to the non-conductive polymers to prevent the build-up of static charges on the surface of the material. It is an emerging area of coal use but highly relevant to developing antistatic and electrically conductive polymer composites.

(iii) The functionality of coal with thermoplastic polymers has been sufficiently discussed in the literature. As revealed in this review, no study has examined the mechanism of coal functionality with thermosetting polymers.

(iv) As confirmed from the review, several factors such as coal type/rank, surface area, particle size distribution, thermal stability, mixing velocity, coupling agent,

dispersion homogeneity, coal-polymer ratio and the processing method can influence the physicochemical properties of the resultant composite. The literature has also shown that it is possible to enhance some properties of the polymer while others deteriorate. Therefore, to achieve balanced composites, it is important to investigate and optimise these parameters to determine their influence on the performance of coal/polymer composites. Therefore, optimisation carried out experimentally, using simulations and/or through theoretical models would be an interesting area to explore in future research.

(v) It is expected that if the flow resistance of the coal/polymer mixture is high, the energy consumption necessary to process this mixture is also high. Therefore, understanding how the factors mentioned in (iv) influence the rheological behaviour of the mixture in terms of dispersion viscosity is essential to developing cost-effective processing techniques.

(vi) Future research should consider tertiary composition by adding coal fly ash, glass waste or coal discard as mineral inclusions to the coal/polymer blend. This combination could have a synergistic effect and may result in improved thermal stability of the blending process.

(vii) To date, bio-based polymers and plastic waste have not been adequately harnessed in the studies of coal/polymer composites. Therefore, the study on the influence of the amount as well as the rank of coal could be extended to bio-based polymers, plastic wastes, and hybrid polymers (petrochemical- and bio-based) in future research.

(viii) Apart from using conventional manufacturing techniques, the use of three-dimensional printing or additive manufacturing techniques holds promise for future research.

(ix) The comprehensive sustainability assessment of coal and polymer composites in terms of economic, environmental, technical, lifecycle, and recyclability assessment is not well documented in the literature. These analyses are important to determine the benefits of coal/polymer composites and to accelerate full-scale application.

Based on this review, it can be concluded that coal and coal-based resources can be used as filler to produce composite materials for different applications. The research position of investigating the suitability of South Africa coal-based waste for the production of building composites is linked to the potential benefits through remediation and elimination of huge stockpiles of this waste. This is the first study investigating the suitability of South African coal waste and using preceramic polymer as the ceramic-forming binder to produce composites for building application. The materials, methods and experimental techniques used in this study are discussed in the next chapter.

# 3 Experimental

This chapter summarises the materials, equipment used, characterisation techniques and experimental procedure employed in achieving the set objectives for this study. Detailed conditions of how the composites were produced and the various characterisation techniques are presented in the subsequent published chapters (Chapters 4 to 7) and were, therefore, omitted in this chapter to avoid repetition.

## 3.1 Chemicals, coal wastes and fabrication of the coal/ceramic composites

The main raw materials used for this study are coal wastes (Likeflow coal slurry (LCS), Greenside tailing slurry (GTS), Proteas coal discard (PCD), GG1 (a discard from the washing plant), GT (a fine from the mined semi-soft coking coal) and GS (from the Witbank coalfield)), a fly ash (FA) sample and two preceramic-forming polymers. The first PCP is proprietary and belongs to the class of polysiloxanes. This polymer was formulated by XMAT®, the Advanced Materials Division of Semplastics, Florida, United States. The other PCP resin (SPR-212) was selected from Starfire Systems, Inc., United States, and also belongs to the class of polysiloxanes. The production step of the monolithic coal/ceramic composites is displayed in Figure 3-1.

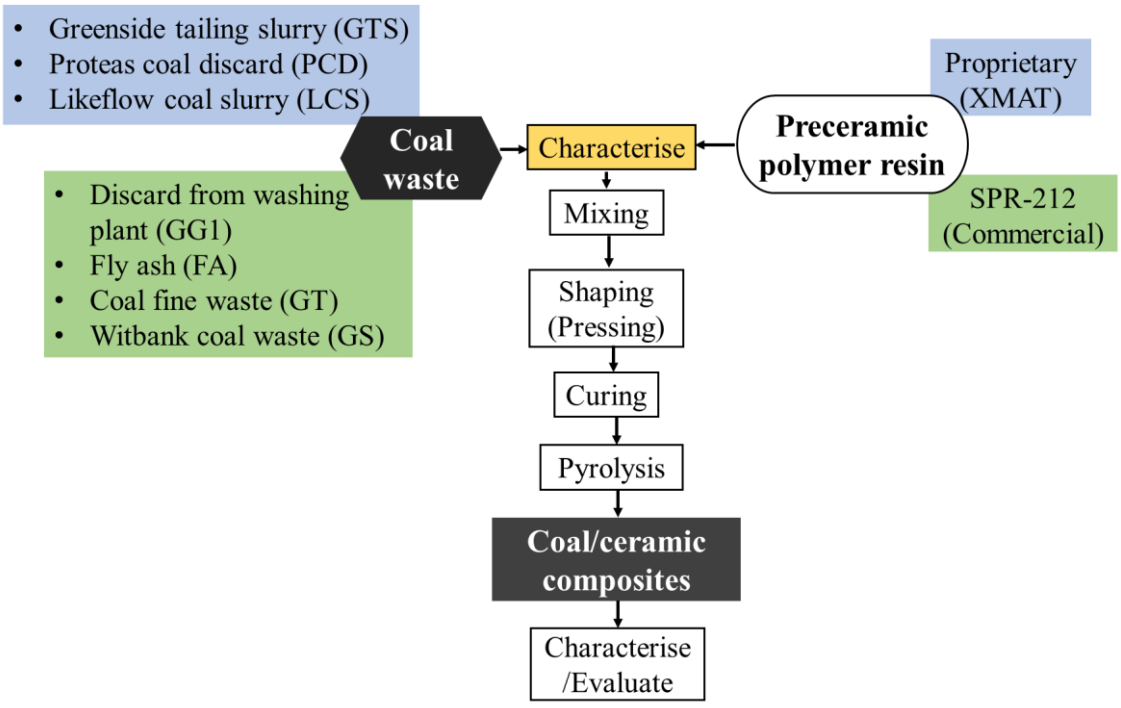



Figure 3-1 Summary of single batch production of the coal composites

## 3.2 Characterisation techniques

The type and grade of coal waste impacts the performance of the coal composite. Therefore, the characterisation of coal wastes used in this study was conducted using the analytical techniques listed below and summarised in Figure 3-2:

(i) Proximate analysis was used to determine the physicochemical properties of the coal waste and the composites such as moisture, volatile matter, ash content and fixed carbon. Proximate analysis was conducted using a TGA701 (LECO Corp., United States) thermogravimetric analyser.

(ii) Ultimate analysis provided information about the absolute measurement of the elemental composition of the coal wastes and the composites, such as total carbon, hydrogen, sulphur, nitrogen, and oxygen content.

(iii) Particle size distribution of the coal wastes was determined using a Malvern Mastersizer 2000 particle size analyser with the Hydro 2000 MU dispersion unit.

(iv) An FTIR spectrometer was used to identify the chemical bond configuration and the functional groups in the coal structure, the PCP resin and the coal composites. FTIR spectrometry was also employed to understand the mechanism of transformation of coal/polymer to coal/ceramics composites.

(v) X-ray diffraction (XRD) analysis was used to compare the mineral phases and the crystallinity of the coal wastes and coal composites.

(vi) X-ray fluorescence (XRF) analysis was required to estimate the oxides in the coal wastes.

(vii) Thermogravimetric analysis (TGA) was used to check the thermal stability of the coal wastes and to compare with the continuous operating temperature of the composites.

(viii) Raman spectroscopy was used to study and compare the graphitisation degree of the carbon phase in the coal waste and coal composites.

(ix) Scanning electron microscopy-electron dispersive spectroscopy (SEM-EDS) was used to examine the morphology and microstructure of the coal composites. The layer of the surface of small coal composites were carbon or palladium-gold (Pd-Au) coated to prevent charging during analysis and to obtain quality images at greater magnifications. EDS provided semi-quantitative chemical composition of the composites.

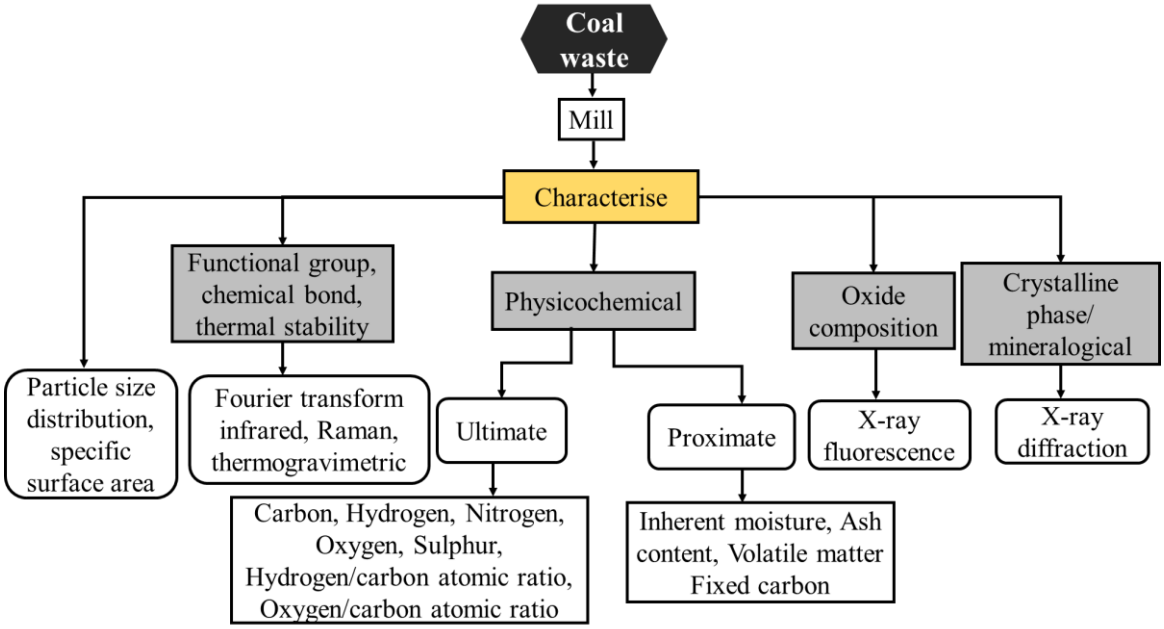



Figure 3-2 A summary of techniques used to analyse the coal wastes

## 3.3 Characterisation of the coal composites

The physicomechanical properties of the coal composite were conducted according to the techniques listed below and summarised in Figure 3-3.

(i) The specific gravity, density, and porosity of pure PDCs and composite structures were measured according to the ASTM C 1167 standard specification for ceramic clay roof tile using an analytical balance and density balance.

(ii) The linear shrinkage was derived from the length of the samples before pyrolysis, $L_G$, and after pyrolysis, $L_{P,}$ and calculated using Equation (2-1).

$$Linear\ Shrinakge, S = \frac{L_G - L_P}{L_G} \times 100\% \quad (2\text{-}1)$$

where $L_G$ is the length (mm) of the green (cured) composites and $L_P$ is the length (mm) of the pyrolysed composites as measured using a calliper or sliding gauge with a precision of ±0.01 mm.

(iii) The water absorption test was conducted to confirm the resistance of the coal composites in water environments. The test was conducted according to the ASTM C 1167 standard specifications for ceramic clay roof tiles. The water absorption of the composites was calculated using Equation (2-2).

$$Water\ absorption, W_R = \frac{M_W - M_D}{M_D} \times 100\% \quad (2\text{-}2)$$

where $M_w$ is the wet mass (g) of the specimen after being removed from the water tank and $M_D$ is the dry mass (g) of the specimens.

(iv) The compressive strength was used to confirm the engineering quality of the composites as building materials. The test was conducted according to the ASTM C 1167 standard test method for clay roof tiles using the universal testing machine.

(v) The efflorescence test was required to detect any presence of soluble salts in the composites. The composites were immersed in water for 24 hours then taken out and allowed to dry in shade. The test will be done according to the ASTM C67 standard test method for sampling and testing structural clay tile.

(vi) The continuous operating temperature/thermal stability of the composites was done to study the weight loss of the composites in flowing air (79% nitrogen gas and 21%

oxygen gas), oxygen and nitrogen atmosphere up to 900 °C. A 10 °C/min heating rate was used.

(vii) The environmental impact of the coal composites in terms of the release of toxic constituents upon contact with liquids may constitute a potential risk to the environment during its end-of-life (i.e., disposal stage). Therefore, laboratory leaching experiments were conducted using distilled water and acetic acid to determine the extent to which toxic constituents might migrate from the coal composites.

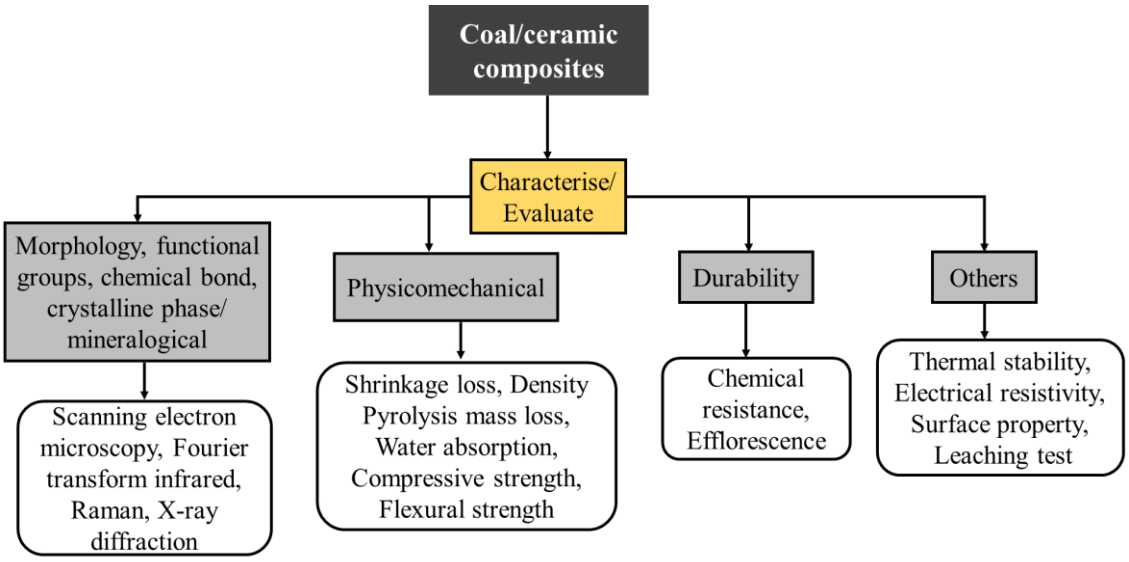



Figure 3-3 A summary of the techniques used to characterise and test the performance of the coal composites

## 3.4 Resources and equipment

The resources used in the fabrication of the coal composites are displayed in Figure 3-4. Some of the products obtained and tests conducted are displayed in Figure 3-5. Table 3-1 presents the list of analytical facilities and equipment used for this research.




Figure 3-4 Resources used in the fabrication of the coal composites: (a) SPR-212 preceramic polymer, (b) 20 mm diameter moulds for shaping, (c) compression moulding machine, (d) oven for curing the moulded mixture of coal and the preceramic polymer, (e) high temperature furnace for pyrolysis of the cured moulded body and (f) compressive strength test equipment

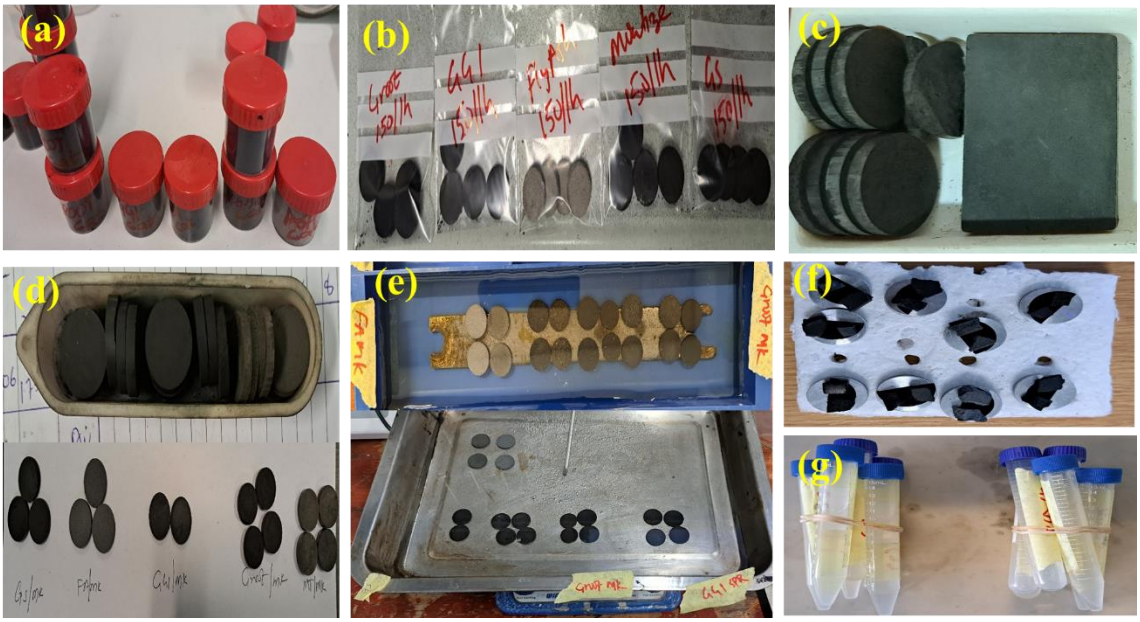



Figure 3-5 Some products obtained and tests conducted: (a) fresh mixture of coal waste and preceramic polymer, (b) cured/green samples, (c, d) pyrolysed samples, (e) efflorescence testing and hot water absorption test, (f) prepared composite sections for scanning electron microscopy analysis, (g) leachate obtained from crushed composite samples and (h, i) pyrolysed samples

Table 3-1 The list of analytical facilities and equipment used for this research

| **Analytical Facility/ Equipment** | **Material / Property** | **Facility Model and Origin** | **Location** |
|---|---|---|---|
| Scanning electron microscope coupled with electron dispersive spectroscopy | Morphology | Sigma 300 VP scanning electron microscope (ZEISS, Germany) | University of the Witwatersrand |
| Light microscope | Surface imaging | Olympus BX41 fluorescence microscope | University of the Witwatersrand |
| Optical contact angle meter | Wettability (contact angle) | OCA 15EC goniometer, DataPhysics instruments, GmbH, Germany | University of the Johannesburg |
| Inductively coupled plasma-mass spectrometry | Heavy metal element determination | - | University of the Johannesburg |
| pH meter | pH value | SevenCompact™ S220 | University of the Witwatersrand |
| Conductivity meter | Electrical conductivity | S230, Mettler-Toledo, GmbH | University of the Witwatersrand |
| Resistance meter | Volume resistivity measurement | 1623-2 Earth Ground Tester, Fluke Corp. United States | University of the Witwatersrand |
| Raman spectroscopy | Molecular bonding/graphitisation degree of the carbon phase | Horiba LabRAM HR Raman spectrometer fitted with an Olympus BX41 microscope | University of the Witwatersrand |
| X-ray fluorescence | Chemical composition | NEX QC+ QuantEZ | University of the Witwatersrand |
| SC-132 analyser | Carbon and sulphur content | LECO Corp. USA | University of the Witwatersrand |
| X-ray powder diffraction | Mineral phases and phase transformation | Bruker D2 phaser diffractometer | University of the Witwatersrand |
| FTIR spectroscopy equipped with an attenuated total reflectance accessory | Functional groups and chemical bonds analysis | Spectrum Two FTIR spectrometer, Perkin Elmer, United States | University of the Witwatersrand |

| | | | |
|---|---|---|---|
| BET surface area analyser | Surface area and pore volume analysis | Quantachrome Instruments, United States | University of the Witwatersrand |
| Laser particle size analyser | Particle size distribution | Malvern 2000 Mastersizer, Hydro2000 MU, Malvern Instrument Ltd., United Kingdom | University of the Witwatersrand |
| Conventional oven | Low-temperature curing | - | Fachbereich Material-Und Geowissenschaften, Technische Universität |
| Tube furnace | High-temperature pyrolysis | - | Fachbereich Material-Und Geowissenschaften, Technische Universität |
| Moulds, pressing equipment | Shaping and pressing | Steel moulds | Semplastics, USA; University of the Witwatersrand; Fachbereich Material-Und Geowissenschaften, Technische Universität |
| Thermogravimetric analyser | Continuous operating temperature, weight loss, proximate analysis | TGA701, LECO Corp. United States | University of the Witwatersrand |
| Balance/platform | Mass, density, pyrolysis mass loss, water absorption, porosity | 120g capacity METTLER TOLEDO - ME104 and Density kit | University of the Witwatersrand |
| Compressive strength test machine | Compressive strength | 10 Tonnes benchtop universal testing machine (H100K-S) | University of the Witwatersrand |
| Flexural strength test machine | Flexural strength | Universal tester machine | Semplastics, USA |

## 3.5 Summary

The procedure and analytical techniques used in producing the composites and analysing/characterising the coal waste samples and the coal or carbon/ceramic composites were presented in this chapter. These characterisation and analytical techniques provided an in-depth information about the various coal wastes and coal composites produced. The results obtained from the experimental investigations of the coal wastes utilised in this study and the coal composites produced thereof are discussed in the subsequent chapters.

# 4 Preparation and characterisation of ceramic composites from South Africa coal discard

This chapter is published in:

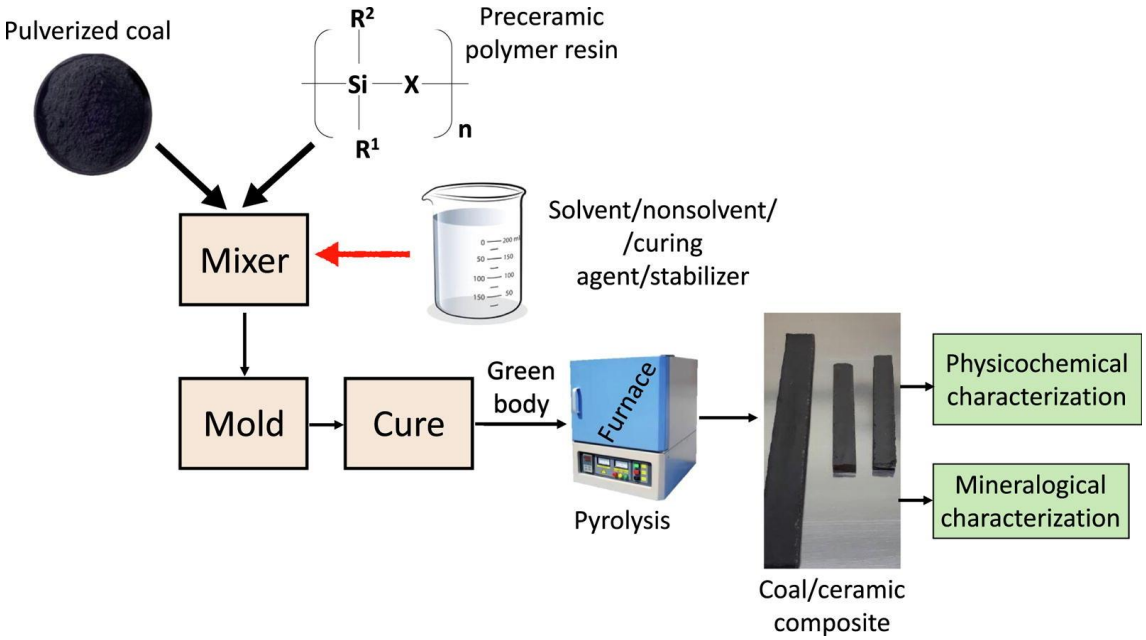
**Eterigho-Ikelegbe, O**., Trammell, R., & Bada, S. (2021). Preparation and characterization of ceramic composites from South Africa coal discard. *Construction and Building Materials*, *302*, 124164.

https://doi.org/10.1016/j.conbuildmat.2021.124164

## Preamble

This chapter presents the findings of the evaluation of coal composites produced from three different South African coal wastes using Semplastics formulated preceramic polymer (X-MAT®) as the ceramic-forming binder. This chapter addresses research question (i).

## Graphical Abstract



**Abstract**

The mining and processing of coal are accompanied by the accumulation of a substantial volume of discard that threatens the environment. Also, the continuous harvesting of natural resources such as clay to produce building materials is not environmentally sustainable. In this study, various South African coal discards were blended with a polysiloxane preceramic polymer (PCP) resin and thereafter pyrolysed to produce coal/ceramic composites. The physicomechanical properties of the composites were evaluated using various ASTM standard test methods. The thermal stability, mineralogy and functional group properties of the raw materials and the composites were checked using thermogravimetric analysis, XRD and Fourier Transform Infrared spectrometry, respectively. The results suggest that carbonyl functional groups and hydrogen bonds in the coal discard promoted bonding with the PCP, thereby improving the physicomechanical properties of the composites. XRD results showed that the total intensity of the diffraction peaks in the coal discard declined after pyrolysis of the blend of coal discard and the PCP. This suggests the amorphisation of the crystalline phases in the coal discard. The developed composites displayed water absorption and flexural strength as low as 1.94 to 10.1% and 27.51 to 36.46 megapascals, respectively. The remarkable mechanical properties of the composites suggest that the coal composites produced in this study could be applicable in the construction industry. However, more tests, such as impact strength, thermal conductivity, etc., are required to characterise the properties of the coal composites fully.

**Keywords:** Coal discard, Composites, Flexural strength, Mechanical properties, Preceramic polymer, Water absorption.

## 4.1 Introduction

With the growing global demand for reliable and low-cost energy, coal remains one of the largest sources of energy in the world. To meet the market specification, an enormous amount of by-products is produced during the extraction and preparation phase. These by-products, sometimes referred to as gangue, slurries, coal slime, tailings, middlings contain small amounts of coal, metallic minerals and a series of incombustible inorganic impurities (Li et al., 2018). To give context to the amount of coal discard produced in South Africa, Belaid et al. (2013) reported that the amount of discard coal stockpiled is more than 1.5 billion tonnes, with approximately 60 million tonnes produced annually. Disposing of this waste has been a challenge to the industry, while stockpiling them results in severe environmental concerns, including leaching, spontaneous combustion, air pollution and contamination of aquifers and useful land space (Addou et al., 2017; Taha et al., 2017; Li et al., 2018).

On the other hand, it is reported that the global construction industry consumes more raw materials than any other economic activity (Pacheco-Torgal & Labrincha, 2013). This continuous exploitation has led to substantial depletion of raw material resources for the building and construction industry. Research efforts to valorise coal discard for building and ceramic applications have emerged and progressed steadily. Information is available in the literature on the use of coal discard as pore-forming agents or as feedstock to produce building ceramic and insulating bricks (Abdrakhimov & Abdrakhimova, 2017; Kairakbaev et al., 2017; Stolboushkin et al., 2017; Fomina & Yu. Stolboushkin, 2019). The research conducted by Fomina and Yu. Stolboushkin (2019) described a procedure to produce ceramic bricks from coal discard and moderately plastic loams. The investigation indicated it was necessary to fire the blend in an oxidising

atmosphere to ensure complete carbon burning. In another investigation conducted by Stolboushkin et al. (2017), pulverised coal discard was subjected to a pressure of 15 to 17 MPa in a press and subsequently fired at 1000 °C to prepare ceramic samples. Based on the analyses, it was established that coal discard with a reduced amount of carbon could be used to produce ceramic bricks of compressive strength 32.4 MPa. Taha et al. (2017) also demonstrated the ability to sustainably produce high mechanical strength bricks from treated coal mine tailings and coal mine waste rocks. Different grades of coal composites have also been produced from coal and coal discard using a polymer as the matrix material (Pusz et al., 2015; Stabik & Chomiak, 2016; Hu et al., 2017; Al-Majali et al., 2019; Bai et al., 2019; Phillips et al., 2019). The results from these studies demonstrated that coal or coal discard could bind to polymers to enhance and modify the polymers with novel properties.

Furthermore, silicon-based ceramic polymers otherwise known as PCP resins, transform into preceramic and ceramic when thermally treated (Wilson et al., 1997; Harshe et al., 2004; Colombo et al., 2010; Martínez-Crespiera et al., 2011; Eckel et al., 2016; Poerschke et al., 2018). According to the literature, PCP resins contain organometallic compounds. These polymers, for example, the polysiloxanes, polycarbosilanes and polysilazanes resins, are used as a precursor to produce silicon carbide, silicon oxycarbide and silicon carbon nitride ceramic, respectively (Riedel et al., 2006; Eckel et al., 2016; Peterson, 2016; Kopeliovich, 2018). They have been used to develop ceramic fibres and carbon-reinforced composites. The composites developed from PCP find a wide range of applications, such as in brake linings, electronics, biotechnology, etc. (Liew et al., 2000; Colombo et al., 2010; Eckel et al., 2016).

Coal-based composites and PCP resin composites have been extensively reported. However, only one study, to our knowledge, examined composites formed by blending coal with PCP resin. Hill and Easter (2019) blended American coal and a polysiloxane PCP resin to produce strong and light composites with potential application as a building material. However, the literature suggests that coal from different regions has different characteristics. According to Falcon (1986), carboniferous coals in the northern hemisphere differ from Permian coals in the southern hemisphere in composition and maturity. The difference in American and South African coals in terms of maturity and mineral composition imposes a need for the technological assessment of South African coal discard when blended with a PCP resin. An innovative solution for the utilisation of South African coal discard to produce structural composites would empower and create a sustainable material for the construction and building industry and an income stream for the coal industry.

In this context, for the first time, this article reports on the preliminary investigation of the blend of South African coal discard with a polysiloxane PCP resin as the binder material. The physical, mechanical, and microstructural properties of the structural composites were investigated using flexural strength, water absorption and compression tests, XRD, FTIR spectrometry, TGA, and SEM.

## 4.2 Experimental

### *4.2.1 Analysis of the coal discard utilised and the synthesised composites*

Three coal discard samples, PCD, GTS, and LCS, were investigated. PCD was obtained from the Northwestern KwaZulu-Natal coal mining area. GTS and LCS were obtained from the Witbank-Middelburg coal mining area in South Africa. A polysiloxane (SPR-212) PCP resin selected from Starfire Systems used in a previous study conducted

at Semplastics was utilised as a binder for developing the composites (Hill & Easter, 2019). Particle size analysis of the coal discard was carried out using a laser particle size analyser (Malvern 2000 Mastersizer, Hydro2000 MU, Malvern Instrument Ltd., United Kingdom). From the analysis, the coal discard samples have similar particle size distributions, with about 80% of the coal discard particles passing 36 µm.

Representative portions of each coal discard sample were pulverised to -212 µm for proximate, ultimate, thermal stability and XRD analysis. Proximate analysis was analysed using a thermogravimetric analyser (TGA701, LECO Corp. United States) according to international standard ASTM D5142. Ultimate analysis was carried out following the ISO 12902-CHN instrumental method (ISO/TS 12902, 2001). The oxygen percentage was calculated by difference. Each analysis was done in duplicate, and the mean values were reported. FTIR spectroscopy (Spectrum Two FTIR spectrometer, Perkin Elmer, United States) equipped with an attenuated total reflectance accessory was used to provide information on the molecular structure of coal discard and coal/ceramic composite samples. The pulverised samples were scanned in the range of 400 to 4000 $cm^{-1}$.

The mineral phases of the coal discard samples and coal composite specimens were recorded using the XRD analytical technique (Bruker D2 phaser diffractometer equipped with Cu-Kα radiation, $\lambda$ = 1.54184 angstroms (Å), operated at 50 kilovolts and 23 milliamperes in the 2-theta range of 10 to 90 °C). The resulting diffraction patterns were matched to a reference database of diffractions using X'Pert Highscore software. The microstructures of the fabricated composite samples (top and fractured surface) were characterised using a Sigma 300 VP scanning electron microscope (ZEISS, Germany).

The samples were coated with carbon to enhance conductivity and obtain high-resolution imaging.

The weight loss of the coal composites and coal discard samples was measured using a thermogravimetric analyser (TGA701, LECO Corp. United States), with approximately 100 mg of fine coal discard and the composite sample placed in a crucible and heated under a nitrogen atmosphere at a heating rate of 10 °C/min from 20 to 900 °C. A schematic representation of the experimental procedure for the development of coal composites is shown in Figure 4-1.

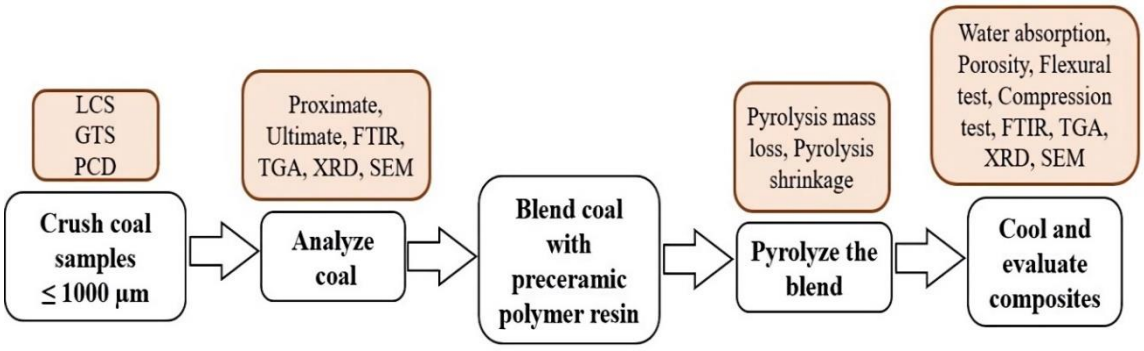



Figure 4-1 A schematic representation of the experimental procedure for producing coal composites

### *4.2.2 Preparation of the composites*

The as-received discard coals were pulverised to fine particles using a mechanical jaw crusher to facilitate the achievement of a greater degree of packing. The pulverised coal was weighed and placed in a mixer, while the PCP resin added in suitable proportions was properly mixed with the coal discard to create a blend that was cast in a prefabricated mould. The PCP resin served as a binder to compact the pulverised coal discard particles. The mixture was poured into a machined steel rectangular mould and subjected to pressing pressure of 6.89 MPa. The moulded shapes were transferred to a retort furnace under a dry nitrogen atmosphere at room temperature and ramped to 1000 °C for ten hours

(Hill & Easter, 2019). During thermal treatment, the constituents were bonded together, chemically turning the blend into a fully dense coal/ceramic composite (Figure 4-2).

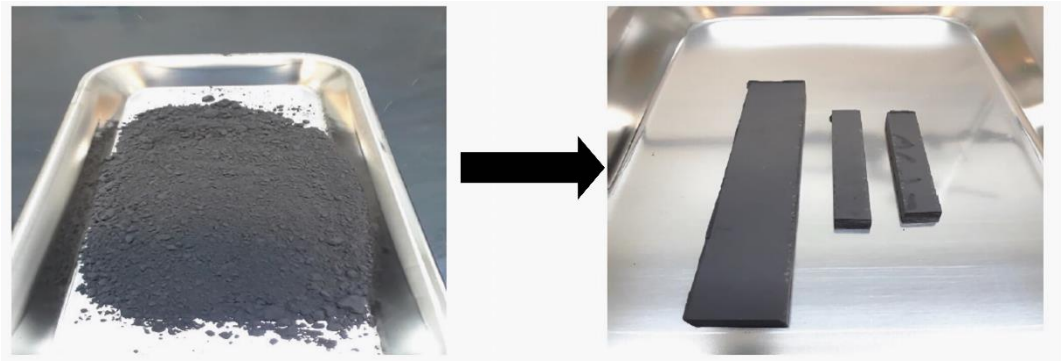


Figure 4-2 Image of coal discard (left) and coal composites formed (right)

### *4.2.3 Physicomechanical characterisation*

The physical and mechanical properties of the developed composites were characterised using different techniques. The mass loss of the composites was determined by weighing the mass of the green bodies before and after pyrolysis, while the pyrolysis shrinkage was calculated as the shrinkage loss before and after pyrolysis. The bulk density, porosity, water absorption and specific gravity of the specimens were determined according to the ASTM C373 standard test method for ceramic tiles using the equations in Table 4-1. According to the ASTM standard procedure, the composites' dry mass, D (g), was obtained after heating in an oven at 110 °C to constant mass. Specimens were then cut from the composite sticks, placed in a glass flask of distilled water, and boiled for five hours. Afterwards, the specimens were soaked for an additional 24 hours in distilled water at room temperature. The suspended mass, S (g), of the impregnated samples was determined while suspended in water. The specimens were then blotted slightly with moistened linen to remove all excess water, and the saturated mass, M (g), in the air was then determined. It was assumed that one cubic centimetre of water weighs one gram, and mass was measured to the nearest 0.01 g.

Table 4-1 Summary of formula

| **Quantity** | **Formula** |
|---|---|
| Apparent porosity, P | [(M–D)/V] 100 |
| Relative density, $\rho$ | 1–P |
| Apparent specific gravity, T | D/(D–S) |
| Bulk density, B | D/V |
| Water absorption, A | [(M–D)/D] 100 |

(D – dry mass (grams); S – suspended mass (grams); M – saturated mass (grams))

The flexural strength of the composites was determined using a universal tester machine under a three-point bending fixture. Compressive strength was used to measure the strength of the composites to resist crushing loads. The test specimen was loaded into a compression test machine with a uniform load ratio of one millimetre/minute until the sample failed. Flexural strength and compression strength were calculated using Equations (4-1) and (4-2) from ASTM C67 and the average of three tests for each specimen was recorded.

$$M = 3\,PL/2bd^2 \tag{4-1}$$

$$C = W/A \tag{4-2}$$

where $M$ is the flexural strength (MPa); $P$ is the load at rupture; $L$ is the distance between supports (mm); $b$ is the width of the specimen (mm); $d$ is the thickness of specimen (mm); $C$ is the compressive strength (MPa); $W$ is the maximum load indicated by the machine; and $A$ is the average of the gross areas of the upper and lower bearing surfaces ($mm^2$).

## 4.3 Results and discussion

### *4.3.1 Proximate and ultimate analysis*

Coal discards vary significantly in characteristics; therefore, the proximate and ultimate analyses were conducted to determine the properties of the three coal discard samples, and the results are presented in Table 4-2. From the table, the proximate analysis

indicates that the LCS sample has the highest volatile matter (23.72%) and can be classified as a medium-volatile matter bituminous coal. The PCD sample has a volatile matter content of 10.67% and can be classified as very lean anthracite coal. The ash content of all the coal discard samples ranges between 15.57% and 39.76%. The ultimate analysis data indicates that the LCS sample has the highest total carbon of 67.20% and total sulphur content of 0.71%. Based on the hydrogen/carbon ratio, it can be inferred that the PCD sample is highly aromatic in structure and more polycondensed due to its low hydrogen/carbon atomic ratio of 0.34 (Solomon, 1981; Davis et al., 1995; Ibarra et al., 1996; ICCP, 1998). The GTS sample, on the other hand, has a hydrogen/carbon atomic ratio of 0.72, indicating that the discard coal may likely contain aliphatic and hydrogen-rich species.

Table 4-2 Summary of properties of coal discard samples and coal composite specimens

| **Parameters** | **PCD** | **GTS** | **LCS** | **PCD composite** | **GTS composite** | **LCS composite** |
|---|---|---|---|---|---|---|
| **Proximate analysis; ad (%)** | | | | | | |
| Inherent moisture content (M) | 4.29 | 3.34 | 3.99 | 0.60 | 0.96 | 0.69 |
| Ash content | 39.76 | 30.69 | 15.57 | 52.67 | 56.22 | 42.41 |
| Volatile matter | 10.67 | 22.57 | 23.72 | 1.50 | 1.78 | 2.03 |
| Fixed carbon (calculation) | 45.31 | 43.42 | 56.74 | 45.23 | 41.04 | 54.87 |
| **Ultimate analysis (%)** | | | | | | |
| Total carbon | 49.40 | 54.20 | 67.20 | - | - | - |
| Hydrogen | 1.64 | 3.24 | 3.67 | - | - | - |
| Nitrogen | 1.38 | 1.39 | 1.64 | - | - | - |
| Oxygen* | 2.99 | 6.46 | 7.22 | - | - | - |
| Total sulphur | 0.54 | 0.68 | 0.71 | - | - | - |
| **Atomic ratio** | | | | | | |
| Hydrogen/carbon | 0.34 | 0.72 | 0.66 | - | - | - |
| Oxygen/carbon | 0.71 | 0.56 | 0.30 | - | - | - |

(Ad – air-dried; GTS – Greenside tailing slurry; LCS – Likeflow coal slurry; PCD – Proteas coal discard; *Oxygen by difference = [100-(M+Ash+sulphur+hydrogen+total carbon+nitrogen)])

### *4.3.2 Fourier Transform Infrared spectroscopy*

Coal is heterogenous by nature and includes a large variety and an abundance of functional groups (Painter et al., 1985). FTIR spectra (Figure 4-3) were used to gain insight into the structural properties of the coal discard and composites. The spectra were interpreted based on previous studies (Painter et al., 1981; Ibarra et al., 1996; Balachandran, 2014; Chen et al., 2015; Okolo et al., 2015). At the 1600 $cm^{-1}$ band, corresponding to the aromatic C=C structure, LCS has the strongest absorption peak intensity. According to Balachandran (2014), strong absorptions at this peak indicate a high carbon content in the coal. This agrees with the highest total carbon content of the LCS sample. The peaks at 2920 $cm^{-1}$ and 2850 $cm^{-1}$ are due to the existence of aliphatic groups in the coal discard samples. The complex band between 900 $cm^{-1}$ and 700 $cm^{-1}$ corresponds to the aromatic structure within the coal discard. The residual band structure on the side of the C=C stretch represents C=O (carbonyl) species in LCS and GTS formed during oxidation (Smyrl & Fuller, 1987; Dun et al., 2013; Zhang et al., 2015; Zhang et al., 2021); they did not appear in PCD. This observation agrees with the oxygen content from the elemental analysis, suggesting that LCS is the most oxidised coal discard. The absorptions on the fingerprint spectrum at 540 $cm^{-1}$, 1030 $cm^{-1}$, and around 3695 $cm^{-1}$ for PCD are an order of magnitude higher in intensity than those of LCS and GTS and are assigned to the vibrations of Si-O-Si in quartz and kaolinite.

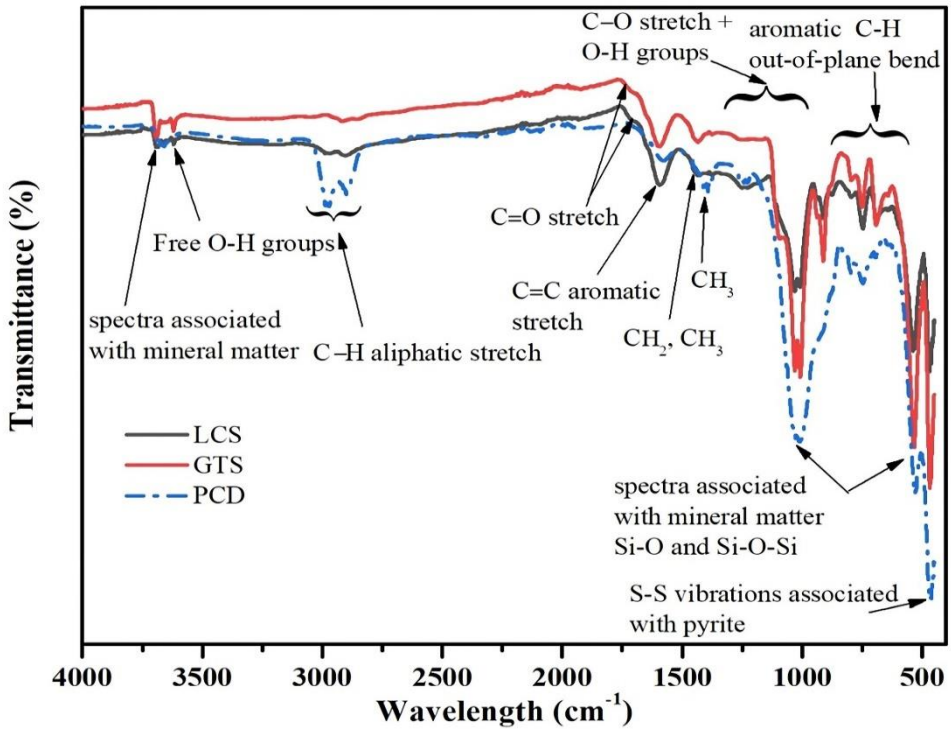



Figure 4-3 Spectra of the raw coal discard samples

(GTS – Greenside tailing slurry; LCS – Likeflow coal slurry; PCD – Proteas coal discard)

The spectra of the coal composites are presented in Figure 4-4. The FTIR results reveal the disappearance of some peaks in the coal discard and the appearance of new peaks in the composite specimens, demonstrating that a binding reaction has taken place between the coal discard and the PCP resin. The intense peak appearing at 3670 $cm^{-1}$ attributed to the O-H stretching vibration is weak in the coal discard samples but is more intense in the composite specimens. The high-intensity O-H vibrations confirm the formation of hydrogen bonds between coal discard and the PCP resin. The peak intensity of the C-H aliphatic stretch occurring at 2978 $cm^{-1}$ and 2904 $cm^{-1}$ in the coal discards (Figure 4-3) substantially increases in the FTIR of the composites (Figure 4-4). This occurrence is due to the combined contribution of C-H alkyl groups present in coal discard and the PCP resin.

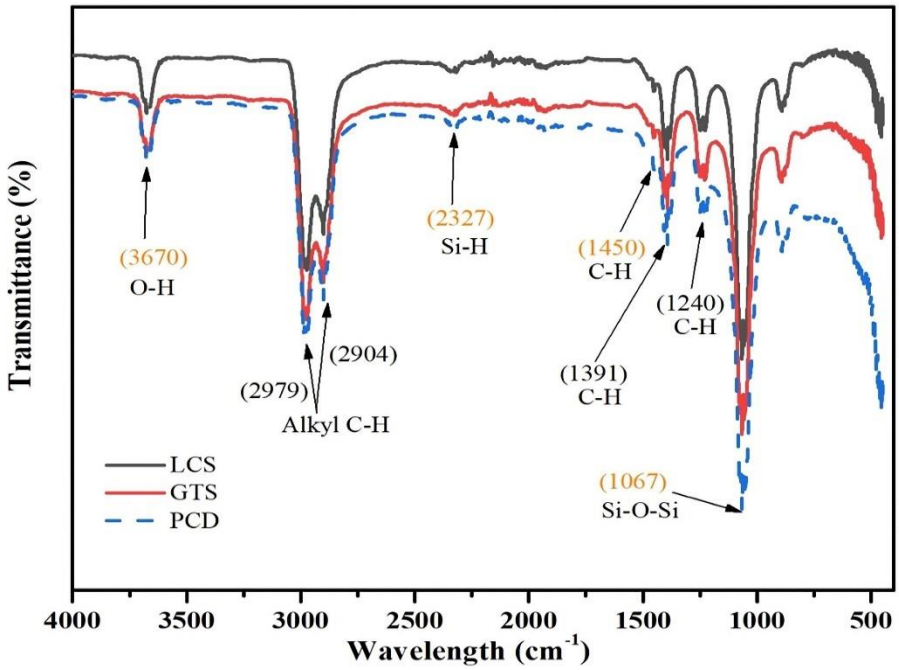



Figure 4-4 Spectra of the coal composites

(GTS – Greenside tailing slurry; LCS – Likeflow coal slurry; PCD – Proteas coal discard)

The residual peaks observed at 2327 $cm^{-1}$ and 1918 $cm^{-1}$ in the FTIR of the composites but absent in coal have been attributed to the Si-H moiety bonds in the PCP resin. The bands at 1391 $cm^{-1}$ and 1240 $cm^{-1}$ are also present in the coal discard samples, but more intense in the composite specimens. These bands have been allocated the symmetric deformation associated with the $-CH_3$ group. The most prominent peak at 1067 $cm^{-1}$ in the composite specimen was identified as the typical vibration Si-O-Si bond in polymer precursors (Harshe et al., 2004; Swaminathan et al., 2010) and silicates in coal combined. The absorption peaks at 773 $cm^{-1}$ and 454 $cm^{-1}$ were allocated to the bending vibrations of the Si-O-Si structure in ceramic (Luo et al., 2019).

### *4.3.3 X-ray diffraction*

The XRD analysis was conducted to determine the mineral phases present in the coal discard and coal/ceramic composites. All phases were matched using X'PERT

HighScore Plus analysis software. The XRD diffractograms obtained for the coal discard samples are presented in Figure 4-5. The GTS and LCS samples have broad peaks typical of coal patterns rich in amorphous phases (Qiu et al., 1999; Cristelo et al., 2016; Yin et al., 2018). The presence of an amorphous hump in the XRD pattern of the LCS sample suggests that the sample is rich in organic matter (Bada et al., 2010; Song et al., 2011).

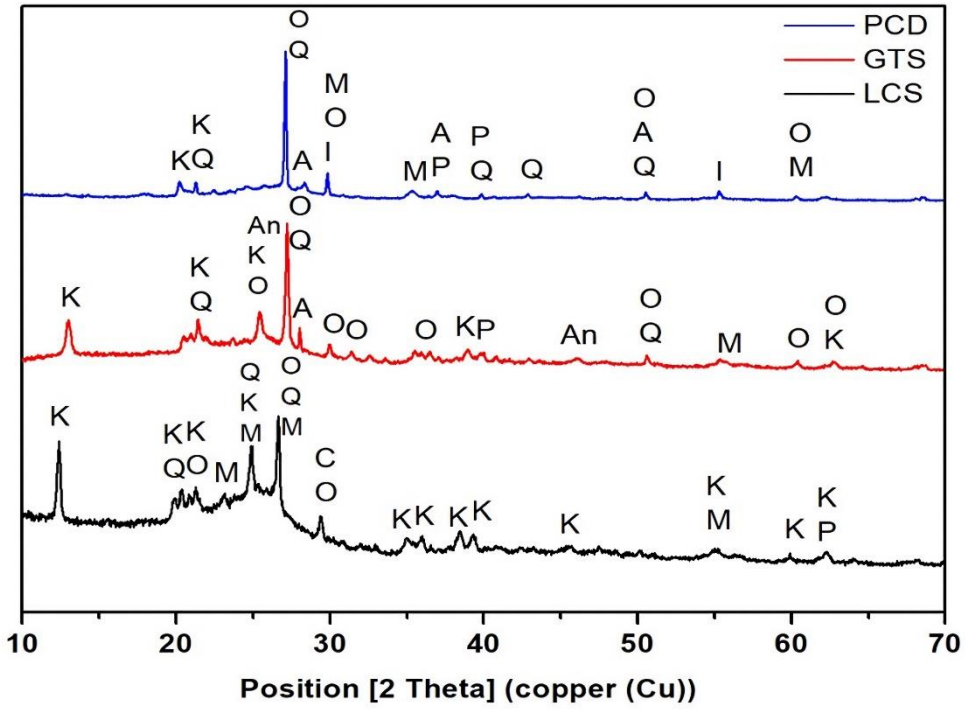



Figure 4-5 X-ray diffraction patterns of pulverised coal discard samples

(K – kaolinite; Q – quartz; M – muscovite; O – orthoclase; P – pyrite; Q – quartz; C – calcite; A – anorthite; An – anatase; I – illite; GTS – Greenside tailing slurry; LCS – Likeflow coal slurry; PCD – Proteas coal discard)

It is evident that the significant proportion of minerals present in the LCS sample are aluminosilicate clay minerals: kaolinite ($Al_2Si_2O_5(OH)_4$) and muscovite ($KAl_2(AlSi_3O_{10})(OH)_2$). The dominant mineral in the PCD sample is the interstratified clay mineral: anorthite and orthoclase accompanied by a small amount of aluminosilicate clay minerals (kaolinite and muscovite). It is anticipated that the difference in the mineral

composition of the coal discard samples would influence the physical and mechanical characteristics of the respective composites produced.

The XRD profiles of the PCD, GTS and LCS composites are shown in Figure 4-6 and are identical. A more intense and broader vitreous structure with an amorphous hump is seen around 24° 2-theta in the LCS composite specimens. In the pyrolysis of polysiloxane PCP resin, Wilson et al. (1997) identified this amorphous hump as networked glass peaks based on its similarity to peaks found in α-silicon dioxide.

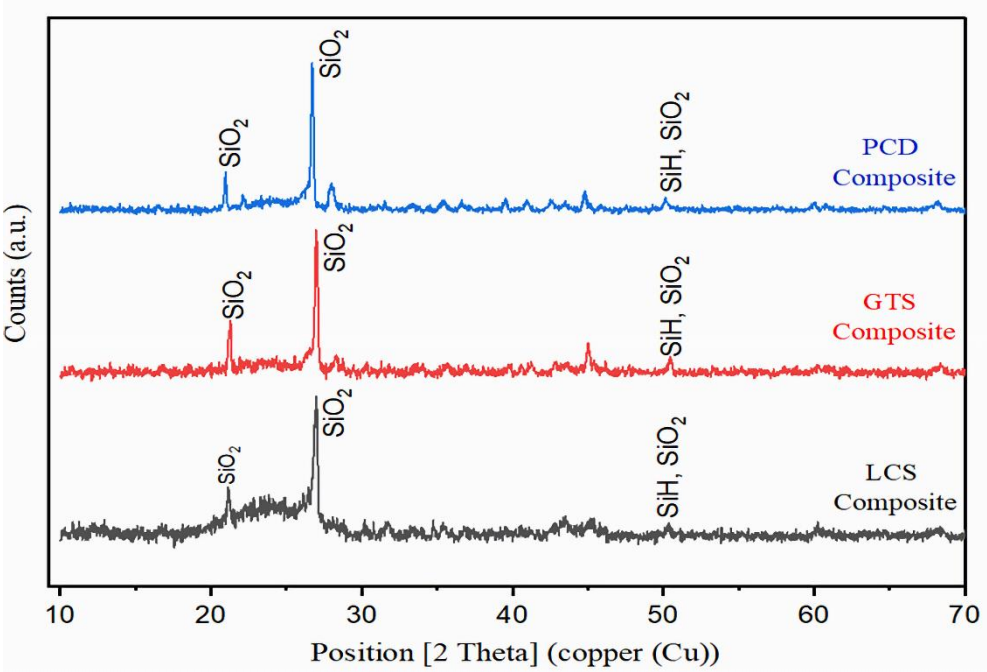



Figure 4-6 X-ray diffraction patterns obtained for coal/ceramic composite specimens (a.u. – arbitrary units; SiH – silicon hydride; $SiO_2$ – silicon dioxide; GTS – Greenside tailing slurry; LCS – Likeflow coal slurry; PCD – Proteas coal discard)

The peaks reflected on the X-ray diffractogram of coal composites (Figure 4-6) indicate the presence of a combined contribution of peaks from the PCP resin and some minerals within the coal. The peak from the PCP resin mostly originates from either the formation of β-silicon carbide or silicon oxycarbide crystals in the amorphous structure or the free carbon of the ceramic-derived materials (Martínez-Crespiera et al., 2011;

Poerschke et al., 2018). The coal discard minerals might be responsible for the complex irreversible reactions and thermal decomposition of the samples with the PCP resin during the pyrolysis treatment. As a result, some residual peaks from the coal discard were observed in addition to new crystalline phases in a low amount that was difficult to identify. This transformation was responsible for the physical and mineralogical properties of the coal ceramic composites.

### *4.3.4 Thermogravimetric analysis*

TGA of the coal discard samples and composites are presented in Figure 4-7. Although the composites produced in this study are intended for use in processes that do not require elevated temperatures, it is important to establish their thermal stability limits. From the figure, it is evident that the decomposition of coal discard samples and composite specimens occurred in a single stage. At temperatures below 300 °C, the coal discard samples show about a 4% loss in weight, which can be attributed to the evaporation of free and physically adsorbed moisture, and the degradation of low molecular volatile organic compounds (Ladner, 1988; Janković et al., 2020). The PCD sample recorded the most thermally stable coal discard largely due to the presence of the incombustible and high amount of minerals as indicated from the proximate result.

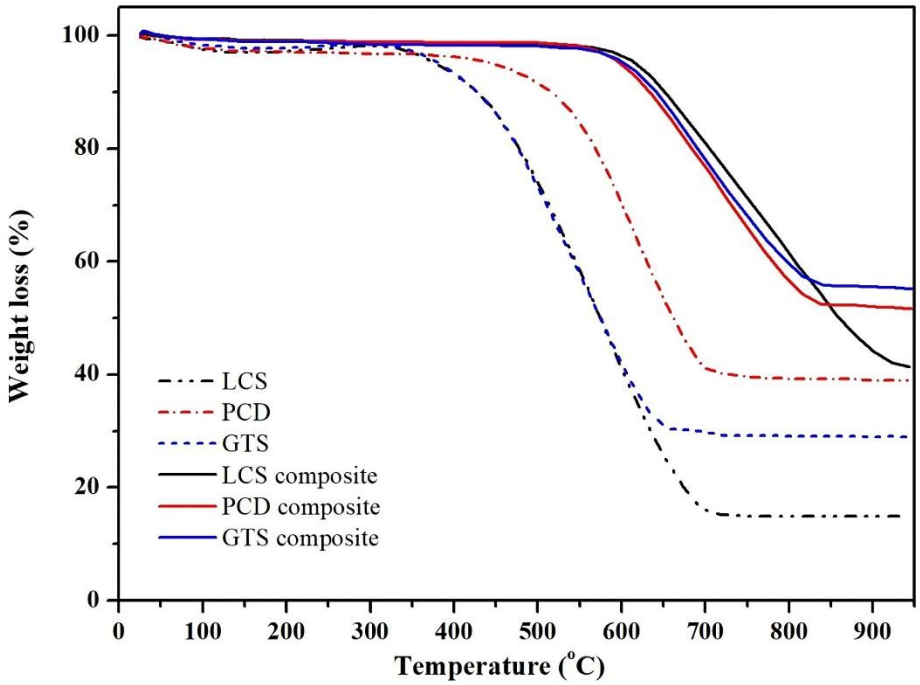



Figure 4-7 Thermogravimetric curves for coal discard samples and coal composite specimens

(GTS – Greenside tailing slurry; LCS – Likeflow coal slurry; PCD – Proteas coal discard)

The thermal stabilities of the developed composites and the respective coal discard samples from which they were formed were compared. In all cases, the initial decomposition temperature of the coal discard samples shifts to a higher temperature region (about 550 °C) after pyrolysis of the coal discard and PCP resin blend. The shift signifies that more stable bonds formed when pyrolysing the blend of coal discard and PCP resin. A total weight loss of around 58.69%, 48.01% and 44.25% at the final temperature (900 °C) was recorded for the LCS, PCD and GTS composites, respectively. The weight loss can be attributed to the release of volatiles from the coal discard samples and the degradation of PCP resin.

From the thermal analysis results, the GTS composite can be adjudged the most stable compared to the PCD and LCS composites. The high hydrogen/carbon ratio (low aromaticity) of the GTS composite suggests that many hydrogen-containing functional

groups could be present in GTS. This could have stimulated strong hydrogen bonding between the GTS and the PCP resin, leading to a better interpenetrating network of the blend. Therefore, high heat was required to break the H-bonds. Highly stable coal-polymer composites developed by Hu et al. (2017) were attributed to strong hydrogen bonding.

### *4.3.5 Morphology*

The degree of surface smoothness and structural order of the composites formed by blending the pulverised coal discard with PCP resin was investigated by SEM. The morphologies of the top and fractured surfaces of the coal ceramic composites are shown in Figures 4-8a to e. It is evident from Figures 4-8a and b that the surface morphology of the LCS and GTS composites is smoother and crack-free, compared to the PCD composite. The surface inhomogeneities of PCD composite and the lack of fusibility (Figure 4-8c) is very significant, giving further evidence of the porous nature of the PCD composite as determined from its apparent porosity (Table 4-3).

The cross-section images of the composite specimens are compared in Figures 4-8d, e and f. The micrographs show connected smooth areas linking the coal discard particles, which is typical for a brittle glassy material derived from the PCP resin pyrolysed at temperatures below 1000 °C (Danko et al., 2000; Berbon et al., 2001; Eckel et al., 2016). Significant nanoporous regions were evident in the coal/matrix interface in the PCD composite (Figure 4-8f). The presence of residual pores, non-uniform size, or spacing as observed in both the surface and cross-sectional area of the composite specimens is indicative of shrinkage of the liquid precursor and gas evolution during pyrolysis. Therefore, based on SEM analysis, it seems likely there is a direct correlation

between the mineral content in coal discard and the level of fusibility of the coal discard and PCP resin.

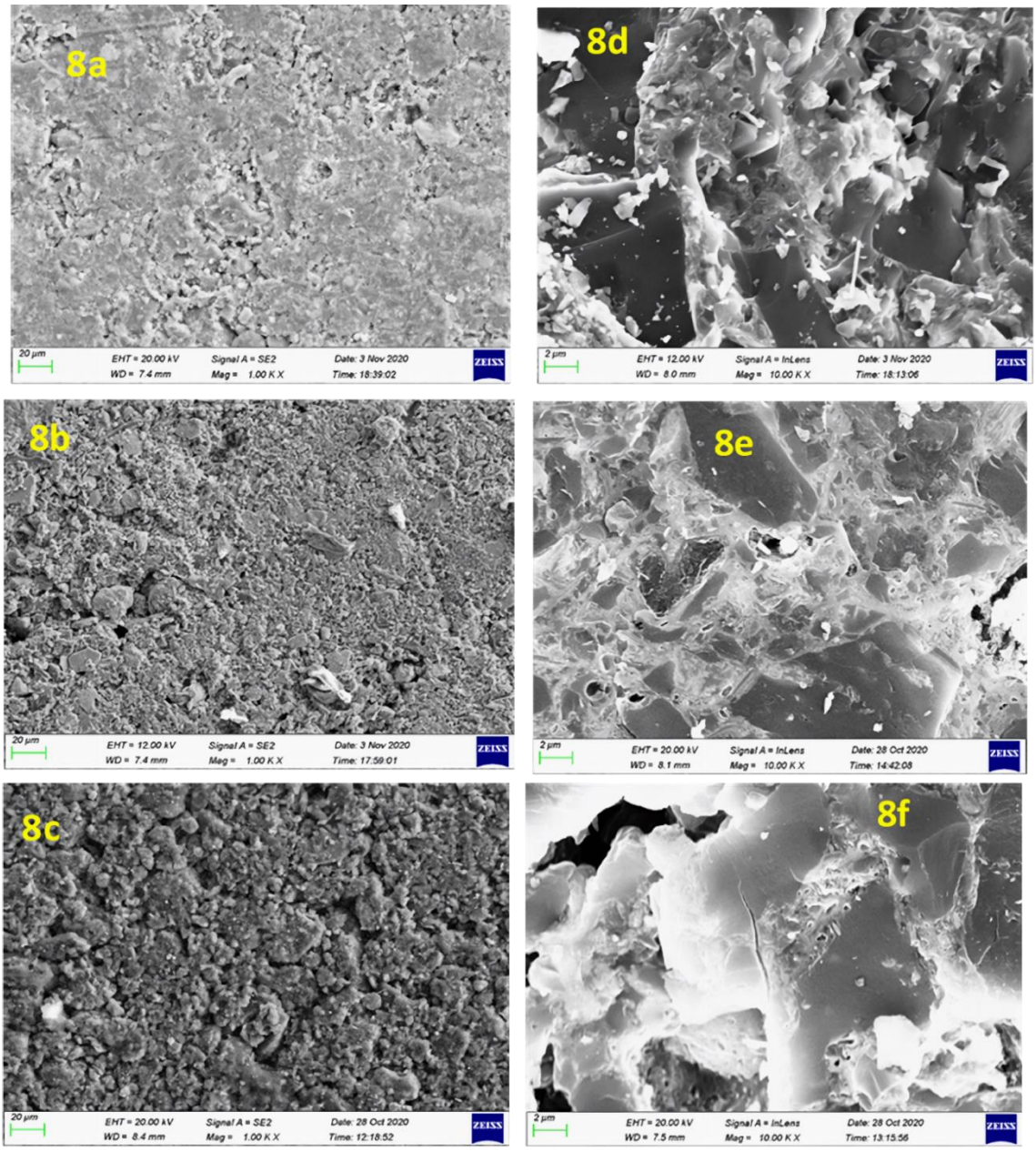



Figure 4-8 Microstructure of the top surface of coal composite specimens (a) Likeflow coal slurry (LCS), (b) Greenside tailing slurry (GTS) and (c) Proteas coal discard (PCD), and the fractured surface of (d) LCS, (e) GTS and (f) PCD

### *4.3.6 Physicomechanical properties*

#### *4.3.6.1 Pyrolysis shrinkage and pyrolysis mass loss of composite specimens*

The composites' pyrolysis mass loss and pyrolysis shrinkage are presented in Figure 4-9. During the pyrolysis of the coal composite, the physical transformation of the composite occurs in parallel with the release of hydrocarbon gases from the PCP and the rapid release of volatiles from the coal discard. As a result, the particles and the PCP resin are expected to have closer interaction (pyrolysis shrinkage) accompanied by mass loss. Generally, the polymer-to-ceramic conversion is intrinsically accompanied by a high mass loss, leading to the formation of porosity and high shrinkage. This transformation is characterised by the evolution of hydrogen and gaseous hydrocarbon species (Galusek et al., 2007; Martínez-Crespiera et al., 2011; Mainzer et al., 2019).

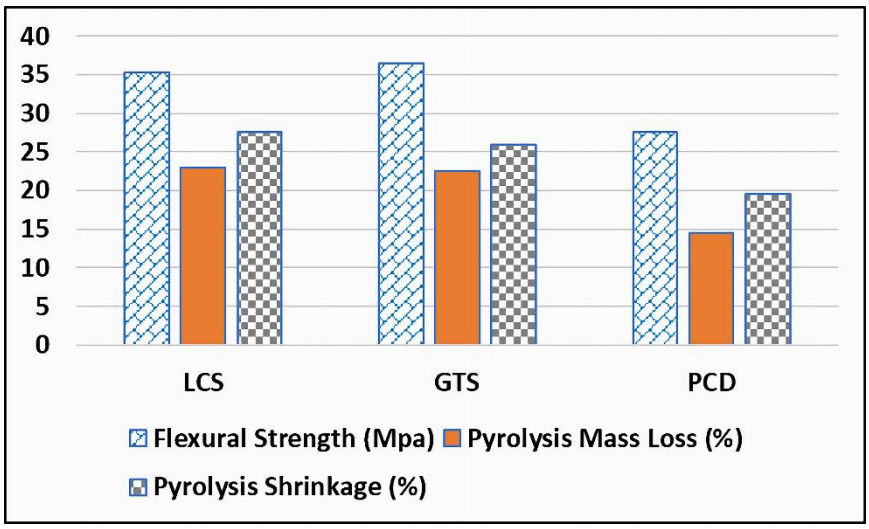



Figure 4-9 Summary of flexural strength, pyrolysis mass loss and pyrolysis shrinkage of coal composite specimens

(GTS – Greenside tailing slurry; LCS – Likeflow coal slurry; PCD – Proteas coal discard)

From the evaluation of the pyrolysis mass loss of the composite specimens (Figure 4-9), the PCD composite has the lowest mass loss of 14.9% and pyrolysis shrinkage of 20%. Based on the proximate data of the coal discard and the composites' pyrolysis loss,

there seems to be a direct relationship between the volatile matter in the coal discard samples, pyrolysis mass loss and pyrolysis shrinkage. The remarkably low pyrolysis mass loss of the PCD composite compared to the LCS and GTS composites could be attributed to the low-volatile matter (10.67%) present in the PCD sample.

Even though the pyrolysis shrinkage results of the composite specimens are moderately high and ideally should lead to deformation, tension and warpage of composite specimens during pyrolysis (Greil, 1995; Xie et al., 2006; Eckel et al., 2016; Peterson, 2016), this was not the case. The authors have attributed this observation to the fine particle size of about 90% coal discard passing -45 um. The pyrolysis shrinkage and pyrolysis mass loss may be overcome by optimising the process.

*4.3.6.2 Porosity and water absorption test*

It is expected that the physical properties of the composites synthesised in this study will be different due to the difference in the inherent properties of the coal discard utilised. A summary of the results obtained from the physical characterisation of the coal composite specimens is presented in Table 4-3.

Table 4-3 Physicomechanical properties of the coal composite specimens

| **Coal composite** | **Bulk density ($g/cm^3$)** | **Apparent specific gravity** | **Water absorption (%)** | **Apparent porosity (%)** | **Compressive strength (MPa)** | **Flexural strength (MPa)** |
|---|---|---|---|---|---|---|
| **LCS** | 1.77 | 1.84 | 1.94 | 3.44 | 208.50 | 35.23 |
| **GTS** | 1.85 | 2.00 | 3.40 | 7.22 | 130.14 | 36.46 |
| **PCD** | 1.69 | 2.03 | 10.1 | 17.08 | 83.67 | 27.51 |

(GTS – Greenside tailing slurry; LCS – Likeflow coal slurry; PCD – Proteas coal discard)

The data in Table 4-3 indicates that the density of composite specimens varies. Density relied on several factors such as the porosity and the degree of interfacial bonding

between coal discard and the PCP resin. The porosity of the developed specimens is in good agreement with the observations from the SEM analysis. The PCD composite, albeit exhibiting the lowest pyrolysis mass loss and shrinkage values, performs remarkably poorly in terms of water absorption, as manifested by its highest porosity value (17.09%). The results suggest that the PCD composite had more void, leading to a reduction in its density.

Meanwhile, water absorption is an important factor to consider for composite materials intended for structural applications, and it is an indirect measure of open porosity. The data from this study suggest that apparent porosities are directly related to the water absorption of composites. From Table 4-3, the LCS composite displays the lowest water absorption rate, which can be explained by the low apparent porosity and high shrinkage. Thus, comparing the water absorption values of the composites, it is reasonable to conclude that the internal structures of the LCS and GTS composites were dense enough to prevent the intrusion of water, meeting the maximum of 6% required by the ASTM C1167-03 standard specification for clay roof tiles.

In this study, the binding mechanism of coal discard and the PCP resin is according to the mechanism depicted in Figure 4-10. Oxygen represents the backbone atom, while $R^1$ and $R^2$ are the side chain functional groups of the polysiloxane PCP resin where R may be hydrogen, or methyl or other aryl or alkyl groups (Colombo et al., 2010; Barroso et al., 2019). During pyrolysis, gases generated, such as methane, hydrogen, carbon monoxide, etc., are given off as the blend of coal and the PCP resin gradually turns into a ceramic structure as observed by Hill and Easter (2019).

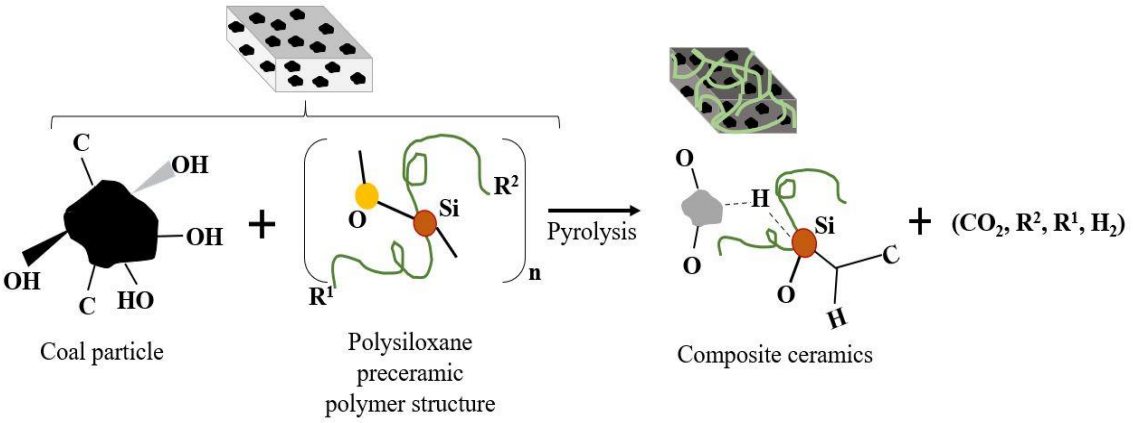



Figure 4-10 Mechanism of the binding scheme between discard coal particles and the preceramic polymer resin

This mechanism is similar to that described by Hu et al. (2017), who stated that hydrogen bonding plays a dominant role in the interaction of coal with other materials. Likewise, in the study by Hill and Easter (2019), the hydrogen functional groups present in the coal were reported to react chemically and bound with the PCP resin. The low hydrogen content (hydrogen = 1.64; hydrogen/carbon ratio = 0.34) of the PCD sample compared to the other coal discard (Table 4-2) suggests that fewer hydrogen-containing functional groups may be present in the PCD sample. As a result, it is possible that the bonding between PCD and the PCP resin is weak. This phenomenon could be responsible for the porous nature and high water absorption recorded for the PCD composite. The low apparent porosity (1.94%) obtained from the LCS composite correlates to strong bonding between the LCS sample and the PCP resin, which could be connected to the high hydrogen/carbon ratio and high volatile matter (23.72%) in the LCS sample. As the coal particles devolatilise during pyrolysis, more pores are created, increasing the microporosity and surface area of the coal discard for more interaction with the PCP resin.

*4.3.6.3 Flexural strength and compression strength*

Flexural strength is a measure of the ultimate strength of a specimen to withstand bending, while compressive strength defines the load-bearing capacity of any structure (Weng et al., 2003; Eliche-Quesada et al., 2011). The results from the compression and flexural testing of the coal composites are summarised in Table 4-3. The GTS composite exhibits the highest flexural strength (36.46 MPa), but not without a slight difference compared to the composites developed using the LCS sample (35.23 MPa). Compared to the reference standard for flexural strength (≥ 35 MPa) for porcelain ceramic tiles (Luo et al., 2019), the composites developed in this study recorded a 4.17% increase, 0.66% increase, and 21.4% decrease for the LCS, GTS and PCD composites, respectively. It has been reported that carbonyl groups in coal (Tan et al., 2019) and in ethyl cellulose polymer (Sam et al., 2017) enhanced binding with other materials. The high value of flexural strength displayed by the GTS and LCS composites may be directly correlated to the carbonyl stretch present in the FTIR spectra of these coal discard. As a result, the carbonyl group ensured the GTS and LCS samples with good reactivity and bonding interactions with the PCP resin. On the other hand, the PCD composite displayed the lowest compressive strength (83 MPa). The poor mechanical strength behaviour of the PCD composites can be attributed to higher porosity and surface inhomogeneity as evident from the SEM analysis, low bulk density, and other imperfections not visible to the microscope.

Table 4-4 compares key data in this study to other composites produced for building applications in the literature. Al-Majali et al. (2019) reported a flexural strength in the range of 30.4 MPa to 42.9 MPa by melt mixing bituminous coal from the United States with HDPE to produce CPCs for building applications. The high flexural strength

reported by the authors was attributed to the strong HDPE material, optimum composite processing parameters and improved dispersion of coal in the polymer matrix. Phillips et al. (2019) blended 30% wt. pulverised bituminous coal with HDPE to form CPCs and obtained a flexural strength of 20.92 MPa. The authors attributed the poor results to weak interfacial adhesion between the coal and HDPE, which led to insufficient stress transfer to the filler particles throughout the polymer matrix. The presence of high mineral content in the coal discard samples utilised in this study was hypothesised to provide rigidity to the pyrolysis of the blend of South African coal discard and PCP resin. Rather, hydrogen content, aromaticity, the PCP resin used and the presence of carbonyl groups in the coal discard played a more obvious role.

Table 4-4 Comparison of key data of the composites developed in this study to other structural composites in the literature

| **Materials** | **Density/ g/cm$^3$** | **Flexural strength/MPa** | **Water absorption/%** | **Reference** |
|---|---|---|---|---|
| Alkali activation of coal fly ash + feldspar + kaolin + bentonite | 2.16 to 1.40 | 41.61 to 58.57 | 0.27 o 1.98 | Luo et al. (2017a) |
| Alkali activation of coal fly ash | 1.92 to 2.55 | 6.99 to 54.49 | 0.00 to 13.33 | Luo et al. (2017b) |
| Plastic waste + fly ash | 0.93 to 1.02 | – | 0.04 to 0.08 | Dhawan et al. (2019) |
| Red mud + aluminium sources | 1.83 to 1.94 | 157.21 to 85.46 | 5.50 to 8.50 | Wang et al. (2020) |
| Waste engine vegetable oil + pulverised fly ash + river sand + sulphuric acid | 1.92 to 1.99 | 7.39 | 5.20 | Sam et al. (2020) |
| Coal discard + preceramic polymer resin | 1.65 to 1.77 | 27.51 to 36.46 | 1.94 to 10.10 | This study |

## 4.4 Conclusion

This study demonstrated a potential reuse application of South African coal discard to synthesise high-value coal composites for the construction industry. Discard coal was blended with a polysiloxane PCP resin and then pyrolysed. The results indicated that coal discard (GTS) with the highest hydrogen/carbon ratio of 0.72 produced composites with a flexural strength of 36.46 MPa and water absorption of 3.40%. These values surpassed the minimum requirement of 35 MPa flexural strength required for porcelain ceramic tile and the maximum water absorption of 6% required by the ASTM C1167 standard specification for clay roof tiles. Thermogravimetric analysis indicated reinforcement of the GTS composites' thermal stability due to strong bonds formed between the South African coal discard and the PCP resin. The results also suggest that coal discard rich in minerals does not necessarily result in higher comparative properties. The remarkable results illustrate a potential practical application of the developed coal composites for building applications. However, more tests such as impact strength, flammability, thermal conductivity are needed to characterise the composites fully.

# 5 Novel composites produced from coal discards with potential application in the building and construction sectors

This chapter is published in:

**Eterigho-Ikelegbe, O**., Trammell, R., & Bada, S. O. (2022). Novel ceramic composites produced from coal discards with potential application in the building and construction sectors. *Journal of the Southern African Institute of Mining and Metallurgy*, *122*(8), 421–428. https://doi.org/10.17159/2411-9717/2001/2022

**Preamble**

This chapter presents the findings of the evaluation of coal composites produced from three different South African coal wastes using Semplastics formulated preceramic polymer (X-MAT®) as the ceramic-forming binder. This chapter addresses research question (ii) and it is different from Chapter 4 in that scientific information not reported in Chapter 4 is presented in Chapter 5 to enhance the understanding of the behavior of the composites in terms of flexural strength, morphology, and water absorption. Furthermore, in Chapter 5, new laboratory results on the continuous operating temperature (chunk composites in air atmosphere), chemical resistance, and efflorescence properties of the composites.

**Abstract**

In response to the enormous amounts of coal discard generated during coal mining and preparation, the development of an efficient and sustainable strategic use of this resource is essential. Furthermore, the rising urban population over the next decades is confronted with the depletion of quality raw materials for building components. To this end, this study reports new information on the morphology, water absorption and flexural strength properties of ceramic composites produced from three different coal discards and polysiloxane preceramic polymer resin. In addition, test results relating to the continuous operating temperature, chemical resistance and efflorescence potential of the composites are presented. The results show that the water absorption and flexural strength of the coal composites up to 1.94% and 36.46 megapascals, respectively exceed the requirements for ceramic and clay roof tiles. The continuous operating temperature of composites was more thermally stable than conventional roofing tiles (concrete and ceramic) between ambient temperature and 600 °C. In addition, the excellent chemical resistance of the composites (94.43% to 99.98%) compared to conventional roofing tiles (67.82% to 99.97%) eliminates the need for additional external coatings. The results documented so far suggest that this technique could be used to produce low-temperature application building products such as bricks, panels, roofing tiles, etc. This new technique of recycling coal discard offers an excellent opportunity to eliminate enormous volumes of coal discard and to advance the circular economy in the coal industry.

**Keywords:** Coal discard, Waste utilisation, Chemical resistance, Circular economy

## 5.1 Introduction

Coal is a relatively low-cost source of energy that has enormously contributed to global economic development. The mining and processing of coal in industrialised and developing countries have led to the production of billions of tonnes of coal discard. With coal meeting about 77% (Department of Mineral and Energy, 2021) of the energy need in South Africa that fosters posterity, industrialisation and domestic growth, coal production will likely remain significant, at least for the foreseeable future. According to the Department of Mineral and Energy, about 60 Mt coal waste is produced each year with an already accumulated surplus of one gigatonne (Gt). These coal discards heaped on arable land or retention ponds could pose enormous environmental hazards, such as spontaneous combustion, if not properly managed. Most of these dumps are known to contain low- to high-quality rich inorganic-organic compounds depending on the source. Although some coal discard dumps can be beneficiated to yield clean coal, the process could be somewhat unattractive when the age of the coal is taken into consideration. Other factors that are considered are the degree of oxidation or weathering of the coal, the potentially high cost of treatment and the subsequent generation of discard after beneficiation.

A panoply of innovative research on the beneficiation of South African coal discard into alternative products exists in the literature. Tambwe et al. (2020) demonstrated laboratory-scale heap leaching potential of pyrite from sulphidic coal discard to reduce its risk of disposal. Nevertheless, the process still leaves behind desulphurised coal discard as waste. The combustion of South African coal discard in a circulating fluidised bed boiler was demonstrated and reported by Belaid et al. (2013). Due to the similar combustion profile of the co-combustion of 70% coal discard and 30%

refuse-derived fuel compared to 100% coal, Isaac and Bada (2020) proposed that the blend could be considered an alternative fuel for use in existing pulverised boilers. Using different South African coal discards to produce activated carbon as porous adsorbents for natural gas storage was reported by Abdulsalam et al. (2019, 2020). Amaral Filho et al. (2020) demonstrated that low-sulphur ultrafine coal discard fabricated topsoil outperformed native soil for rehabilitating coal mine sites. Despite the numerous ongoing investigations on coal discard utilisation, it is worth mentioning that these approaches would not fully utilise the over one Gt of coal discard in South Africa.

An article by Haywood et al. (2019) calls for the introduction and use of mineral waste in the South African economy. The author reported that the secondary utilisation of mining waste is preferred over waste disposal. In a sense, it opens the door to value creation, sustainable development and reducing the responsibilities associated with the waste stream. Globally, the repurposing of coal discard aligns with the concept of waste valorisation, the circular economy and sustainability. In this context, it could be considered a practical solution to pollution problems caused by coal discard dumps. To this end, among the potential reuse strategies of South African coal discard, for the first time, Eterigho-Ikelegbe et al. (2021b) reported on the density, porosity, compression strength, pyrolysis shrinkage, etc. of coal composites produced from South African coal discard and a polysiloxane PCP resin. PCPs are known to convert into thermoset polymers and silicon-based ceramics upon crosslinking and pyrolysis, respectively. The polysiloxanes $(R_1R_2SiO)_n$, contains –Si–O– as the basic backbone or inorganic network with various side reactive and/or inert groups on the silicon atom site. These polymers are ideal precursors for producing silicon oxycarbide bulk ceramic, coatings, foams, energy storage, ceramic fibres, and ceramic matrix composites (Bernardo et al., 2014;

Wen et al., 2020, 2022). By blending a suitable coal discard dump of about one megatonne with a known quantity of PCP resin, following heat treatment, structural coal composites could be produced without generating secondary waste. Whereas, with the washing of this discard dump and cofiring with biomass, additional wastes like fly ash and discard are generated.

In this article, we report new scientific information on the morphology, water absorption and flexural strength of the produced coal composites. Furthermore, the continuous operating temperature, chemical resistance and efflorescence potential of the coal discard composites are presented. Some of the results obtained are then compared with those of standard building materials (concrete and ceramic roof tiles). The performance of the coal composites produced in this study in terms of their temperature resistance up to 600 °C and chemical resistance equivalent to 'thermal stability and durability', respectively, would be of great interest to the building, construction and coal industries. These results suggest the prospect of repurposing South African coal discard to produce ceramic composites for building and construction purposes.

## 5.2 Experimental

### *5.2.1 Materials and method*

Three coal discards were selected that were sourced from the Witbank coalfield and the KwaZulu-Natal coal area. The coal discards are denoted GTS, PCD and LCS. A specially formulated PCP resin by XMAT®, the Advanced Materials Division of Semplastics, Florida, United States was used as a binder to develop the coal composites. The as-received coal discard lumps were crushed and pulverised to about 80% passing 45 μm. The coal particles were thoroughly mixed with the PCP resin, after which the mixture was pressed to 6.89 MPa in low-cost rectangular moulds. The moulds are

machined steel with a smooth matte finish, and a polytetrafluoroethylene release film lining the mould was in direct contact with the material being pressed. The processing of the coal composites occurred in two stages – curing and pyrolysis. The moulded bodies were cured to about 120 °C in an oven to harden and fuse the resin and the coal particles. During crosslinking, the functional groups in the PCP and coal particles presumably undergo a series of reactions – condensation and combination reactions. The cured bodies were pyrolysed in a furnace under a nitrogen flow at 236 millilitres per minute up to 1000 °C for ten hours. The pyrolysis step facilitates the molecular and chemical interactions between the PCP and the coal constituents. In parallel, the elimination of some volatile and hydrogen species occurs during pyrolysis, converting the cured bodies to ceramic-like composites. A schematic of the production process of the coal composites is depicted in Figure 5-1.

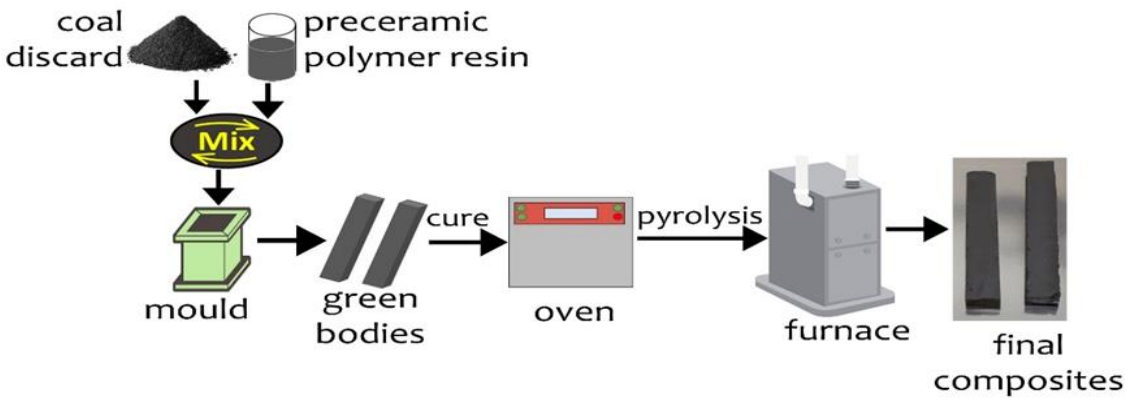



Figure 5-1 Schematic of coal/ceramic composites production

### *5.2.2 Characterisation of coal discard and coal/ceramic composite*

The following techniques were used to characterise the coal discard and the produced coal composites:

(i) Proximate analysis was conducted using approximately one gram of each sample in a thermogravimetric analyser (TGA701, LECO Corp. USA) according to ASTM D5142.

(ii) A benchtop energy dispersive XRF elemental analyser (NEX QC+ QuantEZ) was used to semi-quantitatively determine the major and minor elements of the coal discard.

(iii) Carbon and sulphur content was obtained using a SC-132 analyser (LECO Corp. USA) following the ASTM standard (ASTM D4329, 2018).

(iv) The morphology of the composites was observed under a Sigma 300 VP scanning electron microscope (ZEISS, Germany).

(v) Measurement of water absorption and flexural strength of the composites is described in Eterigho-Ikelegbe et al. (2021b).

(vi) The X-ray diffraction patterns of the powdered coal composites were recorded using a Bruker D2 phaser diffractometer (Bruker Corp., Germany). X-ray source Cu-Kα radiation ($\lambda$ =1.54184 Å) operating at 30 kilovolts and ten milliamperes was used to scan the sample through a 2-theta range from 10° to 70°.

(vii) The thermogravimetric analyser was used to estimate the continuous operating temperature of the composites. For the analysis, one gram of chunk composites was heated in an air atmosphere from room temperature to 950 °C at a ramp rate of 10 °C/min.

(viii) The resistance of the coal composites to different analytical reagent grade chemicals was evaluated according to ISO 10545-13 (2016) for ceramic tiles. The dried composites were immersed in glass bottles containing the chemical for 17 days at ambient temperature and kept covered to minimise evaporation. The chemicals used were:

- ammonium chloride solution (100 g/L (grams per litre))
- hydrochloric acid (18% volume per volume)

- lactic acid solution (5% volume per volume)
- potassium hydroxide solution (100 g/L and 30 g/L)
- citric acid solution (100 g/L)

After immersion, the composites were washed with running water and dried in an oven at 105 °C to a constant weight until the difference between two successive weighings was less than 0.1 g. The chemical resistance of the composites was measured in terms of weight loss using Equation (5-1).

$$Weight\ loss\ (\%) = \frac{W1-W2}{W1} \times 100 \quad (5\text{-}1)$$

where $W1$ and $W2$ are the weights of the composites before immersion and the weight of composites after drying, respectively.

(ix) The efflorescence potential of the coal composites was evaluated according to the ASTM C67 standard test method for structural clay tiles.

## 5.3 Results and discussion

### *5.3.1 Properties of the coal discard samples*

The coal discards differ widely and exhibit different chemical compositions due to the diversity of the coal sources (Table 5-1).

Table 5-1 The major and minor element content of the coal discards

| **Elements (wt.%, a.d.)** | **GTS** | **PCD** | **LCS** |
|---|---|---|---|
| Silicon | 19.65 | 23.56 | 15.68 |
| Aluminium | 10.02 | 10.01 | 9.08 |
| Iron | 9.92 | 6.96 | 9.32 |
| Sulphur | 3.95 | 3.94 | 8.07 |
| Calcium | 5.21 | 3.51 | 7.89 |
| Potassium | 2.05 | 2.17 | 1.48 |
| Titanium | 1.72 | 1.18 | 2.89 |
| Palladium | 0.41 | n.d. | 0.64 |
| Phosphorus | 0.31 | 0.00 | 0.43 |
| Strontium | 0.23 | 0.18 | 0.61 |
| Vanadium | 0.29 | 0.15 | 0.52 |
| Chromium | 0.10 | 0.15 | 0.20 |
| Barium | 0.12 | 0.10 | 0.11 |
| Zirconium | 0.08 | 0.07 | 0.14 |
| Others | 0.38 | 0.25 | 0.49 |
| LOI | 45.56 | 47.78 | 42.46 |

a.d. – air-dried; GTS – Greenside tailing slurry; LCS – Likeflow coal slurry; n.d. – not detected; LOI – loss on ignition PCD – Proteas coal slurry

The data presented in Table 5-1 shows in quantitative terms that the coal discards contain predominantly silicon, aluminium and iron followed by sulphur and calcium in varying quantities. Although the coal discards have similar contents of aluminium, they differ widely in silicon content. This variance is already the first evidence of potential differences in the curing and pyrolysis activity of the three coal/PCP blends. Of the coal discards, PCD has the highest amount of silicon and aluminium combined (33.57%), followed by GTS (29.67%) and LCS (24.76%). The abundance of silicon and aluminium content, especially for PCD, depends largely on the silica minerals (mostly quartz) and aluminosilicates (especially kaolinite) associated with the coal (Huggins, 2002; Mishra et

al., 2016). Due to the refractory nature of quartz, PCD, with the highest content of silicon (23.56%) will degrade at relatively high temperatures compared with GTS and LCS, which contain less silicon. The alkali and alkaline earth metal (potassium + calcium) content in the coal discard average 7.27%, 5.68% and 9.37% for GTS, PCD and LCS, respectively, and are related to the feldspar species in the discard. Feldspar containing coal discard could promote the formation of the glassy or vitreous phase (Nicolas et al., 2020) with the PCP resin during pyrolysis of the mixture. This reaction is important for the densification of coal composites during pyrolysis.

Table 5-2 presents a summary of the physicochemical properties of the coal discard and coal composites. The ash content of PCD (39.76%) compared with GTS (30.69%) and LCS (15.57%) infers that PCD contains a significant amount of refractory and incombustible minerals. It is anticipated that this property might cause PCD to be weakly reactive, leading to a weak bonding interaction between PCD and the PCP resin during pyrolysis. The volatile matter of PCD (10.67%) and LCS (23.72%) infers that PCD and LCS might originate from lean anthracite coal and medium-volatile bituminous coal, respectively (Eterigho-Ikelegbe et al., 2021b). Compared to PCD, the higher volatile matter coal discards (GTS and LCS) could positively influence the reactivity of the mixture during pyrolysis and ultimately on the final properties of the coal composites. From an environmental, scalability and cost perspective, this straightforward technique is attractive because the coal discard does not require a beneficiation process before utilisation to produce the composites. In addition, the carbon within the coal discard is retained in the composites, as seen in Table 5-2.

Table 5-2 Physicochemical properties of the coal discard and coal composites

| Parameters (wt.%, a.d.) | GTS | PCD | LCS | GTS composite | PCD composite | LCS composite |
|---|---|---|---|---|---|---|
| **Fixed carbon** | 43.42 | 45.31 | 56.74 | 41.04 | 45.23 | 54.87 |
| **Volatile matter (M)** | 22.57 | 10.67 | 23.72 | 1.780 | 1.500 | 2.030 |
| **Ash content (Ash)** | 30.69 | 39.76 | 15.57 | 56.22 | 52.67 | 42.41 |
| **Total carbon (C)** | 56.7 | 51.40 | 68.55 | 40.00 | 42.70 | 44.05 |
| **Hydrogen (H)** | 3.24 | 1.64 | 3.67 | - | - | - |
| **Oxygen*** | 6.46 | 2.99 | 7.22 | - | - | - |
| **Total sulphur (S)** | 0.94 | 0.65 | 0.97 | 0.61 | 0.33 | 0.26 |

a.d. – air-dried; GTS – Greenside tailing slurry; LCS – Likeflow coal slurry; PCD – Proteas coal slurry; *Oxygen by difference = [100 - (M + Ash + S + H + C + nitrogen)]

### *5.3.2 Morphological characterisation of the coal composites*

Visualisation of the surface morphology of the composites (Figure 5-2) shows that there is a relationship between the physiochemical properties of the coal discards presented in Table 5-2 and the surface smoothness of the coal composites.

From Figure 5-2, it appears that the surface of the GTS and LCS composites is smoother than that of the PCD composite. The surface unevenness and lack of fusibility of the PCD composite might be related to the physicochemical properties of the coal discard, in particular the oxygen content. As in Table 5-2, the GTS and LCS discards recorded higher oxygen content than PCD. Based on this, it is likely that GTS and LCS are weathered coals and contain a significant amount of oxygen functional groups (Gao et al., 2017; Jian et al., 2019; Nicolas et al., 2020). It could also suggest that GTS and LCS discards likely contain more vitrinite (reactive macerals), whose chemical structure is generally characterised by relatively high oxygen content compared to other maceral groups (Whitehurst, 1978; ICCP, 1998; van Niekerk, 2008; Roberts, 2015). Based on this,

it is possible that coal discard with significant vitrinite maceral and oxygen functional groups, especially if the groups are polar such as hydroxyl or carboxyl, could have enhanced reactivity (Ahamed et al., 2019; Jian et al., 2019) with the PCP during the curing and pyrolysis stages of the blend production. This phenomenon might be responsible for the good fusibility and smooth surfaces of these composites (GTS and LCS). In summary, since the major raw material of the blend is coal discard, to produce composites of satisfactory fusibility and low surface roughness, it is deemed necessary to select coal discard with a significant oxygen content for this process.

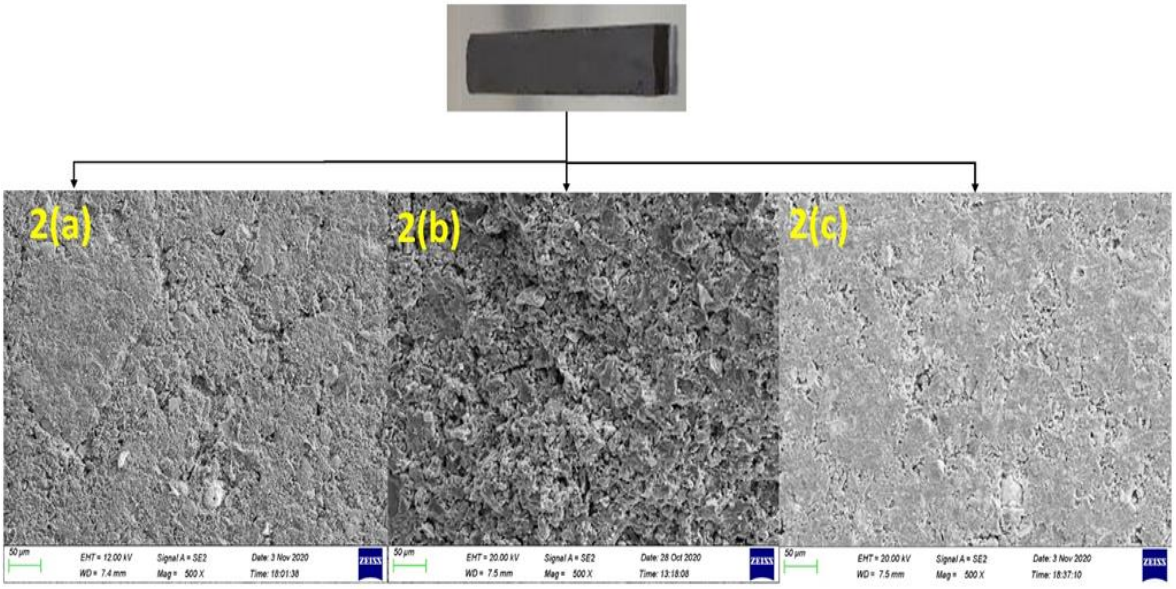



Figure 5-2 Scanning electron microscopy images of the (a) Greenside tailing slurry, (b) Proteas coal discard and (c) Likeflow coal slurry composites

### *5.3.3 Flexural strength and water absorption properties*

High-quality coal composites proposed for use as building materials must be able to satisfy specifications for flexural strength and water absorption. Flexural strength is a parameter used to determine the strength requirement for building materials. For example, ISO 15045-4 (2019) specifies that the minimum average flexural strength for ceramic tiles should be 35 MPa. Three flexural tests were performed on each composite and the

mean values plotted on a bar chart are presented in Figure 5-3. It can be seen from the figure that the PCD composite fails to meet the ISO requirement. However, the flexural strength of the GTS and LCS composites recorded 36.46 MPa and 35.23 MPa respectively, exceeding the 35 MPA requirement for ceramic tiles.

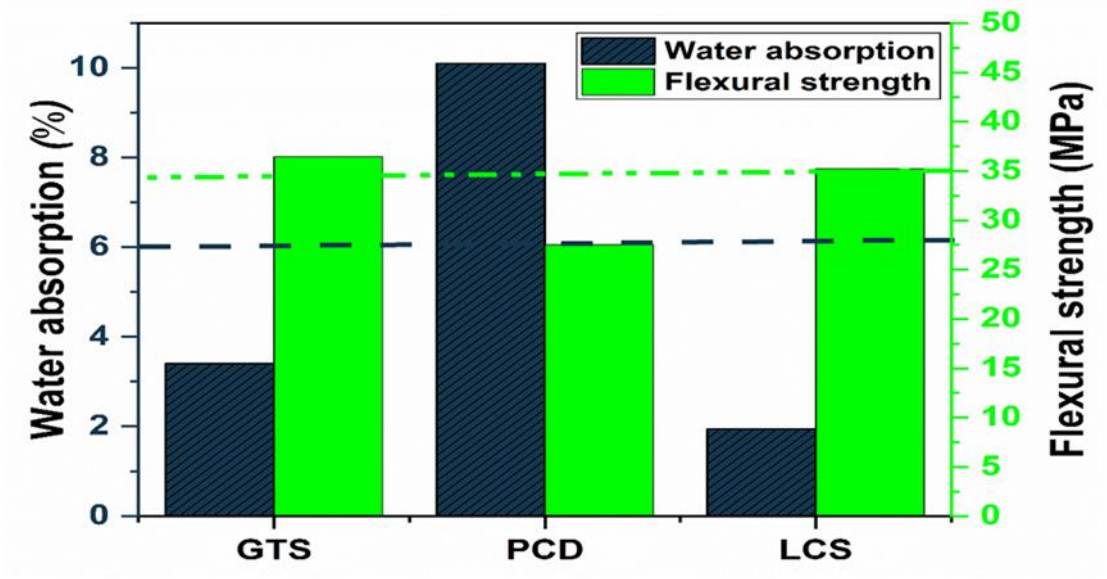



Figure 5-3 Water absorption and flexural strength properties of the composites
(GTS – Greenside tailing slurry; PCD – Proteas coal discard; LCS – Likeflow coal slurry; dotted lines represent the standard cut-off)

A water absorption test provided valuable information on the degree of compactness of the composites. Based on the standard for clay roof tile, the water absorption must not exceed 6% (ASTM C1167; ASTM C373; Taha et al., 2017). Figure 5-3 shows that the GTS (3.4%) and LCS (1.94%) composites recorded lower water absorption than the PCD composite (10.1%). In general terms, the GTS and LCS composites with water absorption that meet the ASTM C1167 standard displayed higher strength. This trend is similar to observations by other researchers (Phonphuak & Thiansem, 2011; Rahman et al., 2015; Yagüe et al., 2018).

Composites GTS and LCS, which meet the required ASTM C1167 standard for water absorption, may have more compact structures. This could be used as a good indicator for predicting the durability of the composites in terms of efflorescence and frost resistance (Eliche-Quesada et al., 2011; Makarov et al., 2019). The superior water absorption and flexural strength properties of the GTS and LCS composites over the PCD composite can be explained based on the studies by Hill and Easter (2019) and Hu et al. (2017). These authors reported that the molecules of low-ranked or weathered coals are rich in hydrogen bonds that could easily be broken to form hydrogen bonds with other materials. As stated previously, the hydrogen content of the PCD (1.64%) reflects that this coal discard might contain a low amount of hydrogen-bonded structures required to form adequate interactions with the PCP resin during pyrolysis. Furthermore, it has been reported that hydrogen bonding probably accounts for the glassy properties of coal (Painter et al., 1987; Painter et al., 2010). Therefore, the ability of the mixture to generate a glassy phase during pyrolysis would enhance the fusibility and compaction of the mixture. Hence, the LCS composites conforming well with the ASTM C1167 standard specification might be a result of the glassy phase formed during the pyrolysis of LCS coal discard and the PCP resin. This is evidenced in the broad hump around 2-theta = 24° of the XRD patterns of the composites (Figure 5-4). Taha et al. (2017) reported that the formation of the glassy phase positively affects the mechanical strength of ceramic composites from coal.

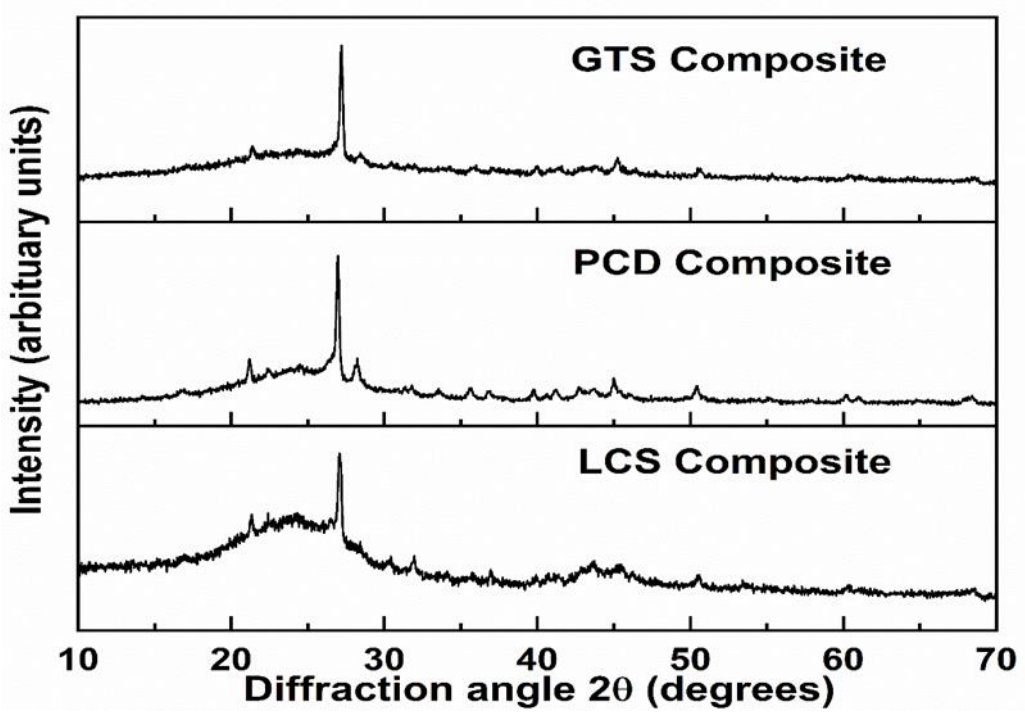



Figure 5-4 X-ray diffraction patterns of the composites

(GTS – Greenside tailing slurry; PCD – Proteas coal discard; LCS – Likeflow coal slurry)

### *5.3.4 Continuous operating temperature*

The extent of the degradation of one gram of chunk coal composites heated in a thermogravimetric analyser under an air atmosphere from 25 °C to 900 °C until constant weight loss is depicted in Figure 5-5a and b. As with sintered ceramic, polymer-derived ceramic or ceramic composites produced from PCP resins are notable for displaying high heat resistance (Ionescu et al., 2010; Ding et al., 2012; Fonblanc et al., 2018; Shen et al., 2018). Therefore, it was anticipated that the composites produced in this study would display appreciable heat resistance.

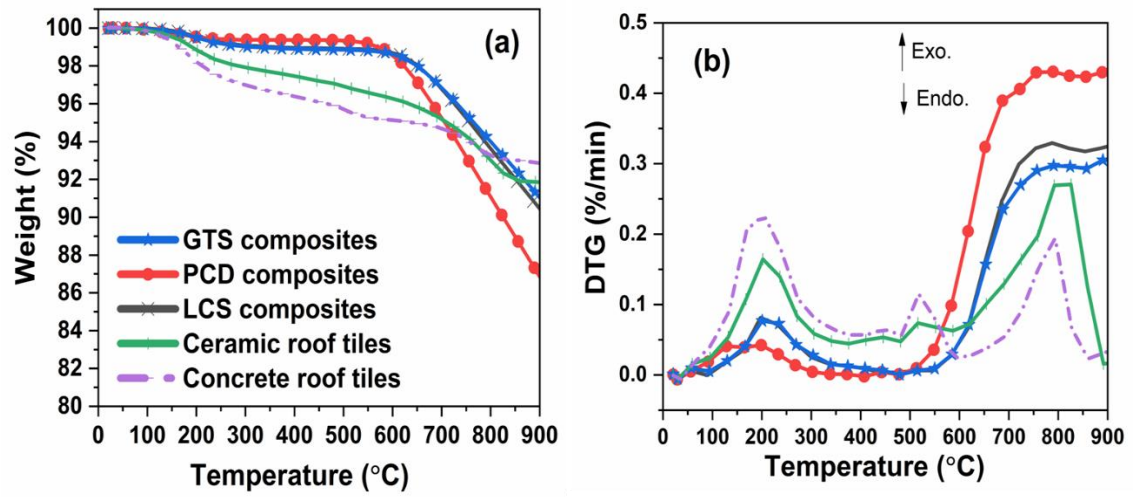



Figure 5-5 (a) Weight loss curves and (b) derivative thermogravimetric (DTG) curves of coal discard composites and conventional roof materials

(GTS – Greenside tailing slurry; PCD – Proteas coal discard; LCS – Likeflow coal slurry)

Weight loss in all the samples occurred in two separate stages. No significant change in weight was noted between 25 °C and 125 °C, whereas above 125 °C, a pronounced degradation in the molecular structure of the conventional roof tiles is observed compared to the coal composites. The peaks at 200 °C (Figure 5-5b) indicate that the coal composites contain fewer volatile compounds than the conventional materials. This observation agrees with the data presented in Table 5-2. Of the three composites, the PCD composite has the lowest volatile matter after devolatilisation. The coal composites are also noted to be more stable up to 600 °C, with about 99% of the original mass of the composites remaining (Figure 5-5a). It can be deduced that the compact structure of the GTS and LCS composites, as confirmed by their low water absorption values, might be responsible. In addition, the ceramic phases formed during the pyrolysis could have contributed to the heat resistance nature of the composites up to 600 °C. The dramatic weight loss experienced by the PCD composite above 600 °C

(Figure 5-5a) could be a result of a loosely compacted structure (bonding) as explained under the morphological characterisation section.

The weight loss of the composites at 900 °C and the temperature at 5% weight loss (T5%) extracted from the thermograms are presented in Table 5-3. The T5% of the coal/ceramic composites is slightly higher than the conventional roofing tiles, confirming their superiority and that thermally stable structures were indeed formed. Furthermore, the percentage weight loss of the composites is comparable with that for the conventional materials after being subjected to thermal degradation up to 900 °C, with PCD displaying the highest degradation of 13%.

Overall, the results demonstrate that the coal composites are superior to conventional roof tiles at temperatures up to 600 °C. The thermal degradation in this range indicates the suitability of the composite as building materials, such as roof tiles, bricks, or panels. In addition, the impressive resistance of the composites to degradation at temperatures up to 600 °C could be considered a desirable property for fire-resistant construction materials.

Table 5-3 Summary of data extracted from the weight loss curves in Figure 5-5a

| **Data** | **GTS** | **PCD** | **LCS** | **Ceramic roof tiles** | **Concrete roof tiles** |
|---|---|---|---|---|---|
| **Temperature at 5% weight loss (°C)** | 765.0 | 706.3 | 757.0 | 704.6 | 671.0 |
| **Weight loss at 900 °C (%)** | 8.9 | 13.0 | 9.4 | 8.1 | 7.1 |

(GTS – Greenside tailing slurry; PCD – Proteas coal discard; LCS – Likeflow coal slurry)

### *5.3.5 Chemical resistance*

The ability of the coal composites as potential building materials to resist degradation or physical corrosion caused by chemical media attacks is of paramount

importance. To confirm this, the composites were exposed to different chemical reagents for 17 days to evaluate their chemical resistance (Figure 5-6).

Table 5-4 provides valuable information on the compatibility of the coal composites in different chemical environments. The results show that the coal composites are moderately affected by base solutions and least affected by acid solutions. This indicates that the bonds of the coal composite structure are more resistant to attack or diffusion of chlorine and hydrogen ions than hydroxide ions. In contrast, conventional roofing materials displayed limited resistance to acidic solutions, as indicated by high-level deterioration and significant weight loss.

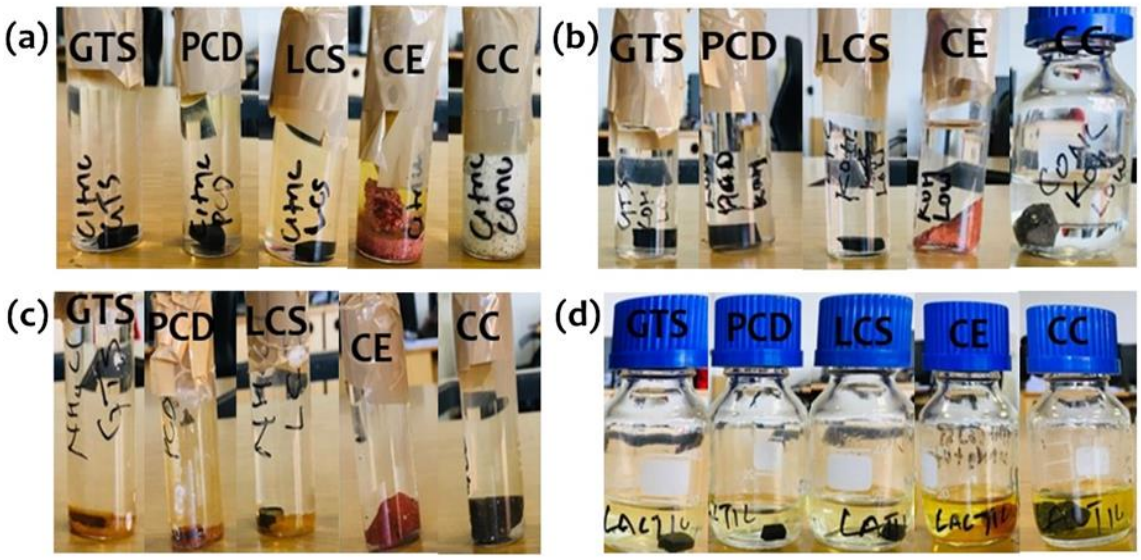



Figure 5-6 Coal composites and conventional roof tiles exposed to different chemicals: (a) citric acid, (b) potassium hydroxide, (c) ammonium chloride and (d) lactic acid solution

(GTS – Greenside tailing slurry; PCD – Proteas coal discard; LCS – Likeflow coal slurry; CC – Concrete; CE – Ceramic)

Table 5-4 Chemical resistance performance of coal composites and conventional roof tiles

| **Medium/Composite** | **Chemical resistance (%)** | | | | |
|---|---|---|---|---|---|
| | **GTS** | **PCD** | **LCS** | **Ceramic roof tile** | **Concrete roof tile** |
| Ammonium chloride solution (100 g/L) | 99.92 | 98.77 | 99.38 | 96.83 | 90.65 |
| Hydrochloric acid solution (18 % V/V) | 97.76 | 97.22 | 99.21 | 71.05 | 67.82 |
| Citric acid solution (100 g/L) | 99.74 | 98.44 | 99.41 | 72.88 | 77.68 |
| Lactic acid solution (5% V/V) | 98.02 | 97.46 | 99.26 | 79.83 | 82.84 |
| Potassium hydroxide solution (100 g/L) | 94.43 | 94.57 | 97.95 | 99.97 | 99.54 |
| Potassium hydroxide solution (30 g/L) | 95.79 | 96.55 | 99.98 | 99.45 | 99.39 |

(GTS – Greenside tailing slurry; PCD – Proteas coal discard; LCS – Likeflow coal slurry)

Interestingly, the chemical resistance of the coal composites can be correlated with the amorphous degree of the composites (XRD spectra in Figure 5-4). This amorphous peak, which was attributed to the presence of glassy-like structures (Eterigho-Ikelegbe et al., 2021b), is more noticeable in the LCS composites. The amorphous nature of the LCS composites could have been responsible for the unprecedented chemical stability (99.21% to 99.98%) compared to the GTS and PCD composites. Furthermore, we recorded the porosity of the GTS, PCD and LCS composites to be 7.22%, 17.08% and 3.44%, respectively (Eterigho-Ikelegbe et al., 2021b). Therefore, composites with porosities that meet the ASTM C1167 standard may have restricted chemical absorption. Thus, in addition to the porosities of the GTS and LCS composites that meet the ASTM C1167 standard, the stabilised bond network of these composites (as mentioned earlier) possibly serves as a protective mechanism against weight loss caused by chemical attack. The results mean that little to no chemical activity took place at the material-solution

interface during the immersion in the solutions, making the composites ideal for long-lasting performance.

Equally important, the physical appearance and colour changes of the reagents at the end of the test validated the superiority of the coal discard composites to chemical attack. It was observed that the colourless chemical solutions remained unchanged after testing. In terms of the physical appearance of the composites, we also observed no surface damage or visual corrosion effects. In contrast, the conventional roof materials formed solid sediments, and the appearance of the clear, colourless chemical solution altered, especially the acid solutions. Admittedly, the composites must be checked to see whether they retained their mechanical strength, water resistance absorption and thermal resistance. In conclusion, the results so far present the first evidence that coal discard composites would perform well in aggressive environments. They may not require additional surface protection coating, additives, or inhibitors to prevent degradation.

### *5.3.6 Efflorescence*

Construction products are exposed to water for long periods, which could result in functional or aesthetic deterioration. Therefore, the efflorescence potential of as-produced coal composites was analysed according to the ASTM C67 standard. This test was performed to assess the potential for migration of water-soluble salts to the composites' surface. To simulate realistic conditions, the coal composites were partially immersed in distilled water for seven days at ambient temperature and then dried in an oven for 24 hours. Based on visual inspection of the faces of the tested composites compared to freshly produced composites, there was no deposition of white deposits (crystalline salts) on the surface. The absence of crystalline salts suggests that the composites contain no soluble salts. This indicates that calcium-containing compounds

such as calcium hydroxide and/or calcium oxide that cause efflorescence are not present in the composites. According to Ibraeva et al. (2017), the migration of soluble salts could weaken the binding network of structural bodies and deteriorate the technical and aesthetic performance of building materials. Furthermore, it should be noted that there was no significant change in the weight and dimension of the coal composites after the efflorescence experiment. This indicates that they are of good quality and can be classified as ‘not efflorescent’.

## 5.4 Conclusions

This study provides additional information on the properties of coal ceramic composites produced using South African coal discards and a polysiloxane PCP resin. The composites displayed excellent resistance to different chemical solutions, are stable at operating temperatures up to 600 °C and contain no soluble salts. Regarding suitability for blending with polysiloxane PCP resin, the high-ash and quartz-rich coal discard (PCD) was deduced to be only weakly reactive until a relatively high temperature is achieved. This resulted in composites with weak molecular bonding. On the other hand, the GTS and LCS coal discards formed composites of good quality that meet building material standards. Coal/ceramic composites that meet or/and exceed building material requirements may also be obtained by investigating other coal discard stockpiles in South Africa and PCP resins. The interesting properties of the coal composites reported in this study indicate that this innovative approach could bode well for avoiding the environmental impact of coal discard and for producing environmentally friendly composite materials for construction applications.

# 6 Mechanism of bonding, surface property, electrical behaviour, and environmental friendliness of carbon/ceramic composites produced via the pyrolysis of coal waste with polysiloxane polymer

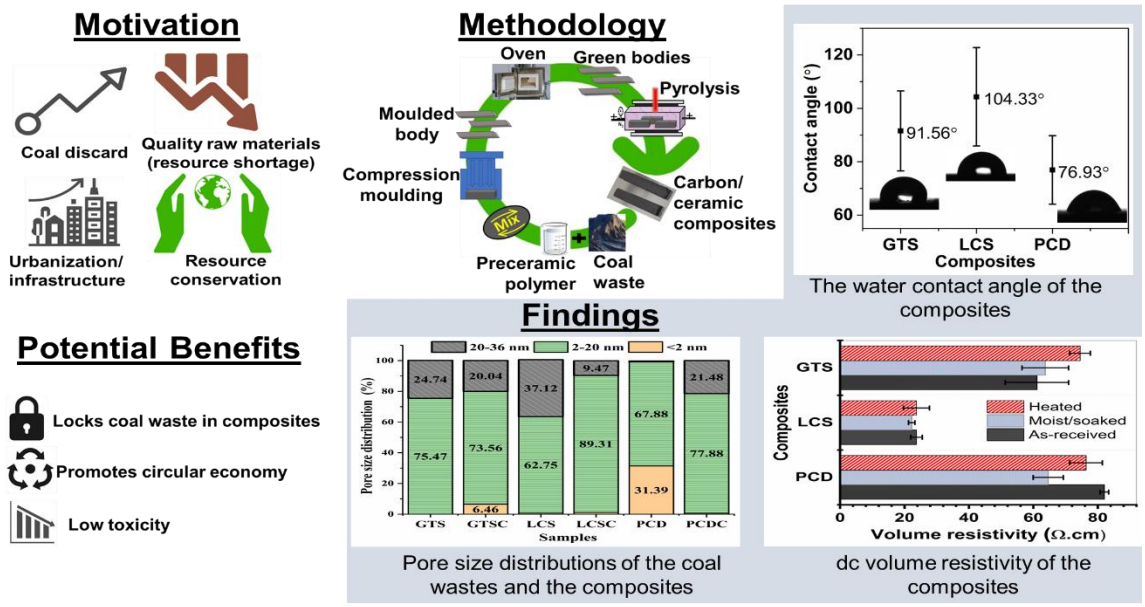
This chapter is published in:

**Eterigho-Ikelegbe, O.**, Trammell, R., Ricohermoso, E., & Bada, S. (2023). Mechanism of bonding, surface property, electrical behaviour, and environmental friendliness of carbon/ceramic composites produced via the pyrolysis of coal waste with polysiloxane polymer. *Environmental Science and Pollution Research*, *30*(41), 93786–93799. https://doi.org/10.1007/s11356-023-28661-z

## Preamble

The proposed mechanism of bonding between coal waste and the preceramic polymer is presented. The combination of analytical techniques such as RAMAN spectroscopy, Brunauer-Emmett-Teller nitrogen adsorption, direct current volume resistivity, water contact angle, and environmental friendliness (leaching studies) were used to evaluate coal composites produced from three different South African coal wastes and Semplastics formulated preceramic polymer (X-MAT®) as the ceramic-forming binder. This chapter addresses research question (iii).

## Graphical Abstract




The water contact angle of the composites

Pore size distributions of the coal wastes and the composites

dc volume resistivity of the composites

**Abstract**

A simple mixing-pressing followed by thermal curing and pyrolysis process was used to upcycle coal waste into high-value composites. Three coal wastes of different physicochemical properties were investigated. The hypothetical mechanisms of bonding between the coal particles and the preceramic polymer are presented. The textural properties of the coals indicated that the lowest volatile coal waste (PCD) had a dense structure. This limited the diffusion and reaction of the preceramic polymer with the coal waste during pyrolysis, thereby leading to low-quality composites. The water contact angles of the composites up to 104° imply hydrophobic surfaces, hence, no external coating might be required. Analysis of the carbon phase confirmed that the amorphous carbon structure is prevalent in the composites compared to the coal wastes. The dc volume resistivity of the composites in the range of 22 to 82 ohms centimetre, implies that the composites are unlikely to suffer electrostatic discharge, which makes them useful in creating self-heating building parts. The leached concentrations of heavy metal elements from the composites based on the end-of-life scenario were below the Toxicity Characteristic Leaching Procedure regulatory limits. Additionally, the release potential or mobility of the metals from the composites was not influenced by the pH of the eluants used. On the basis of the reported results, these carbon/ceramic composites show tremendous prospects as building materials due to their properties.

**Keywords:** Circularity, Coal waste, Contact angle, Leaching, Recycling, Waste utilisation

## 6.1 Introduction

The beneficiation of run-of-mine coal to produce clean coal for power and metallurgical applications and mechanised mining generate coal waste. According to the National Development and Reform Commission of China, the country has already accumulated over 4.5 Gt of coal gangue, which is growing annually with an increase of 370 to 550 Mt (Yang et al., 2018). In South Africa, approximately 60 Mt of coal waste is produced annually with an accumulation already over 1 Gt (Belaid et al., 2013; Isaac & Bada, 2020). Therefore, it can be anticipated that if the global coal demand flattens to around 7.4 Gt by 2025 as predicted by the IEA (IEA, 2020), the amount of coal waste is likely to increase. Unfortunately, only a small proportion of this coal waste is processed into high-value, high-performance products. The remainder is traditionally disposed of in landfills or piled up in arable land, resulting in unintended health, safety, and environmental impacts. While interventions like remediation and reclamation solutions such as mine backfill have evolved significantly, these solutions leave behind risks and liabilities. In addition, their long-term effect is not guaranteed (Lottermoser, 2011; Broadhurst et al., 2019; Zhang & Ling, 2020). Therefore, given the enormous volume of coal waste, immense research attention is devoted to valorisation in line with the objectives of the circular economy model and sustainable development.

Significant research exists in the field of valorisation of coal waste, which includes the synthesis of porous materials for natural gas storage and energy storage, coal briquettes and pellets production, carbon fibre, rare earth extraction, etc. (Abdulsalam et al., 2019, 2020a, b; Eterigho-Ikelegbe et al., 2021a, b, c; Harrar et al., 2022). Of these research fields, recycling coal waste into composites stands out because it is possible to consume huge quantities of coal waste to produce high-volume composites, thus,

preventing their accumulation. Furthermore, composite technologies have been at the forefront of developing advanced materials in recent years, resulting in considerable research attention. This is because composite technology allows the combination of different materials to form products of superior properties compared to products of unit material. Hence, most electronic components, megastructures, sports and packaging equipment, automotive parts, biomedical facilities, construction, etc., are composites (Mohanty et al., 2018; Rajak et al., 2019).

On the other hand, preceramic polymers (PCPs), otherwise known as silicon-based polymers, have been successfully explored to fabricate polymer-derived ceramic (PDC) parts and ceramic matrix composites for more than four decades (Colombo et al., 2010; Ionescu et al., 2010). The PCP route is preferably pursued to realise complex-shaped ceramic bodies and metastable inorganic network structures at relatively low processing temperatures (Colombo et al., 2010; Ding et al., 2012; Ricohermoso et al., 2022). The molecular structure, chemistry and heat treatment conditions of these polymers can be modified to produce custom-made amorphous or nanocrystalline microstructure PDCs of interesting features (Bhandavat et al., 2012; Fonblanc et al., 2018; Shen et al., 2018). Ceramic parts produced via the PCP route include but are not limited to fibres, coatings, energy storage materials, films, monoliths, catalyst support, microelectromechanical systems, and so more (Mutin & Boury, 2003; Colombo et al., 2010; Shen et al., 2018; Wen et al., 2020; Ricohermoso et al., 2021). The PCPs, polysiloxanes, are generally stable in the air and a humid atmosphere, making them easy to manipulate. These polymers are thermally stable, produce no toxic decomposition products, industrially available and inexpensive to produce (Walter et al., 1996; Cordelair & Greil, 2000). Shen et al. (2018) reported the structure of the polysiloxane-derived

ceramic contains nanodomains of silicon dioxide surrounded by carbon nanodomains. This attribute imparts the ceramic with unprecedented chemical and thermal stability, low density and good mechanical properties.

The world's population is expected to quadruple to more than 9.7 billion by 2050 (OECD, 2015). As a result, there is an imminent depletion of building raw materials that are likely to become expensive due to high demand and high energy prices. The material-intensive building industry must, therefore, consider technological waste and composites as an effective strategy to address these challenges. Recently, an innovative approach for producing structural carbon/ceramic composites from two different United States bituminous coal using the polysiloxane PCP as a binder for the coal particles was documented (Hill & Easter 2021; Sherwood et al. 2021). The investigators reported that the lower-grade coal yielded composites of higher linear shrinkage (19.4%) and lower char yield (68.3%). In contrast, the higher-grade coal yielded superior composites of linear shrinkage and char yield of 18% and 80%, respectively. The higher-grade coal contained low volatiles and was less absorbent to the PCP resin than the lower-grade coal. In terms of weight and strength, the higher-grade coal resulted in a lighter and higher-strength composite than the lower-grade coal. Furthermore, a fire test conducted using a propane torch could not cause significant damage to the composites, reflecting their excellent fire resistance. These positive inherent properties of the composites prompt their suitability as a prime alternative to building materials, such as conventional bricks, blocks, panels, roofing sheets and even wood polymer composites.

But variations in the origin, vegetation, and climatic conditions at the time of coal formation, together with subsequent events in the geological history of coal coalification, give rise to coal with different compositions (Falcon, 1986). Interestingly, most South

African coals are bituminous rank (medium rank C) and are of low-sulphur content, but higher in ash and inert organic matter content (inertinite-rich) compared to the northern hemisphere coals (Falcon, 1986; Hancox & Götz, 2014). It is therefore important to match coal or coal waste for specific fields of utilisation because of the differences in the organic and inorganic composition of these coals (Falcon, 1986). Instead of using bituminous coal from the United States, we proposed to investigate South African coal waste (Eterigho-Ikelegbe et al. 2021b). The composites produced by the investigators (Hill & Easter 2021) using different South African coal wastes but with the same procedure and PCP showed that coal waste coded PCD (hydrogen/carbon ratio of 0.34) produced composites with the least desired properties. Specifically, the GTS coal waste manifested the highest hydrogen/carbon ratio of 0.72 and produced good quality composites with a flexural strength of 36.46 MPa and water absorption of 3.40%. In general, water absorption as low as 1.94 to 10.1% and flexural strength in the range of 27.51 to 36.46 MPa was obtained (Eterigho-Ikelegbe et al. 2021b). These values fulfil the requirement or standard specification expected of some building materials, such as ceramic tiles and clay roof tiles. The composites also displayed thermal stability in air and nitrogen atmosphere up to 600 °C and chemical resistance up to 99.97%. It was further shown that most of the carbon in the coal waste was trapped in composites.

This new, yet straightforward technological concept of combining coal waste and PCP to produce composites is a great way to consume a large amount of coal waste. From a social and environmental perspective, this technology concept has several merits, including a reduction in natural resource consumption, a new resource base for building materials, and a reduction in the carbon footprint of coal waste. Furthermore, the concept advances the United Nations Sustainable Development Goals 9, 11 and 12 leading to

2030. Based on this background, this study set forth to shed light on the bonding mechanism between coal waste and the preceramic polymer resin towards the production of carbon/ceramic composites. We investigated the textual properties of the composites compared to the raw coal samples and the surface property of the composites was evaluated using the adsorption of deionised water as the polar liquid to measure the contact angle. Raman spectroscopy was employed to systematically study the graphitisation degree of the carbon phase in the composites and to understand the composites' electrical resistivity behaviour. Finally, using coal waste to produce composites might pose exposure risks of heavy metal elements to the environment and human health when disposed of. As such, the comparison of the leached concentrations of heavy metal elements from the composites to standard leachable concentration thresholds was documented.

## 6.2 Materials and methods

### *6.2.1 Materials*

Coal wastes tagged GTS, PCD and LCS were collected from the KwaZulu-Natal and the Witbank coalfields of South Africa. The assessment of the physicochemical characteristics of the coal wastes (Figure 6-1) shows that PCD has the lowest volatile matter (10.67%) and highest ash content (39.76%) while LCS has the highest fixed carbon (56.74%). The particle size of the coal wastes is such that 80% is less than 45 µm. The ceramic-forming polymer used as the binder for producing the carbon/ceramic composites is a polysiloxane PCP specially formulated by XMAT®, the Advanced Materials Division of Semplastics (Florida, United States). The polysiloxanes are composed of repeated -silicon-oxygen- units (inorganic network) as the backbone and

$CH{=}CH_2$, $H_2$ or $CH_3$ as the organic constituents or side groups attached to the silicon atom.

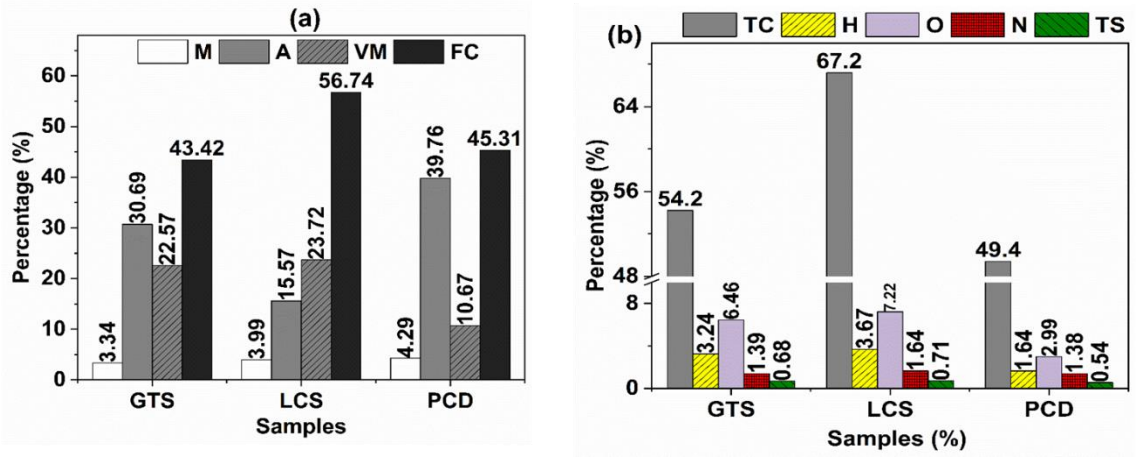



Figure 6-1 Assessment of the physicochemical characteristics of the coal wastes (air-dried) (a) Proximate analysis (b) Ultimate analysis

M: inherent moisture; A: ash content; V: volatile matter; FC: fixed carbon; TC: total carbon; TS: total sulfur; O: oxygen; O: by difference as [100-(M + Ash + C + H + N + S)]; FC: by difference as [100-(VM + Ash + M)]

### *6.2.2 Preparation of the carbon/ceramic composites*

The pulverised coal waste and the liquid PCP resin were sufficiently blended at a predetermined ratio in a mixer to wet the coal particles and fill the voids between the particles. The mouldable mixture is then uniaxially pressed into moulds like standard clay tiles to produce bodies with controlled geometries. The moulded bodies were cured in an oven at 150 °C and the cured bodies were pyrolysed in a retort furnace under a nitrogen atmosphere up to 1000 °C, maintaining the maximum temperature for ten hours. The furnace was allowed to cool to room temperature when the pyrolysis is complete and the cooled composites were analysed and tested. The detailed description of the production of the carbon/ceramic composites is presented in Eterigho-Ikelegbe et al. (2021b). Figure 6-2 displays a summary of the schematic production process of the carbon/ceramic

composites and Figure 6-3 shows the pictorial images of the produced carbon/ceramic composites.

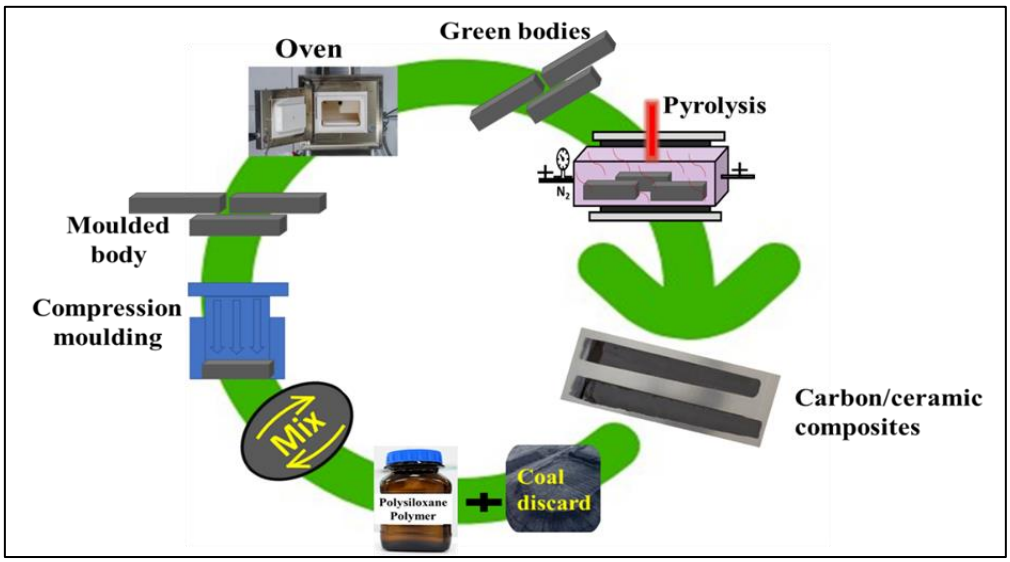



Figure 6-2 A summary of the production of the carbon/ceramic composites

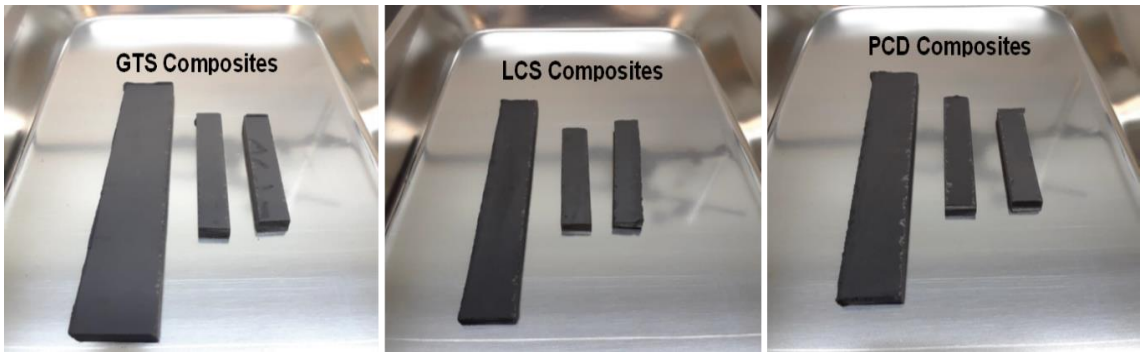



Figure 6-3 Pictorial images of the carbon/ceramic composites

## 6.3 Characterisation and testing

### *6.3.1 Textural properties of the coal samples and the carbon/ceramic composites*

The evaluation of the textural properties of the crushed coal waste and the produced composites was based on Brunauer-Emmett-Teller (BET) nitrogen adsorption analyses of the degassed done at 77 Kelvin. An Autosorb iQ gas sorption instrument (Quantachrome Instruments, United States) with Quantachrome® ASiQwinTM software interfaces the Autosorb iQ to a computer to enable data acquisition and reduction. The

pore size distribution was calculated from the nitrogen adsorption data based on the non-local density functional theory calculation model.

### *6.3.2 Wettability evaluation*

The contact angle measurement device (OCA 15EC goniometer, DataPhysics instruments, GmbH, Germany) equipped with a microsyringe and a high-speed camera provided information about the wetting property (static contact angle) of the composite surface. The surface of the composite was dosed using deionised water at ambient conditions (dosing volume = 3 μL (microlitre); dosing rate = 2 μL/s (microlitre per second) from the syringe prior to measurement. Eight drops at different spots (top and reverse faces) of the composites were recorded after ten seconds and the average value was reported.

### *6.3.3 Form of carbon/Raman analysis*

The microcrystalline carbon structure, such as the degree of ordering and graphitisation of carbon in the coal and composites was characterised using Raman spectroscopy. Raman spectra were obtained for fine samples of the coal and composites using the excitation laser wavelength 514.5 nanometre (nm) line of the Lexel Model-95 SHG argon-ion laser. The instrument is integrated into a Horiba LabRAM HR Raman spectrometer fitted with an Olympus BX41 microscope and the data were acquired using LabSpec v.5 software.

### *6.3.4 Electrical resistivity measurement*

The direct current (dc) volume resistivity of the composite was obtained using a multifunctional resistance analyser (1623-2 Earth Ground Tester, Fluke Corp. United States) in a four-point probe configuration, to gain insight into the electrical properties of

the carbon/ceramic composites. The measurement range of the equipment for our four-point resistance is 0.02 - 19.99 kiloohm (kΩ). A test voltage of 20 volts (V) was applied to measure the volume resistance of the composites. The probe was held firmly to the surface of the composite for 60 seconds and the distance between probes was separated by one-third of the total length of the composite (Figure 6-4). The applied current comes in and out of the composites through the outer probes. The mean representative resistance from five electrical resistance measurements was used to calculate the bulk (volume) resistivity following Equation (6-1).

$$R_C = 2л.a.R_E \quad (6\text{-}1)$$

where $R_C$ is the bulk or volumetric resistivity (Ω.cm) of the composites, $a$ is the probe distance (cm), and $R_E$ is the measured resistance (Ω).

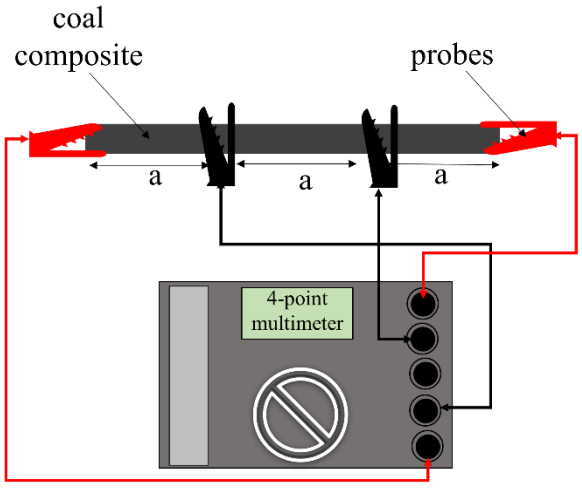



Figure 6-4 Arrangement of the four-point probe resistance measurement of the carbon/ceramic composites

### *6.3.5 Environmental friendliness of the composites*

The end-of-life leaching behaviour of crushed composites was conducted under laboratory conditions using acetate buffer and deionised water as the eluants to determine

the mobility of heavy metal elements. The eluant was added in a liquid-to-solid ratio of 20 mL/g (millilitre per gram) dry matter. The deionised water had a pH of 7.92 while an acetate buffer had a pH of 4.94. The acetate buffer pH was prepared based on Toxicity Characteristic Leaching Procedure (TCLP; US EPA Method 1311, 1992). 5.7 mL glacial acetic acid was added to approximately 900 mL of water to which 64.3 mL of one mole per litre sodium hydroxide solution was added. This solution was then diluted to 1 L with water and thoroughly mixed. The liquid/solid mixture prepared in screw cap bottles was continuously rotated at 30 revolutions per minute for 18 hours using a roller mixer. Thereafter, the mixture was filtered over a 0.45 µm syringe filter to separate it from the solid phase. The pH value and the electrical conductivity of the eluates were recorded using the pH meter and conductivity meter (SevenCompact$^{TM}$ S220 and S230, Mettler-Toledo, GmbH). Inductively coupled plasma-mass spectrometry was subsequently used to determine the concentration of arsenic, barium, cadmium, chromium, lead, zinc, mercury, and selenium in the eluates. The concentrations of inorganic anions – chloride, fluoride, and sulphate were determined using ion chromatography. The results were then compared with the specified TCLP regulatory levels of heavy metal elements (US EPA 1992) and leachable concentration threshold (LCT) from the South African National Environmental Management Waste Act (NEMWA) (Molewa 2013). The end-of-life composite waste is considered hazardous if the determined concentrations of the metals in the eluates exceed both standard levels.

## 6.4 Results and discussion

### *6.4.1 Mechanism of bonding*

As highlighted in Section 6.2, the blend of coal waste and the polysiloxane polymer was pressed into a mould and thermally cured. Crosslinking via an addition

mechanism of the different molecular, reactive and/or functional groups in the blend is activated to yield a weakly bonded body during curing. At the early stage of pyrolysis (150 to 600 °C) of the cured composites under a nitrogen atmosphere, polycondensation and other molecular reactions occur between the coal particles and the PCP. This is accompanied by the release of some of the PCP's side chain groups, hydroxyl structural groups in the raw materials, low molecular weight volatiles in coal, and the volatilisation of the silicon oligomers (Shibuya et al., 2007). As the pyrolysis progresses (at temperatures greater than 600 °C), the bonds in the coal particles are severed and polysiloxane degradation leads to a series of consecutive cleavage of the Si-O, Si-C, C-C, C=H, C-O, O-H and C-H bonds within the mixture. This causes complex recombination reactions between the silicon radicals and the reactive/decomposition products from the mixture. As the constituent of the coal undergoes vitrification and/or mineralisation, the organic components of the PCP transform into inorganic ceramic and graphitised carbon sandwiched into the coal's carbon matrix to obtain dense carbon/ceramic composites. According to Hill and Easter (2021), the illite and kaolinite in the coal mineralise into silica and alumina nanoparticles during pyrolysis. Both the mineralisation (i.e., devolatilisation) and ceramisation process of the raw materials manifest as mass loss and dimensional shrinkage experienced by the body during pyrolysis.

The combination of reactions between the coal particles, the carbon and other moieties of the polysiloxane polymer produces new phases and free carbon embedded in a carbon matrix. Most likely some silicon carbide nanocrystals and nanodomains of silicon dioxide that are surrounded by carbon domains could have been formed as pyrolysis of polysiloxanes is known to result in their growth (Pan et al., 2017; Shen et al.,

2018). Figure 6-5 shows the hypothetical mechanism for composites production from coal waste and PCP resin. $R^1$ and $R^2$ are referred to as organic groups, such as methyl, phenyl, hydrogen, etc., bound to the silicon atom of the PCP. The polar and carbonyl groups in the coal waste react with these organic groups and other constituents of the PCP via hydrogen bonds during curing and pyrolysis to form the carbon/ceramic composites.

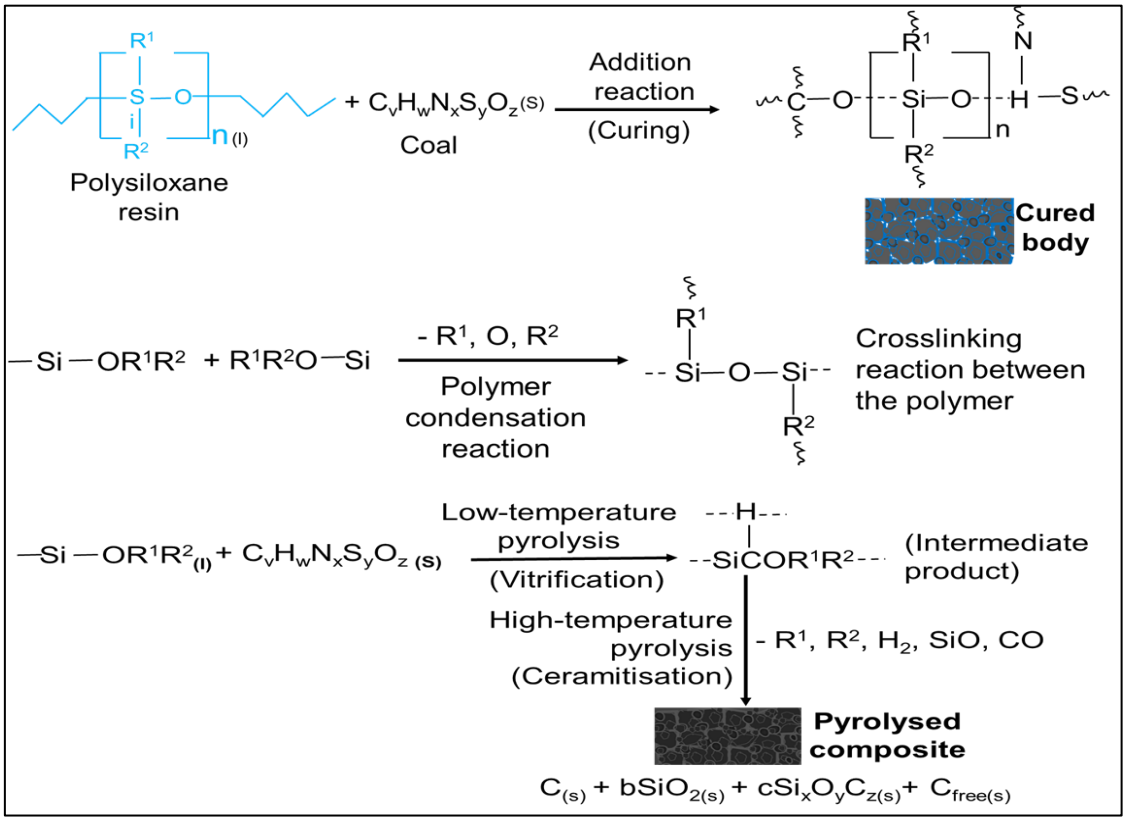



Figure 6-5 Hypothetical mechanisms of the curing and pyrolysis of coal waste and the polysiloxane preceramic polymer

### *6.4.2 Textural analysis of the coal samples and carbon/ceramic composites*

Coal is a heterogeneous material with intrinsic organic and inorganic properties that can influence the textural properties of the composites produced. For instance, the pore network of coal could limit the mass transport, reactivity and diffusivity between coal and the PCP during pyrolysis. Therefore, nitrogen gas physisorption measurements were conducted to characterise the textural properties of the coal samples and

carbon/ceramic composites. Figure 6-6 displays the pore size distribution of the coal waste and the carbon/ceramic composite ceramics based on the density functional theory calculation model. Table 6-1 tabulates the Brunauer-Emmett-Teller surface area, average pore diameter, and total pore volume of the coal samples and respective carbon/ceramic composites.

Table 6-1 Textural information of the coal samples and the carbon/ceramic composites

| Samples | BET SA ($m^2/g$) | APD (nm) | TPV (cc/g) |
|---|---|---|---|
| GTS | 9.791 | 11.56 | 0.019 |
| LCS | 5.174 | 18.08 | 0.013 |
| PCD | 18.113 | 3.34 | 0.014 |
| GTSC | 1.132 | 15.89 | 0.004 |
| LCSC | 2.268 | 6.12 | 0.003 |
| PCDC | 1.565 | 14.44 | 0.004 |

(APD – average pore diameter; BET – Brunauer-Emmett-Teller; GTSC – GTS composite; LCSC – LCS composite; PCDC – PCD composite; SA – surface area; TPV – total pore volume based on non-local density functional theory model)

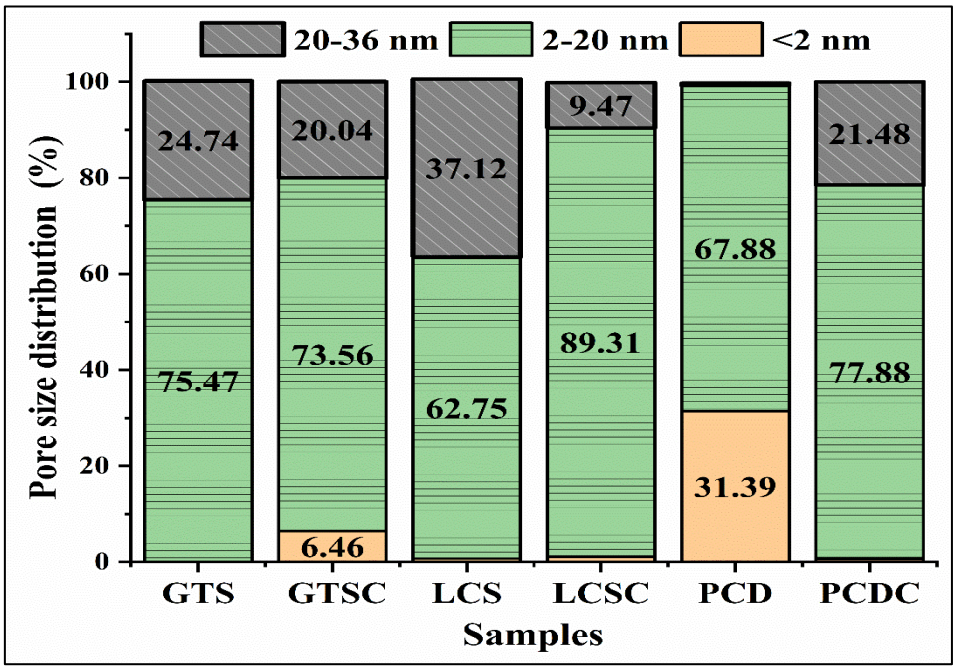



Figure 6-6 Comparison of the pore size distributions of the coal samples and the carbon/ceramic composites

(GTS – Greenside tailing slurry; GTSC – Greenside tailing slurry composite; LCS – Likeflow coal slurry; LCSC – Likeflow coal slurry composite; PCD – Proteas coal discard; PCDC – Proteas coal discard composite)

From Figure 6-6, GTS and LCS (average pore diameter of 11.56 and 18.09 nm) contain less than 0.5% micropore volume. The micropore volume of PCD around 31% (average pore diameter of 3.34 nm) suggests that PCD is from a high-rank coal dump and has a dense structure with low natural porosity and limited adsorption capacity. The dense nature of PCD waste might have impeded the flow of the PCP into the pores of PCD during mixing, limiting the diffusion and reaction between the PCD coal particles and PCP during pyrolysis. Furthermore, Lu and Do (1991) reported that during the pyrolysis of coal waste, volatiles are released. Analysis of the coal wastes indicated that the volatile matter content of GTS, LCS, and PCD is 22.57%, 23.72%, and 10.67%, respectively. As the pyrolysis of the coal/PCP blend progresses, the pores of GTS and LCS are prone to expand or even collapse as a result of volatile liberation. The resultant collapse of the pores might have enhanced the transport and reactivity of the PCP resin into these coal particles, facilitating bonding as the carbon/ceramic composites solidify into a rigid body. Apart from the physicochemical properties, it can be seen that the textural property of the coal waste is an important criterion to consider when selecting coal for this application. As expected, there is a significant decrease in the surface areas of the composites compared to the raw coals (Table 6-1) due to the rigidity of the composite particles. This suggests that the pyrolysis process adequately embedded and bound the ceramic-forming polymer with the coal particles.

### *6.4.3 Water contact angle analysis*

Water penetration significantly impacts the durability or degradation of construction products and engineering composites (Helmi & Hefni, 2014; Li et al., 2021). Since the carbon/ceramic composites could be fabricated into composite building materials for outdoor applications, they must resist water penetration. From this standpoint, the water contact angle (CA) of the composites' surface using deionised water as a polar solvent was measured to examine their hydrophobic performance. The shapes of the sessile drop on the composites (Figure 6-7) indicate that the CA of the PCD composite is of average 76.93° ± 5 and could be considered hydrophilic (CA < 90°). The contact angle of materials is inversely related to hydrophilicity and surface free energy (Azimi & Asselin, 2022). This implies that the surface-free energy of the PCD composite is high, hence, water-shedding on the surface is reduced, and the surface has a high tendency to wet or adsorb water. By contrast, the water CAs of the GTS and LCS composites of 91.56° and 104.33° suggest hydrophobic (CA ≥ 90°) surface properties, poor wettability and the ability to decrease the rates of water adsorption (Duncan et al., 2005; Subedi, 2011; Feyyisa et al., 2017). The relatively large error bar (Figure 6-7) was attributed to the roughness of the composite surfaces. Specifically, the high CA of the GTS and LCS composites infers they may not necessarily require secondary protection to prevent the ingress of water molecules that pose a threat to their degradation. Notable for conventional roofing materials (clay and concrete) that were also tested, it was difficult to capture CA images as the waterdrop spread on the surface and penetrated their pores quickly.

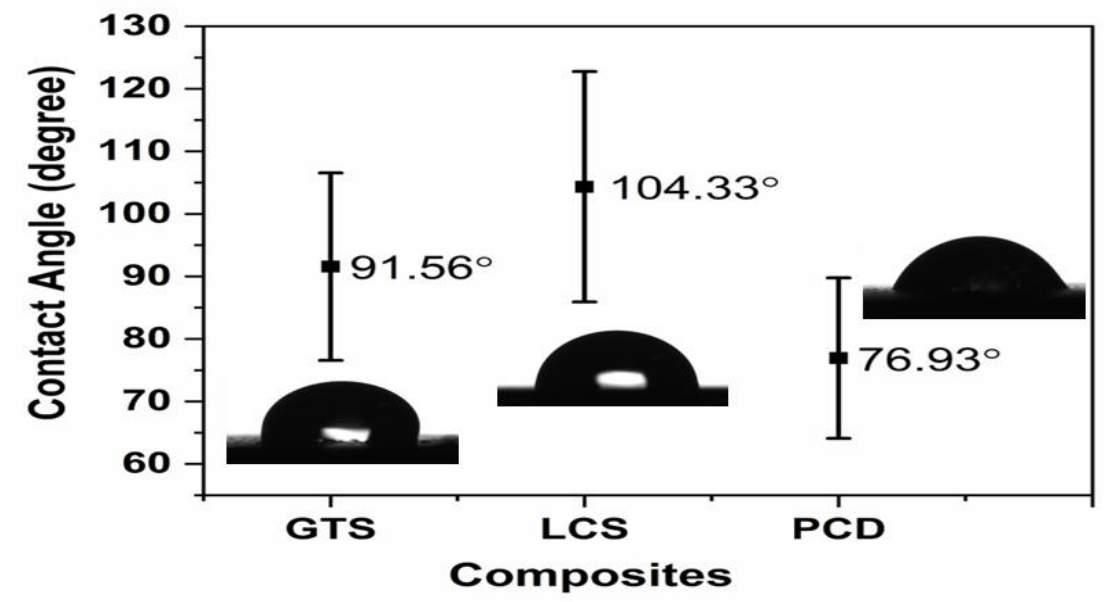



Figure 6-7 The water contact angle of the carbon/ceramic composites at room temperature

(GTS – Greenside tailing slurry; LCS – Likeflow coal slurry; PCD – Proteas coal discard)

### *6.4.4 Raman spectra*

Raman analysis was used to compare the structural state of the carbon atoms in the coal waste and that of the carbon/ceramic composites. The obtained spectra were deconvoluted (curve-fitted) using the Lorentz curve-fitting function (OriginPro 9.1.0 software, OriginLab Corporation, United States) based on the remarks of Angoni (1993). In principle, the structure of the crystallites of polycrystalline carbon materials is described by several parameters to correlate with the nanostructure of these materials. Equations (6-2) to (6-5) were employed to determine the quantitative spectral parameters, such as the peak position, the peak intensity ratio $\left(\frac{A_D}{A_G}\right)$, size of carbon cluster crystallites $(L_a)$ and other graphitisation indices ($L_D$ and $L_{eq}$). The peak intensity ratio was estimated using the ratio of the integrated areas of the D (disordered) and G (graphitic) bands. $A_{2D}$ represents the areas under the 2D peak. Graphitisation parameters of the carbon phase of

the samples derived from the curve-fitted Raman spectrum are summarised in Figure 6-8 and Table 6-2.

$$L_a = C\lambda_L \left(\frac{A_D}{A_G}\right)^{-1} \text{ nm} \tag{6-2}$$

$$L_{eq} = 8.8 \left(\frac{A_{2D}}{A_D}\right) \text{ nm} \tag{6-3}$$

$$n_D = \frac{2.4\times10^{22}}{\lambda_L^4} \left(\frac{A_D}{A_G}\right) \text{ cm}^{-3} \tag{6-4}$$

$$L_D = \sqrt{(1.8 \times 10^{-9})\lambda_L^4 \left(\frac{A_G}{A_D}\right)} \text{ nm} \tag{6-5}$$

From Equation (6-2), $C(514.5) = 4.38$ nm (Ferrari & Robertson, 2000; Jiang et al., 2009; Larouche & Stansfield, 2010; Dalcanale et al., 2014). $L_D$ is the average distance between defects. $L_{eq}$, a graphitisation index introduced by Larouche and Stansfield (2010) describes the average continuous graphene length including tortuosity. This quantity, which gives an estimate of the equivalent phonon mean free path, provided complementary knowledge about the composites. Furthermore, the defect density, $n_D$, and the distance between defects, $L_D$, account for the amount of disorder and were calculated based on work presented in the literature (Cançado et al., 2011; Ricohermoso et al., 2022, 2023).

Table 6-2 Comparison of the other graphitisation indices obtained from deconvoluted Raman spectra of the coal samples and carbon/ceramic composites and calculated using Equations 6-2 to 6-5

| **Sample** | **Carbon content (%)** | **D-band ($cm^{-1}$)** | **G-band ($cm^{-1}$)** | $L_D$ **(nm)** | $n_D$ **[×$10^{11}$] ($cm^{-3}$)** | $L_{eq}$ **(nm)** |
|---|---|---|---|---|---|---|
| **GTS** | 56.70 | 1342 | 1600 | 9.49 | 4.79 | 5.63 |
| **LCS** | 68.55 | 1363 | 1594 | 10.70 | 3.77 | 4.89 |
| **PCD** | 51.40 | 1352 | 1597 | 8.95 | 5.39 | 3.77 |
| **GTS composites** | 40.00 | 1348 | 1598 | 7.41 | 7.86 | 1.47 |
| **LCS composites** | 42.70 | 1356 | 1597 | 7.49 | 7.71 | 1.11 |
| **PCD composites** | 44.05 | 1355 | 1597 | 7.33 | 8.03 | 0.70 |

The first-order Raman spectrum of the coal wastes and carbon/ceramic composites (Figure 6-8) exhibit two prominent features – the fingerprint D-and G-bands at Raman shifts between 1348 - 1363 $cm^{-1}$ and 1594 - 1600 $cm^{-1}$ found in many carbon materials (Ferrari & Robertson, 2000). The D-band is associated with the vibration or breathing mode of the $sp^2$ atoms in rings assigned to the $A_{1g}$ modes observed in small crystallites or boundaries of larger crystallites of graphite. Whereas the G-band, which stems from in-plane bond stretching of $sp^2$ atoms in rings and chains, has been assigned to the $E_{2g}$ modes observed in crystals of graphitic materials (Tuinstra & Koenig, 1970; Ferrari & Robertson, 2000; Sarkar et al., 2011; Dalcanale et al., 2014). Furthermore, two minor peaks corresponding to the 2D and D+G bands in the second-order Raman spectrum between 2400 and 3000 $cm^{-1}$ can be observed in the coal and coal composite samples.

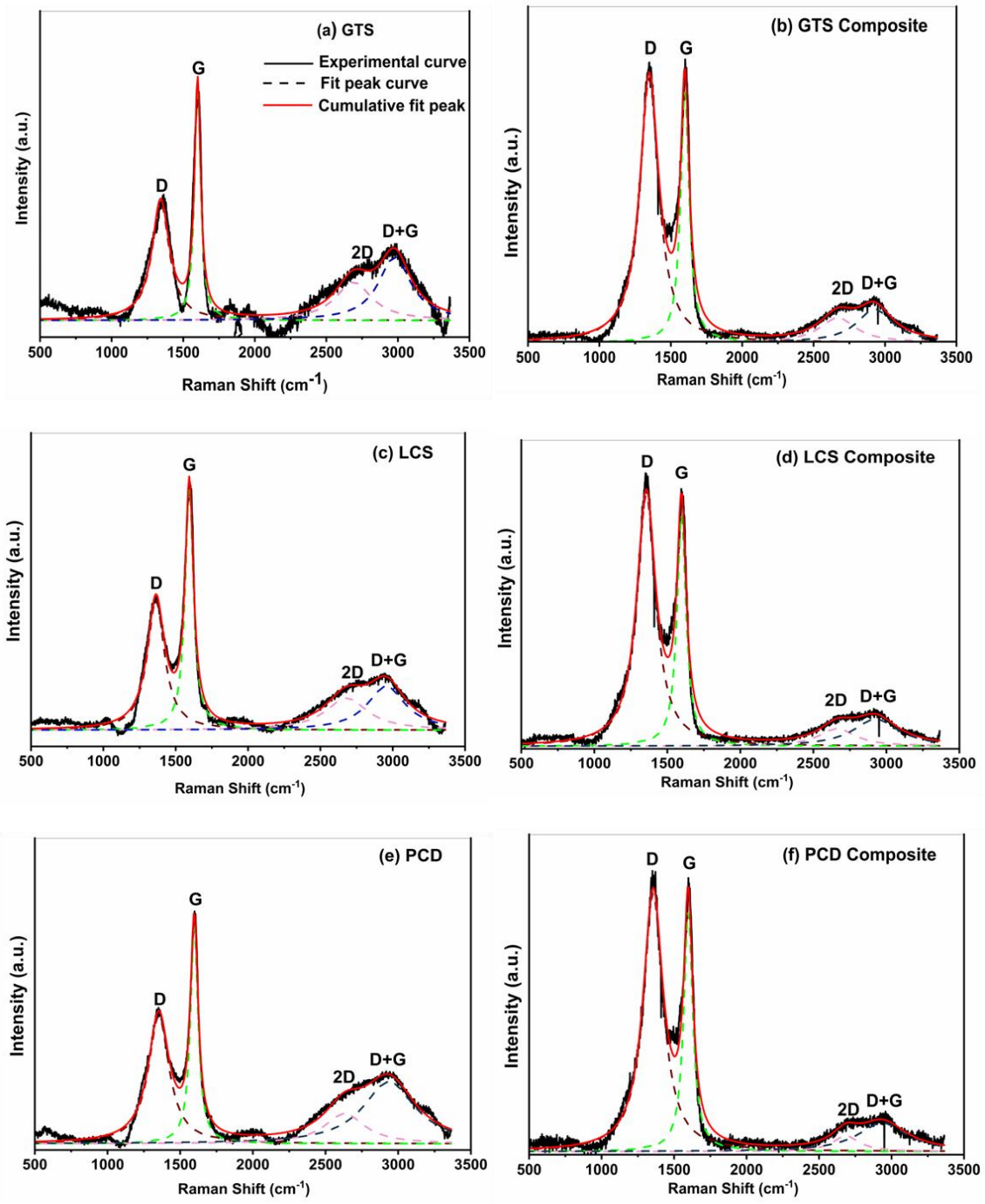



Figure 6-8 Raman spectra of the coal waste and the carbon/ceramic composites with their corresponding curve-fitting bands

(a.u. – arbitrary unit; GTS – Greenside tailing slurry; LCS – Likeflow coal slurry; PCD – Proteas coal discard)

The 2D band observed around 2700 $cm^{-1}$ is usually found in defect free graphite samples while the D+G band is assigned to the disordered state of the carbon

nanostructure in the samples (Gao et al. 2012; Colombo et al. 2010; Wen et al. 2020; Adigun et al. 2022). At close observation, this amorphous state decreases as the coal wastes transform into carbon/ceramic composites. Upon addition of PCP with the coal matrix and further curing/pyrolysis, the disorder degree of the carbon in the composites compared to the coal wastes increases judging from the calculated intensity ratio $A_D/A_G$ (Figure 6-9), meaning there was a progressive conversion of $sp^2$ carbon to $sp^3$ carbon during pyrolysis. This confirms that the amorphous carbon structure (less organised carbon rings) is prevalent in the composites. In principle, the size of carbon crystallites, $L_a$ is reduced; hence, the inter-defect distance ($L_D$) reduces (Dalcanale et al. 2014) compared to the raw coal waste (see Figure 6-9 and Table 6-2). Furthermore, a decrease in $L_D$ of the carbon phases invariably followed an increase in $n_D$ and a corresponding decrease in $L_{eq}$ (Table 6-2). Comparing the composites, $A_D/A_G$ decreases from LCSC<GTSC<PCDC, reflecting that the LCS composite contain more graphitised carbon (He et al. 2017; Moni et al. 2017).

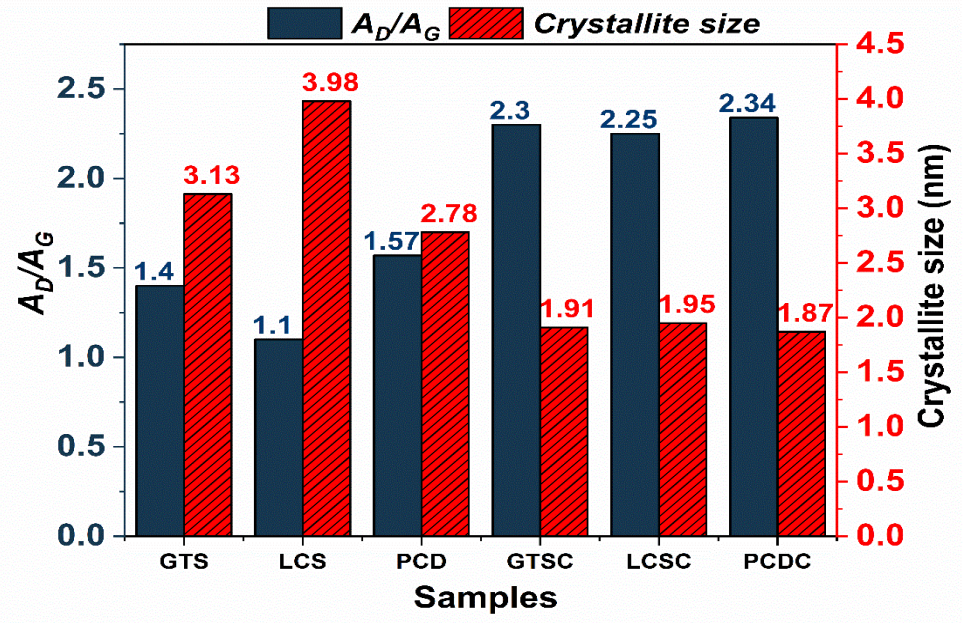



Figure 6-9 Variation in the peak intensity ratio ($A_D/A_G$) and the size of the carbon cluster crystallites of the coal and their composites

(GTS – Greenside tailing slurry; GTSC – Greenside tailing slurry composite; LCS – Likeflow coal slurry; LCSC – Likeflow coal slurry composite; PCD – Proteas coal discard; PCDC – Proteas coal discard composite)

### *6.4.5 Electrical resistivity evaluation*

The direct current volume resistivity of the composites (as-received, heated, and moist (soaked) composites) measured in a four-point probe configuration gave insight into how strongly or weakly the composites resisted the flow of current (Figure 6-10). The standard deviation obtained from five measurements for each composite is less than 5.0% with volume resistivity in the range of 22 to 82 Ω-cm ($4.4998\times10^{-2}$ to $1.2194\times10^{-2}$ Siemens per centimetre in terms of electrical conductivity). The volume resistivity when the as-received composites were soaked in water for three days reduced. However, when heated under the same condition, there was no identifiable trend. Difficulty in maintaining the temperature of the composites in hot state may have led to the resistance being inaccurately measured, although great effort was taken to minimize these errors. The

trend of volume resistivity of the composites at room temperature follows LCS<GTS<PCD. Interestingly, this is similar to the trend of porosity of the composites (LCS<GTS<PCD) but in reverse to the pyrolysis shrinkage (LCS>GTS>PCD) previously reported (Eterigho-Ikelegbe et al., 2021b).

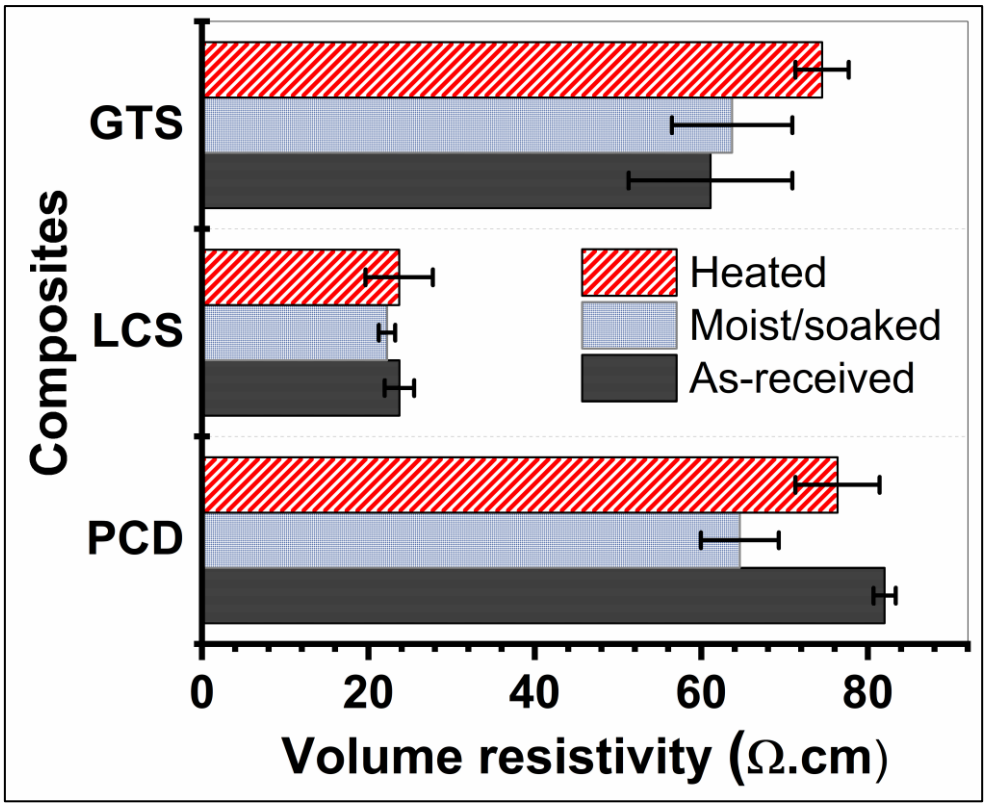



Figure 6-10 Measured volume electrical resistivity of the composites
(GTS – Greenside tailing slurry; LCS – Likeflow coal slurry; PCD – Proteas coal discard)

According to Shibuya et al. (2007), the electrical resistivity of porous composites shows an increasing trend with porosity and is consistent with the composites produced in this study. Presumably, the level of shrinkage that occurred during pyrolysis reduced the interparticle distances and pushed the conducting atoms closer to themselves. Thereby, providing sufficient transport of mobile charge carriers resulting in the LCS composite manifesting the lowest electrical resistance.

Another explanation for the electrical resistivity behaviour of the composites can be drawn from features of the Raman spectra. The LCS composite has the lowest dc electrical resistivity compared to the GTS and PCD composites due to i) lowest defect degree (i.e., highest graphitisation degree of $sp^2$ hybridised carbon); ii) highest carbon cluster size (1.95 nm), meaning the distance between the particles is smaller; thus, the percolation pathway for conduction is highly favoured (Xia et al., 2020; Ricohermoso et al., 2022). Ding et al. (2012) reported that high carbon size enhances the relaxation polarisation and does play a pivotal role in increasing the conductivity of the ceramic. Therefore, $L_a$ and the hybridization state of the carbon atom in the carbon/ceramic composite matrix are believed to exert an influence on the behaviour of the dc volume resistivity of the carbon/ceramic composites.

In general, there is no particular obligation on the electrical resistance performance of building materials. However, the ASTM D257-07 (2021) standard describes a solid material having a volume resistivity between 1 and 10,000000 Ω-cm as moderately conductive. Beyond the physicomechanical properties, other considerations for building materials include dealing with heat build-up, lightning strikes, potential ignition, or explosion risk that arise from the electrostatic charge accumulation on the material surface (Aisenbrey, 2007). As such, in areas where lightning strikes are prevalent, many conventional building materials grouped as insulators are limited in providing pathways for the dissipation of electrical charge accumulation. In fact, in the field of conductive polymer composites, low-volume resistivity composites are least susceptible to static electricity accumulation (Stabik & Chomiak, 2016; Polok-Rubiniec et al., 2021). Moreover, the intrinsic electrically conductive network of carbon-based materials inspires a new generation of smart modern engineering materials. As a result, it

is possible to deploy them as heat-generating elements, lightning strike shielding, and electromagnetic wave shielding (Shintani & Nakamura, 1995; Fiala et al., 2017; Fu & Yuan, 2017; Liu et al., 2022a; Liu et al., 2022b). On the premise of their low-volume resistivity (22 to 82 Ω-cm), these composites may not be affected by electrostatic discharge and can be targeted for cold or icy environments to create self-heating parts that prevent ice build-up or help de-ice (Hill et al., 2022).

### *6.4.6 Leachability analysis*

Coal contains trace amounts of heavy metal elements liable to biological and/or chemical reactions with the environment. Also, the release of soluble constituents from the composites upon contact with liquid may pose a potential risk to the environment during their end-of-life. Therefore, it is important to understand the properties and risks of the composites when disposed of as crushed waste to the environment (end-of-life). The final pH and electrical conductivity of the eluates of the composites subjected to leaching in distilled water (pH 7.92) and acetate buffer solution (pH 4.94) are presented in Table 6-3.

**Table 6-3** pH and electrical conductivity of the leachate

| **Composites** | **Distilled Water** | | **Acetate Buffer** | |
|---|---|---|---|---|
| | **pH** | **EC (µS/cm)** | **pH** | **EC (µS/cm)** |
| GTS | 10.85 ± 0.3 | 33.32 ± 2.05 | 5.345 ± 0.015 | 568.45 ± 6.05 |
| LCS | 10.95 ± 0.34 | 39.45 ± 5.83 | 5.12 ± 0 | 541.4 ± 5 |
| PCD | 10.36 ± 1.12 | 48.62 ± 5.14 | 5.205 ± 0.005 | 560 ± 7 |

(EC – electrical conductivity)

It was observed that the pH values of the eluates based on the distilled water leaching protocol are in the range of 10.55 to 11.48. Whereas the eluates obtained using the Toxicity Characteristic Leaching Procedure based on acetate buffer show a slightly acidic pH ranging between 5.36 and 5.12. In general, the pH of the eluates has slightly

increased by an average of 37% for distilled water and 7% for the acetate buffer solution. It can be concluded that the pH of the eluants influences the final pH values of the eluates after the composites have been through leaching. The electrical conductivity of the eluates from the acetate buffer was found to be about 13 to 14 times higher than that of distilled water, suggesting the high mobility of ions from the crushed composites into the acetate buffer phase. Table 6-4 displays a snapshot of the leachable concentration of the heavy metal elements – arsenic, barium, cadmium, chromium, lead, zinc, mercury, selenium, and inorganic anions – fluoride, chloride, and sulphate from one stage batch test. From the Table, the leached concentrations of these heavy metals from the composites using deionised water and acetate buffer solution are below the TCLP regulatory levels of heavy metal elements (US EPA 1992). Therefore, the composite wastes could be considered non-hazardous at the end of life.

Table 6-4 Leached concentrations of heavy metal elements and inorganic anions from the composites compared with the LCT and TCLP limits

| Metals | Distilled water (mg/L) | | | Acetate buffer solution (mg/l) | | | LCT0 (mg/L) | LCT1 (mg/L) | TCLP Levels (mg/L) |
|---|---|---|---|---|---|---|---|---|---|
| | Composites | | | | | | | | |
| | GTS | LCS | PCD | GTS | LCS | PCD | | | |
| Arsenic | <0.18 | <0.18 | <0.18 | <0.18 | <0.18 | <0.18 | 0.01 | 0.5 | 5.0 |
| Barium | <0 | <0.06 | <0 | <0 | <0.42 | <0 | 0.7 | 35 | 100 |
| Cadmium | <0.02 | <0.02 | <0.02 | <0.02 | <0.02 | <0.02 | 0.003 | 0.15 | 1.0 |
| Chromium | <0.06 | <0.06 | <0.06 | <0.06 | <0.06 | <0.06 | 0.1 | 5 | 5.0 |
| Lead | <0.16 | <0.16 | <0.16 | <0.16 | <0.16 | <0.16 | 0.01 | 0.5 | 5.0 |
| Zinc | <0.02 | <0.02 | <0.02 | <0.02 | <0.02 | <0.02 | 5.0 | 250 | 300 |
| Mercury | <0.02 | <0.02 | <0.02 | <0.02 | <0.02 | <0.02 | 0.006 | 0.3 | 0.2 |
| Selenium | <0.46 | <0.46 | <0.46 | <0.46 | <0.46 | <0.46 | 0.01 | 0.5 | 1.0 |
| **Inorganic anions** | | | | | | | | | |
| Fluoride | 39 | — | — | 744.78 | — | 694.06 | 1.5 | 75 | NA |
| Chloride | 20.76 | 58.98 | 61.96 | 117.4 | 67.23 | 31.42 | 300 | 15000 | NA |
| Sulphate | — | — | — | 40.18 | — | 25.43 | 250 | 12500 | NA |

Note: LCT = Leachable Concentration Threshold; TCLP = Toxicity Characteristic Leaching Procedure; NA = not available; **Type 3 waste**: LCT0 < LC ≤ LCT1 – very low-risk hazardous waste with low potential for contaminant release and must be disposed of on a **Class C** containment barrier design landfill. **Type 2 waste:** LCT1 < LC ≤ LCT2 – Considered low-risk waste with some potential for contaminant release and must be disposed of on a **Class B** containment barrier design landfill. **Green** indicates that the concentration of the waste material is below or equal to LCT0. **Yellow** indicates that the concentration of the waste material is above LCT0 but below LCT1. **Brown** indicates that the concentration is above LCT1 but below LCT2.

Based on the South African classification system, arsenic, cadmium, lead, mercury, and selenium are above LCT0 but below LCT1 (LCT0<LC≤LCT1). As such, the composite waste could be classified as Type 3 waste (see note below Table 6-4). In principle, the low concentration of these heavy metals in the eluate suggests that the pyrolysis of coal and the PCP into composites may have chemically rearranged these metals into stable phases. From Table 6-4 also, it can be seen that the release potential of these metals seemed to have not been influenced by the pH of the extraction fluids. However, the inorganic anions (fluoride, chloride and sulphate) were influenced by pH. Acidic eluant resulted in more mobility of fluoride, chloride, and sulphate, in particular, fluoride, implying that these anions are highly soluble in an acidic solution. In general, when the composites are disposed of as crushed material in landfills, the waste falls between Type 2 and Type 3 waste and can be considered as low to very low hazardous risk waste. The leaching method reported in this study represents the leaching of heavy metals from the crushed composites assuming end-of-life. Overall, the results show that the leaching of these metals is unlikely to endanger the environment. However, this end-of-life approach may be inadequate for assessing the long-term environmental impact of the composites (i.e., use stage). Therefore, the utilisation scenario of the composites based on the tank leaching experiment designed for monolithic specimens should be conducted to estimate the leached concentration of heavy metal elements over a long period.

## 6.5 Conclusion

This research involved investigating the bonding mechanism, textural properties, wettability, electrical behaviour, and the environmental friendliness of composites produced from coal waste and preceramic polymer resin. The evaluation concludes that the textural properties of coal waste (PCD) with the lowest volatile matter (10.67%) and

highest ash content (39.76%) possessed a dense structure. This impeded the reactivity or bonding of the coal particles with the PCP resin during pyrolysis leading to low-quality PCD composites. The water contact angles of LCS and GTS composites were found to be above 90°, as such, the surface of these composites could be considered hydrophobic. The potential of these composites to reduce water penetration when used for outdoor applications is necessary for building materials. The $A_D/A_G$ ratios of the composites were higher than the coal wastes, indicating that the composites contain more amorphous carbon structures. The dc volume resistivity of the composites between 22 and 82 Ω.cm, classified as "moderately conductive", was attributed to the presence of a percolating carbon network in the composites. As a result, the composites may not be prone to static charge accumulation responsible for causing fire hazards. Finally, acceptable levels of heavy metal elements in the eluates of the leached crushed composites suggest that the metals in the coal may have been chemically rearranged into stable phases during pyrolysis with the preceramic polymer resin. Based on the conclusions of the analyses presented in this article, this technique endows coal waste with a beneficial use as raw material to produce carbon/ceramic composites for building applications.

# 7 Strong, lightweight, thermally stable, and hydrophobic structural composites produced from coal-based waste and polymer-derived SiOC ceramics

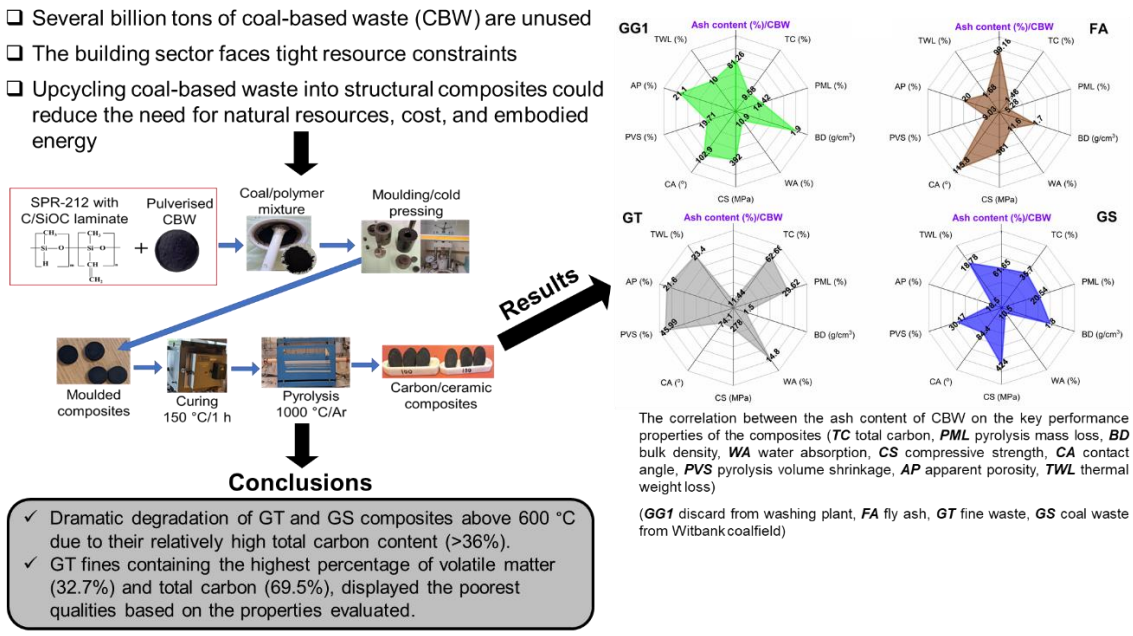
This chapter is published in:

**Eterigho-Ikelegbe, O.**, Ricohermoso, E., Harrar, H., Riedel, R., & Bada, S. (2023). Strong, lightweight, thermally stable, and hydrophobic sustainable structural composites produced from coal-based waste and polymer-derived SiOC ceramics. *Clean Technologies and Environmental Policy*. https://doi.org/10.1007/s10098-023-02589-x

**Preamble**

To broaden the research, the range of South African coal-based waste was extended and a commercial preceramic polymer (SPR-212) was used as the ceramic- forming binder to produce coal composites. Fourier transform infrared spectroscopy, X-ray diffraction, scanning electron microscopic and Raman spectroscopy were used to obtain information about the coal wastes and coal composites. As it relates to building material application, the continuous operating temperature, density, water absorption, apparent porosity, water contact angle measurement and compression strength tests of the composites were reported. This chapter addresses research question (iv) - How does the variations in the physicochemical properties of South African coal wastes affect the behavior of the coal composites fabricated using SPR-212 as the ceramic-forming binder?

## Graphical Abstract




The correlation between the ash content of CBW on the key performance properties of the composites (***TC*** total carbon, ***PML*** pyrolysis mass loss, ***BD*** bulk density, ***WA*** water absorption, ***CS*** compressive strength, ***CA*** contact angle, ***PVS*** pyrolysis volume shrinkage, ***AP*** apparent porosity, ***TWL*** thermal weight loss)

(***GG1*** discard from washing plant, ***FA*** fly ash, ***GT*** fine waste, ***GS*** coal waste from Witbank coalfield)

**Abstract**

Recycling coal-based waste (CBW) into composites suitable as a building material might be a necessary response to combat its risk to the environment. Therefore, the objective of this study was to investigate the microstructure and performance of coal composites produced from CBW and polysiloxane polymer (SPR-212). Four types of CBW that differ in physicochemical properties were examined. Fourier transform infrared spectroscopy results indicated that the higher the intensity of the C=C bonds in the CBW, the higher the pyrolysis mass loss and shrinkage experienced by the composites during pyrolysis. The continuous operating temperature of the composites is up to 600 °C. However, at temperatures above 600 °C, composites containing carbon content greater than 36% manifested dramatic degradation. Pyrolysis mass loss in the range of 5.28 to 29.62% was obtained for all the composites. The density range of the composites is between 1.5 and 1.9 grams per cubic centimetre. The water absorption of all the composites is within the range of 0 to 25% and is comparable to many building materials. Notably, the composites containing total carbon less than 10% registered a water contact angle greater than 90°, indicating the low wettability of their surface. Furthermore, composites that embodied the highest total carbon (63%) displayed the worst structural property. The findings of this study lay the foundation for further development of high-quality structural coal composites from CBW and the SPR-212 polysiloxane polymer through optimisation of the processing conditions.

**Keywords:** Building material; Carbon; Ceramics; Compressive strength; Polysiloxane; Thermal stability

## 7.1 Introduction

As with any mineral extraction activity, coal mining is associated with the disposal of various types of coal wastes (CW) in tailings dumps. Also, coal fly ash (CFA) represents 70-85 wt.% of the total ash generated from coal combustion in thermal power stations. As of 2012, it was estimated that about 800 million tonnes of CFA are generated worldwide annually (Blissett & Rowson 2012; Yao et al. 2014). Traditionally, CW and CFA (grouped as coal-based waste (CBW)) are diverted to landfill and have become a permanent feature around many coal mines and power stations worldwide due to their underutilisation. Undoubtedly, CBW dumps pose adverse implications on the natural environment, social well-being and local resources (Haywood et al., 2019; Li et al., 2018; Mbedzi et al., 2020; Tambwe et al., 2020; Zhao, 2012). There has been progress in the potential application of CFA and CW (Haibin & Zhenling 2010; Blissett & Rowson 2012; Yao et al. 2015; Fecko et al. 2013; Hu 2016). With a focus on circularity worldwide, a forecasted rise in CBW for much of the next 20 years and the unused CBW available in millions of tones, developing multidimensional upcycling strategies can substantially mitigate many of its environmental burdens and enhance global industrial ecology practices. Indeed, this can be seen from the panoply of novel research solutions ongoing to generate value from CBW (Liu et al. 2018; Abdulsalam et al., 2020a; Isaac & Bada, 2020; Morgan & Wade 2021; Hill & Easter, 2021; Eterigho-Ikelegbe et al., 2021a, b, c, 2022; Harrar et al., 2022; Hill et al., 2022). The social and environmental pressures to address concerns over waste reduction drive the incentives for CBW research. At the same time, the built environment and construction sectors are raw material intensive sectors compared to any other economic activity (Pacheco-Torgal & Labrincha, 2013; Hossain et al., 2020). These sectors face increasingly tight resource constraints and a

growing scarcity of good-quality raw materials due to excessive and continuous exploitation (Pacheco-Torgal & Labrincha, 2013; OECD, 2015). 'Resource efficiency/substitution', also known as the use of secondary resources or waste, is a current research trend to address these challenges. The goal of this approach is to promote a circular economy, preserve natural mineral resources, reduce material costs and diminish embodied energy (Hossain et al., 2020).

One of the innovative directions of coal/CBW research is their upcycling into structural or building composites. Major research in this area includes the use of coal as fillers with conventional polymers, followed by moulding (Al-Majali et al., 2019; Bai et al., 2019; Phillips et al., 2019) and firing coal/CBW in itself or mixed with clay for ceramic brick making (Stolboushkin et al., 2016; Xu et al., 2017; Vasić et al., 2021). Recently, some investigators documented a patent using United States raw coal and preceramic polymer (PCP) to produce coal composites for building applications (Hill & Easter, 2021; Hill et al., 2022). The formulation detail of the PCP is unknown as the information is kept proprietary. Of note, PCP, otherwise known as a ceramic-forming polymer, is a special type of polymer precursor that offers simple and inexpensive access to various ceramic systems known as polymer-derived ceramics (PDCs). The PDCs are achieved through a controlled heating process of crosslinking and pyrolysis under an inert or reactive atmosphere. These ceramic-forming polymers are used to produce advanced/technical ceramics, ceramic fibres/matrix composites, monolithic bodies, foams, coatings, membranes, and microelectromechanical systems (MEMS) (e.g., microreactors and microsensors) (Liew et al., 2000; Colombo et al., 2010; Eckel et al., 2016; Wen et al., 2022). The remarkable properties of PDCs stem from the unique

combination of their inherent covalent (polar) Si-O-Si bonds and amorphous nature (Ionescu et al., 2012; Černý et al., 2015).

The manufacturing process of the patented coal composites involves curing the coal/PCP mixture followed by pyrolysis treatment (Hill & Easter, 2021; Sherwood et al., 2021; Hill et al., 2022). Several attributes of the composites include lightweight, adequate strength, thermal stability, fire resistance, etc. These attributes make them suitable for application in the construction industry as roofing tiles, bricks, panels, and blocks. According to the investigators, high volatile matter coals produced composites that were inferior compared to the lower volatile matter coals. The interesting result achieved by Hill and Easter (2021) using the run-of-mine thermal coal for power generation inspired the investigation of South African high-ash coal waste with the same proprietary polymer (Eterigho-Ikelegbe et al., 2021b, 2022). The characterisation of the microstructural and physicomechanical properties of the produced composites has been documented.

For this study, different South African CBWs were investigated to explore the potential of this approach further and to divert them from landfills. As suggested by Hill and Easter (2021), other PCPs capable of being pyrolysed to form ceramic may be selected or tested. Within this context, it becomes necessary to broaden the research using a commercial PCP as the ceramic binder. It is known that the physicochemical properties of CBW vary according to its origin and the seam from where the coal is mined. As such, CBW selection becomes an important factor when considering commercial PCP. Many poly(organosiloxanes) (PSOs) have excellent hydrophobic properties, act as water-repellent coatings and are used in construction as sealants and electro-insulating agents (Greil, 1995; Gumula et al., 2009; Colombo et al., 2010). PSOs are available in high volumes and easily accessible, show excellent physicochemical properties, have a long

storage life, are low cost and are easy to handle under ambient conditions (Greil, 1995; Colombo et al., 2010; Černý et al., 2015). Based on these attributes, SPR-212, a commercial SiOC-yielding PCP under the class of PSOs, was considered the ceramic-forming binder for this study. Fourier transform infrared spectroscopy with attenuated total reflectance (FTIR-ATR) was employed to assess the functional groups and chemical bonds of the raw materials and the pyrolysed composites. X-ray diffraction (XRD), scanning electron microscopic (SEM) and Raman spectroscopy were used to provide information on the mineral composition, microstructure and carbon phases of the composites. Thermogravimetric analysis (TGA) was used to evaluate the thermal stability/continuous operating temperature of the composites. The density, water absorption and apparent porosity of the composites were calculated following ASTM C67 and C373 standards. The surface property of the composites was evaluated using water contact angle measurement while their mechanical performance was studied using compression strength tests.

## 7.2 Experimental and characterisation

### *7.2.1 Materials and preparation of the composites*

The coal-based waste (CBW) used for this study i.e., GT, GG1, and GS were sourced from different collieries in South Africa. GT is a fine from the mined semi-soft coking coal while GG1 is a discard from the washing plant, both from the Waterberg coalfield. GS was collected from the Witbank coalfield and fly ash (FA) was obtained from one of Eskom's coal-fired power stations in the Witbank region. Commercially available low-viscous methylvinylhydrogen polysiloxane (Polyramic® SPR-212 from Starfire Systems Ltd., USA), with a 17 wt.% carbon content, was used as the ceramic-forming binder for the coal matrix. As shown in the inset of Figure 7-1, the polysiloxane

contains monomethylsilane and methylvinylsilane units in the Si-O-Si backbone of the polymer. The polymer was used without solvent or catalyst. The as-received size of GT, GG1 and GS samples from the mines was around -212 µm. These samples were then sent to an external laboratory where it was milled to -106 µm according to ISO 13909 standard (ISO 13909-1, 2016) for coal sampling. FA was used in the as-received state without any pre-treatment. About 60% of the particle size distribution of the CBW is under -82 µm. The particle size distribution and textural property results of the CBW are presented in Table 7-1. The preparation of the composites was based on method adopted from the literature (Hill & Easter, 2021; Sherwood et al., 2021; Hill et al., 2022). In this study, a ratio of CBW to SPR-212 of 80:20 weight per cent was poured into a porcelain mortar and properly hand-mixed for about five minutes with a pestle until homogeneity was achieved. About 1.93 g of the resultant mixture was evenly distributed into a die and compacted using a manual press of applied force, 8 to 10 kilonewtons for about 30 seconds before release to produce circular composites. For the CBW particles to be well laminated by the precursor and to maintain structural integrity during pyrolysis, thermal crosslinking was initiated. The shaped bodies placed in alumina crucibles were heated in an airtight furnace with a ramp rate of 5 °C/min up to 150 °C (below the degradation temperature of the CBW and PCP) and held for one hour. Finally, the resulting cured bodies were pyrolysed in a sealed alumina tube furnace at a rate of 100 °C/h (1.67 °C/min) under flowing argon to 1000 °C and held isothermally for ten hours. After pyrolysis, the furnace was allowed to cool naturally to room temperature at 150 °C/h. Figure 7-1 demonstrates the summary of the production process of the composites.

Table 7-1 Particle size distribution and textural properties of the CBW samples

| Property | GG1 | FA | GT | GS |
|---|---|---|---|---|
| PSD D10, µm | 38.92 | 10.05 | 20.30 | 0.28 |
| PSD D50, µm | 87.07 | 35.56 | 58.79 | 11.22 |
| PSD D90, µm | 99.82 | 55.63 | 70.29 | 43.52 |
| MBET, $m^2/g$ | 9.89 | 1.29 | 3.05 | 3.61 |
| TPV, $10^{-2}$ cc/g | 3.09 | 0.47 | 1.76 | 1.14 |

GG1 – discard from washing plant; FA – fly ash; GT – fine waste; GS – coal waste from Witbank coalfield; PSD – particle size distribution; MBET – multi-point BET surface area measured by nitrogen adsorption; TPV – total pore volume; D10, µm – 10% of GG1 sample has a size of 38.92 µm or smaller

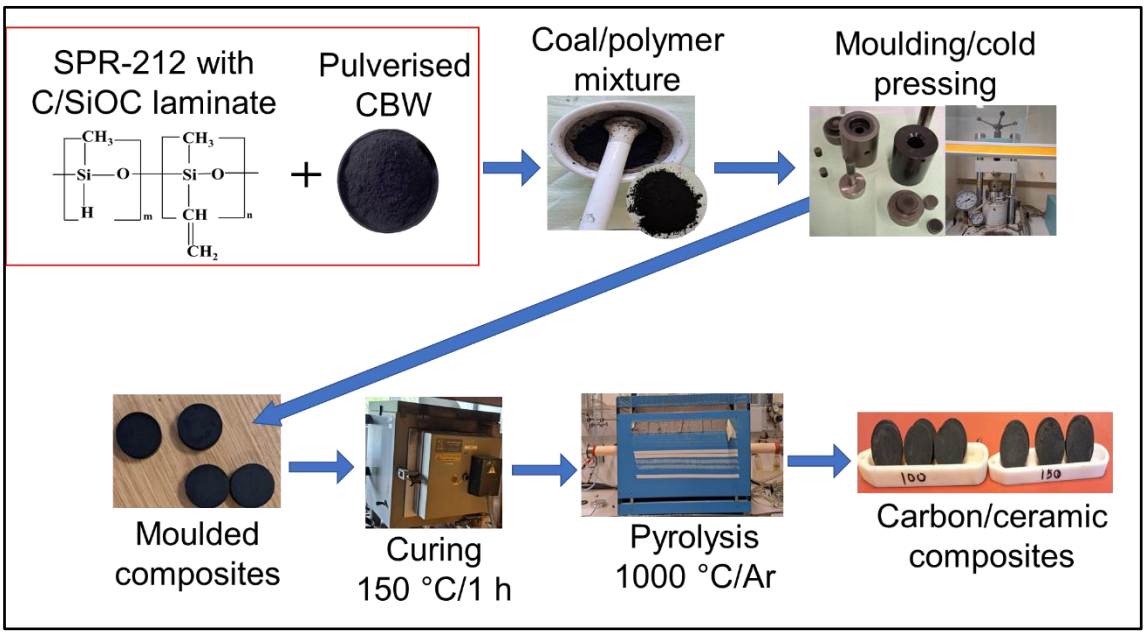



Figure 7-1 Preparation of the composites

*7.2.2 Physicochemical and microstructural characterisation of the coal-based wastes and composites*

Physicochemical analysis was conducted to acquire an understanding of the physical and chemical variation of coal-based waste (CBW). Proximate and ultimate analysis of the CBW was conducted following ASTM D5142 (ASTM D5142, 2009) and

ISO 12902-CHN standards (ISO/TS 12902, 2001), respectively. The elemental composition of the composites was determined using a Flash 2000 CHNS elemental analyser (Thermofisher Scientific). Attenuated total reflectance-FTIR spectroscopy (Spectrum Two™ spectrometer from PerkinElmer) was used to identify the various functional groups in the CBW and composites. Fine samples were scanned in the transmission mode from 400 to 4000 $cm^{-1}$ at a step size of 4 $cm^{-1}$. XRD patterns were obtained using the D2 phaser equipment (Bruker Corporation, Germany) containing an X-ray generator operating at 30 kilovolts and 10 milliamperes with a copper tube radiation (wavelength = 1.54184 Å). The analysis was conducted using a step size of 0.01° and a dwell time of ten seconds per step with a range of diffraction angle from 2-theta of 10 to 90°. The mineralogical phases in the CBW and composites were qualitatively identified using the PANalytical X'Pert software. Surface morphologies of carbon-coated composites were obtained using a scanning electron microscope (Sigma 300 VP, ZEISS, Germany). Energy dispersive X-ray spectroscopy provided semi-quantitative chemical compositions of the composites. The Olympus BX41 fluorescence microscope provided additional information on the microstructure of the composites' surface. The degree of graphitisation of the carbon phase of fine composite ceramics was investigated with a Raman spectrometer (LabRAM HR fitted with an Olympus BX41 microscope and a 514.5 nm laser excitation source of the Lexel Model-95 SHG argon-ion laser). A thermogravimetric analyser (TGA701, LECO Corp., United States) was used to determine the continuous operating temperature of the composites. Approximately one gram of broken pieces of the composites was placed under an air and oxygen atmosphere in the temperature range of 25 to 900 °C and at a ramp rate of 10 °C/min.

### *7.2.3 Physicomechanical and surface properties of the composites*

The properties and performance of the pyrolysed composites were investigated based on their bulk density, firing shrinkage, water absorption and bending strength. The pyrolysis mass loss, radial shrinkage and volume shrinkage experienced by the cured composites upon pyrolysis were determined by measuring the dimensions of the pyrolysed products before and after pyrolysis using Equations (7-1) to (7-3). Five composites were measured using a sliding gauge, and the average value was used to represent the total shrinkage and pyrolysis mass loss to the nearest 0.01%.

$$PML = \frac{M_P - M_C}{M_c} \times 100 \quad (7\text{-}1)$$

$$RS = \frac{L_p - L_C}{L_c} \times 100 \quad (7\text{-}2)$$

$$VS = \frac{V_p - V_C}{V_c} \times 100 \quad (7\text{-}3)$$

where PML is the pyrolysis mass loss (%), RS is the radial shrinkage (%), VS is the volume shrinkage (%), $M_c$ is the cured mass of the composite (g), $M_p$ is the pyrolysed mass of the composite (g), $L_c$ is the cured length of the composite (mm) and $L_p$ is the pyrolysed length of the composite (mm).

Water absorption, bulk density, apparent porosity, and apparent specific gravity were computed with guidance from ASTM C67 (ASTM C67, 2010) and C373 (ASTM C373, 2018) standards and following Eterigho-Ikelegbe et al. (2021b). The uniaxial compressive stress performance of the composites was tested using a benchtop universal testing machine (H100K-S) with a capacity of 10 Tonnes and guidance from ASTM C67 (ASTM C67, 2010) standard. The composite was placed flatwise between two steel loading platens to minimise machine wear. The load was applied continuously at a steady

rate of 1mm/min up to failure. The ultimate compressive stress was automatically generated using Equation 7-4.

$$C = {}^{W}/_{A} \tag{7-4}$$

where *C* is the ultimate compressive stress to the nearest 0.01 MPa, *W* is the maximum load indicated by the testing machine (Kgf or N) and *A* is the average gross area of the upper and lower surfaces of the composite ($mm^2$).

The wetting behaviour/surface property of the composites was investigated based on the static contact angle (CA) measurement. An OCA 15EC goniometer (DataPhysics Instruments, GmbH, Germany) was used for this investigation. The composite surface was dosed with a droplet of water (dosing volume = 3 μL; dosing rate = 2 μL/s) at room temperature for ten seconds. The average water CA was recorded after taking at least seven readings at different spots on both surfaces of the composites.

## 7.3 Results and discussion

### *7.3.1 Physicochemical assessment of the coal-based waste and coal composites*

The physicochemical property of the coal-based waste (CBW) in terms of proximate and elemental compositions is summarised in Table 7-2. The CBW reveal substantial differences regarding their volatile matter, fixed carbon, ash content, and total carbon. GT, being a semi-soft coking coal fine, manifested the lowest ash content, the highest fixed carbon and total carbon. The hydrogen/carbon (H/C) atomic ratios of GG1 (1.68) and GS (0.87) suggest it contains a high proportion of aliphatic chains. In addition, GG1 has a high chance of forming hydrogen bonds with the PCP and it is beneficial for this type of application (Hu et al., 2017; Eterigho-Ikelegbe et al., 2021c). GG1 also has the highest oxygen/carbon (O/C) atomic ratio, implying that it is an oxidised coal rich in

oxygen-containing functional groups (carboxyl, carbonyl, ether, and hydroxyl). These groups impart GG1 with good chemical reactivity (Wang & Zhou, 2011; Tan et al., 2019; Eterigho-Ikelegbe et al., 2021c). The total carbon of the GT composite (63%) from Table 7-3, suggests that a good proportion of its mass contains carbonaceous materials after pyrolysis. The oxygen + silicon fraction in Table 7-3 assumes that no other elements are present in the composites other than the ones listed.

Table 7-2 Physicochemical composition of the coal-based wastes (wt. %, air-dried basis)

| **Sample ID** | **Proximate analysis** | | | | **Elemental composition** | | | | | **Atomic ratio** | |
|---|---|---|---|---|---|---|---|---|---|---|---|
| | **M** | **VM** | **A** | **FC*** | **TC** | **H** | **O*** | **N** | **TS** | **H/C** | **O/C** |
| **GG1** | 3.28 | 10.01 | 81.26 | 5.44 | 7.50 | 1.06 | 5.46 | 1.44 | – | 1.68 | 0.55 |
| **FA** | 0.14 | 0.47 | 99.18 | 0.22 | – | – | – | – | – | – | – |
| **GT** | 3.84 | 32.7 | 11.44 | 52.06 | 69.5 | 4.90 | 7.97 | 1.41 | 0.94 | 0.84 | 0.09 |
| **GS** | 1.71 | 20.37 | 61.65 | 16.27 | 23.77 | 1.74 | 8.02 | 0.63 | 2.48 | 0.87 | 0.25 |

(GG1 – discard from washing plant; FA – fly ash; GT – fine waste; GS – coal waste from Witbank coalfield; A – ash content; FC – fixed carbon; M – inherent moisture; TC – total carbon; TS – total sulphur; VM – volatile matter; *oxygen by calculation = [100-(M + Ash + carbon + hydrogen + nitrogen + sulphur)]; *FC by calculation = [100-(VM + Ash + M)])

Table 7-3 Elemental composition of the pyrolysed composites

| **Sample ID** | **TC** | **H** | **N** | **TS** | **O + Si** |
|---|---|---|---|---|---|
| GG1 | 9.58 | 0.32 | 0.17 | 0.64 | 89.29 |
| FA | 1.46 | 0.26 | 0.07 | 0.28 | 97.93 |
| GT | 62.66 | 0.65 | 0.80 | 0.36 | 35.58 |
| GS | 35.7 | 0.48 | 0.38 | 1.86 | 61.58 |

(GG1 – discard from washing plant; FA – fly ash; GT – fine waste; GS – coal waste from Witbank coalfield; TC – total carbon; H – hydrogen; N – nitrogen; TS – total sulphur; O – oxygen; Si: silicon)

### *7.3.2 Functional group and microstructural analysis of the coal-based wastes and coal composite*

#### *7.3.2.1 Fourier transform infrared spectra analysis*

FTIR spectroscopy was used to determine the functional group composition of the CBW, the SPR-212 polymer, and the resultant composites. FTIR spectroscopy was also useful in probing the chemical interactions that occurred during the pyrolysis of the blend of coal and the SPR-212 polymer. The main functional groups of the SPR-212 resin (Wang, 2019) are shown in the FTIR spectrum of the liquid displayed on an absorbance scale (Figure 7-2). The SPR-212 contains silicon-bonded hydrocarbon constituents, including methyl ($CH_3$) and vinyl groups ($-CH=CH_2$), hydride (Si-H) functionality, Si-O (backbone), and Si-C bond structures. The FTIR spectra of CBW and the resultant composites are compared in Figure 7-3. The summary of functional groups detected in the CBW and coal composites is listed in Table 7-4. The assignment and identification of various functional groups in coal were referenced to work presented in the literature (van Niekerk, 2008; Ferraro & Basile, 2012; van der Merwe et al., 2014). Only GT fines feature the aliphatic C-H stretch ($f_2$) spotted between 2197 and 2852 $cm^{-1}$. FA, a by-product of coal combustion from a power-generating plant did not feature the main bands normally found in coal.

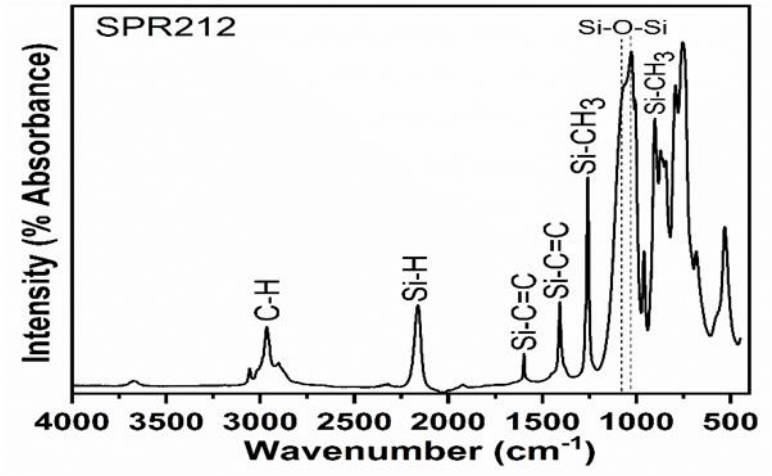



Figure 7-2 Fourier Transform Infrared spectrum of the native polysiloxane SPR-212

From the literature (Hill & Easter, 2021; Sherwood et al., 2021), moisture, low temperature/light volatile molecular species, and hydrocarbon are released creating nanopores within the coal particles and/or coal-PCP interface between 5 and 450 °C. Hence, the bands around 3700 to 3500 $cm^{-1}$ ($s_1$) assigned to the O-H stretching vibrations of the mineral matter in the coal declined in the composites ($p_1$). Absorption bands ($s_2$) observed between 3000 and 2800 $cm^{-1}$ as a result of the aliphatic C-H moieties in coal were more intense in the composites ($p_2$, $p_3$). The disappearance of the Si-vinyl (Si-C=C), Si-hydride (Si-H), and methyl silyl (Si-$CH_3$) peaks in the polymer suggest that these bonds broke down during pyrolysis. The redistribution reactions between these bonds with that of the coal resulted in increased absorbance of the aliphatic structural groups (alky C-H) denoted by $p_2$, $p_3$, $p_4$, and $p_5$. The C-H band is most absorbed in the FA composite and can be linked to an increase in aliphatic molecules emanating from the PCP pyrolysis.

The aromatic C=C bands in coal at about 1600 $cm^{-1}$ (GT>GS>GG1>FA) in terms of absorbance) are heat resistant between 50 and 450 °C (Khare & Baruah, 2014). At the same time, the single bonds in the PCP (Si-H, C-H, and Si-C) and in the coal generate various hydrocarbon radical intermediates (Sharma, 2018) that nucleate on bonding

substrates. It is believed that the intense degradation of the aromatic C=C bonds occurred between 450 and 800 °C with the corresponding evolution of relatively high molecular weight species (devolatilisation). Above 400 °C, the PCP starts transforming to ceramic through the cracking of the Si-C bonds (Černý et al., 2015). According to Taha et al. (2017), the destruction of the double bonds in coal suggests the decomposition of organic matter. As pyrolysis progresses, some of the dissociated bonds recombine with the macromolecular fragments generated during pyrolysis to form new bonds (resolidification). Subsequently, minerals such as kaolinite undergo dihydroxylation to form metakaolin (amorphous kaolinite) and pyrite decomposes into elemental iron and sulphur (O'Gorman & Walker, 1973; Hill & Easter, 2021). Apart from the contribution of weight loss that occurred during the polymer transformation to ceramic, the decomposition of the C=C bonds in coal was directly linked to the pyrolysis mass loss and shrinkage experienced by the composites. It was observed that the higher the intensity of this bond, the higher the mass loss and shrinkage of the composites, as discussed in Section 7.3.3.1.

Above 800 °C, amorphous kaolinite decomposes into nanosized silica (silicon dioxide) and alumina (aluminium oxide) and to amorphous mullite (not detected by XRD). These nanosized products then merge to domains of graphitised carbon and are chemically bound into a ceramic structure through Si-O-Si bonds formed by the transformation of the PCP into ceramic (Solomon, 1981; Hill & Easter, 2021). Referring also to the FTIR spectra presented in Figure 7-3, the $f_3$ peaks of the coals have transformed to $p_6$ in the composites. The disappearance of $f_4$ peaks in the coals assigned to the aromatic C-H vibrations reflects a substitution reaction that had taken place during pyrolysis. The fingerprint region of the CBW ($f_3$-$f_5$), in general, underwent extensive rearrangement

transforming to a dominant band centred around 1065 $cm^{-1}$ ($p_6$) in the composites. This band has been assigned to the -Si-O- stretching vibration associated with quartz and Si-O-Si bonds in ceramics (Gumula et al., 2009), while the weak peaks below 1000 $cm^{-1}$ observed in the composites were ascribed to quartz and Si-C vibrations (Gumula et al., 2009; Taha et al., 2017).

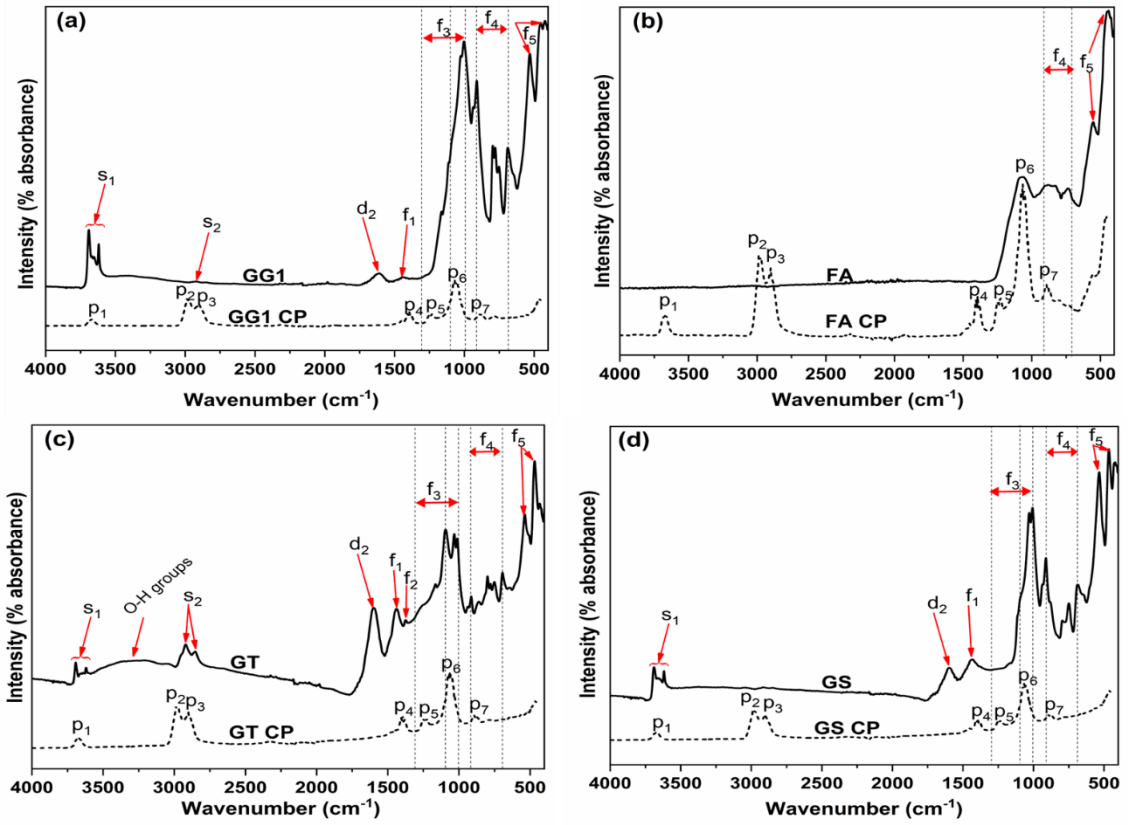



Figure 7-3 Fourier Transform Infrared spectra of the coal waste and their corresponding composites

(CP – composite; GG1 – discard from washing plant; FA – fly ash; GT – fine waste; GS – coal waste from Witbank coalfield)

Table 7-4 Summary of the various functional groups within the coal structure and coal composites

| **Wave number ($cm^{-1}$)** | **Peak/ Vibration** | **Band assignment/functional groups** |
|---|---|---|
| 3690 to 3618 | $s_1$ | O–H stretching vibrations relating to kaolinite, mineral matter (surface and inner surface –OH groups) |
| 2917 to 2852 | $s_2$ | Aliphatic C–H stretch |
| 2917 | | Asymmetric $CH_2$ vibrations |
| 2852 | | Symmetric $CH_2$ and $CH_3$ vibrations |
| 1598 | $d_2$ | Aromatic C=C stretching vibrations |
| 1440 | $f_1$ | $CH_2$, $CH_3$ bending vibrations |
| 1368 | $f_2$ | $CH_3$ groups |
| 1300 to1000 | $f_3$ | C-O stretch, C-C stretch, and O-H bending vibrations alcohols, phenols, ethers, phenoxys and esters |
| 911 to 684 | $f_4$ | Si-O-Si asymmetric stretching vibrations and Al-O-Al symmetric stretching vibrations associated with aluminates and silicates; out-of-plane aromatic C–H bend |
| < 700 | $f_5$ | O–Si–O symmetric bending vibrations/deformations associated with aluminates and silicates; Al–O–Al stretching vibrations associated with minerals; S–S vibrations associated with pyrite |
| **Composites** | | |
| 3700 to 3600 | $p_1$ | O-H stretching vibrations |
| 3000 to 2900 | $p_2/p_3$ | Alkyl C-H stretching vibration |
| 1395 | $p_4$ | C-H stretching vibration |
| 1229 | $p_5$ | C-H stretching vibration |
| 1055 | $p_6$ | Si-O-Si asymmetric stretching vibration |
| 879 | $p_7$ | Quartz vibrations |

*7.3.2.2 X-ray diffraction analysis*

X-ray diffraction was utilised to investigate the mineral phase rearrangement after pyrolysis treatments (Figure 7-4). The absence of an amorphous hump suggests that the FA does not contain the aluminosilicate glass phase. Mineralogically, the association of crystalline quartz (silicon dioxide) and mullite phases is mainly visible in the FA waste. Mullite is an aluminosilicate mineral formed from the decomposition and transformation of kaolinite (a clay mineral) at elevated temperatures (Xu et al., 2017; Rautenbach et al., 2020). Quartz, anorthite, and hematite mineral phases were detected in the FA

composites. The anorthite (calcium aluminosilicate) mineral phase is usually formed by the reaction of mullite and the transformed product of lime (calcium oxide). The detection of anorthite suggests that minor impurities like calcium oxide might be present in the FA (Yuan et al., 2022). Further work is needed to fully characterise the oxides in the coal using X-ray fluorescence analysis. Microcline, a potassium-rich alkali feldspar was detected in GS coal while the kaolinite phase is well present in GG1, GS, and GT. The basic unit of the kaolinite mineral consists of a tetrahedral sheet of silicon dioxide siloxane units and an octahedral sheet of aluminium hydroxide (Zhang et al., 2017). Referring to the mineralogical composition of GG1, GS, and GT composites, the results show that the kaolinite mineral phases in these coals have disappeared. Ideally, kaolinite decomposes at around 700 °C through a process of dihydroxylation (Rautenbach et al., 2020) to form quartz. Besides, some quartz still exists in these composites but in a different phase because at 570 °C quartz undergoes quartz inversion (O'Gorman & Walker, 1973; Wang & Zhou, 2011). Furthermore, quartz is a refractory mineral and is usually non-reactive depending on the mineral association. The new mineral phase rutile (titanium dioxide) detected in the GG1 composite can be attributed to the dissolution reaction of quartz in the presence of kaolinite during pyrolysis. The presence of a broad hump centred at a 2θ-theta value of approximately 10° typical of amorphous carbon or carbonaceous matter (Song et al., 2011) is observed in the diffractogram of GT coal and the GT composite. As stated earlier, GT is a high-rank coal (semi-soft coking coal fines); hence, some graphite crystallite peaks were detected as a result of pyrolysis up to 1000 °C.

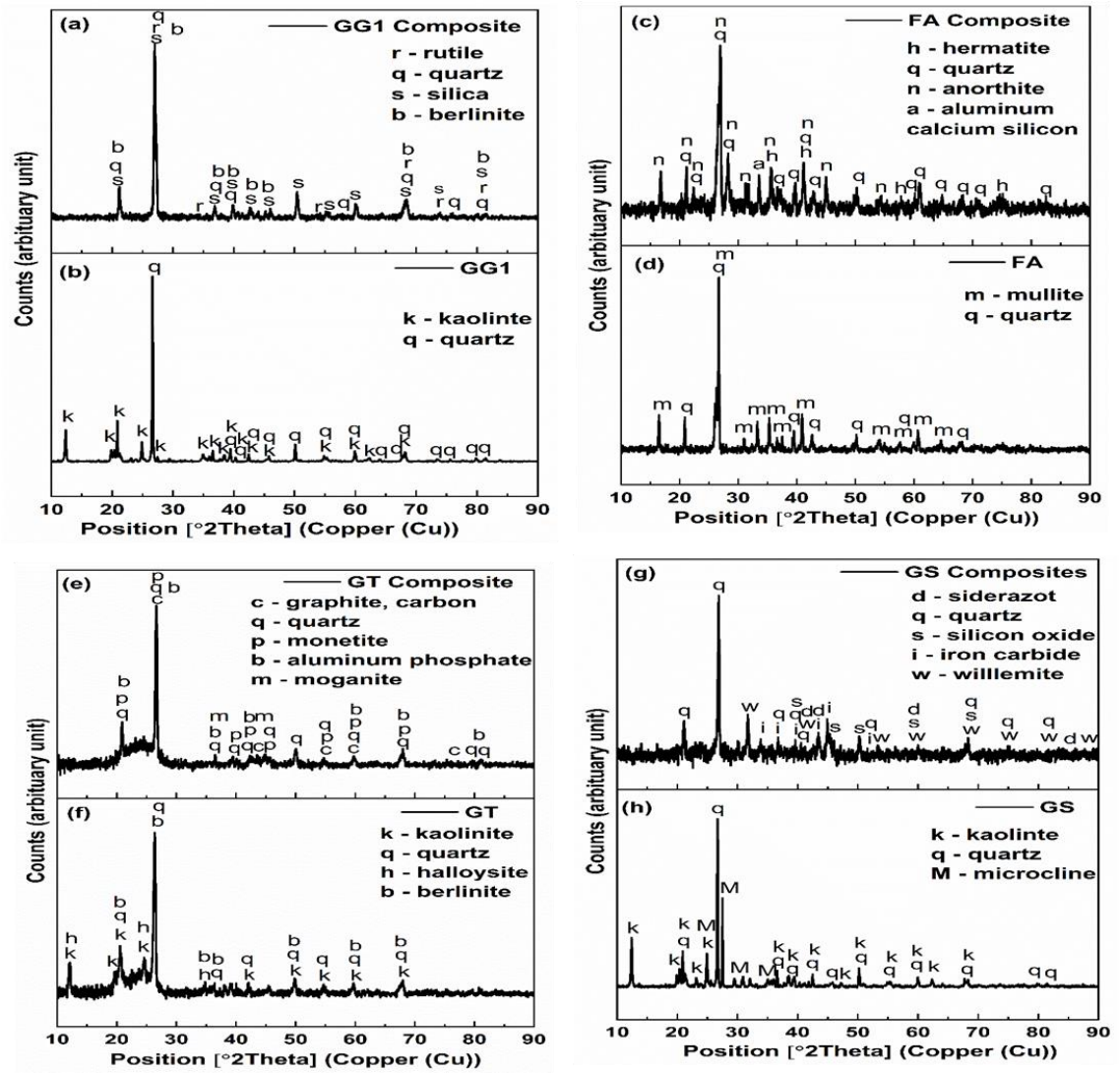



Figure 7-4 A comparison of the X-ray diffraction patterns of the coals and coal composites

(GG1 – discard from washing plant; FA – fly ash; GT – fine waste; GS – coal waste from Witbank coalfield)

*7.3.2.3 Scanning electron and optical imaging*

Scanning electron microscopy-backscattered electron (SEM-BSE) coupled with energy dispersive spectroscopy (EDS) was used to observe the surface morphologies and record the elemental differences of the composites. SEM-BSE images of the carbon-coated composites presented in Figure 7-5 show some cracks on the surface of the composites. These cracks could have been caused by thermal stresses and shrinkage

experienced by the composites during pyrolysis. It could also be possible that the cracks were formed when breaking a small composite sample for SEM imaging. The energy dispersive spectroscopy of an area of the composite surface shows the stoichiometry of the detected elements. The FA composite contains traces of carbon and anorthite grains associated with quartz. In addition, quartz, representing the most abundant phases, seems to be bonded by a carbon matrix formed from the pyrolysis of the PCP. SEM imaging of the GT composite revealed grains of phosphate minerals (monetite). The surface of the GT composite is homogenously darker than the other composites, attributed to the relatively high carbon in the composite. The composites appear smooth; however, at high SEM magnifications, their surfaces are rough. Therefore, to enhance surface smoothness and uniformity, using a polytetrafluoroethylene release film to line the mould in direct contact with the mixture being pressed might be beneficial. Another solution might be to add soluble wetting agents, e.g., water, surfactant, or solvent, to the coal/PCP mixture. The optical microscopic images of fabricated composites (Figures 7-5c, f, i and l) show good incorporation of the mixture content and spatial distribution of minerals on the composites' surface. Large quartz grains can be observed on the FA composite, while apatite grains can be seen on the GS composite (Figure 7-5i).

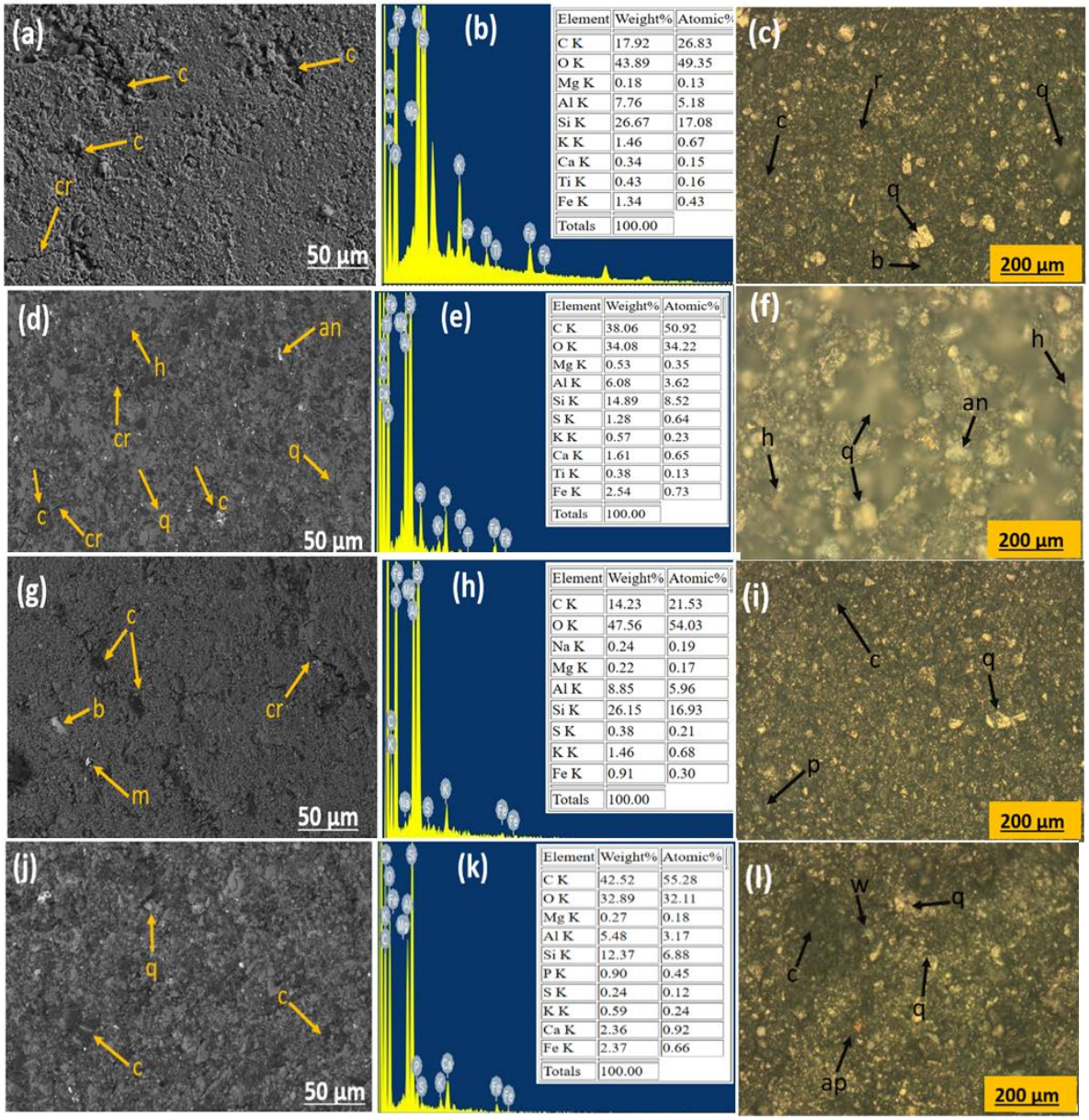



Figure 7-5 Scanning electron microscopy secondary electron image (a), back-scattered images (d, g, j), energy dispersive X-ray spectroscopy analysis (b, e, h, k) and optical micrographs (c, f, i, l) of the as-fabricated composites. (a, b, c) GG1; (d, e, f) FA; (g, h, i) GT; (j, k, l) GS composites.

(an – anorthite; b – aluminium phosphate; c – carbon; cr – crack; h – hematite; m – monetite; q – quartz)

*7.3.2.4 Raman analysis*

The carbon phase is an important component of carbon-bonded composites. As noted earlier, the mixture of the CBW and the PCP pyrolysed up to 1000 °C could have developed a network of graphene fragments or nanodomains of graphitic carbon (Sharma, 2018; Hill & Easter, 2021). Therefore, Raman spectroscopy was used to acquire information pertaining to the carbon structure and the graphitisation degree of the carbon atoms. The Raman spectra of the composites manifest peaks at around 1360 and 1560 $cm^{-1}$, the typical D-band and G-band in carbon-based materials (Figure 7-6). The presence of both bands suggests that the carbon resulting from the pyrolysis of the mixture is in a disorganised state and consists of the infinite repetition of $sp^3$ and $sp^2$ hybridised C-C bonds. Broad peaks centred around 2750 $cm^{-1}$ and 3200 $cm^{-2}$, such as the second-order 2D (or G') and the 2D' bands observed in graphite samples (Ferrari, 2007), are more dominant in the Raman spectra of the GG1 and FA composites. In principle, the 2D-band supports the presence of amorphous carbon and is characteristic of turbostratic carbon (Ruz et al., 2016). Also judging by the existence of the 2D peak in the GG1 and FA composites, as speculated earlier, some graphene layers may have formed (Sazali et al., 2016).

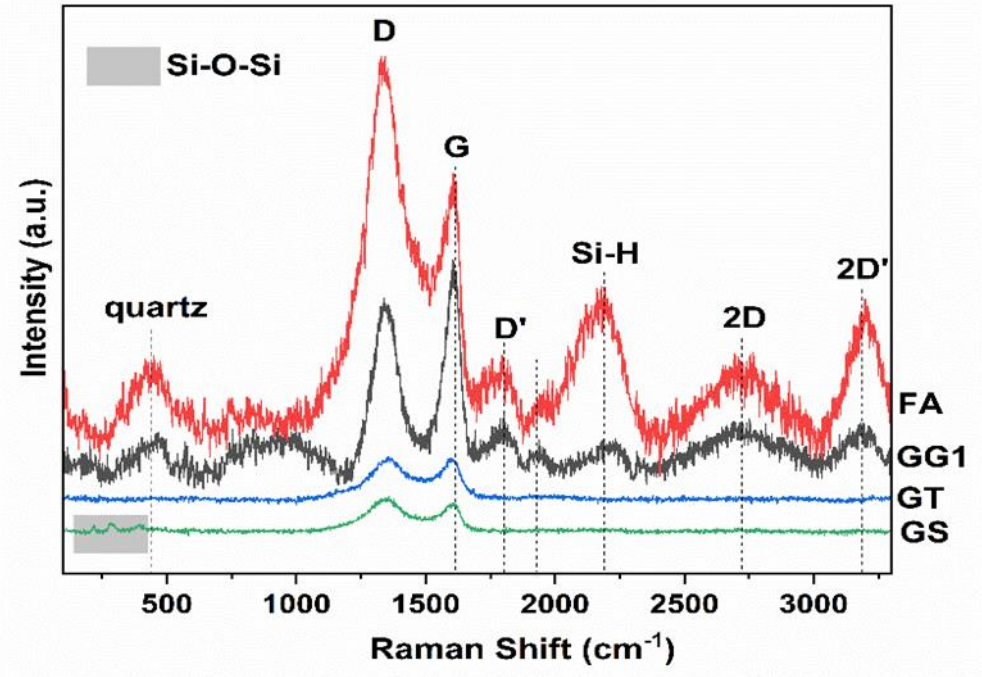



Figure 7-6 Raman spectra of the composites

(GG1 – discard from washing plant; FA – fly ash; GT – fine waste; GS – coal waste from Witbank coalfield)

Table 7-5 Graphitisation indices of the composites

| **Composites/Indices** | **GG1** | **FA** | **GT** | **GS** |
|---|---|---|---|---|
| $A_D/A_G$ | 1.45 | 3.78 | 2.21 | 2.90 |
| $L_a$ | 3.03 | 1.16 | 1.98 | 1.51 |

(GG1 – discard from washing plant; FA – fly ash; GT – fine waste; GS – coal waste from Witbank coalfield; $A_D/A_G$ – peak intensity ratio; $L_a$ – size of carbon crystallites)

The D' peak close to the G-band is usually observed in the nanostructures of disordered carbon materials (Dresselhaus et al., 2010; Pusz et al., 2015), such as those in this study. The emergence of peaks less than 1000 $cm^{-1}$, such as 445 $cm^{-1}$ associated with quartz and 758 $cm^{-1}$ attributed to the Si-C peak, and the presence of the Si-O-Si bond/vibration can be seen in the spectra of the GG1, FA, and GS composites but surprisingly was not Raman active in the GT composites. $A_D/A_G$ was calculated from the ratio of the areas beneath the D- and G-bands, and the size of carbon crystallites ($L_a$) was used to quantify the disorder (Table 7-5). The intensity ratio generally increases with the

amount of carbon phase disorder, and the trend follows FA>GS>GT>GG1, meaning that the least graphitic (i.e., highly defective) carbon phases are dominant in the FA composite. The GG1 composite supports the dominance of the graphitic carbon phases ($sp^2$ C-C bonds) suggesting the formation of fewer defects. $A_D/A_G$ correlates inversely to $L_a$ and agrees with the cluster size of the carbon phase of the composites, FA composites being the least (1.16 nm). As noted earlier, the total carbon of the FA composite (1.46%) was mainly provided by the pyrolysis of the polymer.

*7.3.2.5 Thermal stability/continuous operating temperature of the composites*

The thermal stability of the composites was investigated to monitor the quantitative weight change during the thermal degradation of one gram of composites placed in a TGA furnace under different environments (air and oxygen) at a ramp rate of 10 °C/min to 900 °C. The minimum and maximum weight loss rate temperatures and the decomposition temperature at T5% were used to evaluate the thermal stability of the composites (Table 7-6). Two temperature regions were identified in Figure 7-7 where weight loss occurred. Stage 1 weight loss (less than 200 °C) is related to the loss of adsorbed moisture and low molecular weight volatile matter in the case of the GT composite. The weight loss of the GT and GS composites in an air environment (Figure 7-7b) around 600 °C (stage 2) was about 9.09% and 4.55%, respectively. Above 600 °C, the GT and GS composites show progressive weight loss of about 14.3% and 14.23%, respectively. The GT composite displayed the worst thermal stability performance owing to the thermal decomposition of the carbonaceous materials in the composites. In contrast, a small weight change was recorded for the GG1 and FA composites when heated in an oxygen or air environment. FA, being a non-combustible material, produced the most thermally stable composite. This observation is consistent with the XRD results that

showed highly stable and high melting point minerals e.g., quartz, anorthite, and hematite were detected in the FA composite. Besides, the high thermal stability of the GG1 and FA composites suggests they contain a reasonable amount of Si-O bonds and fewer C-C and C-O bonds compared to the GS and GT composites. The bond dissociation energy of the bonds C-C (82.6 KJ/mol) and C-O (85.2 KJ/mol) are low compared to the Si-O bond (108 KJ/mol) (Jones et al., 2013; Stabler et al., 2018).

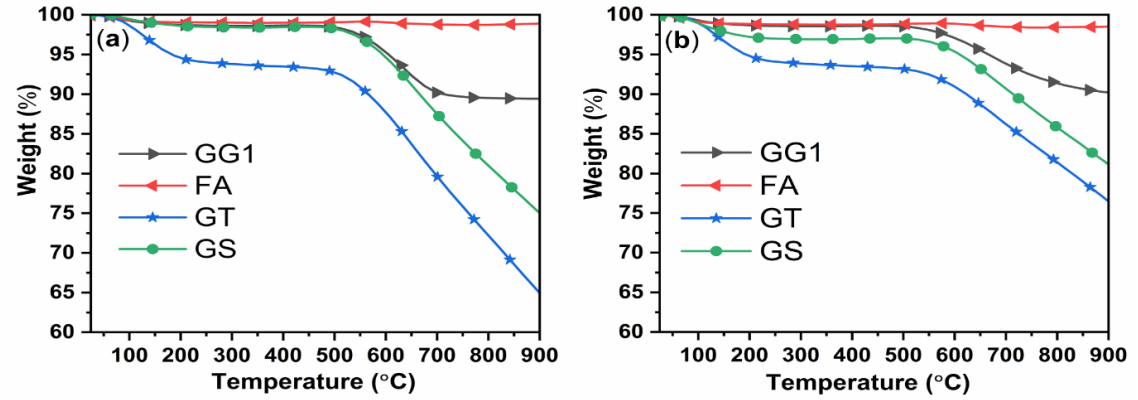



Figure 7-7 Thermal analysis (TGA) profiles of the composites under (a) Oxygen (b) Air environment

Table 7-6 Summary of the thermogravimetric analysis of the composites shown in Figure 7-7

| Composites | $T_1$ (°C) | $T_2$ (°C) | T5% (°C) | Stage 1 weight loss (wt.%) | Stage 2 weight loss (wt.%) | Total weight loss at 900 °C (wt.%) |
|---|---|---|---|---|---|---|
| **(a) Oxygen environment (99.5% purity)** | | | | | | |
| GG1 | 85.85 | 650.83 | 604.14 | 1.40 | 9.10 | 10.50 |
| FA | 89.24 | 633.87 | – | 0.85 | 0.41 | 1.26 |
| GT | 104.51 | 673.97 | 183 | 6.36 | 28.69 | 35.05 |
| GS | 99.21 | 678.76 | 593.77 | 1.54 | 23.59 | 25.13 |
| **(b) Air environment** | | | | | | |
| GG1 | 109.98 | 683.54 | 671.57 | 1.74 | 8.21 | 10 |
| FA | 90.83 | 649.23 | – | 1.12 | 0.55 | 1.68 |
| GT | 139.11 | 681.15 | 191.02 | 6.23 | 17.17 | 23.40 |
| GS | 118.56 | 677.56 | 609.99 | 3.19 | 15.59 | 18.78 |

($T_1$ and $T_2$ – temperature corresponding to the minimum and maximum weight loss rate; T5% – decomposition temperature at 5 % weight loss; GG1 – discard from washing plant; FA – fly ash; GT – fine waste; GS – coal waste from Witbank coalfield)

### *7.3.3 Physical and mechanical analysis of the composites*

The difference in the physiochemical structures of the CBW already indicates the possible differences in terms of the properties of the composites. This section discusses the composites' physical properties (bulk density, apparent porosity, pyrolysis shrinkage and water absorption) and mechanical properties (ultimate compressive stress).

#### *7.3.3.1 Weight loss and shrinkage during pyrolysis*

The shrinkage value after pyrolysis of the cured composites provides useful information on the size of mould or die that would be needed to produce a predetermined composite size. From Figure 7-8, the pyrolysis mass loss of the composites is within the range of 5.28 to 29.62%. All the composites retained their shape, but composites produced from the CBW of high inorganic content (GG1 and FA) presented lower shrinkage values. On the contrary, the GT composite recorded substantial weight loss (29.62%), radial shrinkage (17.97%), and volume shrinkage (46%). This was attributed to the nature of the coal and the high volatile matter content (32.7%). This substantial weight/shrinkage loss,

which implies a reduction in the free volume of the composites, resulted from a high degree of conversion of the C=C bonds in the coal to C-C bonds (as shown in the FTIR results). For a small-sized sample, the volume shrinkage of the GT and GS composites seems quite high. As such, it could present a challenge if large-size composites were produced. High shrinkage tends to be associated with contraction stress, thermal stress, cracks, deformation, and warping during pyrolysis. In principle, the PCP decomposes during pyrolysis, followed by the release of hydrogen and other species containing carbon and hydrogen that results in mass loss, volume shrinkage, and densification. As a result, the composites contain some ceramic phases homogenously dispersed in a carbon matrix. Considering that the ratio of the raw materials is 80 wt.% coal and 20 wt.% PCP, it is believed that the shrinkage that occurred is largely dependent on the physicochemical composition of the coal, which, in turn, dictated the degree of conversion of the composites.

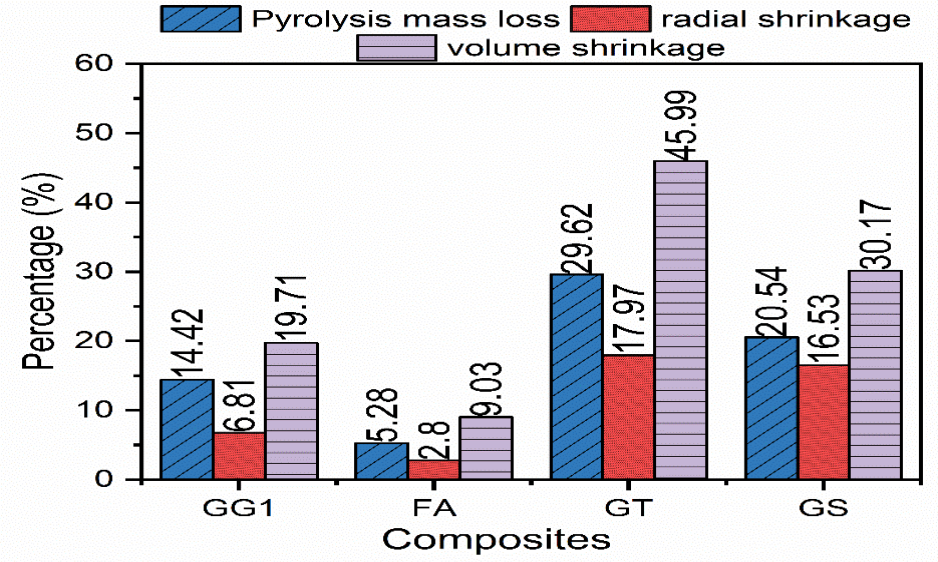



Figure 7-8 Average pyrolysis mass loss and shrinkage of the composites

(GG1 – discard from washing plant; FA – fly ash; GT – fine waste; GS – coal waste from Witbank coalfield)

*7.3.3.2 Density, water absorption and apparent porosity of the composites*

The bulk density, geometric density, and apparent specific gravity of the composites after the water impregnation stages (five-hour cold test, 24-hour cold test, and five-hour boiling test) are displayed in Figure 7-9. According to the data, the 24-hour cold test and the five-hour boiling test did not significantly increase the density of the composites, demonstrating compactness and micro-cracking of the composites. In general, the bulk density of the composites varied between 1.5 g/cm$^3$ and 1.9 g/cm$^3$. The GG1 composite recorded the highest densities while the GT composite had the least overall. The coal from which the GG1 composite was made has the highest ash content, i.e., more inorganic forming minerals. Besides, GG1 is rich in oxygen functional groups, which facilitate curing reactions, as well as physical and chemical interactions with the polymer during pyrolysis. This might have led to the GG1 composite's high density,

considering that the FA is also rich in minerals; yet, the FA composite is of lower density than the GG1 composite.

The high shrinkage experienced by the GT composite is due to the nature of the coal and is reflected in the composite's low density. Furthermore, the high volatile matter (32.7%) of GT coal appears to have accelerated degassing and porosity generation within the composite during pyrolysis. Water absorption, i.e., the mass of water absorbed to the mass of the dry composite, provided an indirect measure of porosity and extent of densification. The apparent porosity expresses the volume of open pores of the composites to its exterior volume as a percentage. As expected, the apparent porosity and water absorption follow the same trend, as displayed in Figure 7-10. Low water absorption of the GS, FA, and GG1 composites indicates a high volume of impervious pores. These low water absorption composites are essential to resist water intrusion from the natural environment, consequently enhancing their durability. With the water absorption of the composites similar to those of conventional building materials (0 to 25%), these composites may be fabricated into pavement tiles, cladding tiles, bricks, blocks, or roof tiles depending on the application.

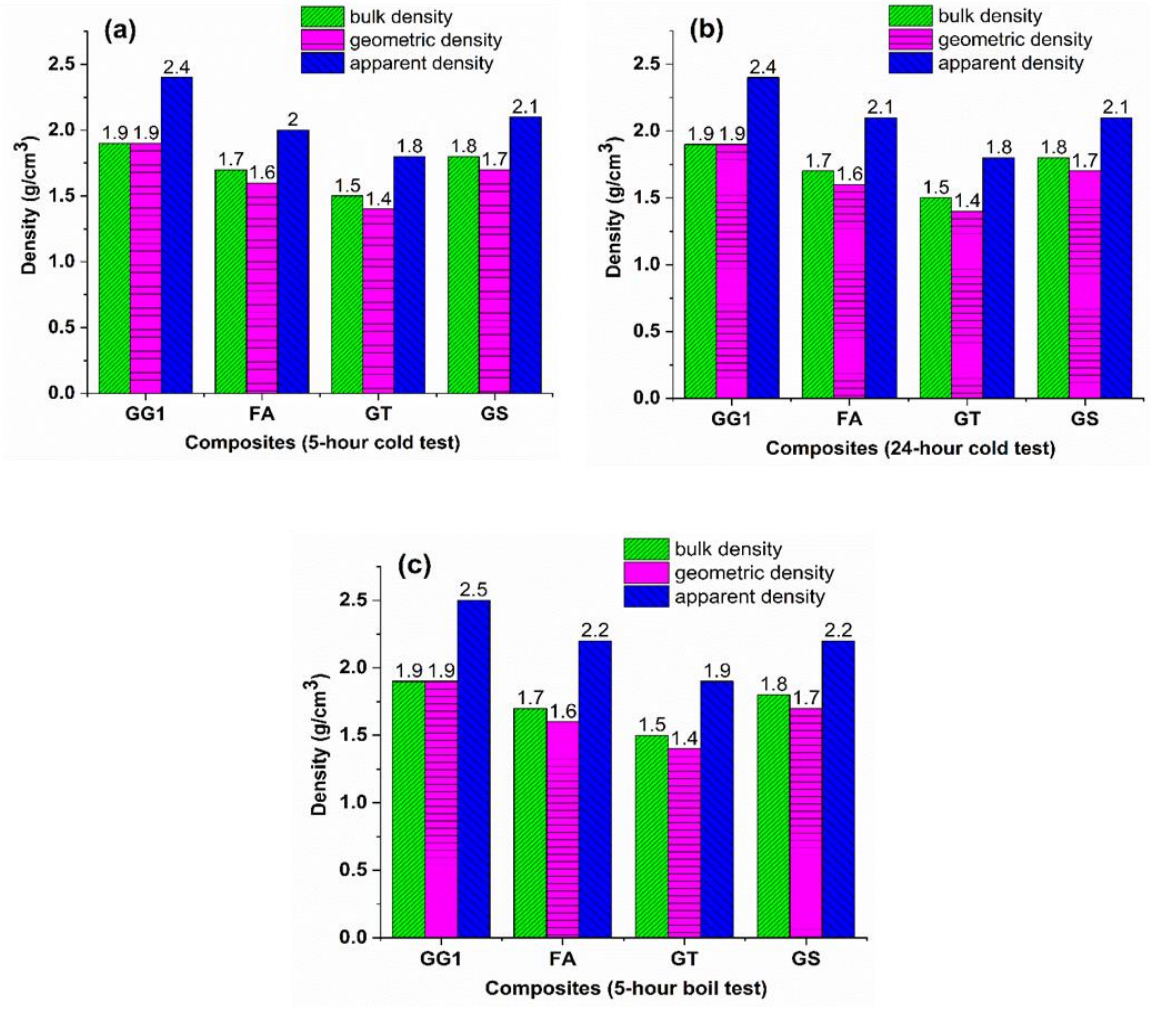



Figure 7-9 Bulk, geometric and apparent densities of the composites

(GG1 – discard from washing plant; FA – fly ash; GT – fine waste; GS – coal waste from Witbank coalfield)

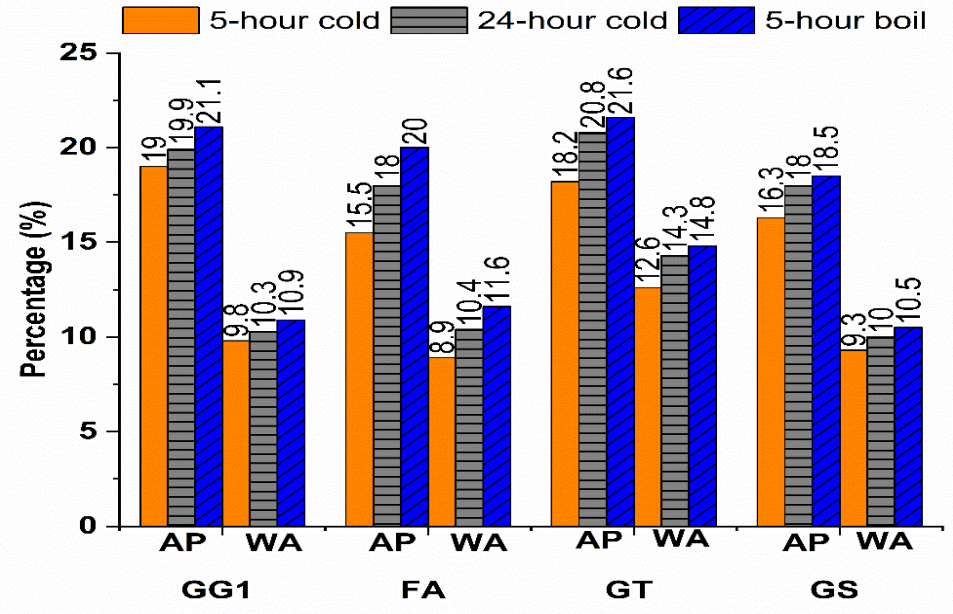



Figure 7-10 Average apparent porosity and water absorption of the composites (AP – average porosity; WA – water absorption; GG1 – discard from washing plant; FA – fly ash; GT – fine waste; GS – coal waste from Witbank coalfield)

*7.3.3.3 Surface property of the composites*

Surface property is a critical indicator in the design of coal composites for construction applications as they could impact the durability of composites. In this work, the surface property of the composites was described in terms of the static CA between water and the composite surfaces. The CA was measured from a minimum of four drops on each side of the composite. The CAs of the GT and GS composites with water are less than 90° (Figure 7-11), can be linked to the nonpolar nature of their surface. This observation implies strong interfacial adhesion between the surface of the composites and water. Therefore, the composites have a high tendency to adsorb water. Therefore, they would be highly susceptible to water wetting and may not be useful in applications where interaction with water is needed. In contrast, the CAs of the FA and GG1 composites are greater than 90°, infer that their surfaces are hydrophobic and the force of attraction of water-to-composite is weak. From a practical point of view, these composites are less

susceptible to water wetting and penetration, which could cause the composites to deteriorate easily. Apart from being dense and less porous, evidence supporting the FA and GG1 composites maintaining a high CA can be linked to the non-polar C-H functional groups bound to their surfaces (Gomez-Caturla et al., 2022). As seen from the FTIR spectra (Figure 7-11), these hydrophobic functional groups (C-H) are more absorbed in the FA and GG1 composites and are responsible for the weak molecular interaction between water and the composite surface.

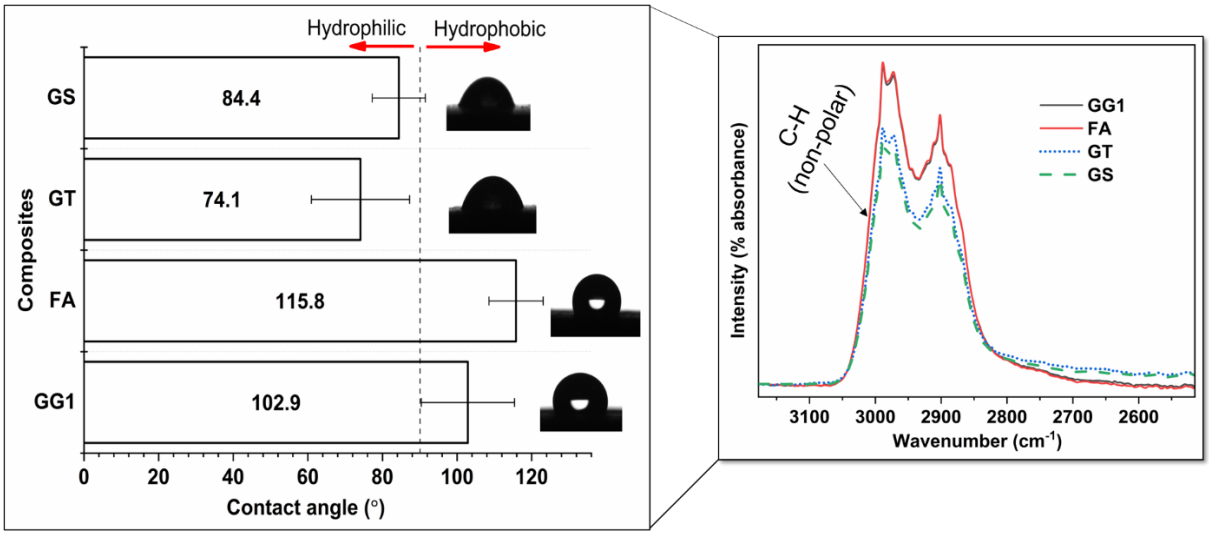



Figure 7-11 The water contact angle of the composites measured by the sessile drop method and FTIR of the nonpolar C-H group (right)

*7.3.3.4 Compressive strength performance*

The mechanical behaviour of the composites produced was studied using compression tests to investigate the strength of the bonds that connect the atoms and crystals inside the composites. The mechanical properties of the composites in terms of their average ultimate compressive stress are presented in Figure 7-12. Given that the various composites offer a difference in their physicochemical properties, the composites produced from the coking coal fines (GT) with 62.66% total carbon and 32% volatile matter, exhibited the lowest resistance to compression (278 MPa). Due to the nature of

this coal, it could be postulated that at lower temperatures, GT swelled and experienced better heat transfer with the polymer than the other wastes. Hence, by pyrolysing the composite up to 1000 °C, it is likely that char-like composites with large pores could have formed. These pores might have constituted stress concentrators under load that led to the low mechanical stability of the composites.

The high compressive strength of the GS, GG1, and FA composites can be linked to their high bulk densities. Increased strength is known to come with increased density (Hill & Easter, 2021). Besides, the formation of the anorthite phase in the FA composite may have contributed to its strength (Kairakbaev et al., 2017). Comparing the bonding strength of the GG1, FA, and GS composites, GS displays the highest strength while FA has the lowest. The lack of reactive sites (inertness of their surfaces) in FA led to weak interactions with the PCP during pyrolysis, consequently lowering the bonding strength. The use of silane coupling agents can provide adequate reaction sites that would significantly enhance the reactions during pyrolysis but with an additional cost. Interestingly, the mechanical response of the GS composite is the best. This suggests that a certain limit of carbon in the CBW may seem sufficient to increase the bonding capacity of the mix and a relatively high carbon content of the CBW could compromise the strength of the final composites. Therefore, it can be postulated that for a relatively high carbon content CBW and depending on the nature of the coal, the bonding strength of the mixture pyrolysed up to 1000 °C would reduce sharply. Comparatively, in terms of their specific compressive strength ($MPa.cm^3/g$), i.e., the strength-to-density ratio, GS recorded the highest, suggesting that the GS composite might be more advantageous for lightweight and high-performance construction material (Ming et al., 2019).

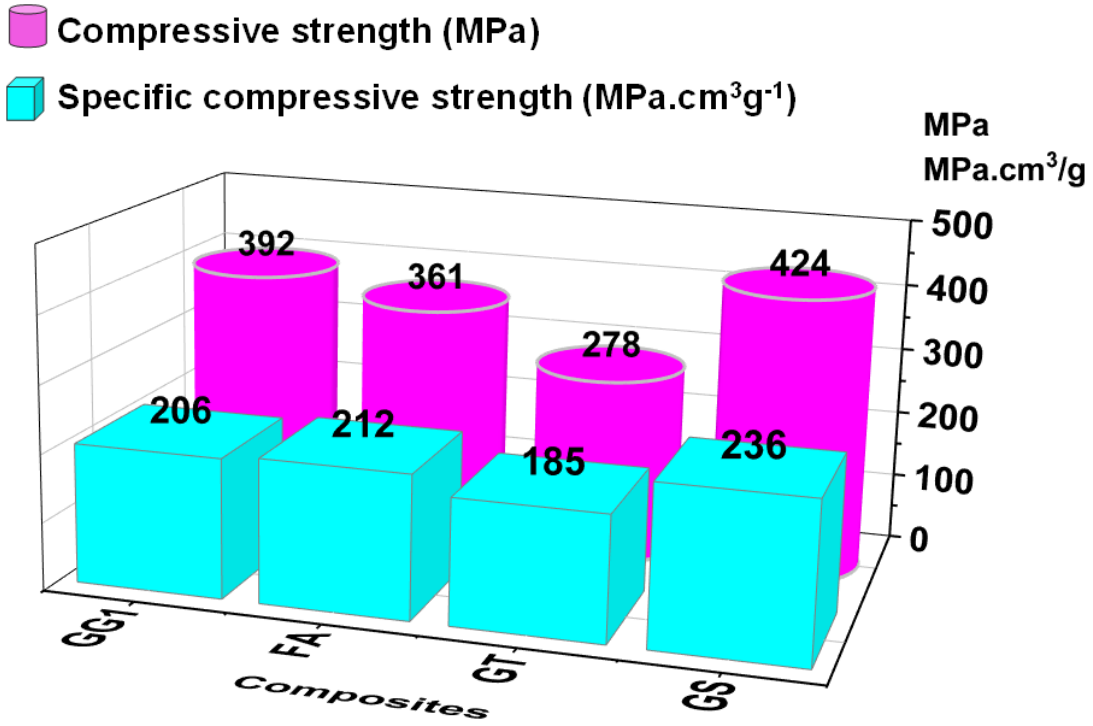
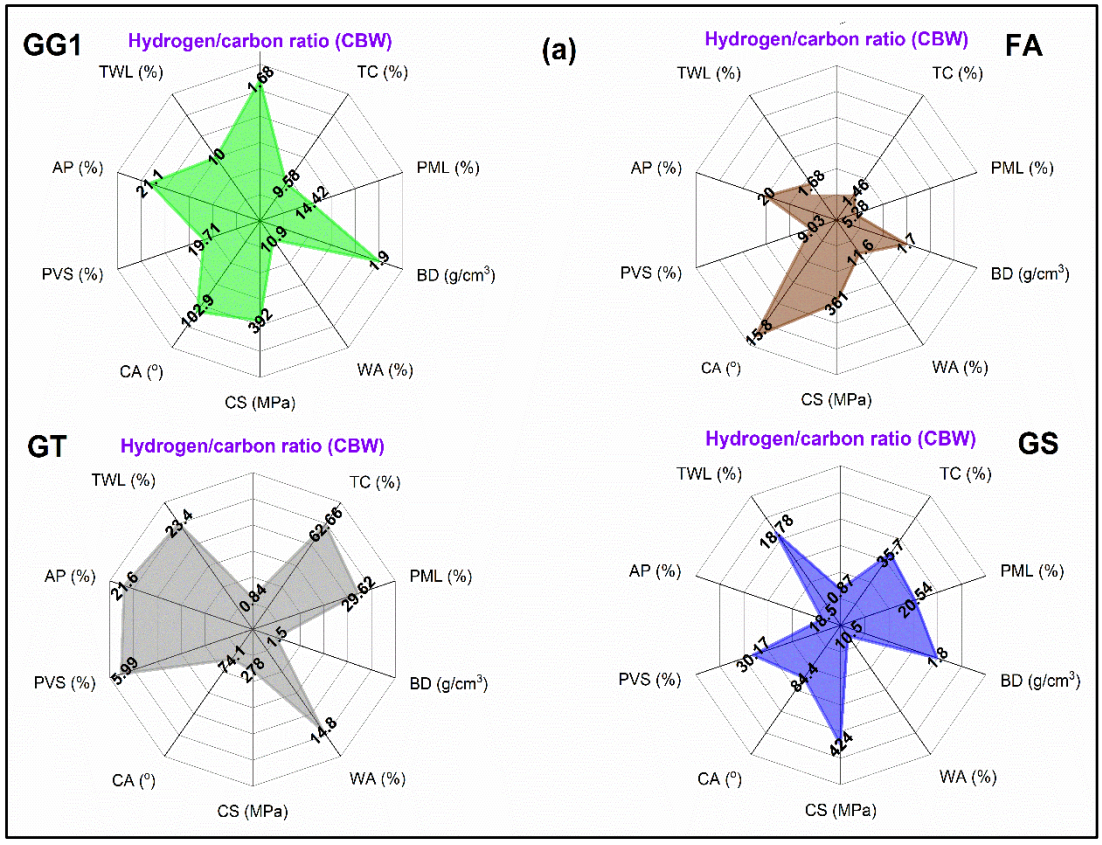


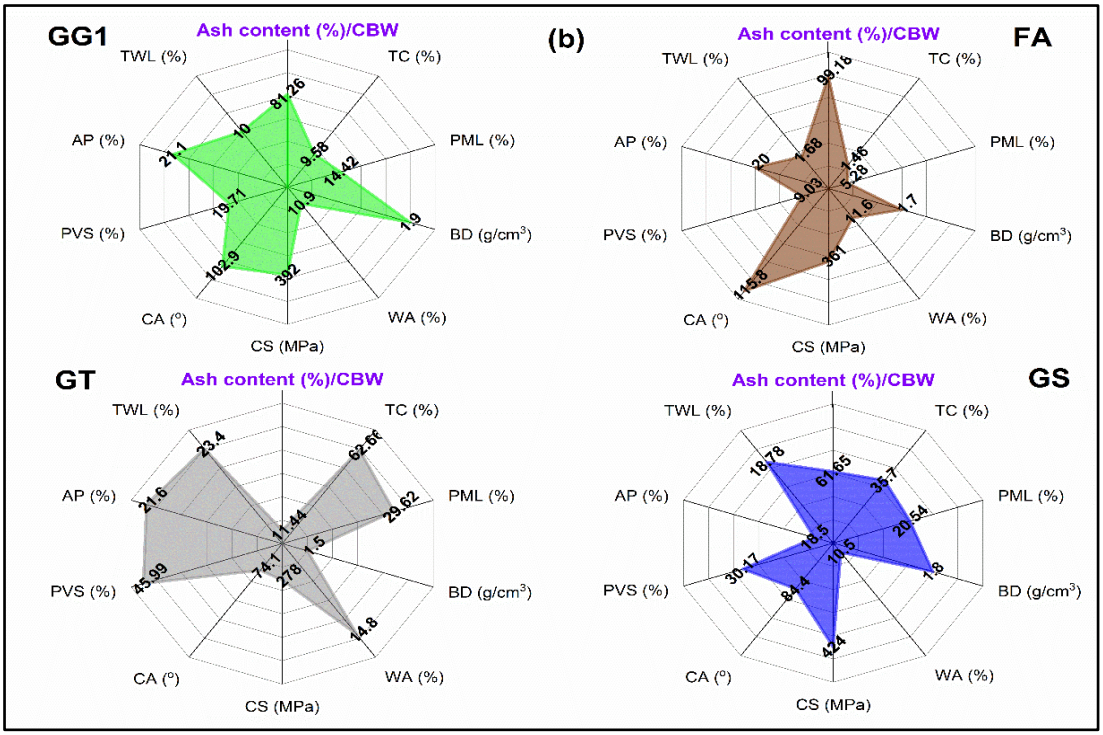

Figure 7-12 Average ultimate compressive stress and specific compressive strength of the composites

(GG1 – discard from washing plant; FA – fly ash; GT – fine waste; GS – coal waste from Witbank coalfield)

The comparison of the physicomechanical performance of the composites produced in this study to other composites for building applications in the literature is listed in Table 7-7. The radar chart (Figure 7-13a, b, c) illustrates the correlation of the hydrogen/carbon ratio, ash content, and volatile matter of CBW on the key performance properties of the coal/PSO composites. It can be seen that higher H/C ratio CBW (GG1) produced the best quality composites in terms of water absorption, compressive strength, and thermal stability. This is because of the many hydrogen bonds contained in the molecules of this waste that enabled it bind effectively with the polymer during pyrolysis (Hu et al., 2017; Hill & Easter, 2019). On the other hand, a clear distinction in the low thermal weight loss and carbon content of the composites produced from high-ash wastes

(GG1 and FA) is due to the presence of many non-combustible materials in these wastes. Finally, high volatile CBW (GT) yielded composites with the least desired properties overall for building applications (lowest compression strength, highest water absorption, and lowest water contact angle).





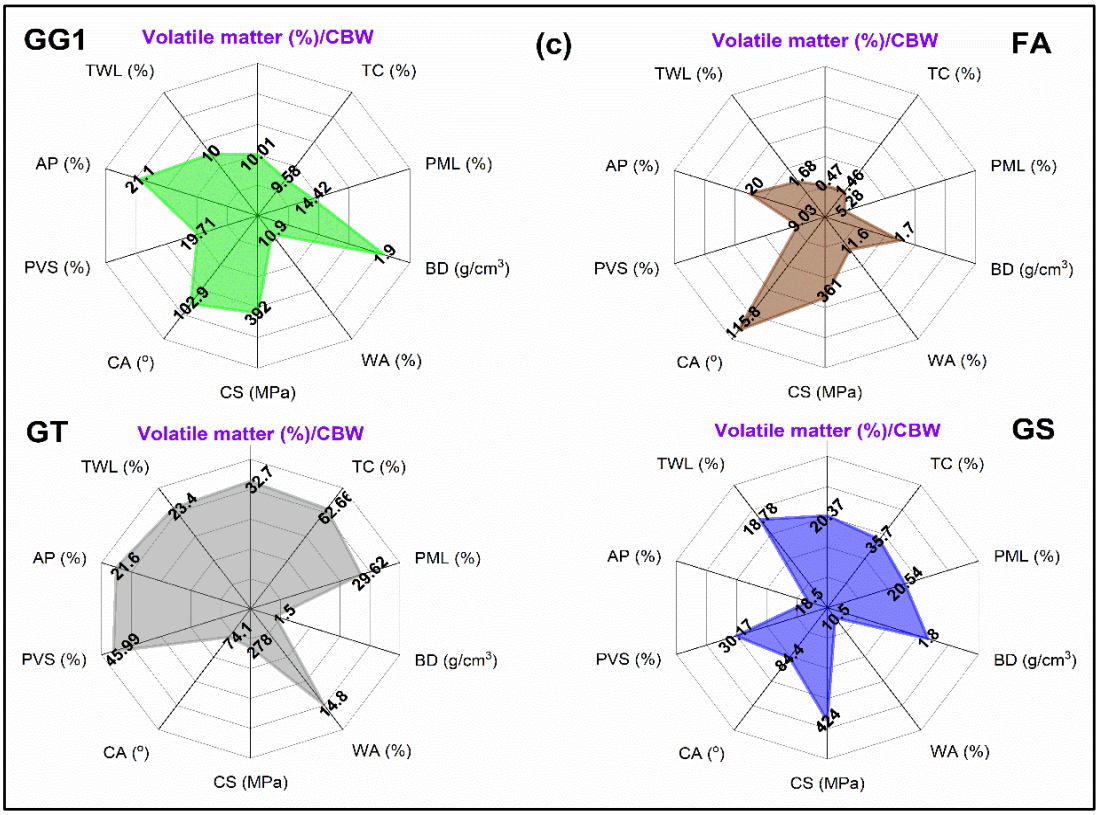




Figure 7-13 The correlation between (a) hydrogen/carbon ratio (b) ash content (c) volatile matter of CBW on the key performance properties of the composites

TC – total carbon; PML – pyrolysis mass loss; BD – bulk density; WA – water absorption; CS – compressive strength; CA – contact angle; PVS – pyrolysis volume shrinkage; AP – apparent porosity; TWL – thermal weight loss
(GG1 – discard from washing plant; FA – fly ash; GT – fine waste; GS – coal waste from Witbank coalfield)

Table 7-7 The physicomechanical performance of the composites produced in this study compared to other composites for building applications in the literature

| **Materials** | **LS (%)** | **BD ($g/cm^3$)** | **WA (%)** | **AP (%)** | **CS/FS (MPa)** | **References** |
|---|---|---|---|---|---|---|
| CFA/NaOH/ feldspar/HPC | 14.94 | - | 0.30 | 0.62 | -/40.25 | Luo et al. (2019) |
| Core sand/clay/ water | 1.8-3.1 | - | 5.9 - 10 | - | - | Alonso-Santurde et al. (2012) |
| Clay/wood pulp/WS/FS | - | < 2 | 10-16 | 29-39 | -/<8 | Quijorna et al. (2012) |
| RM/α-$Al_2O_3$/γ-$Al_2O_3$/ρ-$Al(OH)_3$ | - | 1.83-1.94 | 7.37 | 18.56 | -/185.46 | Wang et al., (2020) |
| CBW/PCP (XMAT) | ~20-~27 | 1.69-1.77 | 1.94-10.1 | 3.44-17.1 | 84-209/28-35 | Eterigho-Ikelegbe et al. (2021b) |
| CBW/clay/ water | - | 1.54-1.77 | 19.4-27.7 | | 18.6-25.8/1.6-2.1 | Gökçe et al. (2018) |
| CBW/clay/water | - | 1.5-1.9 | 20.5-29.5 | 31.2/48.9 | 7-21.3/- | Bonczyk and Rubin (2022) |
| CBW/PCP (XMAT) | 18-19.4 | 1.46-1.7 | - | - | -/35-125 | Hill and Easter (2019) |
| CBW/shale/ IOT/ SS/water | 8.3 | 1.64 | 17.5 | - | 14.24/- | Luo et al. (2020) |
| CBW/SPR-212 | 2.8-16.53 | 1.5-1.9 | 8.9-14.8 | 15.5-21.6 | 278-424/- | Our work |

LS – linear shrinkage; BD – bulk density; WA – water absorption; AP – apparent porosity; CS – compressive strength; FS – flexural strength; CFA – coal fly ash; HPC – high plastic clay; WS – waelz slag; FS – foundry sand; RM – red mud; CBW – coal-based waste; PCP – preceramic polymer; IOT – iron ore tailings; SS – sewage sludge

## 7.4 Conclusion

Processing coal-based waste into high-value composites seems like a good way to manage and transform this problematic waste. The variation in the physicochemical properties of coal-based waste on the resultant composites using the poly(organo)siloxane SPR-212 as the ceramic-forming binder was studied. The GT fines used in this study contain the highest percentage of volatile matter and total carbon. As a result, the GT composite displayed the poorest qualities based on the properties evaluated. The relatively high total carbon (>36%) in the GT and GS composites increased their susceptibility to heat; hence, their dramatic degradation above 600 °C. Furthermore, the evidence appears to suggest that the reactive functional groups present in GG1 waste promoted the reactivity of GG1 with SPR-212. As a result, high-quality GG1 composites were produced compared to the other composites. Despite its chemical inertness, FA yielded composites of interesting properties. The water absorption of the coal composites produced in this study is in the range of 0 and 25%, and their ultimate compressive stress was up to 420 MPa. Based on the promising results documented in this study, these composites may be designed into roofing tiles, blocks, bricks, or cladding tiles for building applications. However, further development in terms of optimizing the process conditions and upscaling the process to produce technical-size coal composites are of great interest for the application of these advanced and sustainable building materials.

# 8 General conclusions and recommendations

The research has successfully demonstrated that South African coal waste can be harnessed to produce dense structural composites containing carbon and ceramic that meet or exceed the properties of many building products. The technique involves blending South African coal waste with PCP in a suitable ratio, curing and further pyrolysis of the moulded mixture under appropriate conditions. On this note and within the scope of this study, the influence of the physicochemical properties of South African coal wastes on the resultant coal composites using ceramic-forming binders was investigated. Proximate, ultimate, total sulphur, hydrogen/carbon ratio, oxygen/carbon ratio and XRF analysis were used as characterisation techniques for the various coal wastes. The composites were characterised using XRD, FTIR, TGA, optical microscopy, SEM and Raman analysis. The coal composites were evaluated using standard mechanical strength (compression tests) for building materials, leaching tests, chemical resistance, electrical resistivity, density measurement (Archimedes' technique), and water contact angle measurements. The produced coal ceramic composites manifested promising structural properties similar to building materials like clay roof tiles, brick, and structural clay tile. Some of the interesting properties of the composites include continuous operating temperatures up to 600 ºC, superior mechanical strength performance, and volume resistivity in the range of 22 to 82 Ω.cm. Major conclusions from the experimental and analysis work conducted in this study are summarised below.

## 8.1 Conclusions

1. Water absorption is one of the most important factors to consider for building materials as it reflects the compactness of the bonds and affects durability. The water absorption of the composites produced in this study is in the range of 2% to 15% and is comparable with the water absorption of ≤ 20% required for many conventional building materials.
2. GT fines used in this study contain the highest volatile matter (32.7%) and total carbon content (69.5%). As a result, the GT composites displayed the poorest overall qualities based on the properties reported. The relatively high total carbon content of the GT composites (62.7%) compromised the strength of the composites and increased their susceptibility to heat. Hence, the fast rapid degradation of these composites above 600 °C.
3. Coal waste (GTS and LCS), with many hydrogen-containing functional groups, as predicted from their hydrogen/carbon atomic ratio is a prerequisite to producing high-quality composites irrespective of the type of preceramic binder used.
4. High-ash coal waste (GG1, FA) produced composites with positive attributes in terms of their excellent thermal stability and low shrinkage/mass loss but high densities (up to 2.5 g/cm$^3$) and high water absorption (<12%) compared to other composites produced in this study (excluding the GT composites).
5. The unprecedented chemical resistance (94.43 to 99.92%) displayed by the composites makes them ideal for harsh chemical environments.
6. The evidence suggests that coal waste (GG1, GTS, LCS) containing the reactive functional groups (hydroxyl, carboxyl, carbonyl) produced higher–quality

composites due to the enhanced reactivity with the PCP during curing and pyrolysis.

The results suggest that these composites could be pressed into various shapes e.g., roofing tiles, blocks, bricks, or cladding tiles for building applications. However, the following recommendations are of great interest for future studies.

## 8.2 Recommendations

1. The study has demonstrated the technical feasibility of this recycling route. Consequently, pilot-scale manufacture of coal composites should be conducted.
2. The environmental and economic benefits of the coal composites compared to conventional building products need to be evaluated.
3. Assessment such as thermal conductivity/thermal shock resistance, flammability, fungus/antibacterial resistance, sound damping (ultrasound), exposure to ultraviolet and sunlight, anti-static behaviour, and the electromagnetic shielding property should be conducted to describe holistically the benefits of the coal composites.
4. The effect of the addition of water or solvent to the mixture of coal waste and PCP resin on the properties of the coal composites should be investigated.
5. Long-term leaching tests should be conducted concerning the release of chemical species of environmental toxicity to ensure that the composites satisfy acceptance and compliance set by the environment agency.
6. Optimising the process conditions (i.e., lower processing temperature and reduced pyrolysis duration) is important to improve the competitiveness of the composites (i.e., lower cost and higher-performance composites).

## References


Abdrakhimov, V. Z., & Abdrakhimova, E. S. (2017). Promising use of waste coal in the production of insulating material without the use of traditional natural materials. *Inorganic Materials: Applied Research*, *8(5)*, 788–794. https://doi.org/10.1134/S2075113317050021.

Abdulsalam, J., Mulopo, J., Bada, S., & Oboirien, B. (2020a). Natural gas storage properties of adsorbents synthesised from three different coal waste in South Africa. *Fuel*, *267*, 117157. https://doi.org/10.1016/j.fuel.2020.117157.

Abdulsalam, J., Mulopo, J., Bada, S. O., & Oboirien, B. (2020b). Equilibria and isosteric heat of adsorption of methane on activated carbons derived from South African coal discards. *ACS Omega*, *5(50)*, 32530–32539. https://doi.org/10.1021/acsomega.0c04744.

Abdulsalam, J., Mulopo, J., Oboirien, B., Bada, S., & Falcon, R. (2019). Experimental evaluation of activated carbon derived from South Africa discard coal for natural gas storage. *International Journal of Coal Science & Technology*, 6*(3)*, 459–477. https://doi.org/10.1007/s40789-019-0262-5.

Addou, R., Hannawi, K., Agbodjan, W. P., & Zenasni, M. (2017). Characterisation of Moroccan coal waste (Jerada Mine): impact on physical properties of mortars made of coal waste. *Journal of Materials & Environmental Science*, *8(10)*, 3473–3482. https://www.jmaterenvironsci.com/Document/vol8/vol8_N10/366-JMES-3282-Addou.pdf.

Adigun, O. D., Ricohermoso, E., Daniyan, A. A., Umoru, L. E., & Ionescu, E. (2022). Structure and electrical properties of carbon-rich polymer derived silicon carbonitride (SiCN). *Ceramics*, *5(4)*, 690–705. https://doi.org/10.3390/ceramics5040050.

Ahamed, M. A. A., Perera, M. S. A., Matthai, S. K., Ranjith, P. G., & Dong-yin, L. (2019). Coal composition and structural variation with rank and its influence on the coal-moisture interactions under coal seam temperature conditions – A review article. *Journal of Petroleum Science & Engineering*, *180*, 901–917. https://doi.org/10.1016/j.petrol.2019.06.007.

Ahmad, I., & Mahanwar, P. A. (2010). Mechanical properties of fly ash filled high density polyethylene. *Journal of Minerals & Materials Characterization & Engineering*, *9(3)*, 183–198. https://doi.org/10.4236/jmmce.2010.93016.

Ahmed, S., & Jones, F. R. (1990). A review of particulate reinforcement theories for polymer composites. *Journal of Materials Science*, *25(12)*, 4933–4942. https://doi.org/10.1007/BF00580110.

Ai, W., Xue, B., Wei, C., Dou, K., & Miao, S. (2018). Mechanical and thermal properties of coal gasification fine slag reinforced low density polyethylene composites. *Journal of Applied Polymer Science*, *135(17)*, 46203. https://doi.org/10.1002/app.46203.

Aisenbrey, T. (2007). Low cost roofing shingles manufactured from conductive loaded resin-based materials. United States Patent No. US7198735B2. Available at: https://patents.google.com/patent/US7198735B2/en.

Alam, M. K., Islam, M. T., Mina, M. F., & Gafur, M. A. (2014). Structural, mechanical, thermal, and electrical properties of carbon black reinforced polyester resin composites. *Journal of Applied Polymer Science*, *131(13)*, 40421. https://doi.org/10.1002/app.40421.

Al-Majali, Y. A., Chirume, C. T., Marcum, E. P., Daramola, D. A., Kappagantula, K. S., & Trembly, J. P. (2019). Coal-filler-based thermoplastic composites as construction materials: A new sustainable end-use application. *ACS Sustainable Chemistry & Engineering*, *7(19)*, 16870–16878. https://doi.org/10.1021/acssuschemeng.9b04453.

Alonso-Santurde, R., Coz, A., Viguri, J. R., & Andrés, A. (2012). Recycling of foundry by-products in the ceramic industry: Green and core sand in clay bricks. *Construction & Building Materials*, *27(1)*, 97–106. https://doi.org/10.1016/j.conbuildmat.2011.08.022.

Amaral Filho, J. R., Firpo, B. A., Broadhurst, J. L., & Harrison, S. T. L. (2020). On the feasibility of South African coal waste for production of 'FabSoil', a Technosol. *Minerals Engineering*, *146*, 106059. https://doi.org/10.1016/j.mineng.2019.106059.

Angoni, K. (1993). Remarks on the structure of carbon materials on the basis of Raman spectra. *Carbon*, *31(4)*, 537–547. https://doi.org/10.1016/0008-6223(93)90106-K.

ASTM C1167-11. (2017). Standard specification for clay roof tiles. Available at: https://www.astm.org/c1167-11r17.html. (Accessed: 24 January 2022).

ASTM C67-05. (2010). Standard test methods for sampling and testing brick and structural clay tile. Available at: https://www.astm.org/c0067-07.html. (Accessed: 24 January 2022).

ASTM D5142-09. (2009). Standard test methods for proximate analysis of the analysis sample of coal and coke by instrumental procedures. Available at: https://webstore.ansi.org/standards/astm/astmd514209. (Accessed: 24 January 2022).

ASTM C373-17. (2018). Standard test methods for determination of water absorption and associated properties by vacuum method for pressed ceramic tiles and glass tiles and boil method for extruded ceramic tiles and non-tile fired ceramic whiteware products. Available at: https://www.astm.org/c0373-17.html. (Accessed: 24 January 2022).

ASTM D257–07. (2021). Standard test methods for DC resistance or conductance of insulating materials. ASTM International, West Conshohocken, PA, 2007. Available at: https://www.astm.org/. (Accessed: 15 April 2023).

ASTM D4239. (2018). Standard Test Method for Sulfur in the Analysis Sample of Coal and Coke Using High-Temperature Tube Furnace Combustion.

Attalla, M. I. (1989). A survey of methods for preparing plastics from coal and coal-related materials. *Fuel Processing Technology*, *23(2)*, 101–115. https://doi.org/10.1016/0378-3820(89)90071-4.

Azimi, M., & Asselin, E. (2022). Improving surface functionality, hydrophilicity, and interfacial adhesion properties of high-density polyethylene with activated peroxides. *ACS Applied Materials & Interfaces*, *14(2)*, 3601–3609. https://doi.org/10.1021/acsami.1c23703.

Bada, S., Tao, D., Honaker, R., Falcon, L., & Falcon, R. (2010). Parametric study of electrostatic separation of South African fine coal. *Mining Science &*

*Technology (China), 20(4),* 535–541. https://doi.org/10.1016/S1674-5264(09)60239-8.

Bai, Y. F., Cao, X. X., Xu, M. L., He, X. F., & Cai, G. H. (2019). Coal powder and ethylene-propylene-diene monomer reinforced hybrid polypropylene composites. *Materials Science Forum, 956,* 192–200. https://doi.org/10.4028/www.scientific.net/msf.956.192.

Balachandran, M. (2014). Role of infrared spectroscopy in coal analysis - An investigation. *American Journal of Analytical Chemistry, 5(6),* 367–372. https://doi.org/10.4236/ajac.2014.56044.

Bardet, M., & Pournou, A. (2017). NMR studies of fossilized wood. In *Annual Reports on NMR Spectroscopy.* Volume 90. G. A. Webb, Ed. Cambridge, Massachusetts: Academic Press. 41–83. https://doi.org/10.1016/bs.arnmr.2016.07.002.

Barroso, G., Li, Q., Bordia, R. K., & Motz, G. (2019). Polymeric and ceramic silicon-based coatings – A review. *Journal of Materials Chemistry A, 7(5),* 1936–1963. https://doi.org/10.1039/C8TA09054H.

Belaid, M., Falcon, R., Vainikka, P., & Patsa, K. V. (2013). Potential and technical basis for utilising coal beneficiation discards in power generation by applying circulating fluidised bed boilers. *2nd International Conference on Chemical, Ecology & Environmental Sciences,* 17-18 June 2013. London: United Kingdom. 17–18. Available at: https://hdl.handle.net/10210/13078.

Berbon, M. Z., Dietrich, D. R., Marshall, D. B., & Hasselman, D. P. H. (2001). Transverse thermal conductivity of thin C/SiC composites fabricated by slurry infiltration and pyrolysis. *Journal of the American Ceramic Society, 84(10),* 2229–2234. https://doi.org/10.1111/j.1151-2916.2001.tb00993.x.

Bernardo, E., Fiocco, L., Parcianello, G., Storti, E., & Colombo, P. (2014). Advanced ceramics from preceramic polymers modified at the nano-scale: A review. *Materials, 7(3),* 1927–1956. https://doi.org/10.3390/ma7031927.

Bhandavat, R., Kuhn, W., Mansfield, E., Lehman, J., & Singh, G. (2012). Synthesis of polymer-derived ceramic Si(B)CN-carbon nanotube composite by microwave-induced interfacial polarization. *ACS Applied Materials & Interfaces, 4(1),* 11–16. https://doi.org/10.1021/am201358s.

Blissett, R. S., & Rowson, N. A. (2012). A review of the multi-component utilisation of coal fly ash. Fuel, *97*, 1–23. https://doi.org/10.1016/j.fuel.2012.03.024.

Bonczyk, M., & Rubin, J. (2022). The application of coal mining waste to the production of construction ceramics: Radiological and mechanical aspects. *Materiales de Construcción*, *72(348)*, Article 348. https://doi.org/10.3989/mc.2022.01822.

BP Statistical Review of World Energy (2019). 68th ed. Available at: https://www.bp.com/content/dam/bp/business-sites/en/global/corporate/pdfs/energy-economics/statistical-review/bp-stats-review-2019-full-report.pdf. (Accessed: 25 April 2023).

BP Statistical Review of World Energy (2020). 69th ed. Available at: https://www.bp.com/content/dam/bp/business-sites/en/global/corporate/pdfs/energy-economics/statistical-review/bp-stats-review-2020-full-report.pdf. (Accessed: 25 April 2023).

Broadhurst, J., Amaral Filho, J., Moyo, A., Nwaila, P., N'Gandu, H. S., Shongwe, B., Sibanda, L., Stander, H. M., & Harrison, S. T. L. (2019). Resource efficient and socially responsible approaches for the integrated management of mine waste: understanding the risks, opportunities, enablers and barriers. (WRC report; no. 2580/1/19). Minerals to metals, Department of Chemical Engineering, University of Cape Town: Water Research Commission.

Cançado, L. G., Jorio, A., Ferreira, E. H. M., Stavale, F., Achete, C. A., Capaz, R. B., Moutinho, M. V. O., Lombardo, A., Kulmala, T. S., & Ferrari, A. C. (2011). Quantifying defects in graphene via Raman spectroscopy at different excitation energies. *Nano Letters*, *11(8)*, 3190–3196. https://doi.org/10.1021/nl201432g.

Černý, M., Chlup, Z., Strachota, A., Halasová, M., Rýglová, Š., Schweigstillová, J., Svítilová, J., & Havelcová, M. (2015). Changes in structure and in mechanical properties during the pyrolysis conversion of crosslinked polymethylsiloxane and polymethylphenylsiloxane resins to silicon oxycarbide glass. *Ceramics International*, *41*(5, Part A), 6237–6247. https://doi.org/10.1016/j.ceramint.2015.01.034.

Chen, Y., Zou, C., Mastalerz, M., Hu, S., Gasaway, C., & Tao, X. (2015). Applications of micro-Fourier transform infrared spectroscopy (FTIR) in the geological

sciences - A review. *International Journal of Molecular Sciences*, *16(12)*, 30223–30250. https://doi.org/10.3390/ijms161226227.

Cheng, G., Tong, B., Tang, Z., Yu, X., Wang, H., & Ding, G. (2014). Surface functionalization of coal powder with different coupling agents for potential applications in organic materials. *Applied Surface Science*, *313*, 954–960. https://doi.org/10.1016/j.apsusc.2014.06.115.

Colombo, P., Mera, G., Riedel, R., & Sorarù, G. D. (2010). Polymer-derived ceramics: 40 years of research and innovation in advanced ceramics. *Journal of the American Ceramic Society*, *93(7)*, 1805–1837. https://doi.org/10.1111/j.1551-2916.2010.03876.x.

Cordelair, J., & Greil, P. (2000). Electrical conductivity measurements as a microprobe for structure transitions in polysiloxane derived Si–O–C ceramics. *Journal of the European Ceramic Society*, *20(12)*, 1947–1957. https://doi.org/10.1016/S0955-2219(00)00068-6.

Cristelo, N., Tavares, P., Lucas, E., Miranda, T., & Oliveira, D. (2016). Quantitative and qualitative assessment of the amorphous phase of a Class F fly ash dissolved during alkali activation reactions – Effect of mechanical activation, solution concentration and temperature. *Composites Part B: Engineering*, *103*, 1–14. https://doi.org/10.1016/j.compositesb.2016.08.001.

Dalcanale, F., Grossenbacher, J., Blugan, G., Gullo, M. R., Lauria, A., Brugger, J., Tevaearai, H., Graule, T., Niederberger, M., & Kuebler, J. (2014). Influence of carbon enrichment on electrical conductivity and processing of polycarbosilane derived ceramic for MEMS applications. *Journal of the European Ceramic Society*, *34(15)*, 3559–3570. https://doi.org/10.1016/j.jeurceramsoc.2014.06.002.

Danko, G. A., Silberglitt, R., Colombo, P., Pippel, E., & Woltersdorf, J. (2000). Comparison of microwave hybrid and conventional heating of preceramic polymers to form silicon carbide and silicon oxycarbide ceramics. *Journal of the American Ceramic Society*, *83(7)*, 1617–1625. https://doi.org/10.1111/j.1151-2916.2000.tb01440.x.

Das, P., Satapathy, A., & Mishra, M. K. (2018). Development and sliding wear response of epoxy composites filled with coal mine overburden material. *IOP Conference Series: Materials Science & Engineering*, *338*, 012032. IOP Conference Series:

Materials Science & Engineering, Volume 338, 7th National Conference on Processing and Characterization of Materials (NCPCM 2017). 8–9 December 2017. Rourkela, India: National Institute of Technology. https://doi.org/10.1088/1757-899X/338/1/012032.

Davidson, R. M. (1982). Molecular structure of coal. In *Coal Science.* M. L. Gorbaty, J. W. Larsen, & I. Wender, Eds. Cambridge, Massachusetts: Academic Press. 83–160. https://doi.org/10.1016/B978-0-12-150701-5.50009-7.

Davis, K. A., Hurt, R. H., Yang, N. Y. C., & Headley, T. J. (1995). Evolution of char chemistry, crystallinity, and ultrafine structure during pulverized-coal combustion. *Combustion & Flame*, *100(1)*, 31–40. https://doi.org/10.1016/0010-2180(94)00062-W.

Department of Mineral and Energy. (2021). Available at: https://www.energy.gov.za/files/coal_frame.html. (Accessed: 25 April 2021)

Derbyshire, F., Jagtoyen, M., Fei, Y. Q., & Kimber, G. (1994). The production of materials and chemicals from coal. *Preprints of Papers-American Chemical Society Division Fuel Chemistry*, *39*, 113–113.

Derbyshire, F., Marzec, A., Schulten, H.-R., Wilson, M. A., Davis, A., Tekely, P., Delpuech, J.-J., Jurkiewicz, A., Bronnimann, C. E., Wind, R. A., Maciel, G. E., Narayan, R., Bartle, K., & Snape, C. (1989). Molecular structure of coals: A debate. *Fuel*, *68(9)*, 1091–1106. https://doi.org/10.1016/0016-2361(89)90178-6.

Dhawan, R., Bisht, B. M. S., Kumar, R., Kumari, S., & Dhawan, S. K. (2019). Recycling of plastic waste into tiles with reduced flammability and improved tensile strength. *Process Safety & Environmental Protection*, *124*, 299–307. https://doi.org/10.1016/j.psep.2019.02.018.

Ding, D., Zhou, W., Zhou, X., Luo, F., & Zhu, D. (2012). Influence of pyrolysis temperature on structure and dielectric properties of polycarbosilane derived silicon carbide ceramic. *Transactions of Nonferrous Metals Society of China*, *22(11)*, 2726–2729. https://doi.org/10.1016/S1003-6326(11)61524-0.

Ding, K., & Laskowski, J. S. (2009). Effect of flotation on preparation of coal-water slurries. *International Journal of Coal Preparation & Utilization*, *29(2)*, 84–98. https://doi.org/10.1080/19392690902784846.

Ding, Y., Wang, T., Dong, D., & Zhang, Y. (2020). Using biochar and coal as the electrode material for supercapacitor applications. *Frontiers in Energy Research*, *7*. Available at: https://www.frontiersin.org/articles/10.3389/fenrg.2019.00159.

Dresselhaus, M. S., Jorio, A., Souza Filho, A. G., & Saito, R. (2010). Defect characterisation in graphene and carbon nanotubes using Raman spectroscopy. *Philosophical Transactions of the Royal Society A: Mathematical, Physical & Engineering Sciences*, *368(1932)*, 5355–5377. https://doi.org/10.1098/rsta.2010.0213.

Dun, W., Guijian, L., Ruoyu, S., & Xiang, F. (2013). Investigation of structural characteristics of thermally metamorphosed coal by FTIR spectroscopy and X-ray diffraction. *Energy & Fuels*, *27(10)*, 5823–5830. https://doi.org/10.1021/ef401276h.

Duncan, B. C., Mera, R. D., Leatherdale, D., Taylor, M., & Musgrove, R. (2005). Techniques for characterising the wetting, coating and spreading of adhesives on surface. NPL Report. DEPC-MPR 020. Available at: http://eprintspublications.npl.co.uk/id/eprint/3172. (Accessed: 18 April 2023).

Eckel, Z. C., Zhou, C., Martin, J. H., Jacobsen, A. J., Carter, W. B., & Schaedler, T. A. (2016). Additive manufacturing of polymer-derived ceramics. *Science*, *351(6268)*, 58–62. https://doi.org/10.1126/science.aad2688.

Eliche-Quesada, D., Martínez-García, C., Martínez-Cartas, M. L., Cotes-Palomino, M. T., Pérez-Villarejo, L., Cruz-Pérez, N., & Corpas-Iglesias, F. A. (2011). The use of different forms of waste in the manufacture of ceramic bricks. *Applied Clay Science*, *52(3)*, 270–276. https://doi.org/10.1016/j.clay.2011.03.003.

Eterigho-Ikelegbe, O., Harrar, H., & Bada, S. (2021a). Rare earth elements from coal and coal discard – A review. *Minerals Engineering*, *173*, 107187. https://doi.org/10.1016/j.mineng.2021.107187.

Eterigho-Ikelegbe, O., Trammell, R., & Bada, S. (2021b). Preparation and characterisation of ceramic composites from South Africa coal discard. *Construction & Building Materials*, *302*, 124164. https://doi.org/10.1016/j.conbuildmat.2021.124164.

Eterigho-Ikelegbe, O., Trammell, R., & Bada, S. O. (2022). Novel ceramic composites produced from coal discards with potential application in the building and

construction sectors. *Journal of the Southern African Institute of Mining & Metallurgy*, *122(8)*, 421–428. https://doi.org/10.17159/2411-9717/2001/2022.

Eterigho-Ikelegbe, O., Yoro, K. O., & Bada, S. (2021c). Coal as a filler in polymer composites: a review. *Resources, Conservation & Recycling*, *174*, 105756. https://doi.org/10.1016/j.resconrec.2021.105756.

Falcon, L. M., & Falcon., R. M. S. (1987). The petrographic composition of southern African coals in relation to friability, hardness, and abrasive indices. *Journal of the Southern African Institute of Mining & Metallurgy*, *87(10)*, 323–336. Available at: https://hdl.handle.net/10520/AJA0038223X_1745.

Falcon, R. M. S. (1986). Classification of coals in southern Africa. In *Mineral Deposits of Southern Africa*. Johannesburg: Geology Society of South Africa. 1899–1921. Available at: http://pascal-francis.inist.fr/vibad/index.php?action=getRecordDetail&idt=7780161.

Fecko, P., Tora, B., & Tod, M. (2013). Coal waste: Handling, pollution impacts and utilization. In *D. Osborne (Ed.), The Coal Handbook: Towards Cleaner Production* (Vol. 2, pp. 63–84). Woodhead Publishing. https://doi.org/10.1533/9781782421177.1.63.

Ferrari, A. C. (2007). Raman spectroscopy of graphene and graphite: Disorder, electron–phonon coupling, doping and nonadiabatic effects. *Solid State Communications*, *143(1)*, 47–57. https://doi.org/10.1016/j.ssc.2007.03.052.

Ferrari, A. C., & Robertson, J. (2000). Interpretation of Raman spectra of disordered and amorphous carbon. *Physical Review B*, *61(20)*, 14095–14107. https://doi.org/10.1103/PhysRevB.61.14095.

Ferraro, J. R., & Basile, L. J. (2012). Fourier transform infrared spectra: Applications to chemical systems. Amsterdam: Elsevier.

Feyyisa, J. L., Daniels, J. L., & Pando, M. A. (2017). Contact angle measurements for use in specifying organosilane-modified coal combustion fly ash. *Journal of Materials in Civil Engineering*, *29(9)*, 04017096. https://doi.org/10.1061/(ASCE)MT.1943-5533.0001943.

Fiala, L., Rovnaník, P., & Černý, R. (2017). Experimental analysis of electrical properties of composite materials. *AIP Conference Proceedings*, *1809(1)*, 020016. https://doi.org/10.1063/1.4975431.

Fomina, O. A., & Yu. Stolboushkin, A. (2019). Development of a novel mould design for manufacturing of hollow ceramic products from coal wastes. *Materials Today: Proceedings*, *11(1)*, 348–353. https://doi.org/10.1016/j.matpr.2018.12.156.

Fonblanc, D., Lopez-Ferber, D., Wynn, M., Lale, A., Soleilhavoup, A., Leriche, A., Iwamoto, Y., Rossignol, F., Gervais, C., & Bernard, S. (2018). Crosslinking chemistry of poly(vinylmethyl-co-methyl)silazanes toward low-temperature formable preceramic polymers as precursors of functional characterise-modified Si–C–N ceramics. *Dalton Transactions*, *47(41)*, 14580–14593. https://doi.org/10.1039/C8DT03076F.

Foresight. (2013). The future of manufacturing: A new era of opportunity and challenge for the UK. Summary Report. *London: The Government Office for Science*. Available at: https://assets.publishing.service.gov.uk/government/uploads/system/uploads/attachment_data/file/255923/13-810-future-manufacturing-summary-report.pdf.

Frank, E., Hermanutz, F., & Buchmeiser, M. R. (2012). Carbon fibres: precursors, manufacturing, and properties. *Macromolecular Materials & Engineering*, *297(6)*, 493–501. https://doi.org/10.1002/mame.201100406.

Fridlyander, I. N., Shevchenko, V. Ya., & Barinov, S. M. (1992). Ceramic composite materials. *Metal Science & Heat Treatment*, *34(2)*, 133–138. https://doi.org/10.1007/BF00769881.

Fu, F., & Yuan, Q. (2017). Electricity functional composite for building construction. In *Advanced High Strength Natural Fibre Composites in Construction*. M. Fan & F. Fu, Eds. Amsterdam: Elsevier. 287–331. https://doi.org/10.1016/B978-0-08-100411-1.00012-1.

Gagarin, H., Sridhar, S., Lange, I., & Bazilian, M. D. (2020). Considering non-power generation uses of coal in the United States. *Renewable & Sustainable Energy Reviews*, *124*, 109790. https://doi.org/10.1016/j.rser.2020.109790.

Galusek, D., Sedláček, J., & Riedel, R. (2007). $Al_2O_3$–SiC composites prepared by warm pressing and sintering of an organosilicon polymer-coated alumina powder. *Journal of the European Ceramic Society*, *27(6)*, 2385–2392. https://doi.org/10.1016/j.jeurceramsoc.2006.09.007.

Gao, Z., Ding, Y., Yang, W., & Han, W. (2017). DFT study of water adsorption on lignite molecule surface. *Journal of Molecular Modeling*, *23(1)*, 27. https://doi.org/10.1007/s00894-016-3194-7.

Gnatowski, A., & Kazik, E. (2019). The research of selected properties and structure of polymeric material modified with hard coal ash. *Acta Physica Polonica*, *135(2)*, 119–121. Proceedings of XIX International Scientific Conference. New Technologies and Achievements in Metallurgy, Material Engineering, Production Engineering and Physics. Częstochowa: Poland, 7-8 June 2018. https://doi.org/10.12693/APHYSPOLA.135.119.

Gökçe, M., Akçaözoğlu, S., & Sinani, B. (2018). Investigation of production of brick with waste coal powder additive. *UBT International Conference*. Available at: https://knowledgecenter.ubt-uni.net/conference/2018/all-events/56.

Gomez-Caturla, J., Balart, R., Ivorra-Martinez, J., Garcia-Garcia, D., Dominici, F., Puglia, D., & Torre, L. (2022). Biopolypropylene-based wood plastic composites reinforced with mango peel flour and compatibilized with an environmentally friendly copolymer from itaconic acid. *ACS Applied Polymer Materials*, *4(6)*, 4398–4410. https://doi.org/10.1021/acsapm.2c00373.

Greil, P. (1995). Active-filler-controlled pyrolysis of preceramic polymers. *Journal of the American Ceramic Society*, *78(4)*, 835–848. https://doi.org/10.1111/j.1151-2916.1995.tb08404.x.

Guang-Heng, W., An-ning, Z., & Xiao-Bing, H. (2006). Effect of coal filler on the properties of soy protein plastics. *Journal of Applied Polymer Science*, *102(4)*, 3134–3143. https://doi.org/10.1002/app.24277.

Gumula, T., Paluszkiewicz, C., & Blazewicz, S. (2009). Study on thermal decomposition processes of polysiloxane polymers - from polymer to nanosized silicon carbide. *Journal of Analytical and Applied Pyrolysis*, *86(2)*, 375–380. https://doi.org/10.1016/j.jaap.2009.09.001.

Haenel, M. W. (1992). Recent progress in coal structure research. *Fuel*, *71(11)*, 1211–1223. https://doi.org/10.1016/0016-2361(92)90046-Q.

Haibin, L., & Zhenling, L. (2010). Recycling utilization patterns of coal mining waste in China. Resources, Conservation & Recycling, 54*(12)*, 1331–1340. https://doi.org/10.1016/j.resconrec.2010.05.005.

Hancox, P. J., & Götz, A. E. (2014). South Africa's coalfields - A 2014 perspective. *International Journal of Coal Geology*, *132*, 170–254. https://doi.org/10.1016/j.coal.2014.06.019.

Harrar, H., Eterigho-Ikelegbe, O., Modiga, A., & Bada, S. (2022). Mineralogy and distribution of rare earth elements in the Waterberg coalfield high ash coals. *Minerals Engineering*, *183*, 107611. https://doi.org/10.1016/j.mineng.2022.107611.

Harshe, R., Balan, C., & Riedel, R. (2004). Amorphous Si(Al)OC ceramic from polysiloxanes: bulk ceramic processing, crystallization behaviour and applications. *Journal of the European Ceramic Society*, *24*(*12)*, 3471–3482. https://doi.org/10.1016/j.jeurceramsoc.2003.10.016.

Haywood, L. K., de Wet, B., de Lange, W., & Oelofse, S. (2019). Legislative challenges hindering mine waste being reused and repurposed in South Africa. *The Extractive Industries & Society*, *6(4)*, 1079–1085. https://doi.org/10.1016/j.exis.2019.10.008.

He, X., Liu, X., Nie, B., & Song, D. (2017). FTIR and Raman spectroscopy characterisation of functional groups in various rank coals. *Fuel*, *206*, 555–563. https://doi.org/10.1016/j.fuel.2017.05.101.

Helmi, F. M., & Hefni, Y. K. (2014). A simple method for measuring the static water contact angle for evaluation the hydrophobicity of the consolidating and protective materials [Working Paper].

Hill, A., & Easter, W. (2019). Carbon ceramic composites and methods. Publication Number 20190292441. Available at: https://patentscope.wipo.int/search/en/detail.jsf?docId=US252246228&docAn=16345577 (Accessed: 19 April 2023).

Hill, A., & Easter, W. (2021). Carbon ceramic composites and methods. United States Patent No. US10988680B2. Available at: https://patents.google.com/patent/US10988680B2/en.

Hill, A., Sherwood, W., Trammell, R., & Easter, W. (2022). High strength, tough, coal and coal by-product based composite ceramics. United States Patent No. US20220144706A1. Available at: https://patents.google.com/patent/US20220144706A1/en.

Honaker, R., Groppo, J., Bhagavatula, A., Rezaee, M., & Zhang, W. (2016). Recovery of rare earth minerals and elements from coal and coal byproducts. *International Coal Preparation Conference*, 25–27. Louisville, Kentucky.

Honaker, R., Yang, X., Chandra, A., Zhang, W., & Werner, J. (2018). Hydrometallurgical extraction of rare earth elements from coal. In *Extraction 2018*. B. R. Davis, M. S. Moats, S. Wang, D. Gregurek, J. Kapusta, T. P. Battle, M. E. Schlesinger, G. R. Alvear Flores, E. Jak, G. Goodall, M. L. Free, E. Asselin, A. Chagnes, D. Dreisinger, M. Jeffrey, J. Lee, G. Miller, J. Petersen, V. S. T. Ciminelli, T. Bhambhani, Eds. New York: Springer International Publishing. 2309–2322. https://doi.org/10.1007/978-3-319-95022-8_193.

Honaker, R. Q., Zhang, W., & Werner, J. (2019). Acid leaching of rare earth elements from coal and coal ash: Implications for using fluidized bed combustion to assist in the recovery of critical materials. *Energy & Fuels*, *33(7)*, 5971–5980. https://doi.org/10.1021/acs.energyfuels.9b00295.

Hossain, Md. U., Ng, S. T., Antwi-Afari, P., & Amor, B. (2020). Circular economy and the construction industry: existing trends, challenges and prospective framework for sustainable construction. *Renewable & Sustainable Energy Reviews*, *130*, 109948. https://doi.org/10.1016/j.rser.2020.109948.

Howard, H. C. (1936). The polymeric character of bituminous coal. *The Journal of Physical Chemistry*, *40*(9), 1103–1112. https://doi.org/10.1021/j150378a003.

Hsissou, R., Seghiri, R., Benzekri, Z., Hilali, M., Rafik, M., & Elharfi, A. (2021). Polymer composite materials: A comprehensive review. *Composite Structures*, *262*, 113640. https://doi.org/10.1016/j.compstruct.2021.113640.

Hu, L. L. (2016). Coal gangue and its application research in building materials. *Materials Science Forum, 873*, 96–104. https://doi.org/10.4028/www.scientific.net/MSF.873.96.

Hu, G., Bian, Z., Xue, R., Huang, W., & Komarneni, S. (2017). Polymer-coal composite as a novel plastic material. *Materials Letters*, *197*, 31–34. https://doi.org/10.1016/j.matlet.2017.03.148.

Huggins, F. E. (2002). Overview of analytical methods for inorganic constituents in coal. *International Journal of Coal Geology*, *50(1-4)*, 169–214. https://doi.org/10.1016/S0166-5162(02)00118-0.

Ibarra, JoséV., Muñoz, E., & Moliner, R. (1996). FTIR study of the evolution of coal structure during the coalification process. *Organic Geochemistry*, *24(6)*, 725–735. https://doi.org/10.1016/0146-6380(96)00063-0.

Ibraeva, Y., Tarasevskii, P., & Zhuravlev, A. (2017). Salt corrosion of brick walls. *MATEC Web of Conferences*, *106*, 03003. https://doi.org/10.1051/matecconf/201710603003.

ICCP. (1998). The new vitrinite classification (ICCP System 1994). *Fuel*, *77(5)*, 349–358. https://doi.org/10.1016/S0016-2361(98)80024-0.

IEA. (2019). World energy outlook 2019. Available at: https://www.iea.org/reports/world-energy-outlook-2019. (Accessed: 25 April 2023).

IEA. (2020). Fuel report 2020. *Analysis and forecast to 2025*. (License: CC BY 4.0) Paris: International Energy Agency (IEA). Available at: https://www.iea.org/reports/coal-2020.

Ionescu, E., Kleebe, H.-J., & Riedel, R. (2012). Silicon-containing polymer-derived ceramic nanocomposites (PDC-NCs): preparative approaches and properties. *Chemical Society Reviews*, *41(15)*, 5032–5052. https://doi.org/10.1039/C2CS15319J.

Ionescu, E., Papendorf, B., Kleebe, H.-J., Poli, F., Müller, K., & Riedel, R. (2010). Polymer-derived silicon oxycarbide/hafnia ceramic nanocomposites. Part I: Phase and microstructure evolution during the ceramization process. *Journal of the American Ceramic Society*, *93(6)*, 1774–1782. https://doi.org/10.1111/j.1551-2916.2010.03765.x.

Isaac, K., & Bada, S. O. (2020). The co-combustion performance and reaction kinetics of refuse derived fuels with South African high ash coal. *Heliyon*, *6(1)*, e03309. https://doi.org/10.1016/j.heliyon.2020.e03309.

ISO 10545-4. (2019). Ceramic tiles – Part 4: Determination of modulus of rupture and breaking strength. Available at: https://www.iso.org/obp/ui/#iso:std:iso:10545:-4:ed-4:v1:en. (Accessed: 24 January 2022).

ISO 10545-13. (2016). Ceramic tiles – Part 13: Determination of chemical resistance. Available at: https://www.iso.org/standard/60975.html. (Accessed: 24 January 2022).

ISO 13909-1. (2016). Hard coal and coke - Mechanical sampling - Part 1: General introduction.

ISO/TS 12902. (2001). Solid mineral fuels - Determination of total carbon, hydrogen, and nitrogen - Instrumental methods.

Jagtoyen, M., Groppo, J., & Derbyshire, F. (1993). Activated carbons from bituminous coals by reaction with $H_3PO_4$: the influence of coal cleaning. *Fuel Processing Technology*, *34(2)*, 85–96. https://doi.org/10.1016/0378-3820(93)90093-J.

Janković, M., Janković, B., Marinović-Cincović, M., Porobić, S., Nikolić, J. K., & Sarap, N. (2020). Experimental study of low-rank coals using simultaneous thermal analysis (TG–DTA) techniques under air conditions and radiation level characterisation. *Journal of Thermal Analysis & Calorimetry*, *142(2)*, 547–564. https://doi.org/10.1007/s10973-020-09288-5.

Jian, K., Chen, G., Guo, C., Ma, G., & Ru, Z. (2019). Biogenic gas simulation of low-rank coal and its structure evolution. *Journal of Petroleum Science & Engineering*, *173*, 1284–1288. https://doi.org/10.1016/j.petrol.2018.11.005.

Jain, N. K., & Gupta, M. K. (2018). Hybrid teak/sal wood flour reinforced composites: Mechanical, thermal and water absorption properties. *Materials Research Express*, *5(12)*, 125306. https://doi.org/10.1088/2053-1591/aae24d.

Jiang, T., Wang, Y., Wang, Y., Orlovskaya, N., & An, L. (2009). Quantitative Raman analysis of free carbon in polymer-derived ceramics. *Journal of the American Ceramic Society*, *92(10)*, 2455–2458. https://doi.org/10.1111/j.1551-2916.2009.03233.x.

Jones, R. G., Ando, W., & Chojnowski, J. (2013). Silicon-containing polymers: The science and technology of their synthesis and applications.

Kairakbaev, A. K., Abdrakhimova, E. S., & Abdrakhimov, V. Z. (2017). Effect of different coal-enrichment wastes on the physical and mechanical properties and phase composition of heat-insulation materials. *Glass & Ceramics*, *74(1)*, 55–59. https://doi.org/10.1007/s10717-017-9928-x.

Keller, B. D., Ferralis, N., & Grossman, J. C. (2016). Rethinking coal: Thin films of solution processed natural carbon nanoparticles for electronic devices. *Nano Letters*, *16(5)*, 2951–2957. https://doi.org/10.1021/acs.nanolett.5b04735.

Keener, T. J., Stuart, R. K., & Brown, T. K. (2004). Maleated coupling agents for natural fibre composites. *Composites Part A: Applied Science & Manufacturing*, *35(3)*, 357–362. https://doi.org/10.1016/j.compositesa.2003.09.014.

Khan, M. Z. R., Srivastava, S. K., & Gupta, M. K. (2019). Hybrid wood particulates composites: Mechanical and thermal properties. *Materials Research Express*, *6(10)*, 105323. https://doi.org/10.1088/2053-1591/ab3835.

Khare, P., & Baruah, B. P. (2014). Thermogravimetric Analysis of Perhydrous Indian Coals. *Energy Sources, Part A: Recovery, Utilization, & Environmental Effects*, *36(7)*, 774–782. https://doi.org/10.1080/15567036.2010.547919.

Kieush, L. (2019). Coal pyrolysis products utilisation for synthesis of carbon nanotubes. *Petroleum & Coal*, *61(3*), 461–466. Available at: https://www.vurup.sk/wp-content/uploads/2019/04/PC-X-2019_Kieusch_17.pdf.

Kijo-Kleczkowska, A., Gnatowski, A., Szumera, M., & Kwiatkowski, D. (2020). Application of thermal analysis methods in research of polyamide, coal fuels and their composites. *Polish Journal of Chemical Technology*, *22(1)*, 6–9. https://doi.org/10.2478/pjct-2020-0002.

Kopeliovich, D. (2018). Advances in manufacture of ceramic matrix composites by infiltration techniques. In *Advances in Ceramic Matrix Composites*. 2nd ed. I. M. Low, Ed. Sawston, Cambridge: Woodhead Publishing. 93–119. https://doi.org/10.1016/B978-0-08-102166-8.00005-0.

Krawczak, P. (2010). Polymer-based functionally graded materials (FGMs): Potential and challenges. *Express Polymer Letters*, *4(6)*, 328–328. https://doi.org/10.3144/expresspolymlett.2010.41.

Kumar, S., Bhattacharya, S., & Mandre, N. R. (2014). Characterization and flocculation studies of fine coal tailings. *Journal of the Southern African Institute of Mining & Metallurgy*, *114(11)*, 945–949. Available at: http://www.scielo.org.za/scielo.php?pid=S2225-62532014001100013&script=sci_arttext.

Kumar, A. P., Mohamed, M. N., Philips, K. K., & Ashwin, J. (2016). Development of novel natural composites with fly ash reinforcements and investigation of their tensile properties. *Applied Mechanics & Materials*, *852*, 55–60. https://doi.org/10.4028/www.scientific.net/AMM.852.55.

Ladner, W. R. (1988). The products of coal pyrolysis: Properties, conversion and reactivity. *Fuel Processing Technology*, *20*, 207–222. https://doi.org/10.1016/0378-3820(88)90021-5.

Larouche, N., & Stansfield, B. L. (2010). Classifying nanostructured carbons using graphitic indices derived from Raman spectra. *Carbon*, *48(3)*, 620–629. https://doi.org/10.1016/j.carbon.2009.10.002.

Laudal, D. A., Benson, S. A., Palo, D., & Addleman, R. S. (2018). Rare earth elements in North Dakota lignite coal and lignite-related materials. *Journal of Energy Resources Technology*, *140(6)*, 062205. https://doi.org/10.1115/1.4039738.

Lemeshev, V. G., Gubin, I. K., Savel'ev, Yu. A., Tumanov, D. V., & Lemeshev, D. O. (2004). Utilization of coal-mining waste in the production of building ceramic materials. *Glass & Ceramics*, *61(9)*, 308–311. https://doi.org/10.1023/B:GLAC.0000048698.58664.97.

Lette, M. J., Ly, E. B., Ndiaye, D., Takasaki, A., & Okabe, T. (2018). Evaluation of sawdust and rice husks as fillers for phenolic resin based wood-polymer composites. *Open Journal of Composite Materials*, *8(3)*, 124–137. https://doi.org/10.4236/ojcm.2018.83010.

Li, D., Wu, D., Xu, F., Lai, J., & Shao, L. (2018). Literature overview of Chinese research in the field of better coal utilization. *Journal of Cleaner Production*, *185*, 959–980. https://doi.org/10.1016/j.jclepro.2018.02.216.

Li, Y. (2012). Effect of coupling agent concentration, fiber content, and size on mechanical properties of wood/HDPE composites. *International Journal of Polymeric Materials & Polymeric Biomaterials*, *61(11)*, 882–890. https://doi.org/10.1080/00914037.2011.617338.

Li, Z., Fei, M.-E., Huyan, C., & Shi, X. (2021). Nano-engineered, fly ash-based geopolymer composites: an overview. *Resources, Conservation & Recycling*, *168*, 105334. https://doi.org/10.1016/j.resconrec.2020.105334.

Liew, L., Zhang, W., An, L., Shah, S., Luo, R., Liu, Y., Cross, T., Dunn, M. L., Bright, V., & Daily, J. W. (2000). Ceramic MEMS - New materials, innovative processing and future applications. *American Ceramic Society Bulletin*, *80(5)*, 25–30.

Liu, X., Wang, Y., & Zhan, L. (2018). Carbon foams prepared from coal tar pitch for building thermal insulation material with low cost. *Chinese Journal of Chemical Engineering, 26(2)*, 415–420. https://doi.org/10.1016/j.cjche.2017.04.012.

Liu, J., Shimanoe, H., Choi, J.-E., Ko, S., Jeon, Y.-P., Nakabayashi, K., Miyawaki, J., & Yoon, S.-H. (2019). Effect of the pre-treated pyrolysis fuel oil: Coal tar pitch ratio on the spinnability and oxidation properties of isotropic pitch precursors and the mechanical properties of derived carbon fibres. *Carbon Letters, 29(2)*, 193–202. https://doi.org/10.1007/s42823-019-00020-4.

Liu, T.-T., Cao, M.-Q., Fang, Y.-S., Zhu, Y.-H., & Cao, M.-S. (2022a). Green building materials lit up by electromagnetic absorption function: A review. *Journal of Materials Science & Technology, 112*, 329–344. https://doi.org/10.1016/j.jmst.2021.10.022.

Liu, X., Liu, H., Xu, H., Xie, W., Li, M., Liu, J., Liu, G., Weidenkaff, A., & Riedel, R. (2022a). Natural wood templated hierarchically cellular NbC/Pyrolytic carbon foams as stiff, lightweight and high-performance electromagnetic shielding materials. *Journal of Colloid & Interface Science, 606(2)*, 1543–1553. https://doi.org/10.1016/j.jcis.2021.08.110.

Longwell, J. P., Rubin, E. S., & Wilson, J. (1995). Coal: energy for the future. *Progress in Energy & Combustion Science, 21(4)*, 269–360. https://doi.org/10.1016/0360-1285(95)00007-0.

Lottermoser, B. G. (2011). Recycling, reuse and rehabilitation of mine wastes. *Elements, 7(6)*, 405–410. https://doi.org/10.2113/gselements.7.6.405.

Lu, G. Q., & Do, D. D. (1991). Structure changes of coal reject char during pyrolysis at low heating rates. *Fuel Processing Technology, 28(3)*, 247–258. https://doi.org/10.1016/0378-3820(91)90078-Q.

Luo, Y., Ma, S., Liu, C., Zhao, Z., Zheng, S., & Wang, X. (2017a). Effect of particle size and alkali activation on coal fly ash and their role in sintered ceramic tiles. *Journal of the European Ceramic Society, 37(4)*, 1847–1856. https://doi.org/10.1016/j.jeurceramsoc.2016.11.032.

Luo, Y., Wu, Y., Ma, S., Zheng, S., & Chu, P. K. (2019). An eco-friendly and cleaner process for preparing architectural ceramics from coal fly ash: Pre-activation of

coal fly ash by a mechanochemical method. *Journal of Cleaner Production*, *214*, 419–428. https://doi.org/10.1016/j.jclepro.2018.12.292.

Luo, Y., Zheng, S., Ma, S., Liu, C., & Wang, X. (2017b). Ceramic tiles derived from coal fly ash: preparation and mechanical characterisation. *Ceramics International*, *43(15)*, 11953–11966. https://doi.org/10.1016/j.ceramint.2017.06.045.

Luo, L., Li, K., Fu, W., Liu, C., & Yang, S. (2020). Preparation, characteristics and mechanisms of the composite sintered bricks produced from shale, sewage sludge, coal gangue powder and iron ore tailings. *Construction & Building Materials*, *232*, 117250. https://doi.org/10.1016/j.conbuildmat.2019.117250.

Magazzino, C., Bekun, F. V., Etokakpan, M. U., & Uzuner, G. (2020). Modeling the dynamic Nexus among coal consumption, pollutant emissions and real income: empirical evidence from South Africa. *Environmental Science & Pollution Research*, *27(8)*, 8772–8782. https://doi.org/10.1007/s11356-019-07345-7.

Magnant, J., Maillé, L., Pailler, R., Ichard, J.-C., Guette, A., Rebillat, F., & Philippe, E. (2012). Carbon fibre/reaction-bonded carbide matrix for composite materials – manufacture and characterisation. *Journal of the European Ceramic Society*, *32(16)*, 4497–4505. https://doi.org/10.1016/j.jeurceramsoc.2012.06.009.

Mainzer, B., Lin, C., Jemmali, R., Frieß, M., Riedel, R., & Koch, D. (2019). Characterisation and application of a novel low viscosity polysilazane for the manufacture of C- and SiC-fibre reinforced SiCN ceramic matrix composites by PIP process. *Journal of the European Ceramic Society*, *39(2-3)*, 212–221. https://doi.org/10.1016/j.jeurceramsoc.2018.09.042.

Makarov, D. V., Suvorova, O. V., & Masloboev, V. A. (2019). Prospects of processing the mining and mineral processing waste in Murmansk Region into ceramic building materials. https://doi.org/10.25702/KSC.978-5-91137-403-7.

Manikandan, V., Richard, S., Thanu, M. C., & Rajadurai, J. S. (2015). Effect of fly ash as filler on mechanical & frictional properties of jute fiber reinforced composite. *International Research Journal of Engineering & Technology*, *2(07)*, 154–158.

Manoj Kumar, B. V., & Kim, Y.-W. (2011). Processing of polysiloxane-derived porous ceramics: A review. *Science & Technology of Advanced Materials*, *11(6)*, 069801. https://doi.org/10.1088/1468-6996/11/6/069801.

Martínez-Crespiera, S., Ionescu, E., Kleebe, H.-J., & Riedel, R. (2011). Pressureless synthesis of fully dense and crack-free SiOC bulk ceramics via photo-crosslinking and pyrolysis of a polysiloxane. *Journal of the European Ceramic Society, 31(5)*, 913–919. https://doi.org/10.1016/j.jeurceramsoc.2010.11.019.

Marzec, A. (2002). Towards an understanding of the coal structure: A review. *Fuel Processing Technology, 77–78*, 25–32. https://doi.org/10.1016/S0378-3820(02)00045-0.

Mbedzi, M. D., van der Poll, H. M., & van der Poll, J. A. (2020). Enhancing a decision-making framework to address environmental impacts of the South African coalmining industry. *Energies, 13(18)*, 4897. https://doi.org/10.3390/en13184897.

Ming, L. Y., Sandu, A. V., Yong, H. C., Tajunnisa, Y., Azzahran, S. F., Bayuji, R., & Loong, F. K. (2019). Compressive strength and thermal conductivity of fly ash geopolymer concrete incorporated with lightweight aggregate, expanded clay aggregate and foaming agent. *Revista de Chimie, 70(11)*, 4021–4028. https://doi.org/10.37358/RC.70.19.11.7695.

Mishra, V., Bhowmick, T., Chakravarty, S., Varma, A. K., & Sharma, M. (2016). Influence of coal quality on combustion behaviour and mineral phases transformations. *Fuel, 186*, 443–455. https://doi.org/10.1016/j.fuel.2016.08.092.

Mistri, E., Bandyopadhyay, N. R., Ghosh, S. N., & Ray, D. (2010). Development of green composites from furfuryl palmitate. *Industrial & Engineering Chemistry Research, 49(22)*, 11357–11362. https://doi.org/10.1021/ie101586s.

Mohanty, A. K., Vivekanandhan, S., Pin, J.-M., & Misra, M. (2018). Composites from renewable and sustainable resources: Challenges and innovations. *Science, 362(6414)*, 536–542. https://doi.org/10.1126/science.aat9072.

Molewa, B. E. E. (2013). The National Environmental Management: Waste Act, 2008 (Act No. 59 of 2008) National norms and standards for the assessment of waste for landfill disposal. Available at: http://sawic.environment.gov.za/documents/2177.pdf. (Accessed: 21 April 2023).

Moni, P., Wilhelm, M., & Rezwan, K. (2017). The influence of carbon nanotubes and graphene oxide sheets on the morphology, porosity, surface characteristics and

thermal and electrical properties of polysiloxane derived ceramics. *RSC Advances*, *7(60)*, 37559–37567. https://doi.org/10.1039/C7RA01937H.

Morgan, D. R., & Wade, F. H. (2021). Coal based silicon carbide foam (United States Patent US20210395096A1). Available at: https://patents.google.com/patent/US20210395096A1/en.

Moyo, A., Amaral Filho, J. R. do, T. L. Harrison, S., & Broadhurst, J. L. (2019). Implications of sulfur speciation on the assessment of acid rock drainage generating potential: A study of South African coal processing wastes. *Minerals*, *9(12)*, Article 12. https://doi.org/10.3390/min9120776.

Moyo, A., Filho, J. A., Harrison, S., & Broadhurst, J. (2018). Characterising the environmental risks of coal preparation wastes: A study of fine coal slurry waste and discards from South African collieries. *IMWA 2018 Annual Conference; Pretoria, South Africa*.

Munawer, M. E. (2018). Human health and environmental impacts of coal combustion and post-combustion wastes. *Journal of Sustainable Mining*, *17(2)*, 87–96. https://doi.org/10.1016/j.jsm.2017.12.007.

Mutin, P. H., & Boury, B. (2003). Ceramics, chemical processing of. In *Encyclopedia of Physical Science and Technology*. 3rd ed. R. A. Meyers, Ed. Cambridge, Massachusetts: Academic Press. 621–636. https://doi.org/10.1016/B0-12-227410-5/00093-4.

NCC. (2019). Coal in a new carbon age. Available at: http://www.nationalcoalcouncil.org/studies/2019/New-Carbon-Age-Report-Fact-Sheet.pdf. (Accessed: 2 April 2023).

Nicolas, M. F., Vlasova, M., Aguilar, P. A. M., Kakazey, M., Cano, M. M. C., Matus, R. A., & Puig, T. P. (2020). Development of an energy-saving technology for sintering of bricks from high-siliceous clay by the plastic molding method. *Construction & Building Materials*, *242*, 118142. https://doi.org/10.1016/j.conbuildmat.2020.118142.

Nip, M., De Leeuw, J. W., & Crelling, J. C. (1992). Chemical structure of bituminous coal and its constituting maceral fractions as revealed by flash pyrolysis. *Energy & Fuels*, *6(2)*, 125–136. https://doi.org/10.1021/ef00032a003.

Odalanowska, M., Woźniak, M., Ratajczak, I., Zielińska, D., Cofta, G., & Borysiak, S. (2021). Propolis and organosilanes as innovative hybrid modifiers in wood-based polymer composites. *Materials, 14(2)*, 464. https://doi.org/10.3390/ma14020464.

OECD. (2015). Material resources, productivity and the environment. Organisation for Economic Co-operation and Development. OECD Green Growth Studies. *OECDiLibrary*. https://doi.org/10.1787/9789264190504-en.

O'Gorman, J. V., & Walker, P. L. (1973). Thermal behaviour of mineral fractions separated from selected American coals. *Fuel, 52(1)*, 71–79. https://doi.org/10.1016/0016-2361(73)90016-1.

Okolo, G. N., Neomagus, H. W. J. P., Everson, R. C., Roberts, M. J., Bunt, J. R., Sakurovs, R., & Mathews, J. P. (2015). Chemical–structural properties of South African bituminous coals: Insights from wide angle XRD–carbon fraction analysis, ATR–FTIR, solid state $^{13}$C NMR, and HRTEM techniques. *Fuel, 158*, 779–792. https://doi.org/10.1016/j.fuel.2015.06.027.

Pacheco-Torgal, F., & Labrincha, J. A. (2013). The future of construction materials research and the seventh UN Millennium Development Goal: A few insights. *Construction & Building Materials, 40*, 729–737. https://doi.org/10.1016/j.conbuildmat.2012.11.007.

Painter, P. C., Snyder, R. W., Starsinic, M., Coleman, M. M., Kuehn, D. W., & Davis, A. (1981). Concerning the application of FT-IR to the study of coal: A critical assessment of band assignments and the application of spectral analysis programs. *Applied Spectroscopy, 35(5)*, 475–485. https://doi.org/10.1366/0003702814732256.

Painter, P. C., Sobkowiak, M., & Youtcheff, J. (1987). FT-i.r. study of hydrogen bonding in coal. *Fuel, 66(7)*, 973–978. https://doi.org/10.1016/0016-2361(87)90338-3.

Painter, P., Pulati, N., Cetiner, R., Sobkowiak, M., Mitchell, G., & Mathews, J. (2010). Dissolution and dispersion of coal in ionic liquids. *Energy & Fuels, 24(3)*, 1848–1853. https://doi.org/10.1021/ef9013955.

Painter, P., Starsinic, M., & Coleman, M. (1985). Determination of functional groups in coal by fourier transform interferometry. In *Fourier Transform Infrared Spectra.*

*Applications to Chemical Systems*. J.R. Ferraro & L.J. Basile, Eds. Cambridge, Massachusetts: Academic Press. 169–241. https://doi.org/10.1016/B978-0-12-254104-9.50011-0.

Pan, J., Ren, J., Xie, Y., Wei, X., Guan, Y., Yan, X., Tang, H., & Cheng, X. (2017). Porous SiOC composites fabricated from preceramic polymers and wood powders for efficient dye adsorption and removal. *Research on Chemical Intermediates*, *43(7)*, 3813–3832. https://doi.org/10.1007/s11164-016-2850-y.

Pardo, S. G., Bernal, C., Ares, A., Abad, M. J., & Cano, J. (2010). Rheological, thermal, and mechanical characterization of fly ash-thermoplastic composites with different coupling agents. *Polymer Composites*, *31(10)*, 1722–1730. https://doi.org/10.1002/pc.20962.

Peterson, R. J. (2016). Literature review of polymer derived ceramics (Report no. LA-UR-16-23706). Los Alamos National Lab. (LANL), Los Alamos, NM (United States). https://doi.org/10.2172/1254934.

Phillips, L. N., Kappagantula, K. S., & Trembly, J. P. (2019). Mechanical performance of thermoplastic composites using bituminous coal as filler: study of a potentially sustainable end-use application for Appalachian coal. *Polymer Composites*, *40(2)*, 591–599. https://doi.org/10.1002/pc.24696.

Phonphuak, N., & Thiansem, S. (2011). Effects of charcoal on physical and mechanical properties of fired test briquettes. *Science Asia*, *37*, 120–124. https://doi.org/10.2306/scienceasia1513-1874.2011.37.120.

Phua, J.-L., Teh, P.-L., Ghani, S. A., & Yeoh, C.-K. (2017). Influence of thermoplastic spacer on the mechanical, electrical, and thermal properties of carbon black filled epoxy adhesives. *Polymers for Advanced Technologies*, *28(3)*, 345–352. https://doi.org/10.1002/pat.3894.

Poerschke, D. L., Braithwaite, A., Park, D., & Lauten, F. (2018). Crystallization behaviour of polymer-derived Si-O-C for ceramic matrix composite processing. *Acta Materialia*, *147*, 329–341. https://doi.org/10.1016/j.actamat.2018.01.052.

Polok-Rubiniec, M., Włodarczyk-Fligier, A., & Chmielnicki, B. (2021). The properties of a polypropylene matrix composite with anthracite filler. *Archives of Metallurgy & Materials*, *66(1)*, 305–311. https://doi.org/10.24425/amm.2021.134788.

Pudasainee, D., Kurian, V., & Gupta, R. (2020). Coal: past, present, and future sustainable use. In *Future Energy.* 3rd ed. T. M. Letcher, Ed. Amsterdam: Elsevier. 21–48. https://doi.org/10.1016/B978-0-08-102886-5.00002-5.

Pusz, S., Szeluga, U., Nagel, B., Czajkowska, S., Galina, H., & Strzezik, J. (2015). The influence of structural order of anthracite fillers on the curing behaviour, morphology, and dynamic mechanical thermal properties of epoxy composites. *Polymer Composites*, *36(2)*, 336–347. https://doi.org/10.1002/pc.22948.

Qi, F., Tang, M., Wang, N., Liu, N., Chen, X., Zhang, Z., Zhang, K., & Lu, X. (2017). Efficient organic–inorganic intumescent interfacial flame retardants to prepare flame retarded polypropylene with excellent performance. *RSC Advances*, *7(50)*, 31696–31706. https://doi.org/10.1039/C7RA04232A.

Qi, G., Zhang, C., & Hu, H. (2006). Effects of precoating and calcination on microstructure of 3D silica fiber reinforced silicon nitride based composites. *Transactions of Nonferrous Metals Society of China*, *16(4)*, 824–827. https://doi.org/10.1016/S1003-6326(06)60333-6.

Qiu, J.-R., Li, F., & Zheng, C.-G. (1999). Mineral transformation during combustion of coal blends. *International Journal of Energy Research*, *23(5)*, 453–463. https://doi.org/10.1002/(SICI)1099-114X(199904)23:5<453::AID-ER493>3.0.CO;2-E.

Quijorna, N., Coz, A., Andres, A., & Cheeseman, C. (2012). Recycling of Waelz slag and waste foundry sand in red clay bricks. *Resources, Conservation & Recycling*, *65*, 1–10. https://doi.org/10.1016/j.resconrec.2012.05.004.

Raether, F. (2013). Ceramic matrix composites - an alternative for challenging construction tasks. *Ceramic Applications*, *1(1)*, 45–49. Available at: https://www.htl.fraunhofer.de/content/dam/htl/en/Über%20uns/publikationen/Komposite/Ceramic%20Matrix%20Composites%20in%20Ceramic%20Applications%20Raether%20042013.pdf. (Accessed: 21 April 2023).

Rahman, Md. H., Islam, Md. T., Minhaj, T. I., Azad, M. A. K., Hasan, Md. M., & Haque, A. A. Md. R. (2015). Study of thermal conductivity and mechanical property of insulating firebrick produced by local clay and petroleum coal dust as raw materials. *Procedia Engineering*, *105*, 121–128. https://doi.org/10.1016/j.proeng.2015.05.019.

Rajak, D. K., Pagar, D. D., Kumar, R., & Pruncu, C. I. (2019). Recent progress of reinforcement materials: A comprehensive overview of composite materials. *Journal of Materials Research & Technology*, *8(6)*, 6354–6374. https://doi.org/10.1016/j.jmrt.2019.09.068.

Ramachandran, M., & Kalita, K. (2014). Effect of coal ash as a filler on mechanical properties of glass fiber reinforced material. *International Journal of Applied Engineering Research*, *9(22)*, 14269–14277.

Rautenbach, R., Matjie, R. H., Strydom, C. A., Bunt, J. R., Ward, C. R., French, D., & Van Alphen, C. (2020). Evaluation of mineral matter transformations in low-temperature ashes of South African coal feedstock samples and their density separated cuts using high-temperature X-ray diffraction. *International Journal of Coal Preparation & Utilization*, *40(4–5)*, 320–347. https://doi.org/10.1080/19392699.2019.1677629.

Reid, I. (2018). Non-energy uses of coal. (Report no. CCC/291). *IEA Clean Coal Centre Executive Summary, 91*. International Centre for Sustainable Carbon. Available at: https://www.sustainable-carbon.org/report/non-energy-uses-of-coal-report-ccc291/. (Accessed: 20 April 2023).

Ricohermoso, E. I., Heripre, E., Solano-Arana, S., Riedel, R., & Ionescu, E. (2023). Hierarchical microstructure growth in a precursor-derived SiOC thin film prepared on silicon substrate. *International Journal of Applied Ceramic Technology*, *20(2)*, 735–746. https://doi.org/10.1111/ijac.14185.

Ricohermoso, E. I., Klug, F., Schlaak, H., Riedel, R., & Ionescu, E. (2022). Electrically conductive silicon oxycarbide thin films prepared from preceramic polymers. *International Journal of Applied Ceramic Technology*, *19(1)*, 149–164. https://doi.org/10.1111/ijac.13800.

Ricohermoso, E., Rosenburg, F., Klug, F., Nicoloso, N., Schlaak, H. F., Riedel, R., & Ionescu, E. (2021). Piezoresistive carbon-containing ceramic nanocomposites – A review. *Open Ceramics*, *5*, 100057. https://doi.org/10.1016/j.oceram.2021.100057.

Riedel, R., Mera, G., Hauser, R., & Klonczynski, A. (2006). Silicon-based polymer-derived ceramics: synthesis properties and applications-a review. *Journal of the*

*Ceramic Society of Japan*, *114(1330)*, 425–444. https://doi.org/10.2109/jcersj.114.425.

Roberts, M. (2015). The molecular structure of selected South African coal-chars to elucidate fundamental principles of coal gasification. PhD thesis. North-West University. https://www.academia.edu/69936058/The_molecular_structure_of_selected_South_African_coal_chars_to_elucidate_fundamental_principles_of_coal_gasification.

Rojek, M., Szymiczek, M., Suchoń, Ł., & Wróbel, G. (2011). Mechanical properties of polyamide matrix composites filled with titanates modified-coal. *Journal of Achievements in Materials & Manufacturing Engineering*, *46(1)*, 25–32.

Romey, I., & Hein, M. (1981). Carbon fibres from coal-tar pitch. *Fuel*, *60(9)*, 848–850. https://doi.org/10.1016/0016-2361(81)90148-4.

Ruz, P., Banerjee, S., Pandey, M., Sudarsan, V., Sastry, P. U., & Kshirsagar, R. J. (2016). Structural evolution of turbostratic carbon: implications in $H_2$ storage. *Solid State Sciences*, *62*, 105–111. https://doi.org/10.1016/j.solidstatesciences.2016.10.017.

Saha, B. K., Rose, M. T., Wong, V. N. L., Cavagnaro, T. R., & Patti, A. F. (2018). Nitrogen dynamics in soil fertilized with slow release brown coal-urea fertilizers. *Scientific Reports*, *8(1)*, 14577. https://doi.org/10.1038/s41598-018-32787-3.

Sam, S. S., Habib, N. Z., Aun, N. C., Yong, C. S., Bashir, M. J. K., & Ping, T. W. (2020). Blended waste oil as alternative binder for the production of environmental friendly roofing tiles. *Journal of Cleaner Production*, *258*, 120937. https://doi.org/10.1016/j.jclepro.2020.120937.

Sam, S. S., Ng, C., Chee, S. Y., Habib, N., Nadeem, H., & Teoh, W. P. (2017). Utilization of ethyl cellulose polymer and waste materials for roofing tile production. *IOP Conference Series: Earth & Environmental Science*, *67(1)*, 012005. https://doi.org/10.1088/1755-1315/67/1/012005.

Sarkar, S., Gan, Z., An, L., & Zhai, L. (2011). Structural evolution of polymer-derived amorphous SiBCN ceramics at high temperature. *The Journal of Physical Chemistry C*, *115(50)*, 24993–25000. https://doi.org/10.1021/jp203287h.

Sazali, N. E. S., Deraman, M., Omar, R., Othman, M. a. R., Suleman, M., Shamsudin, S. A., Tajuddin, N. S. M., Hanappi, M. F. Y. M., Hamdan, E., Nor, N. S. M., & Basri, N. H. (2016). Preparation and structural characterisation of turbostratic-carbon/graphene derived from amylose film. *AIP Conference Proceedings*, *1784(1)*, 040009. https://doi.org/10.1063/1.4966795.

Schmitz, K. S. (2018). Ecology. In *Physical Chemistry*. K. S. Schmitz, Ed. Amsterdam: Elsevier. 833–974. https://doi.org/10.1016/B978-0-12-800513-2.00005-X.

Schobert, H. H., & Song, C. (2002). Chemicals and materials from coal in the 21st century. *Fuel*, *81(1)*, 15–32. https://doi.org/10.1016/S0016-2361(00)00203-9.

Schweinfurth, S. P. (2003). Coal – a complex natural resource: An overview of factors affecting coal quality and use in the United States. United States Printing Office, Washington: US Department of the Interior, US Geological Survey Circular. https://doi.org/10.3133/cir1143.

Sekhohola, L. M., Igbinigie, E. E., & Cowan, A. K. (2013). Biological degradation and solubilisation of coal. *Biodegradation*, *24(3)*, 305–318. https://doi.org/10.1007/s10532-012-9594-1.

Sharma, S. (2018). Glassy carbon: a promising material for micro- and nanomanufacturing. *Materials*, *11(10)*, 1857. https://doi.org/10.3390/ma11101857.

Shen, C., Barrios, E., & Zhai, L. (2018). Bulk polymer-derived ceramic composites of graphene oxide. *ACS Omega*, *3(4)*, 4006–4016. https://doi.org/10.1021/acsomega.8b00492.

Sengupta, S., Pal, K., Ray, D., & Mukhopadhyay, A. (2011). Furfuryl palmitate coated fly ash used as filler in recycled polypropylene matrix composites. *Composites Part B: Engineering*, *42(7)*, 1834–1839. https://doi.org/10.1016/j.compositesb.2011.06.021.

Sengupta, S., Ray, D., & Mukhopadhyay, A. (2012). Thermal and structural characterization of furfuryl palmitate coated fly ash reinforced recycled polypropylene matrix composites. *Advanced Materials Research*, *584*, 551–555. https://doi.org/ 10.4028/www.scientific.net/AMR.584.551.

Sengupta, S., Ray, D., & Mukhopadhyay, A. (2013). Sustainable materials: Value-added composites from recycled polypropylene and fly ash using a green

coupling agent. *ACS Sustainable Chemistry & Engineering*, *1(6)*, 574–584. https://doi.org/10.1021/sc3000948.

Sherwood, W., Hill, A., Nameni, G., & Easter, W. (2021). Composite tile and method of manufacture. United States Patent No. US11136270B2. https://patents.google.com/patent/US11136270B2/en.

Shibuya, M., Sakurai, M., & Takahashi, T. (2007). Preparation and characteristics of a vapor-grown carbon fibre/ceramic composite using a methylsilicone precursor. *Composites Science & Technology*, *67(15-16)*, 3338–3344. https://doi.org/10.1016/j.compscitech.2007.03.023.

Shinn, J. H. (1984). From coal to single-stage and two-stage products: A reactive model of coal structure. *Fuel*, *63(9)*, 1187–1196. https://doi.org/10.1016/0016-2361(84)90422-8.

Shintani, T., & Nakamura, M. (1995). Electromagnetic wave shielding building material. United States Patent No. US5422174A. https://patents.google.com/patent/US5422174.

Silva, L. F. O., Crissien, T. J., Tutikian, B. F., & Sampaio, C. H. (2020). Rare earth elements and carbon nanotubes in coal mine around spontaneous combustions. *Journal of Cleaner Production*, *253*, 120068. https://doi.org/10.1016/j.jclepro.2020.120068.

Smyrl, N. R., & Fuller, E. L. (1987). Diffuse Reflectance Infrared Fourier Transform (DRIFT) spectroscopic studies of coals: in situ studies of acetylation. *Applied Spectroscopy*, *41(6)*, 1023–1028. https://doi.org/10.1366/0003702874447923.

Solomon, P. R. (1981). Coal structure and thermal decomposition. In *New Approaches in Coal Chemistry. Chapter 4. ACS Symposium Series*, *169*, 61–71. American Chemical Society. https://doi.org/10.1021/bk-1981-0169.ch004.

Song, C., Hou, L., Saini, A. K., Hatcher, P. G., & Schobert, H. H. (1993). CPMAS 13C NMR and pyrolysis-GC-MS studies of structure and liquefaction reactions of Montana subbituminous coal. *Fuel Processing Technology*, *34(3)*, 249–276. https://doi.org/10.1016/0378-3820(93)90069-G.

Song, C., Saini, A., Huang, L., Wenzel, K., Hatcher, P. G., & Schobert, H. H. (1992). Effects of low-temperature catalytic pretreatments on coal structure and reactivity in liquefaction. *Technical progress report, October 1991–December*

*1991*. (Report no. DOE/PC/91042-T2, ON: DE93004362). Pennsylvania State University, University Park, PA (United States): Department of Materials Science and Engineering. https://doi.org/10.2172/6911546.

Song, C., Schobert, H. H., & Andreson, J. M. (2005). Premium carbon products and organic chemicals from coal. (Report No. CCC-98). IEA Clean Coal Centre, London (United Kingdom). Available at: https://www.osti.gov/etdeweb/biblio/20674218.

Song, D., Yang, C., Zhang, X., Su, X., & Zhang, X. (2011). Structure of the organic crystallite unit in coal as determined by X-ray diffraction. *Mining Science & Technology (China)*, *21(5)*, 667–671. https://doi.org/10.1016/j.mstc.2011.10.004.

Stabik, J., & Chomiak, M. (2011). Influence of casting velocity on surface resistivity of epoxy-hard coal graded composites. *Archives of Materials Science & Engineering, 47 (1)*, 48–56.

Stabik, J., Rojek, M., Suchoń, Ł., & Mrowiec, K. (2012). Carbon materials as fillers for polymer matrix composites. *Archives of Materials Science & Engineering*, *Vol. 53, nr 1*, 29–37. Available at: https://www.infona.pl//resource/bwmeta1.element.baztech-article-BSL7-0056-0002.

Stabik, J., & Chomiak, M. (2013). Wear resistance of epoxy-hard coal composites. *Archives of Materials Science & Engineering*, *64(2*), 168–174.

Stabik, J., & Chomiak, M. (2016a). Graded epoxy-hard coal composites: Analysis of filler particle distribution in the epoxy matrix. *Journal of Composite Materials, 50(26)*, 3663–3677. https://doi.org/10.1177/0021998315623626.

Stabik, J., & Chomiak, M. (2016b). Graded epoxy–hard coal composites: surface resistivity study. *Journal of Composite Materials, 50(27)*, 3765–3777. https://doi.org/10.1177/0021998315625452.

Stabik, J., Suchoń, Ł., Rojek, M., & Szczepanik, M. (2009). Investigation of processing properties of polyamide filled with hard coal. *Journal of Achievements in Materials & Manufacturing Engineering, 33(2)*, 142–149.

Stabik, J., Szczepanik, M., Dybowska, A., & Suchoń, Ł. (2010). Electrical properties of polymeric gradient materials based on epoxy resin filled with hard coal. *Journal of Achievements in Materials & Manufacturing Engineering, 38(1)*, 56–63.

Stabler, C., Ionescu, E., Graczyk-Zajac, M., Gonzalo-Juan, I., & Riedel, R. (2018). Silicon oxycarbide glasses and glass-ceramics: "All-Rounder" materials for advanced structural and functional applications. *Journal of the American Ceramic Society, 101(11)*, 4817–4856. https://doi.org/10.1111/jace.15932.

Stolboushkin, A. Yu., Ivanov, A. I., & Fomina, O. A. (2016). Use of coal-mining and processing wastes in production of bricks and fuel for their burning. *Procedia Engineering, 150*, 1496–1502. https://doi.org/10.1016/j.proeng.2016.07.089.

Stolboushkin, A. Y., Akst, D. V., Fomina, O. A., Ivanov, A. I., & Syromyasov, V. A. (2017). Analysis of waste coal from the enterprises of Kemerovo region as raw materials for production of ceramic materials. *IOP Conference Series: Earth and Environmental Science, 84*, 012037. *International Scientific and Research Conference on Knowledge-based Technologies in Development and Utilization of Mineral Resources (KTDMUR2017).* 6–9 June 2017. Novokuznetsk, Russian Federation. https://doi.org/10.1088/1755-1315/84/1/012037.

Subedi, D. P. (2011). Contact angle measurement for the surface characterisation of solids. *Himalayan Physics, 2(2)*, 1–4. https://doi.org/10.3126/hj.v2i2.5201.

Sun, W., Wang, N., Chu, W., & Jiang, C. (2015). The role of volatiles and coal structural variation in coal methane adsorption. *Science Bulletin, 60(5)*, 532–540. https://doi.org/10.1007/s11434-015-0747-6.

Swaminathan, B., Painuly, A., Manwatkar, S., & Shanmugam, P. (2010). Preceramic polymer-derived C/C-SiC and C/C-SiBCO composites for high temperature applications. In *High Temperature Ceramic Materials & Composites*. W. Krenkel & J. Lamon, Eds. Berlin: Aviso Verlagsgesellschaft mbH. 724-730.

Taha, Y., Benzaazoua, M., Hakkou, R., & Mansori, M. (2017). Coal mine wastes recycling for coal recovery and eco-friendly bricks production. *Minerals Engineering, 107*, 123–138. https://doi.org/10.1016/j.mineng.2016.09.001.

Tambwe, O., Kotsiopoulos, A., & Harrison, S. T. L. (2020). Desulphurising high sulphur coal discards using an accelerated heap leach approach.

*Hydrometallurgy*, *197*, 105472. https://doi.org/10.1016/j.hydromet.2020.105472.

Tan, J., Cheng, H., Wei, L., Wei, C., Xing, Y., & Gui, X. (2019). Using low-rank coal slime as an eco-friendly replacement for carbon black filler in styrene butadiene rubber. *Journal of Cleaner Production*, *234*, 949–960. https://doi.org/10.1016/j.jclepro.2019.06.221.

Tanzi, M. C., Farè, S., & Candiani, G. (2019). Organization, structure, and properties of materials. In *Foundations of Biomaterials Engineering*. M. C. Tanzi, S. Farè, & G. Candiani, Eds. Cambridge, Massachusetts: Academic Press. 3–103. https://doi.org/10.1016/B978-0-08-101034-1.00001-3.

Tsyntsarski, B., Petrova, B., Budinova, T., Petrov, N., Krzesinska, M., Pusz, S., Majewska, J., & Tzvetkov, P. (2010). Carbon foam derived from pitches modified with mineral acids by a low pressure foaming process. *Carbon*, *48(12)*, 3523–3530. https://doi.org/10.1016/j.carbon.2010.05.048.

Tuinstra, F., & Koenig, J. L. (1970). Raman spectrum of graphite. *The Journal of Chemical Physics*, *53(3)*, 1126–1130. https://doi.org/10.1063/1.1674108.

U.S. EPA. (1992). Method 1311 Toxicity characteristic leaching procedure SW-846. United States Environmental Protection Agency. Available at: https://www.epa.gov/sites/default/files/2015-12/documents/1311.pdf; https://www.epa.gov/sitesdefault/files/2020-04/documents/sw_846_ch7.pdf. (Accessed: 21 April 2023).

van der Merwe, E. M., Prinsloo, L. C., Mathebula, C. L., Swart, H. C., Coetsee, E., & Doucet, F. J. (2014). Surface and bulk characterisation of an ultrafine South African coal fly ash with reference to polymer applications. *Applied Surface Science*, *317*, 73–83. https://doi.org/10.1016/j.apsusc.2014.08.080.

van Niekerk, D. (2008). Structural elucidation, molecular representation and solvent interactions of vitrinite-rich and inertinite-rich South African coals. PhD thesis. The Pennsylvania State University.

Vasić, M. V., Goel, G., Vasić, M., & Radojević, Z. (2021). Recycling of waste coal dust for the energy-efficient fabrication of bricks: A laboratory to industrial-scale study. *Environmental Technology & Innovation*, *21*, 101350. https://doi.org/10.1016/j.eti.2020.101350.

Walter, S., Suttor, D., Erny, T., Hahn, B., & Greil, P. (1996). Injection moulding of polysiloxane/filler mixtures for oxycarbide ceramic composites. *Journal of the European Ceramic Society*, *16(4)*, 387–393. https://doi.org/10.1016/0955-2219(95)00120-4.

Wang, G. H., & Zhou, A. N. (2011). Effect of coal structure on mechanical and thermal properties of coal filled soy protein composites. *Advanced Materials Research*, *236–238*, 288–291. https://doi.org/10.4028/www.scientific.net/AMR.236-238.288.

Wang, W., Sun, K., & Liu, H. (2020). Effects of different aluminium sources on morphologies and properties of ceramic floor tiles from red mud. *Construction & Building Materials*, *241*, 118119. https://doi.org/10.1016/j.conbuildmat.2020.118119.

Wang, X. (2019). Photoinduced thiol-ene click chemistry assisted additive manufacturing and freeze casting of polymer-derived ceramics. Universitätsverlag der TU Berlin.

Wang, X., Schmidt, F., Hanaor, D., Kamm, P. H., Li, S., & Gurlo, A. (2019). Additive manufacturing of ceramics from preceramic polymers: A versatile stereolithographic approach assisted by thiol-ene click chemistry. *Additive Manufacturing*, *27*, 80–90. https://doi.org/10.1016/j.addma.2019.02.012.

Weller, M., & Wert, C. A. (1983). Internal friction of coal and of other natural macromolecular solids. *Le Journal de Physique Colloques*, *44(C9)*, C9–191. https://doi.org/ 10.1051/jphyscol:1983924.

Wen, Q., Qu, F., Yu, Z., Graczyk-Zajac, M., Xiong, X., & Riedel, R. (2022). Si-based polymer-derived ceramics for energy conversion and storage. *Journal of Advanced Ceramics*, *11(2)*, 197–246. https://doi.org/10.1007/s40145-021-0562-2.

Wen, Q., Yu, Z., & Riedel, R. (2020). The fate and role of in situ formed carbon in polymer-derived ceramics. *Progress in Materials Science*, *109*, 100623. https://doi.org/10.1016/j.pmatsci.2019.100623.

Weng, C.-H., Lin, D.-F., & Chiang, P.-C. (2003). Utilization of sludge as brick materials. *Advances in Environmental Research*, *7(3)*, 679–685. https://doi.org/10.1016/S1093-0191(02)00037-0.

Wert, C. A., & Weller, M. (1982). Polymeric character of coal. *Journal of Applied Physics, 53(10)*, 6505–6512. https://doi.org/10.1063/1.330076.

Whitehurst, D. D. (1978). A primer on the chemistry and constitution of coal. In *Organic Chemistry of Coal*. *Chapter 1*. *ACS Symposium Series, 71*, 1–35. American Chemical Society. https://doi.org/10.1021/bk-1978-0071.ch001.

Wilson, A. M., Zank, G., Eguchi, K., Xing, W., Yates, B., & Dahn, J. R. (1997). Polysiloxane pyrolysis. *Chemistry of Materials, 9(7)*, 1601–1606. https://doi.org/10.1021/cm970002r.

Wu, C., Tuo, J., Zhang, L., Zhang, M., Li, J., Liu, Y., & Qian, Y. (2017). Pore characteristics differences between clay-rich and clay-poor shales of the Lower Cambrian Niutitang Formation in the Northern Guizhou area, and insights into shale gas storage mechanisms. *International Journal of Coal Geology*, *178*, 13–25. https://doi.org/10.1016/j.coal.2017.04.009.

Xia, A., Yin, J., Chen, X., Liu, X., & Huang, Z. (2020). Polymer-derived Si-based ceramics: recent developments and perspectives. *Crystals*, *10(9)*, 824. https://doi.org/10.3390/cryst10090824.

Xie, Z., Wang, S., & Chen, Z. (2006). Active filler (Aluminium–Aluminium Nitride) controlled polycarbosilane pyrolysis. *Journal of Inorganic & Organometallic Polymers & Materials, 16(1)*, 69–81. https://doi.org/10.1007/s10904-006-9030-2.

Wang, X. (2019). Photoinduced thiol-ene click chemistry assisted additive manufacturing and freeze casting of polymer-derived ceramics. Universitätsverlag der TU Berlin. Available at: https://d-nb.info/1196200122/34. (Accessed: 21 April 2023).

Xu, H., Song, W., Cao, W., Shao, G., Lu, H., Yang, D., Chen, D., & Zhang, R. (2017). Utilization of coal gangue for the production of brick. *Journal of Material Cycles & Waste Management*, *19(3)*, 1270–1278. https://doi.org/10.1007/s10163-016-0521-0.

Yang, J., Su, Y., He, X., Tan, H., Jiang, Y., Zeng, L., & Strnadel, B. (2018). Pore structure evaluation of cementing composites blended with coal by-products: Calcined coal gangue and coal fly ash. *Fuel Processing Technology*, *181*, 75–90. https://doi.org/10.1016/j.fuproc.2018.09.013.

Yang, Z., Wang, D., Meng, Z., & Li, Y. (2019). Adsorption separation of $CH_4/N_2$ on modified coal-based carbon molecular sieve. *Separation & Purification Technology*, *218*, 130–137. https://doi.org/10.1016/j.seppur.2019.02.048.

Yao, Z. T., Ji, X. S., Sarker, P. K., Tang, J. H., Ge, L. Q., Xia, M. S., & Xi, Y. Q. (2015). A comprehensive review on the applications of coal fly ash. *Earth-Science Reviews*, *141*, 105–121. https://doi.org/10.1016/j.earscirev.2014.11.016.

Yao, Z. T., Xia, M. S., Sarker, P. K., & Chen, T. (2014). A review of the alumina recovery from coal fly ash, with a focus in China. *Fuel*, *120*, 74–85. https://doi.org/10.1016/j.fuel.2013.12.003.

Yagüe, S., Sánchez, I., Vigil de la Villa, R., García-Giménez, R., Zapardiel, A., & Frías, M. (2018). Coal-mining tailings as a pozzolanic material in cements industry. *Minerals*, *8(2)*, 46. https://doi.org/10.3390/min8020046.

Yin, Y., Yin, J., Zhang, W., Tian, H., Hu, Z., Ruan, M., Xu, H., Liu, L., Yan, X., & Chen, D. (2018). FT-IR and micro-Raman spectroscopic characterisation of minerals in high-calcium coal ashes. *Journal of the Energy Institute*, *91(3)*, 389–396. https://doi.org/10.1016/j.joei.2017.02.003.

Yuan, Q., Robert, D., Mohajerani, A., Tran, P., & Pramanik, B. K. (2022). Utilisation of waste-to-energy fly ash in ceramic tiles. *Construction & Building Materials*, *347*, 128475. https://doi.org/10.1016/j.conbuildmat.2022.128475.

Zabihi, O., Shafei, S., Fakhrhoseini, S. M., Ahmadi, M., Ajdari Nazarloo, H., Stanger, R., Anh Tran, Q., Lucas, J., Wall, T., & Naebe, M. (2019). Low-Cost carbon fibre derived from sustainable coal tar pitch and polyacrylonitrile: Fabrication and characterisation. *Materials*, *12(8)*, 1281. https://doi.org/10.3390/ma12081281.

Zhang, W., & Honaker, R. (2020). Characterization and recovery of rare earth elements and other critical metals (Co, Cr, Li, Mn, Sr, and V) from the calcination products of a coal refuse sample. *Fuel*, *267*, 117236. https://doi.org/10.1016/j.fuel.2020.117236.

Zhang, W., Jiang, S., Wang, K., Wang, L., Xu, Y., Wu, Z., Shao, H., Wang, Y., & Miao, M. (2015). Thermogravimetric dynamics and FTIR analysis on oxidation properties of low-rank coal at low and moderate temperatures. *International*

*Journal of Coal Preparation & Utilization*, *35(1)*, 39–50. https://doi.org/10.1080/19392699.2013.873421.

Zhang, W., Yang, X., & Honaker, R. Q. (2018). Association characteristic study and preliminary recovery investigation of rare earth elements from Fire Clay seam coal middlings. *Fuel*, *215*, 551–560. https://doi.org/10.1016/j.fuel.2017.11.075.

Zhang, Y., Liu, Q., Zhang, S., Zhang, Y., Zhang, Y., & Liang, P. (2016). Characterization of kaolinite/styrene butadiene rubber composite: Mechanical properties and thermal stability. *Applied Clay Science*, *124–125*, 167–174. https://doi.org/10.1016/j.clay.2016.02.002.

Zhang, Y., Song, H., Liu, Q., Zhang, S., & Zhang, Y. (2017). Dynamic mechanical property of kaolinite/styrene-butadiene rubber composites. *Mechanics, Materials Science & Engineering Journal*, *8*. https://doi.org/10.2412/mmse.61.54.732.

Zhang, Y., & Ling, T.-C. (2020). Reactivity activation of waste coal gangue and its impact on the properties of cement-based materials – A review. *Construction & Building Materials*, *234*, 117424. https://doi.org/10.1016/j.conbuildmat.2019.117424.

Zhang, Y., Zhang, X., & Hu, S. (2021). Structural transformations of coal at low temperature oxidation via in-situ FTIR. *Combustion Science & Technology*, *193(11)*, 1885–1902. https://doi.org/10.1080/00102202.2020.1716341.

Zhao, B. (2012). Environmental assessment of Durban Navigation Colliery discard dumps in the Klip River coalfield, Kwazulu-Natal province of South Africa. *Environmental Earth Sciences*, *67(3)*, 743–757. https://doi.org/10.1007/s12665-012-1533-2.

Zhao, H., Wang, L., Jia, D., Xia, W., Li, J., & Guo, Z. (2014). Coal based activated carbon nanofibres prepared by electrospinning. *Journal of Materials Chemistry A*, *2(24)*, 9338–9344. https://doi.org/10.1039/C4TA00069B.

Zhou, G., Xu, C., Cheng, W., Zhang, Q., & Nie, W. (2015). Effects of oxygen element and oxygen-containing functional groups on surface wettability of coal dust with various metamorphic degrees based on xps experiment. *Journal of Analytical Methods in Chemistry*; *Hindawi*, *467242*. https://doi.org/10.1155/2015/467242.

Zhu, X., Pan, Q., Xu, H., & Lu, J. (2010). Effects of coal and ammonium polyphosphate on thermal degradation and flame retardancy of polyethylene terephthalate. *Journal of Polymer Research, 17(5)*, 621–629. https://doi.org/10.1007/s10965-009-9350-3.

# Appendix A

# Published Papers

## A.1 'Coal as a Filler in Polymer Composites: A Review'.

Contents lists available at ScienceDirect

Resources, Conservation & Recycling

journal homepage: www.elsevier.com/locate/resconrec



Review

# Coal as a Filler in Polymer Composites: A Review

Orevaoghene Eterigho-Ikelegbe [a,*], Kelvin O. Yoro [b], Samson Bada [a]

[a] DSI-NRF SARChI Clean Coal Technology Research Group, School of Chemical and Metallurgical Engineering, Faculty of Engineering and the Built Environment, University of the Witwatersrand, Wits 2050, Johannesburg, South Africa
[b] Energy Technologies Area, Lawrence Berkeley National Laboratory, 1 Cyclotron Road, Berkeley CA 94720, United States

ARTICLE INFO

*Keywords:*
Agglomeration
Coal
Organic filler
Preceramic polymer
Reinforcement

ABSTRACT

There is rapidly growing interest in non-energy coal applications. In addition, the demand for non-traditional specialized materials is on the rise. Therefore, this review systematically presents cutting-edge updates on the development of polymer composites using coal as a filler feedstock. The review begins by exploring the polymeric nature and macromolecular structure of coal. The study then reviews the results of published experimental studies relating to the use of coal as a filler in polymeric composites. Previous studies have demonstrated that coal can serve as a filler to extend the use and processing of polymer materials. Based on the articles reviewed, the content of coal, the structure of the coal, and the interfacial bonding between coal particles and the polymer matrix are the main factors that influence the mechanical performance of the final coal/polymer composite material. Not to mention, coupling agents could be introduced to alter the surface of the coal particles as a strategy to increase the compatibility between coal and polymer and ultimately the composite performance. However, further studies involving the use of modeling and simulation capable of predicting the influence of processing parameters on the overall performance of the final composites are necessary. More positive results demonstrating the technical feasibility and sustainable utilization of coal as a filler in polymer composites production beyond the laboratory scale could pave the way for its large-scale applications.

### Introduction

Coal is a heterogeneous complex rock containing organic materials with inorganic mineralized inclusions dispersed within and around its internal structure (Davidson, 1982; Schweinfurth, 2003; Pudasainee et al., 2020). Coal is abundantly available and for many decades has been used as a source of affordable energy, thereby enhancing industrial and economic growth globally (Magazzino et al., 2020). Currently, the most significant use of coal is for the generation of steam for electricity production (IEA, 2019). Energy projections indicated that coal would continue to play an indispensable role as a source of fuel for the world's electricity generation, petrochemical, metallurgical reductant, and for the production of cement, aluminum, and glass (IEA, 2019). However, a recent report on world energy by the bp Statistical Review, (2020) indicates that the use of coal is declining steadily, especially in power generation. This decline could be attributed to the long-term concerns regarding greenhouse gas emissions, which puts pressure on the environment. Furthermore, the preference for renewables and the stiff pricing competition of coal with natural gas for power generation also contribute to the current decline in coal usage (bp statistical review of world energy 2019, 2020; Gagarin et al., 2020). As countries switch to natural gas and renewables for electricity generation, there is a need to diversify the use of coal beyond the production of electricity and chemicals.

Research to combat the environmental impacts of coal combustion has progressed massively in recent times with significant attention shifting towards diversifying the inherently rich carbon and mineral chemistry of coal to produce sustainable non-energy products. One of the non-energy products derived from coal to enhance its economic and environmental value is the production of composite materials. Composite or hybrid materials are increasingly gaining popularity due to their attractiveness and the significant roles they play in modern applications such as biomedical implants, electronic components; construction, and auto-parts structures (Mohanty et al., 2018; Rajak et al., 2019). In producing composites, two or more components synergistically combine to produce a new material with improved mechanical, electrical, and physicochemical properties compared to a single material (Rajak et al., 2019). Research and development regarding the use of coal

* Corresponding author.
*E-mail address:* 1794557@students.wits.ac.za (O. Eterigho-Ikelegbe).

https://doi.org/10.1016/j.resconrec.2021.105756
Received 1 March 2021; Received in revised form 23 May 2021; Accepted 16 June 2021

## A.2 'Preparation and characterisation of ceramic composites from South Africa coal discard'.

Construction and Building Materials 302 (2021) 124164

Contents lists available at ScienceDirect

Construction and Building Materials

journal homepage: www.elsevier.com/locate/conbuildmat

# Preparation and characterization of ceramic composites from South Africa coal discard

Orevaoghene Eterigho-Ikelegbe [a,*], Ryan Trammell [b], Samson Bada [a]

[a] DSI-NRF SARChI Clean Coal Technology Research Group, School of Chemical and Metallurgical Engineering, Faculty of Engineering and the Built Environment, University of the Witwatersrand, Private Bag X3, Wits 2050, Johannesburg, South Africa
[b] Samplastics, 269 Aulin Avenue, Suite 1003, Oviedo, FL 32765, USA

ARTICLE INFO

*Keywords:*
Coal discard
Composites
Flexural strength
Mechanical properties
Preceramic polymer
Water absorption

ABSTRACT

The mining and processing of coal are accompanied by the accumulation of a substantial volume of discard that threatens the environment. Also, the continuous harvesting of natural resources such as clay to produce building materials is not environmentally sustainable. In this study, various South Africa coal discard was blended with a polysiloxane preceramic polymer resin and thereafter pyrolyzed to produce coal/ceramic composites. The physicomechanical properties of the composites were evaluated using various ASTM standard test methods. The thermal stability, mineralogy, and functional group properties of the raw materials and the composites were checked using TGA, XRD, and FTIR respectively. The results suggest that carbonyl functional groups and hydrogen bond in the coal discard promoted bonding with the preceramic polymer, therby improving the physicomechanical properties of the composites. XRD results showed that the total intensity of the diffraction peaks in the coals discards declined after pyrolysis of the blend of coal discard and the preceramic polymer. This suggests the amorphization of the crystalline phases in the coal discards. The developed composites displayed water absorption and flexural strength as low as 1.94–10.1% and 27.51–36.46 MPa respectively. The remarkable mechanical properties of the composites suggest that the coal composites produced in this study could be applicable in the construction industry. However, more tests like impact strength, thermal conductivity, etc. are required to fully characterize the properties of the coal composites.

### 1. Introduction

With growing global demand for reliable and low-cost energy, coal remains one of the largest sources of energy in the world. To meet the market specification, an enormous amount of byproducts is produced during the extraction and preparation phase. These by-products sometimes referred to as gangue, slurries, coal slime, tailings, middlings, etc. contain small amounts of coal, metallic minerals, and a series of incombustible inorganic impurities [38]. To give context to the amount of coal discard produced in South Africa, Belaid et al. [12] reported that the amount of discard coal stockpiled is more than 1.5 billion tons, with approximately 60 million tons produced annually. Disposing of this waste has been a challenge to the industry, while stockpiling them results in severe environmental concerns, including leaching, spontaneous combustion, air pollution, and contamination of aquifers and useful land space [2,38,63].

On the other hand, it is reported that the global construction industry consumes more amount of raw materials than any other economic activity [46]. This continuous exploitation has led to substantial depletion of raw material resources for the building and construction industry. Research efforts to valorize coal discard for building and ceramic applications have emerged and progressed steadily. Information is available in the literature on the use of coal discard as pore-forming agents or as feedstock for the production of building ceramic and insulating bricks [1,25,35,61]. The research conducted by Fomina and Stolboushkin [25] described a procedure to produce ceramic bricks from coal discard and moderately plastic loams. The investigation indicated it was necessary to fire the blend in an oxidizing atmosphere to ensure complete carbon burning. In another investigation conducted by Stolboushkin et al. [61], pulverized coal discard was subjected to a pressure of 15–17 MPa in a press and subsequently fired at 1000 °C to prepare ceramic samples. Based on the analyses carried out, it was established that coal discard with a reduced amount of carbon could be used to produce ceramic bricks of compressive strength 32.4 MPa. Taha et al. [63] also

* Corresponding author.
*E-mail address:* 1794557@students.wits.ac.za (O. Eterigho-Ikelegbe).

https://doi.org/10.1016/j.conbuildmat.2021.124164
Received 26 May 2021; Received in revised form 17 June 2021; Accepted 4 July 2021
0950-0618/© 2021 Elsevier Ltd. All rights reserved.

## A.3 'Novel ceramic composites produced from coal discards with potential application in the building and construction sectors'.



# Novel ceramic composites produced from coal discards with potential application in the building and construction sectors

by O. Eterigho-Ikelegbe[1], R. Trammell[2], and S.O. Bada[1]

Affiliation:
[1]DSI-NRF SARChI Clean Coal Technology Research Group, School of Chemical & Metallurgy, Faculty of Engineering and the Built Environment, University of the Witwatersrand, South Africa.
[2]Semplastics, United States.

Correspondence to:
O. Eterigho-Ikelegbe

Email:
eterighoo@gmail.com

Dates:
Received: 25 Jan. 2022
Revised: 19 May 2022
Accepted: 22 Jun. 2022
Published: August 2022

How to cite:
Eterigho-Ikelegbe, O., Trammel, R., and Bada, S.O. 2022
Novel ceramic composites produced from coal discards with potential application in the building and construction sectors.
Journal of the Southern African Institute of Mining and Metallurgy, vol. 122, no. 8, pp. 421–428

DOI ID:
http://dx.doi.org/10.17159/2411-9717/2001/2022

ORCID:
S.O. Bada
https://orcid.org/0000-0002-1079-3492
O. Eterigho-Ikelegbe
https://orcid.org/0000-0001-6384-7741

This paper was first presented at the Southern African Coal Processing Society, Biannual International Coal Conference, 12-14th October 2021, Secunda

### Synopsis

**In response to the enormous amounts of coal discard generated during coal mining and preparation, the development of an efficient and sustainable strategic use of this resource is essential. Furthermore, the rising urban population over the next decades is confronted with the depletion of quality raw materials for building components. To this end, this study reports new information on the morphology, water absorption, and flexural strength properties of ceramic composites produced from three different coal discards and polysiloxane pre-ceramic polymer (PCP) resin. In addition, test results relating to the continuous operating temperature, chemical resistance, and efflorescence potential of the composites are presented. The results show that the water absorption and flexural strength of the coal composites, up to 1.94% and 36.46 MPa respectively, exceed the requirements for ceramic and clay roof tiles. The continuous operating temperature of composites is found to be more thermally stable than conventional roofing tiles (concrete and ceramic) between ambient temperature and 600°C. In addition, the excellent chemical resistance of the composites (94.43%–99.98%) compared to conventional roofing tiles (67.82%–99.97%) eliminates the need for additional external coatings. The interesting results documented so far suggest that this technique could be used to produce low-temperature application building products such as bricks, panels, roofing tiles, *etc*. This new recycling technique offers an excellent opportunity to eliminate enormous volumes of coal discard and to advance the circular economy in the coal industry.**

### Keywords

**coal discard, waste utilization, composites, chemical resistance, circular economy.**

### Introduction

Coal is a relatively low-cost source of energy that has contributed enormously to global economic development. The mining and processing of coal in the industrialized and developing countries has led to the production of billions of tons of coal discard. With coal meeting about 77% (http://www.energy.gov.za) of the energy needs in South Africa, coal production will likely remain significant, at least for the foreseeable future. According to the website, about 60 Mt coal waste are produced each year, adding to an already accumulated surplus of 1 Gt. These coal discards heaped on arable land or retention ponds could pose enormous environmental hazards such as spontaneous combustion if not properly managed. Most of these dumps are known to contain low- to high-quality rich inorganic-organic compounds, depending on the source. Although some coal discard dumps can be beneficiated to yield clean coal, the process could be somewhat unattractive when the age of the coal is taken into consideration. Other factors that are considered are the degree of oxidation or weathering of the coal, the potentially high cost of treatment, and the subsequent generation of discard after beneficiation.

A panoply of innovative research on the beneficiation of South Africa´s coal discard into alternative products exists in the literature. Tambwe, Kotsiopoulos, and Harrison. (2020) demonstrated the laboratory-scale heap leaching potential of pyrite from sulphidic coal discard to reduce its risk of disposal. Nevertheless, the process still leaves behind desulphurized coal discard as waste. The combustion of SA coal discard in a circulating fluidized bed (CFB) boiler was demonstrated and reported by Belaid *et al.* (2013). Due to the similar combustion profile of the co-combustion of 70% coal discard and 30% refuse-derived fuel compared to 100% coal, Isaac and Bada (2020) proposed that the blend could be considered an alternative fuel for use in existing pulverized boilers. The use of different South African coal discards to produce activated carbon as porous adsorbents for natural gas storage was reported by Abdulsalam *et al.* (2019; 2020). Amaral Filho *et al.* (2020) demonstrated that low-sulphur ultrafine coal discard fabricated topsoil outperformed native soil for rehabilitating coal mine sites. Despite the numerous

**A.4 'Mechanism of bonding, surface property, electrical behaviour, and environmental friendliness of carbon/ceramic composites produced via the pyrolysis of coal waste with polysiloxane polymer'.**

Environmental Science and Pollution Research (2023) 30:93786–93799
https://doi.org/10.1007/s11356-023-28661-z

RESEARCH ARTICLE

# Mechanism of bonding, surface property, electrical behaviour, and environmental friendliness of carbon/ceramic composites produced via the pyrolysis of coal waste with polysiloxane polymer

Orevaoghene Eterigho-Ikelegbe[1,2] · Ryan Trammell[3] · Emmanuel Ricohermoso III[2] · Samson Bada[1]

Received: 2 April 2023 / Accepted: 3 July 2023 / Published online: 29 July 2023
© The Author(s) 2023

**Abstract**
A simple mixing-pressing followed by thermal curing and pyrolysis process was used to upcycle coal waste into high-value composites. Three coal wastes of different physicochemical properties were investigated. The hypothetical mechanisms of bonding between the coal particles and the preceramic polymer are presented. The textural properties of the coals indicated that the lowest volatile coal waste (PCD) had a dense structure. This limited the diffusion and reaction of the preceramic polymer with the coal waste during pyrolysis, thereby leading to low-quality composites. The water contact angles of the composites up to 104° imply hydrophobic surfaces, hence, no external coating might be required. Analysis of the carbon phase confirmed that the amorphous carbon structure is prevalent in the composites compared to the coal wastes. The dc volume resistivity of the composites in the range of 22 to 82 Ω-cm infers that the composites are unlikely to suffer electrostatic discharge, which makes them useful in creating self-heating building parts. The leached concentrations of heavy metal elements from the composites based on the end-of-life scenario were below the Toxicity Characteristic Leaching Procedure regulatory limits. Additionally, the release potential or mobility of the metals from the composites was not influenced by the pH of the eluants used. On the basis of the reported results, these carbon/ceramic composites show tremendous prospects as building materials due to these properties.

**Keywords** Circularity · Coal waste · Contact angle · Leaching · Recycling · Waste utilisation

## Introduction

The beneficiation of run-of-mine coal to produce clean coal for power and metallurgical applications and mechanised mining generate coal waste. According to the National Development and Reform Commission of China, the country has already accumulated over 4.5 Gt of coal gangue, which is growing annually with an increase of 370 to 550 Mt (Yang et al. 2018). In South Africa, approximately 60 Mt of coal waste is produced annually with an accumulation already over 1 Gt (Belaid et al. 2013; Isaac and Bada 2020). Therefore, it can be anticipated that if the global coal demand flattens to around 7.4 Gt by 2025 as predicted by the IEA (IEA 2020), the amount of coal waste is likely to increase. Unfortunately, only a small proportion of this coal waste is processed into high-value, high-performance products. The remainder is traditionally disposed of in landfills or piled up in arable land, resulting in unintended health, safety, and environmental impacts. While interventions like remediation and reclamation solutions such as mine backfill have evolved significantly, these solutions leave behind risks and liabilities. In addition, their long-term effect is not guaranteed (Lottermoser 2011; Broadhurst et al. 2019; Zhang and Ling 2020). Therefore, given the enormous volume of coal waste, immense research attention is devoted to valorisation in line with the objectives of the circular economy model and sustainable development.

Responsible Editor: George Z. Kyzas

**Highlights**
- The hypothetical mechanisms of the curing and pyrolysis are presented.
- The amorphous carbon structure is prevalent in the composites.
- The carbon/ceramic composites manifested water contact angle of up to 104°.
- The dc resistivity of the composites is between 22 and 82 Ω.cm.
- Concentrations of heavy metal elements from the composites were below the TCLP limits.

Extended author information available on the last page of the article

## A.5 'Strong, lightweight, thermally stable, and hydrophobic sustainable structural composites produced from coal-based waste and polymer-derived SiOC ceramics'.

Clean Technologies and Environmental Policy
https://doi.org/10.1007/s10098-023-02589-x

ORIGINAL PAPER

# Strong, lightweight, thermally stable, and hydrophobic sustainable structural composites produced from coal-based waste and polymer-derived SiOC ceramics

Orevaoghene Eterigho-Ikelegbe[1] · Emmanuel Ricohermoso III[2] · Hamza Harrar[1] · Ralf Riedel[2] · Samson Bada[1]

Received: 13 March 2023 / Accepted: 12 July 2023
© The Author(s) 2023, corrected publication 2023

**Abstract**
Recycling coal-based waste (CBW) into composites suitable as a building material might be a necessary response to combat its risk to the environment. Therefore, the objective of this study was to investigate the microstructure and performance of coal composites produced from CBW and polysiloxane polymer (SPR-212). Four types of CBW that differ in physicochemical properties were examined. Fourier transform infrared spectroscopy results indicated that the higher the intensity of the C=C bonds in the CBW, the higher the pyrolysis mass loss and shrinkage experienced by the composites during pyrolysis. The continuous operating temperature of the composites is up to 600 °C. However, at temperatures above 600 °C, composites containing carbon content greater than 36% manifested dramatic degradation. Pyrolysis mass loss in the range of 5.28 to 29.62% was obtained for all the composites. The density range of the composites is between 1.5 and 1.9 g per cubic centimetre. The water absorption of all the composites is within the range of 0 to 25% and is comparable to many building materials. Notably, the composites containing total carbon less than 10% registered a water contact angle greater than 90°, indicating the low wettability of their surface. Furthermore, composites that embodied the highest total carbon (63%) displayed the worst structural property. The findings of this study lay the foundation for further development of high-quality structural coal composites from CBW and the SPR-212 preceramic polymer through optimisation of the processing conditions.

✉ Orevaoghene Eterigho-Ikelegbe
1794557@students.wits.ac.za; eterighoo@gmail.com

[1] Faculty of Engineering and the Built Environment, DSI-NRF SARChI Clean Coal Technology Research Group, School of Chemical and Metallurgical Engineering, University of the Witwatersrand, Private Bag X3, Wits 2050, Johannesburg, South Africa

[2] Fachbereich Material-und Geowissenschaften, Technische Universität Darmstadt, Otto-Berndt-Straße 3, 4287 Darmstadt, Germany

Published online: 29 July 2023

**A.6 Report contribution – 'The alternative uses of coal in the production of advanced materials and lightweight products for the sustainability of the South African coal industry'.**




**THE ALTERNATIVE USES OF COAL IN THE PRODUCTION OF ADVANCED MATERIALS AND LIGHTWEIGHT PRODUCTS FOR THE SUSTAINABILITY OF THE SOUTH AFRICAN COAL INDUSTRY**

**Report Chair**

**Samson BADA**

**Clean Coal Technology Group, University of the Witwatersrand**

**Report Chapter Leads**

**Samson BADA, University of the Witwatersrand**

**Jibril Abdulsalam, University of the Witwatersrand**

**Orevaoghene Eterigho-Ikelegbe, University of the Witwatersrand**

**Project Number: P2023 – 1**

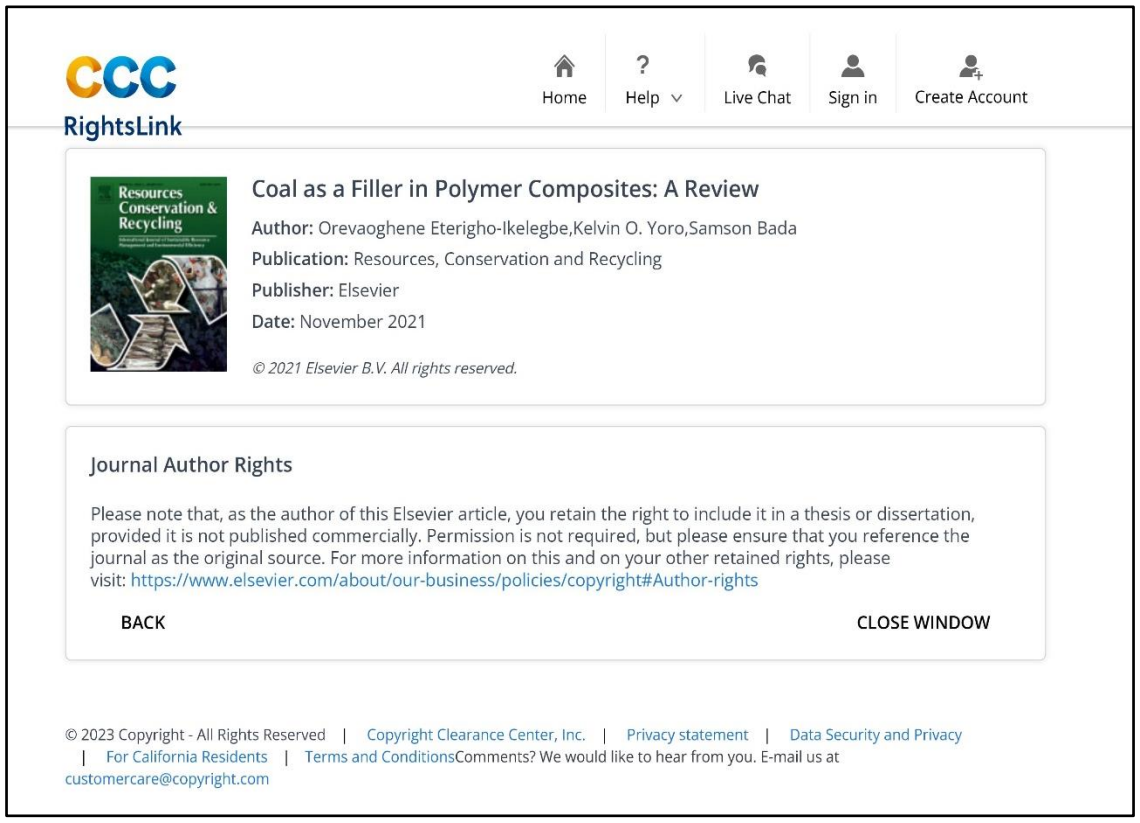
**2023**

# Appendix B

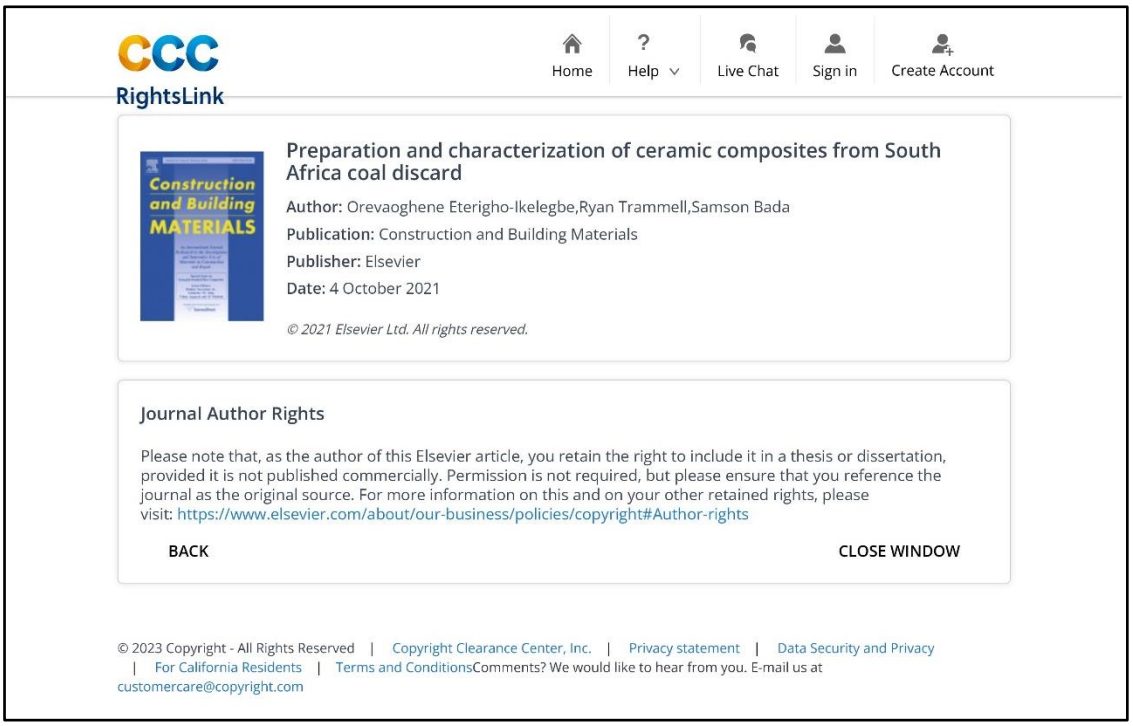
## Author Copyright Permissions

All copyright permissions of articles used in this thesis were requested from Copyright Clearance Centre.

### B.1 Copyright Clearance Center Permission for 'Coal as a Filler in Polymer Composites: A Review'.



## B.2 Copyright Clearance Center Permission for ‘Preparation and characterisation of ceramic composites from South Africa coal discard'.



**B.3 Permission for 'Novel ceramic composites produced from coal discards with potential application in the building and construction sectors'.**

Creative Commons — Attribution 4.0 International — CC BY 4.0 https://creativecommons.org/licenses/by/4.0/deed.en

This page is available in the following languages:

# Creative Commons License Deed

**Attribution 4.0 International (CC BY 4.0)**

This is a human-readable summary of (and not a substitute for) the license.

## You are free to:

**Share** — copy and redistribute the material in any medium or format

**Adapt** — remix, transform, and build upon the material

for any purpose, even commercially.

The licensor cannot revoke these freedoms as long as you follow the license terms.

## Under the following terms:

**Attribution** — You must give appropriate credit, provide a link to the license, and indicate if changes were made. You may do so in any reasonable manner, but not in any way that suggests the licensor endorses you or your use.

**No additional restrictions** — You may not apply legal terms or technological measures that legally restrict others from doing anything the license permits.

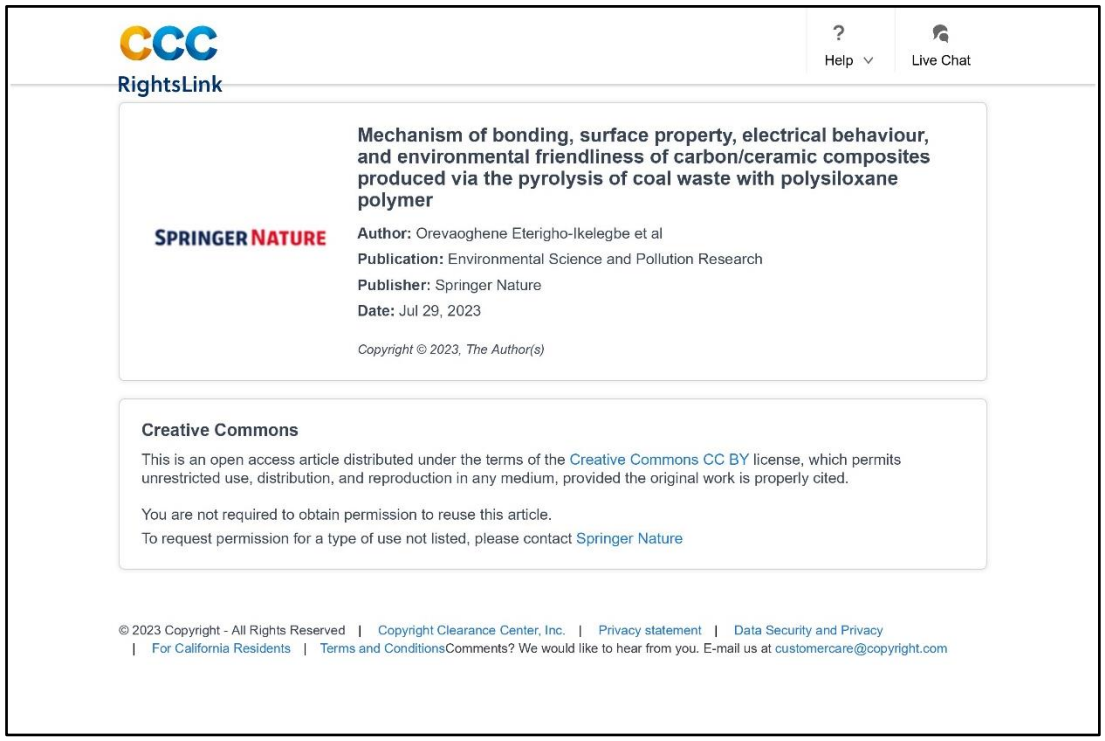
## Notices:

You do not have to comply with the license for elements of the material in the public domain or where your use is permitted by an applicable exception or limitation.

No warranties are given. The license may not give you all of the

1 of 2 2023/09/12, 23:27

**B.4 Copyright Clearance Center Permission for 'Mechanism of bonding, surface property, electrical behaviour, and environmental friendliness of carbon/ceramic composites produced via the pyrolysis of coal waste with polysiloxane polymer'.**



CCC RightsLink

Help | Live Chat

SPRINGER NATURE

**Mechanism of bonding, surface property, electrical behaviour, and environmental friendliness of carbon/ceramic composites produced via the pyrolysis of coal waste with polysiloxane polymer**

**Author:** Orevaoghene Eterigho-Ikelegbe et al

**Publication:** Environmental Science and Pollution Research

**Publisher:** Springer Nature

**Date:** Jul 29, 2023

*Copyright © 2023, The Author(s)*

**Creative Commons**

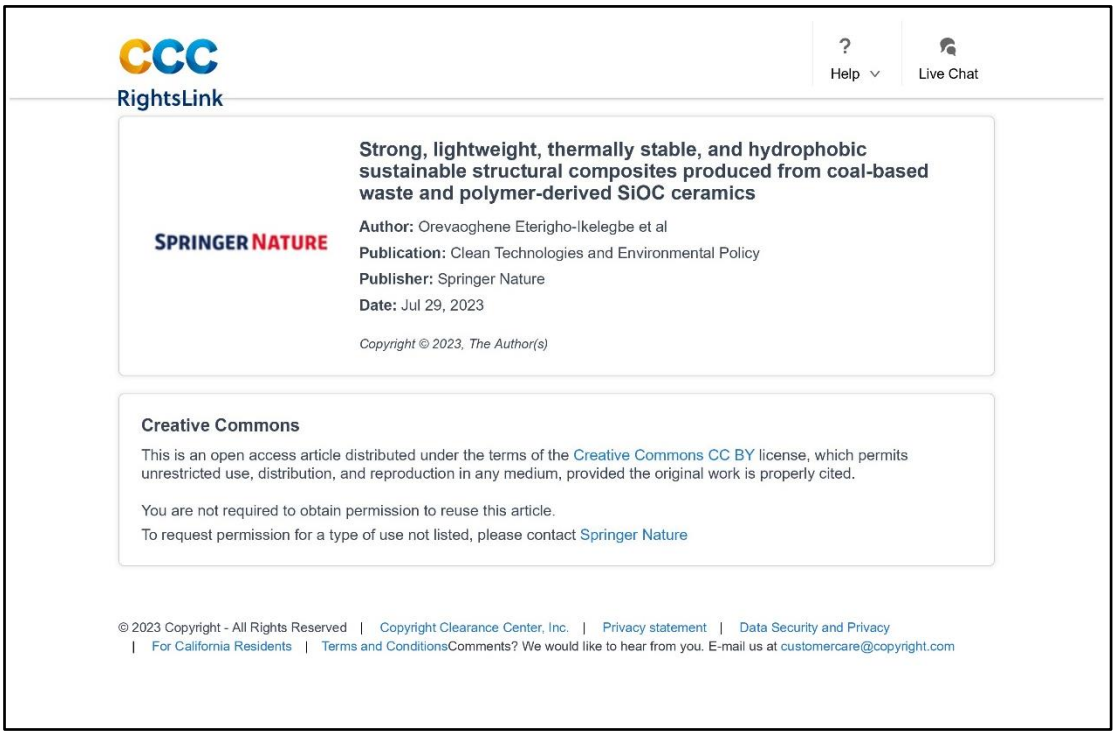
This is an open access article distributed under the terms of the Creative Commons CC BY license, which permits unrestricted use, distribution, and reproduction in any medium, provided the original work is properly cited.

You are not required to obtain permission to reuse this article.

To request permission for a type of use not listed, please contact Springer Nature

© 2023 Copyright - All Rights Reserved | Copyright Clearance Center, Inc. | Privacy statement | Data Security and Privacy | For California Residents | Terms and ConditionsComments? We would like to hear from you. E-mail us at customercare@copyright.com

**B.5 Copyright Clearance Center Permission for 'Strong, lightweight, thermally stable, and hydrophobic sustainable structural composites produced from coal-based waste and polymer-derived SiOC ceramics'.**



CCC RightsLink

Help | Live Chat

**Strong, lightweight, thermally stable, and hydrophobic sustainable structural composites produced from coal-based waste and polymer-derived SiOC ceramics**

SPRINGER NATURE

**Author:** Orevaoghene Eterigho-Ikelegbe et al
**Publication:** Clean Technologies and Environmental Policy
**Publisher:** Springer Nature
**Date:** Jul 29, 2023

*Copyright © 2023, The Author(s)*

**Creative Commons**

This is an open access article distributed under the terms of the Creative Commons CC BY license, which permits unrestricted use, distribution, and reproduction in any medium, provided the original work is properly cited.

You are not required to obtain permission to reuse this article.

To request permission for a type of use not listed, please contact Springer Nature

© 2023 Copyright - All Rights Reserved | Copyright Clearance Center, Inc. | Privacy statement | Data Security and Privacy | For California Residents | Terms and ConditionsComments? We would like to hear from you. E-mail us at customercare@copyright.com

# Appendix C

## Award and Seminar Participation

DAAD Deutscher Akademischer Austauschdienst
German Academic Exchange Service

### DOCUMENT OF AWARD

The German Academic Exchange Service (DAAD) is a joint organization
of the universities and other institutions of higher education in the Federal Republic of Germany.
Supported from public funds, the DAAD promotes international academic cooperation,
especially through the exchange of students and academics.
DAAD scholarships are awarded by selection committees comprising a panel of independent academics.

**Orevaoghene Eterigho-Ikelegbe**

has been awarded a scholarship by the DAAD for further study and training.

I would like to congratulate you on your award and wish you every success for your further studies. It would give me great pleasure, if you would maintain contact with your academic partners and the DAAD after completion of your scholarship.

Bonn, 07/12/2021

Prof. Dr. Joybrato Mukherjee
President of the DAAD

This document will only come into effect in connection with a letter of award (Stipendienzusage) from the DAAD office.



# Postgraduate Seminar

**(CHEMET-PGS-2023)**

This certificate is presented to

*Orevaoghene Eterigho-Ikelegbe*

for the presentation titled

**Coal composites: An option for coal waste in the circular economy**

in the CHEMET-PGS-2023 on

30 May 2023

Organised by the School of Chemical and Metallurgical Engineering, University of the Witwatersrand

Smarte Anekwe
CHEMET PG committee chairperson

Josias Van der Merwe
CHEMET Head of School

CHEMET
CHEMICAL AND METALLURGICAL ENGINEERING

UNIVERSITY OF THE WITWATERSRAND JOHANNESBURG 1922 2022


UNIVERSITY OF THE WITWATERSRAND, JOHANNESBURG
Postgraduate Affairs
Research Office
CERTIFICATE
AWARDED TO
OREVAOGHENE ETERIGHO-IKELEGBE
FOR PARTICIPATION AT
THE WITS PhD SEMINAR
12 - 13 September 2022
Professor Lynn Morris
DVC: Research & Innovation
Professor Robert Muponde
HEAD: Postgraduate Liaison (Wits Research Office)